Postnatal development of the purinergic signaling system in the preBötzinger Complex; implications for the hypoxic ventilatory response

by

Robert J. Reklow

A thesis submitted in partial fulfillment of the requirements for the degree of

Doctor of Philosophy

Department of Physiology
University of Alberta

Abstract

Low oxygen (hypoxia) evokes the biphasic hypoxic ventilatory response (HVR), in which carotid-body chemoreceptors trigger a rapid increase in ventilation ($\dot{V}_E$) followed by a centrally-mediated, secondary hypoxic depression of respiration (HRD) and metabolic rate ($\dot{V}_{O_2}$) that involves adenosine. In adults, $\dot{V}_E$ and $\dot{V}_E/\dot{V}_{O_2}$ remain above baseline throughout the HRD. However, in neonates $\dot{V}_E$ can fall below baseline, more than the hypoxia-induced decrease in $\dot{V}_{O_2}$, such that neither $\dot{V}_E$ nor $\dot{V}_E/\dot{V}_{O_2}$ remain above baseline, which can become life-threatening. Astrocytes in the preBötzinger Complex (preBötC, brain site that generates inspiratory rhythm) sense hypoxia and release ATP, which binds $P2Y_1$ receptors (Rs), increases $\dot{V}_E$ and attenuates the HRD. ATP, however, is rapidly degraded to adenosine, which, via P1Rs, depresses breathing. Thus, the HRD is influenced by an interaction in the preBötC between ATP excitation and adenosine inhibition that changes developmentally. Multiple factors, collectively called the purinome, influence this balance, including P2Rs, P1Rs, ectonucleotidases that terminate ATP signaling and produce adenosine, and transporters and enzymes that terminate the actions of adenosine.

My first aim asked how individual purinome components contribute to postnatal changes in the net signaling actions of ATP in the preBötC by comparing how manipulating specific purinome components affected baseline preBötC behaviour and its responses to P1 and P2R-related agents applied to medullary slices from mice between postnatal day 0 (P0) and P12. My second aim assessed whether developmental changes in the purinome identified in Aim 1 shape the HVR in vivo and contribute to the blunted HVR of neonatal rodents. My final Aim tested the controversial hypothesis that the HVR of neonatal mammals (rodents) is not blunted; i.e., greater reductions in

$\dot{V}_E$ during hypoxia in neonates reflects a greater depression of $\dot{V}_{O_2}$ such that mammals of all ages respond to hypoxia with an adaptive increase in $\dot{V}_E/\dot{V}_{O_2}$ (hyperventilation).

Data from Aim 1 revealed that ATP excitation of preBötC frequency increased developmentally to match the $P2Y_1R$ excitation, which was constant postnatally. Differences between ATP and $P2Y_1R$ actions were not due to developmental reductions in ectonucleotidase activity or adenosine inhibition; ATP degradation by preBötC tissue increased with age and the adenosine-evoked decrease in frequency remained constant between P0 and P12. Removing equilibrative nucleoside transporters (ENT1 and 2) that clear adenosine prolonged adenosine inhibition in P0–12 slices, suggesting ENTs are unlikely to mediate developmental changes. In contrast, expression of adenosine kinase (ADK), which metabolizes adenosine and facilitates ENT-mediated adenosine clearance, was barely detectable at P0, and reached adult levels by P21. Functionally, ADK inhibition only affected baseline frequency in older slices.

To test the role of adenosine clearance mechanisms in the development of the HVR (Aim 2), I used plethysmography to measure the development (P0–adult) of ventilatory and metabolic responses evoked by 10% O_2 in ENT1/2 knockout mice and ADKtg mice. ENT1/2 knockout had surprisingly modest effects on the HVR. In contrast, neonatal ADKtg mice that express adult levels of ADK responded to hypoxia with an adult-like, sustained hyperventilation, while $\dot{V}_E/\dot{V}_{O_2}$ did not change in neonatal wild-type mice. These strain differences disappeared by P6, supporting a critical role of ADK in development of the HVR. Surprisingly, the adult-like HVR in neonatal ADKtg mice was not due to an enhanced ventilatory response but a hypoxia-induced decrease in $\dot{V}_{O_2}$ not seen in wild-types.

To test whether the greater HRD in neonates reflects greater hypoxic depression of $\dot{V}O_2$ (Aim 3), I measured $\dot{V}E$ and $\dot{V}O_2$ responses of C57BL/6J and FVB mice and SD rats to 10% O_2 daily starting at P0. Hypoxia never depressed $\dot{V}O_2$ in P0 rodents; nor did it evoke in P0 mice a sustained increase in $\dot{V}E/\dot{V}O_2$. Hypoxia-induced reductions in $\dot{V}O_2$ emerged after P3 in C57BL/6J mice and at P1 in FVB mice and SD rats, demonstrating that the mechanisms underlying the adaptive depression of $\dot{V}O_2$ by hypoxia develop after postnatally.

These data demonstrate that puringeric signaling in the preBötC network shifts toward excitation postnatally, in part due to increased ADK activity and enhanced adenosine clearance. ENT and especially ADK activity contribute to a more sustained HVR with development. Most surprising, adult-like ADK expression in neonates bestows an ability for hypoxia to inhibit metabolism. Thus, purinergic modulation of central networks may impact development of adaptive ventilatory and metabolic responses to hypoxia.

Preface

Ethics Approval

This thesis is an original work by Robert Reklow. The research presented in this thesis is described in two Animal Use Protocols that were reviewed and approved by the University of Alberta's Health Sciences Animal Care and Use Committee in accordance with the guidelines of the Canadian Council on Animal Care. The approved ethics protocols are entitled:

i) "Neuromodulation of inspiratory network activity in vitro", No. AUP00000255, 2013 (renewed through to 2024)
ii) "In vivo approaches to deciphering the differential modulation of respiratory rhythm generation and pattern forming networks by ATP", No. AUP00000256, 2016 (Renewed through to 2023)

Collaborations:

Chapter 1 of this thesis is based upon a review that I wrote for the journal *Frontiers in Cellular Neuroscience* in 2019. (Reklow, R.J., Alvares, T.S., Zhang, Y., Tapia, A.P.M., Biancardi, V., Katzell, A.K., Frangos, S.M., Hansen, M.A., Toohey, A.W., Cass, C.E., Young, J.D., Pagliardini, S., Boison, D., Funk, G.D., 2019. The purinome and the preBötzinger Complex - a ménage of unexplored mechanisms that may modulate/shape the hypoxic ventilatory response. *Frontiers in Cellular Neuroscience* 13, 365). However, Chapter 1 contains significant changes to the published review that were included to incorporate new literature that has emerged since the initial publication and to incorporate the specific aims of my thesis into the relevant sections of the review. This was done so that the background and rationale for each aim was clear. Despite the revisions, the majority of the Chapter 1 review are the same as in published review.

As first author, I worked closely with GDF in conception, design, organization of the entire manuscript. I was primarily responsible for a majority of the writing but GDF, YZ, AT, VB, AK, SF, MH, and AT contributed to specific sections. The manuscript is primarily a review, but it also includes some novel data. I contributed to conception and design of experiments described in Figure 1.3, completed these studies and performed the statistical analysis with some assistance from TA. JDY and CEC are included as they provided the ENT knockout mice that were used to

generate Fig 1.3. DB consulted on ADK biochemistry and edited the manuscript. All authors participated in manuscript revision and approved the submitted version.

In addition to my own work, chapters 2, 3 and 4 of this thesis include work contributed by honors/summer students who were trained by me and under my supervision (bolded below; Steven Qiu; Tristan Sinnatamby; Sara Frangos and Meghan Hansen), Suey van Baarle (lab technician), Tucaauê Alvares (lab technician), and Daniel B. Zoccal (visiting faculty member from São Paulo State University). TA, SVB, **SQ** conducted phosphate assay experiments in section 2.3.2ii and Fig 2.4, and **SQ** analyzed these data. **SMF** and **MAH** conducted in vitro experiments measuring the effect of NBMPR on neonate slices (2.3.3i and Fig. 1.5). SVB conducted genotyping for ENT KO confirmation (2.3.3ii and Fig 2.6). SVB and **TS** conducted and analyzed western-blots for ADK expression (2.3.3iv, 2.3.3v and Fig. 2.7, 2.8). DBZ conducted in vivo hypoxia experiments with ENT1/2 KO mice (3.3.2 and Fig. 3.2-3.3). **TS** conducted in vivo 8% O_2 hypoxia experiments with ADKtg mice (3.3.3; 4.3.3 and Fig. 3.8; 4.4) and daily hypoxia experiments in SD rats (4.3.6 and Fig 4.7). I completed synthesis of all data and figures for their inclusion in this document. All data interpretation and discussion are my original work.

Acknowledgements

First, I would like to recognize my supervisor, Dr. Gregory Funk. His patience, knowledge and mentorship have been instrumental in my growth as a scientist and I will be forever grateful for his enthusiasm and advice in my academic and personal endevours. I am appreciative for the opportunities provided by Greg to attend international conferences, contribute to important collaborations and work amongst a team of exceptional scientists. Greg is an outstanding mentor and even better friend. Next, I thank the members of my supervisory committee; Dr. Simon Gosgnach and Dr. Silvia Pagliardini, as well as external examining members, Dr. Joanna MacLean and Dr. Christopher Wilson for their role in the examination process. I would also like to recognize Dr. Peter Smith who was a member of my original supervisory committee. I am very grateful for my extraordinary colleagues in the Funk and neighbouring labs, including: Neeharika Reddy, Suey van Baarle, Jun Ren, Vivian Biancardi, Ana Miranda Tapia, Yong Zhang, Venkatesh Jalubula, Vishaal Rajani, Ann Revill, Annette Pisanski, Tara Janes, Vladimir Rancic, Farhia Haque, Jasmeen Saini, Tristan Sinnatamby, Steven Qiu, Alex Toohey, Megan Hansen, Sara Frangos, Alexis Katzell, and Jashan Saini, as well as a visiting faculty member, Dr. Daniel Zoccal. I would be remiss to not mention another former colleague and very close friend, Tucaauê Alvares, who was responsible for teaching me many of the techniques used in this thesis and was an extremely knowledgeable resource for troubleshooting many hurdles in my experimental protocols. Finally, thank you to my family and friends for their immense support throughout my studies. I am thankful for the encouragement of the Smith-Winnitoy family. To my sisters, Laura and Emily, thank you for lifting my spirits and inspiring me through your own incredible endevours – keep being awesome. To Eileen and Jeff, more personally known as Mom and Dad, thank you for your endless support, guidance and inspiration to pursue science and persevere through many challenging moments in my degree. I'm very grateful to finally celebrate this achievement with both of you. Lastly, to my amazing partner, Lauren, thank you for keeping me grounded, well-fed and sparking optimism in many difficult moments while I completed this thesis. Your love and dedication is an inspiration for me to be a better human every day and I cannot overstate the positive impact you have made in my life. Thank you for constantly expanding my world and supporting me to become the best version of myself.

Funding Sources: CIHR, NSERC, SCHF through WCHRI

Table of Contents

List of Figures

List of Abbreviations

Abbreviation	Definition
$[Ca^{2+}]_i$	intracellular calcium
ABT 702	adenosine kinase inhibitor
aCSF	artificial cerebral spinal fluid
ADK	adenosine kinase
ADKtg	transgenic overexpression of ADK
ADO	adenosine (i, intracellular; e, extracellular)
ADP	adenosine diphosphate
AMP	adenosine monophosphate
AMPA	glutamatergic receptor
AMPK	AMP-activated protein kinase
ANOVA	analysis of variance
AOP	apnea of prematurity
ATP	adenosine triphosphate
ATPɣS	non-hydrolyzable ATP
BK	large conductance calcium activated potassium currents
C57BL/6J	C57 black 6 inbred mouse from Jackson Laboratories
CA1	hippocampal pyramidal neurons
cAMP	cyclic AMP
Cd39	ectonucleoside triphosphate diphosphohydrolase 1
CD73	ecto-5′-nucleotidase
cDNA	complementary DNA
CNS	central nervous system
CNT	concentrative nucleoside transporter
CV 1808	A_2 receptor agonist
DMSO	dimethyl sulfoxide
DPCPX	A_1 receptor antagonist
E-NTPDase	5'-triphosphate ectonucleosidase
ECTO	ectonucleotidase
ENT	equilibrative nucleoside transporter
EPSP	excitatory post synaptic potential
EtOH	ethanol
$FeCO_2$	outflow CO_2 fraction
FeO_2	outflow O_2 fraction
$FiCO_2$	inflow CO_2 fraction
FiO_2	inflow O_2 fraction
FR	flowrate
Freq	frequency
FVB	inbred mouse with Friend leukemia virus B allele
GABA	gamma-aminobutyric acid
Gaq/Gs/Gi/Go	G protein-coupled receptors
H_2O_2	hydrogen peroxide
HD	Huntington's Disease
HRD	hypoxic respiratory depression

Abbreviation	Definition
$HVR_{\dot{V}E}$	hypoxic ventilatory response
$HVR_{\dot{V}E/\dot{V}O2}$	hypoxic ventilatory and metabolic response
i.p.	intraperitoneal
I_{CAN}	calcium activated non-specific cation current
kD	kilodalton
KNCQ	potassium channel
MAPK	mitogen-activated protein kinase
mGluR	metabotropic glutamate receptor
MRS 2179/2279	selective $P2Y_1$ receptor antagonist
MRS 2365	selective $P2Y_1$ receptor agonist
NBMPR	equilibrative nucleoside transporter inhibitor
NMDA	N-methyl-D-aspartate
OGD	oxygen-glucose
P1	adenosine (A) receptor
P2X	purinergic receptor
P2Y	purinergic receptor
$PaCO_2$	arterial partial pressure of carbon dioxide
PaO_2	arterial partial pressure of oxygen
P_B	barometric pressure
P_C	chamber water vapour pressure
PCR	polymerase chain reaction
P_K	calibration pressure deflection
PNA	phrenic nerve activity
POM1	E-NTPDases inhibitor
PPADS	nonselective P2 antagonist
P_R	water vapour pressure
preBötC	preBötzinger Complex
P_T	respiratory pressure deflection
RT-PCR	reverse transcription polymerase chain reaction
RTN	retrotrapezoid nucleus
SD	sprague-dawley
SEM	standard error of mean
SIDS	sudden infant death syndrome
SK	small conductance calcium activated potassium currents
SP	Substance P
SpO_2	oxygen saturation
SUDEP	sudden unexplained death in epilepsy
Swiss CD	inbred mouse strain
T_A	air temperature within chamber
TASK	TWIK-related aid sensitive K+ channel
Tb	body temperature
TIRF	total internal reflection fluorescence
TNAP	tissue-nonspecific alkaline phosphatase
TTX	tetrodotoxin

Abbreviation	Definition
$\dot{V}_E$	minute ventilation
$\dot{V}_E/\dot{V}_{O_2}$	air convection requirement
V_K	calibration volume
$\dot{V}_{O_2}$	metabolic rate
VRC	ventral respiratory column
V_T	tidal volume
WT	wild type
∫XII	integrated hypoglossal nerve activity

Chapter 1: Literature Review

(Section 1.2 of this introductory chapter has been modified from Reklow et al., 2019. The Purinome and the preBötzinger Complex - A Ménage of Unexplored Mechanisms That May Modulate/Shape the Hypoxic Ventilatory Response. Frontiers in Cellular Neuroscience 13, 365)

1.1 Overview

The HVR is a vital homeostatic reflex in which substantial reductions in the partial pressure of O_2 in the arterial blood (PaO_2) and brain evoke a biphasic ventilatory response. The term HVR is most commonly used to describe how ventilation ($\dot{V}E$) changes during hypoxia, especially in clinical research where it can be difficult to simultaneously measure metabolic rate ($\dot{V}O_2$). However, it is also used to describe how the ratio of $\dot{V}E/\dot{V}O_2$, the air convection requirement, changes during hypoxia. The importance of distinguishing between these two definitions is discussed below and in the final section of the literature review. For clarity, when the HVR is used to describe changes in ventilation during hypoxia I will refer to it as the $HVR_{\dot{V}E}$. When HVR is used to describe changes in $\dot{V}E/\dot{V}O_2$ during hypoxia I will refer to it as $HVR_{\dot{V}E/\dot{V}O_2}$. The $HVR_{\dot{V}E}$ comprises an initial, carotid body-mediated, rapid (~1 min) increase in ventilation (Phase 1) that is followed by a centrally mediated secondary depression during which ventilation falls slowly (4–5 min) to a lower steady state Phase 2 level that, in adults, remains above baseline (Bissonnette, 2000; Martin-Body et al., 1985; Mayer et al., 2006; Mortola, 1996; Moss, 2000; Serra et al., 2001). The mechanisms underlying the secondary depression are not fully understood, but it is believed to be mediated by the central nervous system (CNS) and involve adenosinergic and GABAergic signaling (Fiore et al., 2013; Funk, 2013; Herlenius et al., 2002; Koos et al., 1997; Paolillo and Picone, 2013; Reklow et al., 2019). Premature and newborn infants and newborn mammals also show a biphasic $HVR_{\dot{V}E}$. The main difference between the $HVR_{\dot{V}E}$ in the very young compared to mature mammals is that the secondary depression of ventilation is much greater in neonates such that ventilation can fall below baseline, which can become life-threatening (Bonora et al., 1984; Carroll and Bureau, 1987; Cross and Oppe, 1952). Therefore, of significant interest is understanding the mechanisms that shape the $HVR_{\dot{V}E}$, especially those that act after the initial Phase 1 peak and are responsible the greater hypoxic respiratory depression in the youngest mammals, including humans.

Over the last 20 years, purinergic signaling, defined as signaling mediated by ATP and its breakdown products, adenosine diphosphate (ADP) and adenosine (ADO), has emerged as important player in shaping the $HVR_{\dot{V}E}$ (Gourine et al., 2005). Compelling evidence accumulating since 2005 has challenged the long-standing view that the only role of the CNS in the $HVR_{\dot{V}E}$ is inhibitory – i.e., that CNS mechanisms are responsible for the secondary respiratory depression

but do not contribute to the excitatory component of the HVR$\dot{V}_E$ underlying the increase in $\dot{V}E$ evoked by hypoxia. These data suggest that following peripheral, carotid-body-mediated Phase 1 excitation, interactions between central excitatory and inhibitory purinergic mechanisms shape this key homeostatic reflex (Angelova et al., 2015; Rajani et al., 2017). An objective of this literature review is to present our working model of how purinergic signaling modulates inspiratory activity in the preBötzinger Complex (preBötC; key site of inspiratory rhythm generation) to shape the HVR$\dot{V}_E$. It is based on the perspective that the actions of extracellular ATP are determined by a complex signaling system, the purinome, which is described in detail below. Briefly, the purinome includes not only the excitatory actions of ATP and ADO at P2 and P1 receptors, respectively, but diverse families of enzymes and transporters that collectively determine the rate of ATP degradation, ADO accumulation and extracellular ADO (ADOe) clearance (Reklow et al., 2019). In this context, the net actions of ATP when released in the preBötC during hypoxia are determined by the balance between the excitatory actions of ATP at P2Rs and the inhibitory actions of ADO at P1Rs (Huxtable et al., 2009; Zwicker et al., 2011), a balance that is determined by the various components of the purinome and how they change during development. I summarize current knowledge of the roles played by these different purinergic elements in shaping the HVR$\dot{V}_E$, often drawing on examples from other brain regions because little is known of how these elements change during development in the brainstem and preBötC. Thus, an additional goal of this review is to provide the background and rationale for the aims of this thesis, the overarching objective of which is to advance understanding of the role of purinergic signaling within the preBötC in shaping the HVR$\dot{V}_E$ during development.

The first aim, presented in Chapter 2, is to characterize during the first two weeks of postnatal development (postnatal day 0–12, P0–12) how the different components of the purinome affect inspiratory-related preBötC rhythm and its modulation by ATP and ADO. To directly assess the signaling actions of these compounds on preBötC-generated inspiratory rhythm, experiments were performed in vitro using preBötC-containing medullary slices that continue to generate an inspiratory-related rhythm "in a dish" where the preBötC can be studied in isolation (Funk and Greer, 2013; Smith et al., 1991). These experiments were designed to identify the purinergic elements most likely to underlie developmental changes in the HVR$\dot{V}_E$ to inform the design of in vivo studies to explore the role of those elements in shaping the HVR$\dot{V}_E$. My observation in Chapter

2 that the duration of the inhibition evoked by ADO in the preBötC decreases with development identified ADOe clearance mechanisms, specifically ENTs and ADK, as the most likely candidates. Thus, the second aim of my thesis, described in Chapter 3, is to test the hypothesis in vivo that the immature HVR ($HVR_{\dot{V}_E}$ and $HVR_{\dot{V}_E/\dot{V}_{O_2}}$); i.e., the inability to produce a sustained increase in ventilation during hypoxia, is due to the limited capacity of newborns to clear ADOe.

The third and final aim of my thesis, described in Chapter 4, is to re-visit a decades-old, but unresolved debate about the functional maturity of the HVR and its underlying network. The HVR is operational at birth but not fully mature, as demonstrated by developmental differences in the temporal profile of the $HVR_{\dot{V}_E}$ and the $HVR_{\dot{V}_E/\dot{V}_{O_2}}$. Thus, a key question is whether the network that underlies the HVR is sufficiently developed at birth to maintain O_2 homeostasis. Simultaneous measurement of the $HVR_{\dot{V}_E/\dot{V}_{O_2}}$ and blood gases is required to directly address this question, but technical limitations (multiple blood samples from neonatal mice) and ethical concerns (exposing premature infants to hypoxia) are challenges. Nevertheless, inferences can be made from careful measurement of adaptive hypoxic responses. In fact, developmental measurements of $HVR_{\dot{V}_E/\dot{V}_{O_2}}$ using C57BL/6J mice (Chapter 3) and the observation that hypoxia did not evoke an increase in $\dot{V}_E/\dot{V}_{O_2}$ until animals are between 4–6 days old strongly suggests that the HVR, whether reported as $HVR_{\dot{V}_E}$ or $HVR_{\dot{V}_E/\dot{V}_{O_2}}$, is compromised in neonates. Chapter 4 was therefore designed to more thoroughly assess whether neonatal rodents have a compromised HVR by comparing in two strains of mice and SD rats daily changes in the $HVR_{\dot{V}_E}$ and $HVR_{\dot{V}_E/\dot{V}_{O_2}}$.

Chapter 4 is then followed by a general discussion that integrates the data from Chapters 2–4 to summarize the contributions of this thesis, provide an updated overview of the role played by the purinome in shaping the HVR during development and discuss clinical implications and next steps.

The remainder of this chapter (Section 1.2) is a modified version of a first-authored review published in 2019 entitled “The Purinome and the preBötzinger Complex – A Ménage of Unexplored Mechanisms That May Modulate/Shape the Hypoxic Ventilatory Response” (Reklow et al., 2019). The published review has been updated here to include relevant research published since 2019 and to integrate into relevant sections the specific aims of my thesis to clarify the rationale for each aim. This review also includes a new section, Section 1.3 that provides the

background and rationale for my third aim that reopens an old but unresolved debate about whether it is most appropriate to report the HVR as $HVR_{\dot{V}E}$ or $HVR_{\dot{V}E/\dot{V}O_2}$ and whether premature and neonatal mammals actually have a compromised/inadequate response to hypoxia.

1.2 The purinome and the preBötzinger Complex - a ménage of unexplored mechanisms that may modulate/shape the hypoxic ventilatory response.

1.2.1 Introduction

The mammalian brain depends on a constant supply of O_2 to meet its energy needs, and a host of adaptive responses have evolved to protect brain O_2 levels. Prominent among these is the biphasic $HVR_{\dot{V}E}$ (Mortola, 1996) in which a fall in arterial O_2 detected at the carotid body chemoreceptors triggers, within the first minute of exposure, an adaptive (Phase 1) increase in breathing. If this increase does not immediately restore arterial O_2, the brain becomes hypoxic, triggering changes in brain chemistry and a maladaptive secondary hypoxic respiratory depression during which ventilation gradually decreases (4–5 min) to a lower steady-state (Phase 2) level. The secondary depression is especially pronounced in premature mammals, where ventilation falls below baseline and can become life-threatening (Bissonnette, 2000; Mortola, 1996; Moss, 2000).

Mechanistically, the biphasic $HVR_{\dot{V}E}$ has been viewed for decades as the result of just two interacting processes; an initial peripheral, carotid body-mediated (Phase 1) excitation and a slower, centrally-mediated hypoxic respiratory depression to a steady-state Phase 2 level of breathing (Mortola, 1996; Moss, 2000). The mechanisms underlying this depression are not fully understood, but adenosine is strongly implicated (Bissonnette, 2000; Mortola, 1996; Moss, 2000). The key point is that according to this conventional view of the $HVR_{\dot{V}E}$, excitation of breathing during hypoxia derives solely from the peripheral nervous system; i.e., the only contribution of the central nervous system to the $HVR_{\dot{V}E}$ is depression.

New evidence from key cardiorespiratory control sites is challenging this dogma. In relation to the cardiovascular system, C1 noradrenergic neurons involved in control of heart rate and blood pressure are powerfully excited by hypoxia and this excitation is important for homeostatic control (Guyenet, 2006). In the respiratory network, while the Phase 1 component of the $HVR_{\dot{V}E}$ is mediated peripherally, our data from rodents strongly suggest that during hypoxia, astrocytes in

the preBötC detect hypoxia and release ATP, which, via $P2Y_1$ receptors, excites inspiratory neurons and increases ventilation, thereby attenuating the hypoxic respiratory depression (Angelova et al., 2015; Gourine et al., 2005; Rajani et al., 2017; Sheikhbahaei et al., 2018). Thus, unlike the majority of brain regions where hypoxia has depressant actions, the astroglial network of the preBötC appears to mount an excitatory response that partially counteracts the hypoxic respiratory depression, contributing to a vital homeostatic reflex.

The effects of extracellular ATP (ATPe), however, are not determined solely by its actions on P2 receptors. ATPe is rapidly broken down by ectonucleotidases (e.g., Cd39, CD73) into extracellular adenosine diphosphate (ADPe), adenosine monophosphate (AMPe) and ultimately adenosine (ADOe), a transmitter in its own right that signals via 4 types of P1 receptors, A_1, A_{2A}, A_{2B} and A_3 (Haas and Selbach, 2000; Sebastião and Ribeiro, 2009). Indeed, a predominant effect of hypoxia (and ischemia) on brain chemistry is a widespread increase in the concentration of extracellular adenosine (ADOe) (reviewed by (Dale and Frenguelli, 2009) that can derive from multiple sources including vesicular release of ATP as a transmitter/co-transmitter that is subsequently degraded, and export of intracellular ADO (ADOi) (reviewed by Latini and Pedata, 2001). In the brain ADOe acts primarily through low affinity A_1 and A_{2A} receptors to elicit a host of region-specific effects, largely by modulating glutamatergic transmission. A_1 receptor-mediated inhibitory mechanisms, pre- and postsynaptic, are widespread and can be considered neuroprotective (Boison, 2013a, 2016; Wei et al., 2011). A_{2A} receptors are primarily excitatory and engaged in adaptive processes, as heralded by their key role in synaptic plasticity in different brain areas (Canas et al., 2018; Cunha, 2016; Lopes et al., 2019; Pedata et al., 2001; Thauerer et al., 2012; Yacoubi et al., 2001, 2009). Within the brainstem network that generates and controls breathing, ADOe is largely inhibitory, which in this network is maladaptive; i.e., for the body/brain to recover from hypoxia and restore O_2 homeostasis, ventilation and cardiac activity must increase. ADOe inhibits breathing most potently in premature and newborn mammals via A_1 receptors in the preBötC (Herlenius et al., 1997; Herlenius and Lagercrantz, 1999; Huxtable et al., 2009; Zwicker et al., 2011) and A_{2A} receptor-mediated excitation of brainstem GABAergic neurons (Koos et al., 2001, 2004; Mayer et al., 2006; Wilson et al., 2004). Indeed the inhibitory actions of ADOe on the central respiratory network are strongly implicated in the respiratory depression that is life-threatening in apnea of prematurity (AOP) (Burnstock and Dale, 2015; Funk, 2013; Martin and Abu-Shaweesh,

2005; Paolillo and Picone, 2013), and fatal in sudden infant death syndrome (SIDS) and sudden unexpected death in epilepsy (SUDEP) (Boison, 2013b; Richerson et al., 2016).

Thus, the actions of ATP in the preBötC are likely determined by the balance between the excitatory actions of ATP (and ADP) at P2 receptors and the inhibitory actions of its main metabolite, ADO, at P1 receptors (Fig. 1.1). Indeed, this balance, which is controlled by a complex signaling system referred to as the *purinome* (Volonté and D'Ambrosi, 2009) (Fig. 1.2), is emerging as important in determining the degree of hypoxic respiratory depression (Angelova et al., 2015; Funk, 2013; Funk and Gourine, 2018a; Gourine and Funk, 2017; Rajani et al., 2017). The purinome includes: ATPe and P2 receptors (1,2 in Fig. 1.2), ADOe and P1 receptors (4); ectonucleotidases that degrade ATP into ADO (3); equilibrative and concentrative nucleoside transporters (ENTs and CNTs, respectively) (King et al., 2006; Parkinson et al., 2011; Young et al., 2013) that move ADO across membranes down (ENTs) or against (CNTs) the ADO concentration gradient (5); and intracellular metabolic enzymes such as adenosine kinase (ADK) (Boison, 2013b) that keep ADOi levels low and control the direction of ADO transport by ENTs (7) (Boison, 2013b). Astrocytes also contribute through their ability to release and respond to ATP and ADO, degrade ATP and remove ADOe. This integrated view of the purinome has influenced epilepsy researchers in the development of novel strategies for manipulating endogenous levels of ADOe to combat seizures (Boison, 2012a; Richerson et al., 2016). Previous work exploring the contribution of purinergic signaling to the HVR$\dot{V}_E$ has been neurocentric and focused primarily on the actions of ADO at P1 receptors. Thus, contrary to the long-held view that the biphasic HVR$\dot{V}_E$ is due to two competing processes, we propose at least three processes, a peripheral carotid body mediated excitation that underlies Phase 1, as well as central excitatory and inhibitory processes that interact to determine the time course and magnitude of the secondary depression; we also propose a key role for glia in this central excitation. Here we first discuss the clinical significance of understanding the HVR$\dot{V}_E$. We then present our working hypothesis of the significance of purinergic signaling in the HVR$\dot{V}_E$ from the broader perspective of the purinome, summarize what is known about the roles played by each component of the purinome in this response and highlight some of the important challenges/questions that remain. Our purpose is not to provide an exhaustive review of all purinergic mechanisms and their influence on information processing in

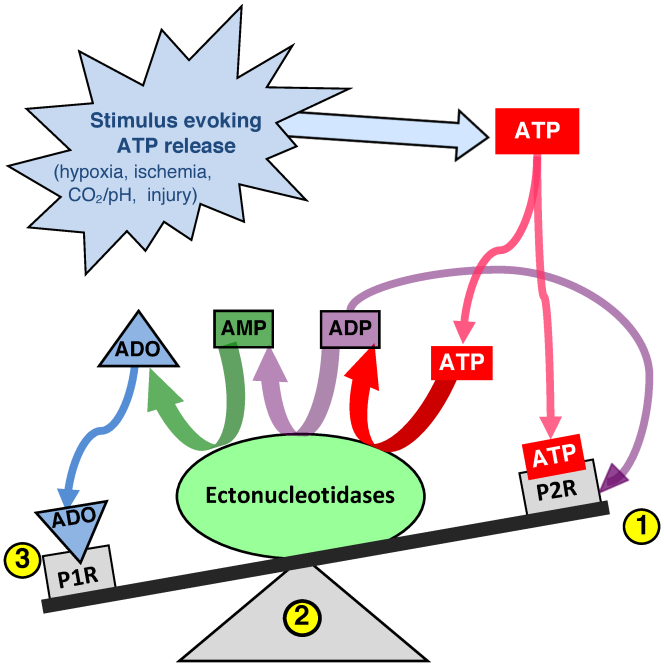

Figure 1.1. The effects of ATP released into the extracellular space is determined by a balance between actions of ATP at P2 receptors and ADO, its main metabolite, at P1 receptors.

Extracellular ATP has two fates, binding to P2 receptors (1) or degradation by diverse ectonucleotidases (2) with differential substrate affinities that degrade ATP and its by-products ultimately to adenosine (ADO). Extracellular ADO has three fates, binding to P1 receptors, transport into the intracellular compartments (astrocytes in adults) or remain where it is. The balance is dynamic and determined by a complex system referred to as the purinome (see Fig. 1.2) (Modified with permission from Funk 2013).

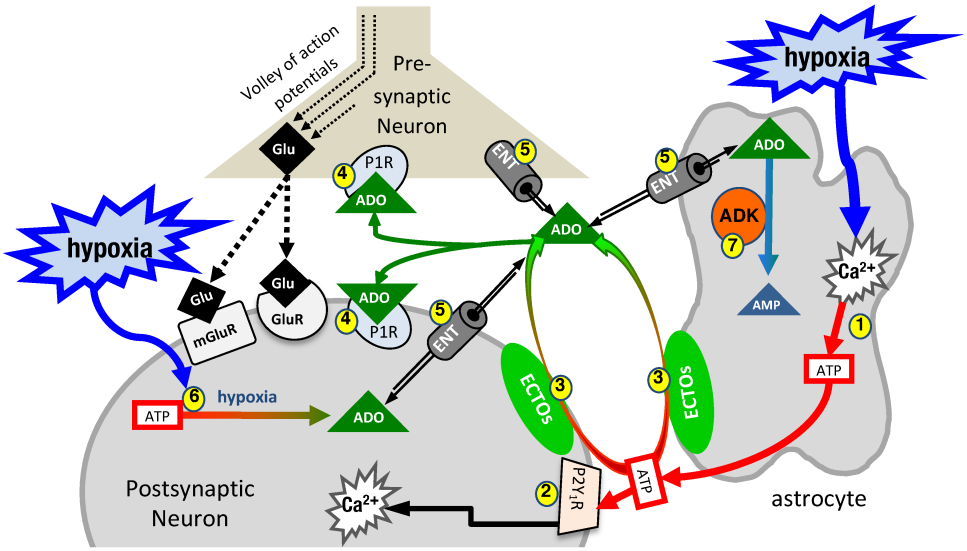

Figure 1.2. Simplified schematic of the purinome at a glutamatergic, inspiratory, preBötC synapse: multiple factors determine the balance between ATP and ADO signaling. During inspiration, a volley of action potentials in the presynaptic neuron evokes glutamate release that depolarizes the postsynaptic inspiratory neuron via activation of glutamate receptors (ionotropic and metabotropic, mGluR). Hypoxia stimulates astrocytes, via a mitochondrial mechanism (not shown) that evokes increased intracellular Ca^{2+} and vesicular ATP release (1). Hypoxia also causes accumulation of intracellular ADO (ADOi) from ATPi hydrolysis (2). 3) ATPe acts via neuronal P2 (including $P2Y_1$) receptors to excite inspiratory neurons and increase ventilation via a process involving increased intracellular Ca^{2+}. Extracellular ADO (ADOe) increases through breakdown of ATPe by ECTOs (4) or ENT transport of accumulating ADOi (5). ADO acts pre- and postsynaptically via A_1 (or A_2 receptors on GABAergic neurons, not shown) to inhibit ventilation (6). The direction of ADO transport via ENTs (5) is dependent on the [ADO] gradient. ADK phospohorylates ADO into AMP (7), keeping ADOi low so that ENTs remove ADOe. The cytoplasmic form of ADK, at least in adult brain, is limited to astrocytes so that removal of ADOe becomes an astrocyte dependent process. (Modified with permission from Funk 2013).

the CNS, but to focus on those most relevant to understanding purinergic signaling in the preBötC and its contribution to the HVR$\dot{V}_E$. We draw from the insights about purinergic signaling that come from other systems, especially the Schaffer collateral-CA1 pyramidal neuron synapse in the hippocampus and consider potential implications of identified mechanisms in the context of what is known in respiratory control. For those interested in the control of breathing, the goal is familiarity with the complexities of purinergic systems and potential implications for respiratory control in health and disease. For those with expertise in purinergic signaling, the goal is an appreciation of the unique opportunities for advancing understanding of purinergic signaling that might come with analysis of the central neuro-glial networks that control breathing (the contribution of purinergic signaling to hypoxia sensing in the carotid body is reviewed elsewhere) (Conde et al., 2017; Lahiri et al., 2007; Leonard et al., 2018; Nurse et al., 2018).

1.2.2 Clinical significance of the Hypoxic Ventilatory Response

Hypoxia and the secondary hypoxic respiratory depression are most severe and life threatening in infants born prematurely. This reflects that the brain circuits responsible for the generation and control of ventilation are immature and produce a breathing pattern that is interrupted by frequent apneas (periods where breathing stops; apnea of prematurity). Thus, a potentially fatal positive feedback loop can develop in which an apnea causes hypoxia, hypoxia evokes the HVR$\dot{V}_E$ that features a strong secondary respiratory depression that can exacerbate the hypoxia…and so on. Apnea of prematurity affects ~1% of all births in Canada; ~3000 babies/year (Statistics Canada, 2022). Risk decreases dramatically with gestational age; ~15% of infants are affected at 32–33 weeks gestational age but nearly 100% at < 29 weeks (Paolillo and Picone, 2013). The mechanisms underlying the hypoxic respiratory depression and the greater depression in prematurity are not fully understood. The literature is confusing because the hypoxic respiratory depression varies greatly between species, changes developmentally, and likely involves multiple mechanisms. Hypoxia also affects metabolic rate, which is homeostatically linked to ventilation, therefore this is an important consideration when examining the hypoxic respiratory depression (Section 1.3). It also depends on whether the experimental apparatus used to deliver the hypoxic gas can deliver a rapid, step change in oxygen. The hypoxia-evoked, Phase 1 increase in ventilation peaks within the first minute. If the transition from normoxia to hypoxia produced by the gas delivery system is too slow, the hypoxic stimulus will peak after secondary depressive mechanisms have been

activated. The result is that the magnitude of both the Phase 1 increase in ventilation and the secondary depression will be underestimated. Nevertheless, it is clear that while the secondary depression is not entirely due to ADOe, ADOe plays a significant role (Burnstock and Dale, 2015; Funk, 2013; Martin and Abu-Shaweesh, 2005; Paolillo and Picone, 2013). Blockade of the respiratory depression by ADO receptor antagonists in a host of species suggests a causative role for ADOe (Burnstock and Dale, 2015; Funk, 2013; Martin and Abu-Shaweesh, 2005; Paolillo and Picone, 2013). Virtually all infants born prematurely who have apnea are treated with methylxanthines, purine based respiratory stimulants that antagonize the inhibitory actions of ADO (Schmidt et al., 2012, 2007). At higher doses that may be relevant clinically, methylxanthines may also inhibit phosphodiesterase activity (preventing cAMP breakdown) and voltage-gated calcium channels (Comer et al., 2001); i.e., the actions of caffeine may not all be mediated by P1 receptors.

Caffeine is the preferred methylxanthine for treatment of apnea of prematurity, due to its better safety profile, and efficacy (Shrestha and Jawa, 2017). However, there is still a need for alternate treatment strategies. First, ~20% of apnea of prematurity patients do not respond to caffeine (Schmidt et al., 2012, 2007). On average such infants will spend an extra week on ventilator support and face greater rates of lung pathology, cognitive delay and cerebral palsy (Schmidt et al., 2012, 2007). Second, while generally a very safe drug, acute side effects include tachycardia, hypertension and tremors. In addition, while high concentrations (which are more effective at reducing apneas) in preterm infants increase the incidence of cerebellar hemorrhage two years later, are associated with significant changes in motor performance (McPherson et al., 2015) and status epilepticus (Boison, 2011; Shrestha and Jawa, 2017). There is also the potential for long-term effects on sleep (Montandon et al., 2009). Hypoxia and hypoxic respiratory depression are also implicated in SUDEP, the sudden, unexplained death of persons with epilepsy (Boison, 2013b; Richerson et al., 2016; Vilella et al., 2018). SUDEP is a catastrophic event for which all persons with epilepsy are at risk; most deaths occur in middle age, but it can happen at any age. The risk for SUDEP is not trivial. A cohort of children with epilepsy was observed for 40 years; SUDEP occurred in 9% of all patients and accounted for 38% of all deaths (Boison, 2012b; Matti and Shlomo, 2010). Respiratory arrest appears to be the major cause for SUDEP (Devinsky, 2011); a leading hypothesis, the ADO hypothesis of SUDEP, proposes that hypoxia and accumulation of

ADOe during a seizure causes a fatal depression of the brainstem respiratory networks (Shen et al., 2010). No preventative strategies exist for SUDEP.

Intermittent hypoxia is also common in various forms of sleep disordered breathing in which a combination of a collapsible airway, high arousability, and high loop gain in chemosensory control systems give rise to cyclic apneas (Dempsey et al., 2012) and a dramatic increase in the risk of cardiovascular disease (Leung and Bradley, 2001; Punjabi, 2008; Young et al., 1993; Young and Peppard, 2000). While the HVR$\dot{V}_E$ and hypoxic respiratory depression are not directly implicated in the cyclic apneas of obstructive sleep apnea, understanding all chemosensory systems, including the novel central hypoxia sensing mechanism under discussion here, is essential to resolve how central and peripheral chemosensory systems interact to cause high loop gain and cyclic apneas that are common in sleep disordered breathing (Dempsey et al., 2012, 2010; Dempsey and Smith, 2019).

Efforts to understand purinergic signaling in the HVR$\dot{V}_E$ have largely focused on the inhibitory actions of ADO at P1 receptors, primarily because ADO is so strongly implicated in the profound hypoxic depression in apnea of prematurity (Burnstock and Dale, 2015; Funk, 2013; Martin and Abu-Shaweesh, 2005; Paolillo and Picone, 2013). Given the emerging picture that the balance between ATP and ADO signaling in the preBötC is important in determining the degree of respiratory depression during the HVR$\dot{V}_E$, this focus on ADO receptors needs to expand to other components of the purinome. Understanding how the various components of the purinome affect the balance between ATP and ADO signaling is key to manipulating purinergic signaling to modulate breathing. Indeed, the therapeutic potential of the purinome lies in the diversity of its ATP and ADO receptors, transporters, and enzymes. This is fertile ground that has led to clinical drug trials for cardiac arrhythmias, pain, thrombosis, Parkinson's disease, psoriasis, dry eye, cystic fibrosis, glaucoma and cancer (Boison, 2013b; Burnstock, 2006; Gendron et al., 2002; Jacobson et al., 2012; Koles et al., 2005).

1.2.3 Working model of purinergic signaling in the preBötC inspiratory synapse during hypoxia

We first provide a brief summary of our working model of how the various components of the purinome in the preBötC might shape the HVR$\dot{V}_E$; note that not all of the indicated pathways have been demonstrated. This summary is followed by a detailed discussion of the data supporting involvement of purinergic signaling in each step of the proposed model that focuses on the types of preparations from which data were derived (culture, in vitro, or in vivo anesthetized/paralyzed/freely moving). When relevant data are not available from analysis of the respiratory network, we draw on insights made from analysis of glutamatergic synapses in other brain regions, in particular the hippocampus, where the modulation of glutamatergic signaling by purines (and all components of the purinome) is more completely understood.

At the core of the model (Fig. 1.2) are three preBötC cells including an astrocyte, a presynaptic inspiratory glutamatergic neuron, and a postsynaptic, inspiratory glutamatergic neuron. During inspiration a volley of action potentials arrives at the presynaptic terminal, triggers the release of glutamate that acts at ionotropic (primarily AMPA) and metabotropic glutamate receptors and evokes an inspiratory burst. Modulation of rhythm by ATP and ADO during hypoxia is hypothesized to occur through modulation of excitability at multiple synapses like this one between key inspiratory, preBötC neurons that generate rhythm based on their excitatory connections with each other (Del Negro et al., 2018). During hypoxia, astrocytes in the preBötC respond with an increase in intracellular Ca^{2+} and vesicular release of ATP (1). ATPe has two fates. It binds to P2, primarily $P2Y_1$, receptors on inspiratory neurons causing excitation and increased inspiratory frequency, at least in part via activation of G_q proteins and increasing intracellular Ca^{2+} (Rajani et al., 2017) (2). ATPe, once released into the extracellular space, also immediately begins to undergo degradation by ectonucleotidases (3), producing extracellular ADPe (which is excitatory at $P2Y_1$ receptors), AMPe and finally ADOe, which binds to pre- and postsynaptic A_1 receptors that inhibit inspiratory rhythm (4). This sets up the very dynamic interaction between the excitatory actions of ATPe (and ADPe) at P2 receptors (2) and inhibitory actions of ADOe at A_1 receptors (4). The dynamics will be determined by the elements of the purinome that likely vary between brain regions, with development and also between the same brain region in different species (see discussion below comparing rat vs mice (Zwicker et al.,

2011)). Excitation will be determined by the amount of ATP released, local P2 receptor expression patterns and levels, their downstream signaling cascades, as well as the expression level and local complement of ectonucleotidases that determine the rate of ATP removal. In addition, because different ectonucleotidases have different substrate affinities and reaction products with some preferentially producing ADP (which is excitatory via $P2Y_1$ receptors) while others preferentially produce ADO, the mixture of agonists that develops following ATP release depends on the local complement of ectonucleotidases. Inhibition will be determined by local P1 receptor expression patterns and levels, their downstream signaling cascades and the local concentration of ADOe. ADOe accumulates from ectonucleotidase-mediated degradation of adenine nucleotides but it can also come from ENT-mediated transport of ADOi (5) if the concentration of ADO accumulating inside cells from ATP hydrolysis (6) during hypoxia exceeds ADOe. Importantly, the availability of ADOe and hence the level of neuronal ADO receptor activation is largely under the control of ADK (7), expressed in astrocytes (at least in adults). Intracellular phosphorylation of ADO into AMP in astrocytes keeps ADOi levels sufficiently low to drive the influx of ADOe into astrocytes via ENT facilitated transport. Thereby, astrocytes assume a role as a metabolic sink for ADOe and for the termination of ADO receptor activation. The main points of Fig. 1.2 are first that the balance between P2 and P1 receptor signaling is very dynamic and determined by multiple factors, many of which remain to be examined for their impact on the $HVR\dot{V}_E$. Second, in contrast to the long-held view that the biphasic $HVR\dot{V}_E$ results from just two interacting processes (an initial peripheral, carotid body-mediated (Phase 1) excitation and a slower, centrally-mediated hypoxic respiratory depression (Mortola, 1996; Moss, 2000), we propose that following the Phase 1 increase, central purinergic mechanisms, excitatory and inhibitory, interact in the preBötC and perhaps elsewhere to shape the remainder of the $HVR\dot{V}_E$.

While the initial increase indeed appears to be mediated by peripheral chemoreceptors, whether a central excitatory component helps shape the $HVR\dot{V}_E$ during phase 2 remains controversial and readers are referred to a recent Cross-Talk debate in the Journal of Physiology for a detailed discussion (Funk and Gourine, 2018a, 2018b; Teppema, 2018a, 2018b). Several points of consensus came from that Cross-Talk. First, there was general agreement that gradual recovery, or lack of recovery, of an excitatory component to the $HVR\dot{V}_E$ following carotid body denervation is unlikely to be informative as the same data could be interpreted to support or refute either position.

For example, while the frequently observed loss of a hypoxia-evoked increase in ventilation after carotid body denervation is compelling evidence that there is no central contribution to the hypoxia-induced increase in ventilation, there is an alternate interpretation. The lack of response could result from the loss of a tonic, non-chemosensory related carotid body input that is necessary for central hypoxia sensing mechanisms to be expressed. Indeed, unanesthetized dogs and goats with separately perfused, normoxic carotid bodies respond to central hypoxia with a slow onset increase in ventilation that is lost once the normoxic carotid bodies are denervated (Curran et al., 2000; Daristotle et al., 1991). Conversely, gradual recovery of an excitatory ventilatory response to hypoxia in carotid body-denervated animals is often cited as strong evidence of a central contribution, but this recovered response is also dismissed as the result of plasticity. Indeed, carotid body denervation triggers considerable plasticity in peripheral and central neural networks involved in the control of breathing (Teppema and Dahan, 2010). Second, the need for reduced preparations to delineate cellular/ionic/molecular mechanisms of O_2 sensing was acknowledged, but so was the importance of acknowledging the limitations of data derived from such preparations. Finally, there was consensus that the real arbiter of the physiological relevance of central hypoxia sensing mechanisms is what happens in unanesthetized animals with intact carotid bodies when putative central oxygen sensing mechanisms are selectively (and reversibly, if possible) perturbed. Progress toward this goal, via the application of viral approaches to selectively manipulate central purinergic and glial signaling mechanisms in vivo, is summarized below.

1.2.4 Components of the purinome and their role(s) in the hypoxic ventilatory response

Role for ATP and astrocytes

Hypoxia-evoked ATP release of unknown origin was first detected using ATP sensors placed on the ventral medullary surface of anesthetized rats (Angelova et al., 2015; Gourine et al., 2005; Rajani et al., 2017). Hypoxia-induced increases in intracellular Ca^{2+} fluorescence of cortical astrocytes in anesthetized rats suggest that astrocytes are directly sensitive to hypoxia. Direct sensitivity was confirmed by isolating astrocytes in culture where they responded to hypoxia with an increase in mitochondrial reactive oxygen species that activated PLC, causing an increase in intracellular Ca^{2+} that triggered exocytotic release of ATP (not shown in Fig 1.2); ATP release was shown directly using TIRF (total internal reflection fluorescence) imaging to reveal hypoxia-

induced disappearance of ATP-containing vesicles from the intracellular surface of astrocyte membranes (Angelova et al., 2015).

Astrocytic ATP release was also shown indirectly in awake, carotid body-intact animals using viral approaches to block astroglial vesicular release mechanisms (injection of adenoviral vectors that expressed light chain tetanus toxin in astrocytes) or increase ATP degradation (injection of lentiviral vector that increased ectonucleotidase expression on all cells) at the level of the preBötC; both treatments consistently reduced the $HVR_{\dot{V}E}$ (Angelova et al., 2015; Sheikhbahaei et al., 2018). These treatments in anaesthetized carotid body intact or carotid body denervated rats similarly decreased the $HVR_{\dot{V}E}$ (Angelova et al., 2015; Rajani et al., 2017).

These data make a strong case for an ATP-mediated, excitatory contribution to the $HVR_{\dot{V}E}$. A caveat remains regarding the case for an astrocytic contribution. The recent demonstrations that disruption of vesicular release mechanisms in astrocytes using the same viral tools attenuates the hypercapnic ventilatory response and exercise capacity as well as the $HVR_{\dot{V}E}$ (Marina et al., 2018; Sheikhbahaei et al., 2018) have raised the concern that viral injection disrupts baseline astrocyte functions and impairs preBötC excitability. We consider this unlikely because control viruses were without effect on the $HVR_{\dot{V}E}$, the hypercapnic ventilatory response and exercise capacity. Thus, while it will be important to demonstrate that the viral tools used to disrupt astrocytic signaling in vivo do not globally impair preBötC responsiveness, we propose that the attenuation of respiratory responses to elevated ventilatory drive or metabolic demand following block of vesicular release mechanisms in preBötC astrocytes supports that astrocytes act as brain metabolic sensors (Marina et al., 2018).

P2 Receptors

ATP acts through seven subtypes of ionotropic P2X and eight subtypes of metabotropic P2Y receptors (Abbracchio et al., 2009; Burnstock, 2015; Burnstock and Dale, 2015). Our focus is on $P2Y_1$ receptors because they are exclusively responsible for the marked frequency increase evoked by ATP in the preBötC in medullary slices that generate inspiratory-related rhythm in vitro. However, $P2Y_1$ receptor effects are not always excitatory and vary between brain regions. For example, in the hippocampus, $P2Y_1$ receptor activation reduces glutamate release (Rodrigues et

al., 2005), but also excites inhibitory interneurons (Kawamura et al., 2004). Lamina IX spinal cord neurons are also directly excited by $P2Y_1$ receptor activation (Aoyama et al., 2010). In the preBötC, MRS 2179 and MRS 2279 ($P2Y_1$ receptor antagonists) completely block the network response evoked by exogenous ATP in vitro, while PPADS and Suramin (general P2 antagonists with low affinity for $P2Y_1$ receptors) and TNP-ATP ($P2X_{1,3}$ antagonist) are without effect (Huxtable et al., 2010, 2009; Lorier et al., 2007). In vivo, bathing the ventral medullary surface of anesthetized rats with PPADS (10 μM) or unilaterally injecting the $P2Y_1$ antagonist MRS 2279 into the preBötC of paralyzed rats reduces the $HVR_{\dot{V}E}$, indicating that $P2Y_1$ receptors, and possibly other P2 receptors, contribute to the central, hypoxia-mediated increase in ventilation (Angelova et al., 2015; Gourine et al., 2005; Rajani et al., 2017). Potentiation of $P2Y_1$ receptor signaling may therefore be one approach through which respiratory activity could be enhanced to counteract respiratory depression. Developmental changes in $P2Y_1$ receptor activation within central respiratory networks have not been characterized past the first days of life. Increases in $P2Y_1$ receptor sensitivity of the preBötC inspiratory network may also contribute to developmental reductions in hypoxic respiratory depression by enhancing the excitatory effects of ATP, therefore the effects of ATP and MRS 2365 on preBötC activity are assessed during the first two weeks of postnatal life in mice, in vitro (Chapter 2).

These data add to a growing body of evidence that the preBötC is unique. Not only is it key for inspiratory rhythm generation (Feldman and Del Negro, 2006), generation of sighs (Li et al., 2016) and coordinating multiple orofacial behaviours (Kleinfeld et al., 2014a, 2014b), it also mounts an excitatory response to hypoxia (Angelova et al., 2015; Gourine and Funk, 2017; Rajani et al., 2017). An important remaining task is to define 2^{nd} messenger cascades, ionic mechanisms and neuronal phenotype(s) that underlie the ATP excitation of the preBötC that occurs during hypoxia. $P2Y_1$ receptors conventionally signal via the G_q cascade (Abbracchio et al., 2006), but the cascade activated in the preBötC has not been identified. Candidate ion channels, i.e., those that affect preBötC rhythm and are also modulated by $P2Y_1$ receptors, include TASK, KCNQ, L-, P-, Q-, and N-type voltage-gated Ca^{2+} channels, BK and SK, and I_{CAN} (Ca^{2+}-activated non-selective cation channels) (Rajani et al., 2016). A key question is whether the subgroup of preBötC neurons that respond to $P2Y_1$ receptor activation and mediate the increase in network frequency are excitatory (i.e., glutamatergic) or inhibitory (GABA- or glycinergic). The model in Fig. 1.2 depicts

glutamatergic neurons as responsible but recent data indicate that preBötC rhythm can be more dramatically increased via the activation of inhibitory preBötC neurons (Baertsch et al., 2018).

Ectonucleotidases

There are seven extracellular ectonucleotidase isoforms in the brain grouped into four families: E-NTPDase-1-3; E-NPP1 and 3; tissue non-specific alkaline phosphatase (TNAP); and ecto-5'-nucleotidase (Abbracchio et al., 2009; Langer et al., 2008). This diversity, combined with isoform diversity in substrate and end-product preferences and differential distribution in the brain underlies significant clinical potential and ongoing efforts to produce selective ectonucleotidase agonists/antagonists (al-Rashida and Iqbal, 2014). There is little doubt that ectonucleotidases help determine the balance between ATP and ADO signaling in the preBötC (Funk et al., 2008; Huxtable et al., 2009; Zwicker et al., 2011). However, that most ectonucleotidases inhibitors lack specificity and have off-target actions that interfere with respiratory network function means that most evidence is indirect. Evidence that ectonucleotidases affect preBötC network responses to ATP derives primarily from analysis of rhythmically-active medullary slices in vitro and includes that: i) hydrolysis-resistant ATP analogs, such as ATPγS (Lorier et al., 2007) and MRS 2365 (Huxtable et al., 2009) evoke greater frequency responses than ATP; ii) frequency responses evoked by injection of ATP into the preBötC of rat and especially mouse slices are enhanced by the A_1 receptor antagonist, DPCPX (Huxtable et al., 2009; Zwicker et al., 2011); iii) diffusion of ATP through the preBötC is enhanced in tissue with reduced ectonucleotidase activity (Huxtable et al., 2009); iv) ATP degradation, measured as the rate of phosphate produced by preBötC tissue punches incubated with ATP, is greatly slowed by the ectonucleotidase inhibitor POM1 (Huxtable et al., 2009); v) ATP applied to the saline solution bathing rhythmically-active slices has very poor access into the tissue; i.e., for an ATP sensor placed just above the slice surface to record the same ATP signal as when the same sensor is placed just 200 μm below the slice surface in the preBötC, the concentration of ATP in the bath must be raised 100-fold, suggesting limited diffusion but more likely significant ATP degradation (Funk et al., 2008).

Indirect evidence that differential ectonucleotidase expression is an important factor in shaping network response dynamics to ATP comes from comparing the responses evoked by injecting ATP into the preBötC of slices from rats and mice and correlating these data with real-time PCR data

quantifying the relative expression patterns of ectonucleotidase transcripts in the preBötC of the two species. When applied to the preBötC of Wistar or Sprague-Dawley rats, a brief injection of ATP (10 sec) evokes a two- to four-fold increase in frequency that peaks in the first 20–30 sec then falls, typically below baseline between 30–60 sec postinjection before returning to baseline. In mice, however, the same ATP injection either has no effect or a much smaller effect on frequency (Fig. 1.3A) (Zwicker et al., 2011). Importantly, the response of the mouse preBötC to ATP is the same as the rat if A_1 ADO receptors are first blocked (Fig. 1.3C). Rat and mouse responses to the selective $P2Y_1$ receptor agonist MRS 2365 are also very similar (Fig. 1. 3B). Thus, both networks share a common P2 receptor-mediated excitation (Zwicker et al., 2011). In mouse, however, it appears that ATP is degraded so quickly to ADO that the ATP excitation and ADO inhibition almost cancel each other out. That the complement of ectonucleotidases might be a factor in this differential ATP sensitivity is supported by the real-time PCR analysis of mRNA extracted from preBötC showing that the protein encoded by the dominant ectonucleotidase transcript in mice, TNAP (tissue non-specific alkaline phosphatase; comprises 80% of total ectonucleotidase mRNA), converts ATPe directly to ADOe. In rats, however, the dominant isoform is ENTPDase 2 (its transcripts comprise 55% of total ectonucleotidase mRNA), which has a much higher affinity for ATP than ADP so will preferentially produce ADP, an agonist at excitatory $P2Y_1$ receptors. What remains is to determine protein expression (rather than mRNA) and enzyme activities in these different species as well as between different brain regions. The development of inhibitors that are selective for the different ectonucleotidase isoforms that are also devoid of off-target actions will open the door to answering key questions about the significance and therapeutic potential of manipulating ectonucleotidase activities. Given the important contribution ectonucleotidases have in determining overall excitatory and inhibitory effects evoked by ATP, postnatal changes in ectonucleotidase activity within the medulla, including in preBötC tissue punches, are assessed in Chapter 2.

Adenosine and Adenosine (P1) receptors

ADO actions are mediated via four subtypes of G-protein coupled, P1 receptors; these are the A_1 and A_{2A} high-affinity subtypes and the A_{2B}, and A_3 low-affinity subtypes (Burnstock et al., 2011; Sebastião and Ribeiro, 2009). While dogma holds that A_1 and A_3 receptors act through Gi/Go to inhibit, while A_{2A} and A_{2B} receptors act through Gs to stimulate, the classical adenylate cyclase –

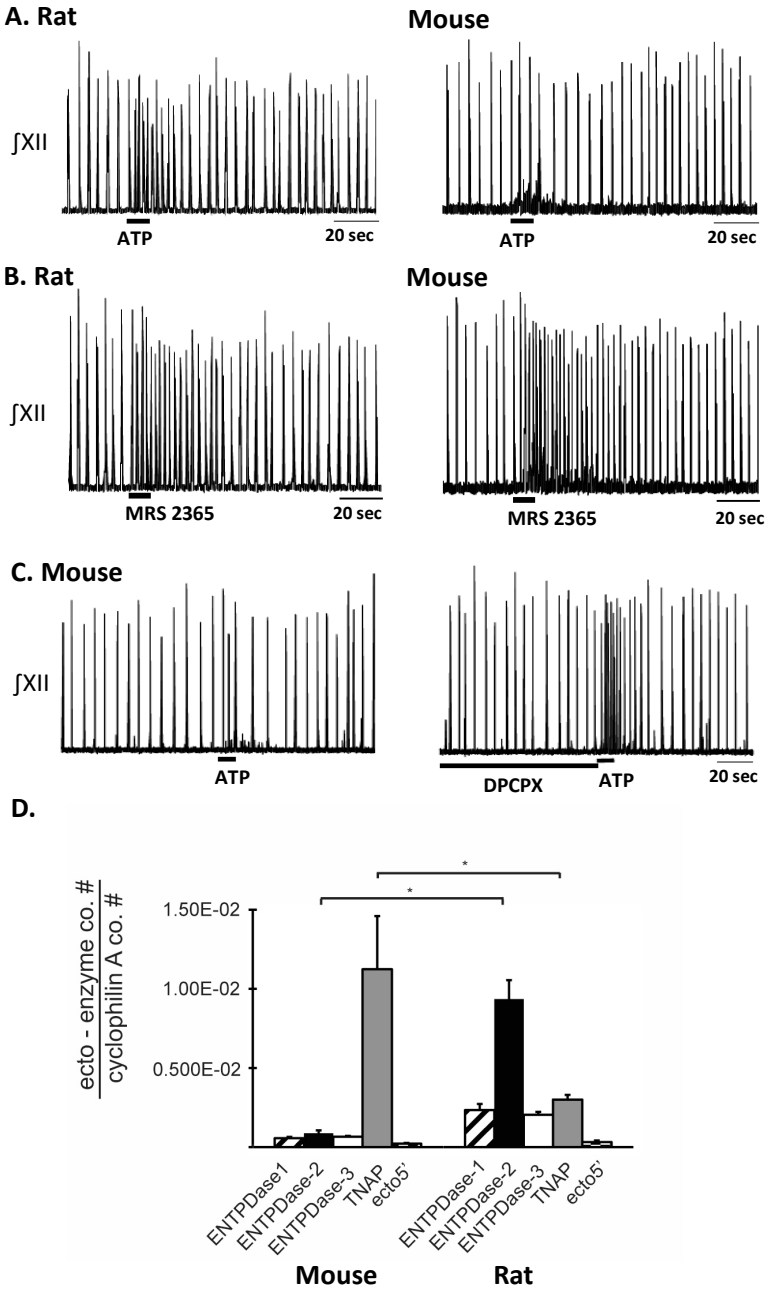

Figure 1.3. Differential balance between the actions of ATP and ADO in rhythmic preBötC-containing slices from neonatal rat and mouse.
Integrated XII nerve recordings (∫XII) from rhythmic slices of rat and mice showing baseline inspiratory-related rhythm in vitro and responses to local injection of ATP (A) or the $P2Y_1$ receptor agonist, MRS 2365 (B) into the preBötC. C) Response of a mouse slice to ATP under control conditions and after preBotC injection of the A1 receptor antagonist DPCPX. D) Real-time PCR analysis showing the percentage contribution of each ectonucleotidase isoform to the total ectonucleotidase mRNA extracted from mouse and rat preBötC punches. Error bars indicate SEM. *Significant difference between the compared columns. Reproduced with permission from Zwicker et al., 2011).

cAMP – protein kinase A signaling pathway (Fredholm et al., 2001; Thauerer et al., 2012), in the brain cAMP does not appear to be the main transducing system operated by A_1 or A_{2A} receptors (Cunha, 2016). P1 receptors may also signal through phospholipase C, Ca^{2+} and mitogen-activated protein kinases (MAPKs) (Abbracchio et al., 1995; Calker et al., 1979; Fredholm et al., 2001; Linden, 1991; Linden et al., 1991; Schulte and Fredholm, 2003; Tomaselli et al., 2008). A_{2A} receptors in the striatum can also couple to G_{olf} rather than Gs (Kull et al., 2000). All receptor subtypes are present in the CNS, but the high-affinity A_1 and A_{2A} subtypes are functionally the most important (Fredholm et al., 2001; Thauerer et al., 2012).

Measurements of ADOe concentrations made using multiple methods, all with limitations, underlie estimates of basal ADOe levels between 30–250 nM (Latini and Pedata, 2001). During hypoxia, local or global ischemia, or traumatic brain injury the concentration of ADOe is estimated to increase up to 100-fold into the μM range (3–30 μM) (Dunwiddie and Masino, 2001; Pedata et al., 2001; Wei et al., 2011). When considered in relation to the binding affinity of the different subtypes for ADO (calculated from in vitro binding studies; 3–30 nM for A_1, 1–20 nM for A_{2A}, 5 ± 20 μM for A_{2B} and > 1 μM for A_3 (Fredholm et al., 1994)), ADOe concentration data suggest that basal levels of ADOe are sufficient to tonically activate A_1 and A_{2A} receptors. However, basal ADOe transmission appears to primarily involve A_1 receptors (Lopes et al., 2019). Lower affinity A_{2B} and A_3 receptors may be activated during hypoxia/ischemia/brain injury when ADOe concentrations increase pathologically (Latini and Pedata, 2001; Pedata et al., 2001).

A_1 receptors are distributed throughout the body with the highest levels of expression in the brain, especially the cortex, hippocampus, cerebellum and dorsal horn of the spinal cord (Dixon et al., 1996; Fredholm et al., 2000; Mahan et al., 1991; Wei et al., 2011), A_1 receptor expression is also high in brainstem regions essential for respiratory control (Reppert et al., 1991). As reviewed by Gomes (2011), neuronal A_1 receptors are located pre-, post- and extrasynaptically. A_1 receptors are highly expressed in presynaptic terminals, especially at excitatory synapses (glutamatergic, cholinergic, serotonergic) (Gomes et al., 2011; Thauerer et al., 2012), where their activation generally inhibits neurotransmitter release (Gomes et al., 2011; Wu and Saggau, 1994; Yawo and Chuhma, 1993) and reduces evoked PSPs and the frequency of mEPSPs. The main mechanisms underlying this inhibition include inhibition of voltage-gated Ca^{2+} channels and reduced sensitivity

of the vesicular release apparatus to Ca^{2+} (Ambrósio et al., 1997; Scanziani et al., 1992; Scholz and Miller, 1992; Silinsky, 1984). Postsynaptic A_1 receptors are primarily located in the postsynaptic density (Rebola et al., 2003) and their activation reduces the responses of hippocampal neurons to excitatory inputs via the inhibition of N-type Ca^{2+} channels, and NMDA receptor-mediated (but not AMPA receptor-mediated) synaptic inputs (Mendonça et al., 1995).

At the level of the brainstem respiratory network, particularly the preBötC, A_1 receptor actions appear dominant (Funk, 2013). A_1 receptor antagonists increase basal frequency in vitro and in vivo and block the inhibitory actions of ADO in respiratory rhythm (Huxtable et al., 2009; Kawai et al., 1995; Kobayashi et al., 2001; Koos et al., 2001, 2004; Schmidt et al., 1995; Wang et al., 2005; Zwicker et al., 2011). In contrast, A_{2A} and A_{2B} receptor agonists have no effect on basal activity of mouse rhythmic medullary slices (Mironov et al., 1999), or brainstem spinal cord preparation (Brockhaus and Ballanyi, 2000), nor the ADO-mediated inhibition of mouse slices (Mironov et al., 1999). As is well-documented in hippocampus and striatum, A_1 receptor activation appears to modulate respiratory neuron and network excitability via pre- and postsynaptic mechanisms, but effects differ between subtypes of respiratory neuron, species and with development. Presynaptic A_1 receptor-mediated inhibition of synaptic transmission has only been directly shown with miniPSC analysis in phrenic motoneurons in neonatal rats (Dong and Feldman, 1995). However, presynaptic A_1 receptor mediated inhibition of inspiratory, excitatory and inhibitory inputs to rat XII motoneurons in vitro (Bellingham and Berger, 1994), mouse inspiratory neurons in vitro (Herlenius et al., 1997; Herlenius and Lagercrantz, 1999; Mironov et al., 1999) and cat stage 2 expiratory neurons in vivo (Schmidt et al., 1995) is inferred from A_1 agonist-mediated reductions in respiratory (excitatory and inhibitory), evoked or spontaneous synaptic inputs (Brockhaus and Ballanyi, 2000). A_1 receptor-mediated presynaptic inhibition may also be input or neuron specific because the inspiratory synaptic inputs to some inspiratory neurons in the brainstem spinal cord preparation are not unaffected by ADO while excitatory PSPs arriving during expiration are inhibited (Brockhaus and Ballanyi, 2000). Detailed analysis of the effects of ADO and A_1 receptor agonists on the frequency and amplitude of miniPSCs in the different subtypes of respiratory neurons is essential to establish which synapses are under presynaptic A_1 receptor-mediated control.

Postsynaptically, A_1 receptor activation hyperpolarizes stage 2 expiratory neurons in adult cat in vivo via activation of postsynaptic conductance (likely a K^+ conductance) that decreases input resistance (Schmidt et al., 1995). Similarly, in brainstem spinal cord preparation A_1 receptors hyperpolarize expiratory neurons and reduce input resistance (effects that persist in TTX), suggesting activation of a postsynaptic K^+ conductance (Herlenius and Lagercrantz, 1999). The membrane potential and input resistance of biphasic expiratory (Herlenius and Lagercrantz, 1999) and inspiratory neurons was unaffected by ADO in the absence (Brockhaus and Ballanyi, 2000) (or presence) of TTX (Herlenius and Lagercrantz, 1999). In inspiratory preBötC neurons of rhythmic mouse slices, A_1 receptors inhibit intracellular cAMP production, which results in K_{ATP} activation and membrane hyperpolarization (Mironov et al., 1999). Similarly, A_1 receptor-mediated hyperpolarization of inspiratory neurons in preBötC island preparations from mice is associated with significant reductions in neuronal input resistance (Vandam et al., 2008). Developmental and species differences must also be taken into account. For example, the A_1 receptor mediated inhibition of inspiratory rhythm in the rhythmic slice or brainstem spinal-cord preparation of rat is gone by postnatal day 2–3 (Herlenius et al., 2002, 1997; Huxtable et al., 2009). The preBötC network of neonatal mice (Swiss CD) is very sensitive to the inhibitory actions of ADO via A_1 receptors, whether the ADO is applied directly or subsequent to the application of ATP and its degradation to ADO (Zwicker et al., 2011). Whether this sensitivity diminishes with postnatal development, therefore reducing the overall inhibitory effects of the purinome within the preBötC as seen in the rat, or remains constant will be explored in Chapter 2.

Postsynaptic A_1 receptors are also located at extrasynaptic sites (Tetzlaff et al., 1987). Their activation in hippocampal neurons enhances background K^+ currents and causes neuronal hyperpolarization (Greene and Haas, 1991). Basal ADOe tone in the CSF should be sufficient to activate these extrasynaptic receptors and contribute to a tonic, ADO-mediated inhibitory drive. The observation that global inhibition of ADO or A_1Rs enhances respiratory rhythm in anesthetized adult cats (Schmidt et al., 1995), unanesthetized fetal sheep (Koos et al., 2001), lambs (Koos et al., 2004), rats in vivo, neonatal rats in vitro (Kawai et al., 1995; Wang et al., 2005), as well as fetal breathing movements in embryonic rats in vivo (Kobayashi et al., 2001) and fictive breathing in vitro (Huxtable et al., 2009), suggests that the respiratory network is also under tonic A_1 receptor inhibitory control. However, whether this tone reflects activation of synaptic or

extrasynaptic receptors is not known. Whether A_1 receptors on astrocytes and microglia (Calker and Biber, 2005; Haselkorn et al., 2010) influence respiratory network function also remains to be determined.

A2A receptors are expressed widely but more variably throughout the CNS compared to A_1 receptors. Expression levels are greatest in the olfactory tubercle and on medium spiny neurons of the striatum (Rosin et al., 1998; Svenningsson et al., 1997b, 1997a). The majority of A_{2A} receptors are located in synapses. In the striatum this includes significant pre-synaptic A_{2A} receptor expression, but the majority of A_{2A} receptors are postsynaptic (Rebola et al., 2005). While A_{2A} expression levels in most other brain regions (including the cortex and hippocampus that show the highest levels of A_1R expression (Dixon et al., 1996; Svenningsson et al., 1997a) are substantially lower than in the striatum, levels are still sufficient to modulate neuronal excitability. For example, activation of presynaptic A_{2A} receptors facilitates glutamatergic transmission in hippocampal CA1 neurons by blocking the inhibitory actions of presynaptic A_1 receptors on glutamate release (Lopes et al., 2002, 1999). Postsynaptic A_{2A} receptor mechanisms include potentiation of synaptic, but not extrasynaptic, NMDA receptor responses in hippocampal CA1 neurons (Mouro et al., 2018) and inhibition of the slow AHP in pyramidal neurons of the basolateral amygdala (Rau et al., 2015). As reviewed by Cunha (2016) and Wei et al. (2011), the blockade of A_{2A} receptor-mediated effects appears to have little impact on synaptic transmission under baseline conditions but pharmacological or genetic block of A_{2A} signaling attenuates synaptic plasticity/LTP at specific excitatory synapses. Neuronal and glial expression of A_{2A} receptors can also change dramatically in response to specific conditions/stimuli such as epilepsy, suggesting an important role in brain plasticity (Cunha, 2005).

Within the brainstem and preBötC, A_1 receptor mechanisms appear to dominate but at higher levels of the CNS, possibly at the thalamus (Koos et al., 2000, 1998), A_{2A} receptors also modulate breathing and contribute to the hypoxic respiratory depression. Injection of A_{2A} receptor antagonists into the cisterna magna of sheep pigs and rats reduces the hypoxic respiratory depression (Koos et al., 2004; Mayer et al., 2006; Wilson et al., 2004). Importantly, in pigs and rats the actions of the A_{2A} antagonist on the hypoxic respiratory depression are reversed by the GABA receptor antagonist, bicuculline (Mayer et al., 2006; Wilson et al., 2004), suggesting that

the A_{2A} receptor-mediated inhibition is indirect via excitation of GABAergic neurons. The site of GABAergic neurons that receive the A_{2A} mediated excitation is not known but it is likely rostral to the medulla and pons since A_2 receptor antagonists have no effect on the actions of ADO in the rhythmic medullary slice (Mironov et al., 1999) or brainstem spinal cord preparation (Brockhaus and Ballanyi, 2000). Lack of an A_{2A} receptor effect under these conditions does not mean A_{2A} receptors have no role in modulation of respiratory networks. Just as A_{2A} receptors appear important in plasticity in cortical circuits (Cunha, 2016; Gomes et al., 2011), activation of A_{2A} receptors on phrenic motoneurons that drive the main inspiratory pump muscle of mammals can induce phrenic motor facilitation (Golder et al., 2008), a form of inducible plasticity in which inspiratory inputs to the phrenic motoneurons are potentiated. The critical role of the brainstem respiratory network in homeostasis has fueled the long-held view of the respiratory network as a hard-wired, immutable structure. This construct is gradually being replaced with the view that plasticity is likely key to the network's ability to adapt throughout life to diverse demands that are constantly changing on multiple time scales (e.g., during development, disease, aging, transitions to altitude, exercise, phonation, speech). A role for A_{2A} receptors in plasticity at the motor output level of this network is clear (Fuller and Mitchell, 2017a, 2017b; Golder et al., 2008; Johnson and Mitchell, 2013). Exploration of mechanisms that might underlie frequency plasticity within respiratory rhythm generating networks is in its infancy (Johnson et al., 2019).

The actions of high-affinity A_{2B} and A_3 receptors on respiratory networks are not known, but both have been implicated in modulating synaptic plasticity through actions on A_1 receptor signaling. A_{2B} receptors are located at glutamatergic terminals of the Schaffer collateral-CA1 pyramidal neuron synapse where they counteract the predominant A_1 receptor-mediated inhibition of synaptic transmission (Gonçalves et al., 2015). Similarly, an A_3 receptor antagonist was reported to reduce the A1 receptor-mediated inhibition of excitatory inputs at these same synapses (Dunwiddie et al., 1997a; Lopes et al., 2003).

In summary, multiple lines of evidence indicate that ADOe plays an important role in modulating respiratory network activity and in shaping the HVR$\dot{V}_E$ [see (Ballanyi, 2004) for review of other modulators that may contribute]. ADOe applied exogenously or derived from the hydrolysis of extracellular ATP or from accumulated intracellular ADO that is transported to the extracellular

compartment via equilibrative nucleoside transporters depresses ventilation in virtually all mammals tested, at fetal (Bissonnette et al., 1991, 1990; Koos and Matsuda, 1990), newborn (Hedner et al., 1985, 1984; Herlenius et al., 1997; Lagercrantz et al., 1984; Runold et al., 1989, 1986), and adult stages (Eldridge et al., 1984; Wessberg et al., 1984; Yamamoto et al., 1994). In addition, despite significant species differences in the sensitivity of the secondary hypoxic respiratory depression to ADO antagonists [reviewed in (Ballanyi, 2004)], ADO receptor antagonists consistently attenuate the secondary hypoxic respiratory depression (Bissonnette et al., 1991, 1990; Koos and Matsuda, 1990; Koos et al., 2004; Koos and Maeda, 2001; Runold et al., 1989; Yan et al., 1995) and counteract respiratory depression in apnea of prematurity (Bhatt-Mehta and Schumacher, 2003). Despite this abundance of data (Burnstock and Dale, 2015; Funk, 2013; Koos et al., 2001, 2004; Martin and Abu-Shaweesh, 2005; Wilson et al., 2004), the relative contribution of ADOe and the four subtypes of ADO (P1) receptor to the respiratory depression and their site(s) of action are not clear. Variations in protocol, drugs, and developmental stage as well as species differences confound the animal literature (Funk, 2013; Heitzmann et al., 2016). A_1 receptor signaling appears to dominate in the preBötC (Angelova et al., 2015; Huxtable et al., 2009; Lorier et al., 2008, 2007; Zwicker et al., 2011), where it may be the only P1 receptor mechanism operating, at least in newborn rodents (rats and mice) (Brockhaus and Ballanyi, 2000; Mironov et al., 1999). Even within the confines of the preBötC, the action of A_1 receptor activation varies developmentally and between species (Herlenius et al., 2002, 1997; Herlenius and Lagercrantz, 1999; Huxtable et al., 2009; Zwicker et al., 2011). There is significant need to understand in many species, throughout development, how the effects of ADO on preBötC activity change, as well as the magnitude of the increase in ventilation that can be achieved by inhibiting ADO receptors within the preBötC. Outside the preBötC, the neuroglial substrate responsible for the A_{2A} receptor-mediated component of the hypoxic respiratory depression has yet to be defined and nothing is known in respiratory networks of the potential actions of A_{2B} and A_3 receptors.

Despite the efficacy of ADO receptor antagonists, especially caffeine, as respiratory stimulants that are highly effective in apnea of prematurity, ADO receptors may not be the best target for long-term manipulation of the balance between ATP and ADO signaling. First, as mentioned above, the observation that not all apnea of prematurity patients respond to ADO receptor antagonists highlights the need for alternate, non-ADO receptor focused methods of manipulating

this balance. Second, P1 receptors are expressed throughout the body and brain, and potential for cardiovascular side-effects is high (Stella et al., 1993). Thus, even if more selective, higher affinity A_1 receptor antagonists/agonists become available, it is unlikely that their oral or intravenous delivery would alter breathing without significant side-effects. A_{2A} receptors are less widely expressed than A_1 receptors but manipulation of their activity as a means to counteract hypoxic respiratory depression is not known. Blockade of presynaptic A_{2A} receptor actions (which will inhibit glutamatergic transmission) is generally considered as neuroprotective but activation, rather than inhibition of post- and extrasynaptic A_{2A} receptors may be beneficial (Gomes et al., 2011). In the context of Huntington's Disease, it remains unclear whether A_{2A} agonism or antagonism is clinically favourable. In contrast, A_{2A} receptor antagonists improve motor performance in animal models of Parkinson's Disease (Gomes et al., 2011), and are under examination for their potential clinical utility as a therapeutic strategy for Parkinson's Disease (Takahashi et al., 2018). In the context of SUDEP, caffeine increases survival time in animal models, hypothetically by reducing the inhibitory actions of ADOe on breathing (Shen et al., 2010). However, caffeine (Chrościńska-Krawczyk et al., 2011), or treatments that reduce ADOe, promote seizure (Fedele et al., 2005).

Sources of extracellular adenosine. A key piece of information lacking for the preBötC (and all parts of the respiratory network) that is critical for the rational development of alternate approaches to manipulate the purinome to enhance P2 and inhibit P1 signaling is the source, or sources, of ADOe. The source of endogenous ADOe during normal synaptic activity, during hypoxia or during any physiological/pathophysiological process is not known. Clearly the source of elevated endogenous ADOe (e.g. via export of ADOi or degradation of ATPe) will dictate the strategies that can be used to modify ADOe. ADOe can derive from multiple sources and release mechanisms that may differ depending on the nature and severity/duration of the stimulus (synaptic activity, hypoxia/ischemia, inflammation, excitotoxicity/traumatic brain injury) brain region and even cell type (Latini and Pedata, 2001). That the cellular source of ADOe can vary with stimulus was elegantly demonstrated when cultured neurons, astrocytes, and microglia (from rat) were deprived of oxygen-glucose (OGD, to model energy failure), exposed to H_2O_2 (to simulate oxidative stress), or given glutamate (to induce excitotoxicity) (Jackson et al., 2017). Cultured neurons were the primarily source of ADOe during OGD or glutamate exposure while microglia were the main

source during oxidative stress. As reviewed by Latini and Pedata (2001) and in agreement with early studies in culture and using hippocampal slices (Brundege and Dunwiddie, 1996; Lloyd et al., 1993; Meghji et al., 1989), a majority of studies indicate that during ischemic or hypoxic conditions the main source of ADOe is formed intracellularly and exported. Importantly, while glia may be a dominant source of ADOe during hypoxia, elevated ADOe during hypoxia could come from endothelial cells, glial cells, and also neurons from anywhere along their cell membrane; i.e., not limited to synapses (Latini and Pedata, 2001). ADO release during hypoxia is only partially sensitive to TTX and Ca^{2+}-independent. This pattern of release differs markedly from normoxic conditions when depolarizing stimuli evoke an ADOe increase that is completely blocked by TTX, Ca^{2+}-sensitive and derived from presynaptic neuronal release of ATP that is subsequently degraded (i.e., ADOe production is sensitive to ecto-5-nucleotidase inhibitors) (Brundege and Dunwiddie, 1996; Latini and Pedata, 2001; Lietsche et al., 2016; Lloyd et al., 1993; Meghji et al., 1989; Parkinson et al., 2005; Wall and Dale, 2008; Zhang et al., 2012). The proposal that ADO can be released via exocytosis from synaptic vesicles (Corti et al., 2013; Klyuch et al., 2012, 2011; Wall and Dale, 2008, 2007) remains controversial, reflecting in part the speed with which ATP can be converted into ADOe and therefore the difficulty of excluding ATP as a source of ADOe (Cunha, 2016). It was shown early on that the actions of ATP at P2 receptors in different brain regions are followed by inhibitory actions that are caused by the rapid degradation of ATP via ectonucleotidases into ADO and activation of P1 receptors (Cunha et al., 1998; Dunwiddie et al., 1997b). The kinetics of this biphasic ATP-ADOe signaling action appear strongly influenced by the properties of ecto-5'-nucleotidase, the main extracellular enzyme that converts AMP into ADO. During periods of intense presynaptic activity and high ATP/ADP levels, it was proposed that ADO production from AMP is delayed until activity ceases and ATP/ADP levels decline, which removes the ATP/ADP inhibition of ecto-5'-nucleotidase (Dunwiddie et al., 1997b; Latini and Pedata, 2001). Such a biphasic response is clearly seen when ATP is applied exogenously into the preBötC of neonatal rats, but not in Swiss CD mice where the excitatory actions of ATP and inhibitory actions of ADOe more or less cancel each other out (Zwicker et al., 2011). This difference may reflect differential expression of ectoATPases in the two species. As mentioned above, the dominant ectonucleotidase transcript in mice is TNAP, which converts ATPe directly to ADOe, while the dominant isoform in rat is ENTPDase 2 that will preferentially produce ADP from ATP (Zwicker et al., 2011). The kinetics of the ATP/ADO interaction that evolves in the

preBötC in response to endogenously released ATP, and the involvement of specific ectoATPases in this relationship is not known. However, there is evidence that enzyme activity may be distributed to achieve spatially specific adenosine receptor activation. In hippocampus, production of ADOe by ecto-5'-nucleotidase has presynaptic inhibitory actions but also contributes to A_{2A} receptor-mediated long-term potentiation of NMDA EPSCs (Rebola et al., 2008). In the striatum, ecto-5'-nucleotidase is localized to astrocytes but also prominently localized to A_{2A} receptor-containing postsynaptic terminals where it mediates hypolocomotion and modulates working memory (Augusto et al., 2013).

Although the majority of studies (primarily in hippocampus) indicate that the main source of ADOe during ischemic or hypoxic conditions is formed intracellularly (Brundege and Dunwiddie, 1996; Lloyd et al., 1993; Meghji et al., 1989), this may not be case for regions involved in respiratory control. During hypoxia in fetal sheep, an important source of ADOe in the thalamic parafascicular locus, where A_{2A} receptors contribute to the secondary hypoxic respiratory depression (Koos et al., 1998), appears to be extracellular; i.e. the hypoxia-induced increase in ADOe is unaffected by ENT inhibitors but reduced by inhibitors of ecto-5'- nucleotidase (Koos et al., 1997). Within the preBötC we also propose an extracellular source of ADOe during hypoxia; i.e. that hypoxia evokes ATP release from astrocytes via exocytosis, which is then degraded to ADOe. Whether ATPe released via exocytosis, and the subsequently produced ADOe, will diffuse to extrasynaptic receptors and have broad, generalized effects over the entire network, or have localized actions on specific preBötC neurons/synapses is not known. However, within the framework of the localized, bidirectional communication that is proposed to occur between pre- and postsynaptic terminals and astrocytes in the tripartite synapse (Araque et al., 1999; Covelo and Araque, 2018), and the observation that preBötC respiratory neurons differ markedly in their sensitivity ATP/$P2Y_1$ and ADO receptor activation (Herlenius and Lagercrantz, 1999; Lorier et al., 2008, 2007; Mironov et al., 1999; Thomas and Spyer, 2000), neuro-glial interactions in the preBötC are likely to be highly specialized, regionally and functionally; i.e., the effects of ATP/ADP/ADO released from astrocytes during hypoxia are likely reflect activation of specific synapses and neurons.

Equilibrative nucleoside transporters

There are four ENT isoforms that move ADO passively, and bidirectionally across cell membranes. The direction of ADO transport is determined by the ADO concentration gradient. ENT1 and 2 carry out the majority of ADO transport across the outer cell membrane (Parkinson et al., 2011). ENT3 is intracellular and irrelevant in determining ADOe while ENT4 appears to function primarily in monoamine transport. Three isoforms of concentrative nucleoside transporters (CNTs) in the CNS are Na^+-coupled and indirectly consume ATP to move ADO against its concentration gradient, but there is no evidence that CNTs regulate ADOe under normal physiological conditions (Chu et al., 2013; Parkinson et al., 2011). Thus, our focus is on ENT1 and ENT2, which are widely expressed throughout the brain in both neurons and astrocytes (Chen et al., 2023; Jennings et al., 2001; Nagai et al., 2005).

Under baseline conditions these transporters play a key role in removing ADOe, as demonstrated by significant increases in ADOe in multiple brain areas following transporter inhibition (Ballarín et al., 1991; Choi et al., 2004; Tanaka et al., 2011). Conversely, ENT-mediated disruption of adenosine tone is associated with a host of neuropsychiatric disorders, including anxiety and depression (Cheffer et al., 2018) and neurodegenerative disorders such as Huntington's Disease (HD) and mouse models of HD where the increased expression and activity of ENT1 and/or ENT2 are associated with reductions in ADOe tone (Kao et al., 2017). Moreover, ENT inhibitors or genetic removal of ENT1 enhances survival in mouse models of Huntington's disease (Kao et al., 2017). ENTs are increasingly recognized as potential targets in drug discovery, in part because ADOe is implicated in a broad range of CNS disorders, including sleep disorders (King et al., 2006), epilepsy (Boison, 2016), and the examples mentioned above.

ENT transport of ADO is bidirectional. Thus, targeted manipulation of ENTs to increase or decrease ADOe requires that the source of the increased ADOe is known (Funk, 2013; Martín et al., 2007; Pascual et al., 2005; Pearson et al., 2003). As discussed above (*Sources of extracellular ADO*) if the main source of ADOe during hypoxia is from the ENT-mediated export of ADOi that accumulates during hypoxia, then ENT inhibition would be required to reduce ADOe in the preBötC. If, however, the main source of ADOe is from degradation of ATPe that is released in response to hypoxia, then the objective would be to potentiate inward ENT-mediated transport and

the clearance of ADOe. Multiple sources and mechanisms can contribute to a hypoxia-induced increase in ADOe. While ENT-mediated export may be a dominant source of ADOe during hypoxia/ischemia in some parts of the brain (Brundege and Dunwiddie, 1996; Latini and Pedata, 2001; Lloyd et al., 1993; Meghji et al., 1989), this may not be the case in the respiratory network. For example, in fetal sheep, a major source of ADOe implicated in the hypoxic respiratory depression (Koos et al., 1998) is from degradation of extracellular adenine nucleotides (Koos et al., 1997), not transport of ADOi.

Our measurements of the HVR (from whole-body plethysmography to record absolute frequency; relative V_T; relative $\dot{V}_E$) evoked by 10% O_2 (10 min) in WT and three strains of adult transgenic mice from which ENT1, ENT2 or ENT1 and 2 were knocked out from conception are consistent with these observations in fetal sheep (Koos et al., 1997). Hypoxia evoked a biphasic ventilatory response in all strains. After the initial increase from baseline to the peak in Phase 1 (reported as 100%), ventilation fell by ~30% in WT and ENT2 KO mice, ~45% in ENT1 KO mice and 100% in ENT1/2 double knockout mice; i.e., ventilation fell back to baseline in the ENT1/2 KO mice (Fig. 1.4). These data, which show a progressive increase in the hypoxic respiratory depression with reductions in ENT activity, suggest that the main source of ADOe causing the hypoxic depression comes from breakdown of ATPe. If ADOe that caused the secondary depression came via ENT-mediated outward transport of ADOi, one would expect the opposite – that ADOe would not increase in the ENT KOs and there would be no depression. Limitations of these data include that measurements of V_T and $\dot{V}_E$ were not absolute, but relative to baseline. In addition, metabolic rate was not recorded. As discussed briefly in Section 1.1 and expanded upon in Section 1.3, ventilation serves homeostatic control of blood and brain pH, PCO_2 and PO_2 and is therefore intimately linked to metabolism. Hypoxia not only evokes biphasic changes in ventilation but also developmentally-dependent reductions in metabolic rate, which means that $\dot{V}_E$ and $\dot{V}_{O_2}$ must both be measured to properly interpret whether ventilatory responses to hypoxia are adequate or compromised. In hypoxia, the adaptive response is hyperventilation, a disproportionate increase in $\dot{V}_E$ relative to metabolic rate such that $\dot{V}_E/\dot{V}_{O_2}$ increases. This corresponds to delivering a greater volume of O_2 deficient gas to the exchange surface per unit if O_2 is consumed by metabolism. In the context of the different ENT KO mouse strains, the greater depression in $\dot{V}_E$ in the ENT1/2 KO suggests a much greater ventilatory depression and an inadequate ventilatory response. This holds

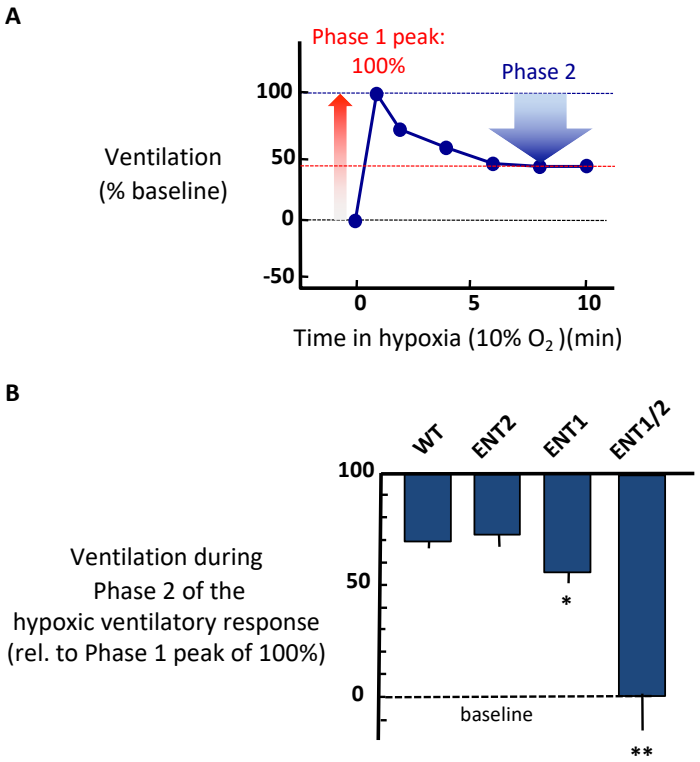

Figure 1.4. Global knockout of ENTs increases the secondary hypoxic respiratory depression.

A) Cartoon showing the biphasic hypoxic ventilatory response, which comprises a Phase 1 increase followed by a secondary depression to a lower, steady-state level of ventilation in Phase 2. The Phase 1 increase was reported as 100%. Ventilation during Phase 2 was calculated as a percentage of the peak increase during Phase 1. In this mock example, ventilation during phase 2 was ~45% of the phase 1 increase; i.e., ventilation fell by ~55% from the peak during the hypoxic respiratory depression. B) The level of ventilation (measured using whole-body plethysmography) during Phase 2 of the hypoxic ventilatory response is reported relative to the Phase 1 peak increase for unanesthetized wild type (WT), ENT2, ENT1 and ENT1/2 double knockout mice. *represents sig. difference from WT, $p<0.05$ or ** $p<0.01$. ANOVA was used in conjunction with Bonferroni post hoc multiple comparison test.

if hypoxia induced changes in $\dot{V}O_2$ are the same in all strains. However, if the reduction in $\dot{V}E$ of each strain is proportionate to the hypoxia-induced reduction on $\dot{V}O_2$ (i.e., ENT1/2 KO mice show a proportionately greater reduction in metabolic rate), then all strains are responding appropriately. Thus, in Chapter 3, I have repeated these in vivo experiments using ENT1/2 KO mouse and plethysmography methods that allow absolute measurements of V_T, $\dot{V}E$ and $\dot{V}O_2$ to more thoroughly explore the role of ENTs in shaping the ventilatory (and metabolic) responses to hypoxia during development.

A final limitation of the ENT data is that ENTs are knocked out globally from birth in these animals, including from the carotid body. Thus, additional work with conditional and/or localized deletion/inhibition of ENT activity is required to fully evaluate in respiratory networks the source of elevated ADOe during hypoxia, and the role of ENTs in the $HVR_{\dot{V}E}$. Such information is required to inform strategies on how to manipulate ENT function to reduce hypoxic respiratory depression. The role of ENTs in regulating ADOe during hypoxia has not been examined specifically in the preBötC. Under baseline conditions in the brainstem spinal cord of neonatal rats, the ENT1 and ENT2 inhibitor, dipyridamole, decreases inspiratory-related burst frequency, indicating that at least under these conditions ENT activity is important for clearing ADOe from brainstem regions that modulate inspiratory rhythm (Herlenius et al., 1997). Whether ENTs specifically within the preBötC of can affect inspiratory rhythm will be examined in Chapter 2 by comparing the effects of ENT inhibition on baseline rhythm in vitro, and whether the effect of injecting ADO into the preBötC differs between P0–12 WT and ENT1/2 KO mice.

Adenosine kinase.

The impact of manipulating ENT activity on ADOe emphasizes the importance of ADOe clearance mechanisms in regulating ADOe under baseline, hypoxic and pathological conditions. ENT activity, however, is only part of the ADOe clearance equation. The direction of ADO transport by ENTs is determined by the ADO concentration gradient across the extracellular membrane; ADOi must be maintained below ADOe for ENTs to effectively remove ADOe. As demonstrated in rat hippocampal slices (Lloyd and Fredholm, 1995), ADOi and ADOe are influenced by several intracellular enzymes. These include S-adenosyl homocysteine hydrolase, the low affinity, high-capacity metabolic enzyme adenosine deaminase, which that converts ADO into inosine, and the

high affinity, low-capacity enzyme, adenosine kinase (ADK), that phosphorylates ADOi to AMPi. We focused on ADK because it has a higher affinity for ADO than adenosine deaminase, and in hippocampal and cortical networks it is the most important enzyme affecting intracellular levels of ADO and in controlling neuronal excitability and ADO signaling (Boison, 2013b; Pak et al., 1994). It is important to note that in the adult cortex ADK is primarily expressed in astrocytes. Thus, ADOe and its activation of neuronal P1 receptors is under the control of astrocyte-based ADOe clearance mechanisms. Dysregulation of ADK may be causative in some forms of epilepsy. The ADK hypothesis of epilepsy posits that acute insults to the brain lead to an initial and transient downregulation of ADK and an acute elevation of ADOe that is protective in the short term. However, the acute changes trigger maladaptive, long-term changes of the purinome including downregulation of astrocytic A_1 receptors, upregulation of A_{2A} receptors, astrogliosis in conjunction with chronic overexpression of ADK, reduced ADOe and ultimately spontaneous focal seizure activity in astrogliotic regions (Boison, 2008). Pharmacological inhibition of ADK (Kowaluk and Jarvis, 2000), or ADO augmentation therapies developed to inhibit ADK and raise ADOe greatly reduce seizures in animal models of epilepsy (Boison, 2012a), whereas transgenic overexpression of ADK triggers seizures (Fedele et al., 2005). A challenge with therapies based on inhibition of ADK to increase ADOe and reduce seizure activity is that ADOe inhibits breathing. Thus, ADK inhibition has the potential to increase the risk of respiratory depression, and possibly SUDEP. For example, global pharmacological inhibition of ADK prolongs the depression of phrenic nerve activity (PNA) following kainic acid-induced seizures. Restoration of PNA activity with caffeine, a P1R antagonist, supports that the depression of phrenic activity following ADK inhibition is due to elevated ADO levels (Ashraf et al., 2021). Blocking ADK activity had a positive effect by delaying the onset of induced seizures. However, ADO-mediated suppression of breathing following ADK inhibition contributed to sudden death following seizure in two mice, supporting the hypothesis that ADK activity reduces the accumulation of ADOe in respiratory networks, which has been implicated in both SUDEP and apnea of prematurity.

Most exciting in terms of respiratory control is that the expression pattern of ADK, which comes in long nuclear (ADK-L) and short cytoplasmic isoforms (ADK-S), changes dramatically during postnatal development (Boison, 2013b). During fetal and the early postnatal period, the predominant isoform is ADK-L, which is preferentially distributed in neurons, has an epigenetic

role as a regulator of DNA methylation. It also supports DNA synthesis and neuronal proliferation (Gebril et al., 2021). ADK-S is barely detectable at birth. With development ADK-S becomes the dominant isoform that is preferentially distributed in astrocytes. The cytoplasmic form ADK-S converts ADOi into AMP and is responsible for regulating extracellular levels of adenosine and therefore ADO receptor activation (Williams-Karnesky et al., 2013, Boison 2013b). While the role of ADK seems to transition during development from a dominant role as an epigenetic regulator of brain development towards the regulation of ADOe, it is important to note that ADK-L does not disappear with development. It persists into adulthood in several brain regions, especially those where neurogenesis continues into adulthood, including the cerebellum (Gebril et al., 2021), olfactory bulb (Gouder et al., 2004) and hippocampus (Fábera et al., 2022; Gebril et al., 2020; Studer et al., 2006). Nonetheless, in the hippocampus (Fábera et al., 2022; Fedele et al., 2005), cerebral cortex (Studer et al., 2006), and cerebellum (Gebril et al., 2021), a major system responsible for clearing ADOe (ADK-S) is immature at birth. If the maturation of ADK follows a similar developmental profile in the brainstem respiratory network, it could contribute to the greater susceptibility of premature animals to hypoxic respiratory depression (Moss and Inman, 1989). Tools developed to study the role of ADK in epilepsy, including transgenic mouse lines (Boison et al., 2002; Fedele et al., 2004; Tronche et al., 1999) and adeno-associated viral vectors that knockdown ADK specifically in neurons or astrocytes (Theofilas et al., 2011), should be very instructive in advancing our understanding of the role played by ADK in respiratory control and the HVR$\dot{V}_E$. In this thesis, I test the hypothesis that developmental changes in ADK-S activity, which increases developmentally to set ADOe tone in other regions of the brain, influences preBötC activity and contributes to maturation of the HVR. In Chapter 2, I characterize the developmental profile of ADK-S vs ADK-L expression in medulla compared to the cortex and cerebellum, then functionally assess its role in determining baseline preBötC activity during development and its impact on shaping responses to exogenous ADO in vitro. Based on these observations, in Chapter 3, I will test the hypothesis that lack of ADK-S at birth contributes to the immature HVR, in vivo.

1.3 Understanding development of the hypoxic ventilatory response must also consider developmental changes in the effects of hypoxia on metabolic rate.

Characterization of the HVR and its development has largely focused on changes in minute ventilation ($\dot{V}E$) during hypoxia, without also characterizing changes in $\dot{V}O_2$ and their contribution to an animal's capacity to overcome hypoxic challenges. The biphasic nature of the $HVR_{\dot{V}E}$ and the consistent observation in multiple species that the increase in $\dot{V}E$ evoked by hypoxia in neonates is transient, returning to or below baseline during the hypoxic exposure, but sustained in adults strongly suggests that this key homeostatic reflex is immature at birth (Bissonnette, 2000; Bonora et al., 1984; Carroll and Bureau, 1987; Cross and Oppe, 1952; Fiore et al., 2013; Moss, 2000). For example, most recently Zannin et al. (2023) showed that reductions in F_IO_2 during sleep decreased $\dot{V}E$ after 4–5 minutes in nearly two-thirds of premature infants studied and produced periodic breathing that increased SpO_2 variability in about one-third of these infants. This supports the notion that premature human infants cannot sustain increases in $\dot{V}E$ as is usually observed in most adult mammals.

However, a major limitation of reporting the HVR only in terms of how $\dot{V}E$ changes over time is that hypoxia also causes reductions in metabolic rate ($\dot{V}O_2$) that are greater in neonates and decrease thereafter. $\dot{V}E$ is inextricably linked to $\dot{V}O_2$ through homeostatic feedback loops, such that a hypoxia-induced change in $\dot{V}O_2$ will have direct effects on $\dot{V}E$ over and above the effects of hypoxia on $\dot{V}E$. Thus, the greater depression of $\dot{V}E$ that occurs during hypoxia in neonates could reflect a greater depression of $\dot{V}O_2$. Defining the HVR in terms of how hypoxia affects the relationship between $\dot{V}E$ and $\dot{V}O_2$ ($\dot{V}E/\dot{V}O_2$, air convection requirement) is therefore considered more informative than reporting $HVR_{\dot{V}E}$. When assessed from this perspective, most mammals increase $\dot{V}E$ and depress $\dot{V}O_2$ to produce a sustained increase in $\dot{V}E/\dot{V}O_2$ (Barros et al., 2001; Cross et al., 1958; Frappell et al., 1992; Gill and Pugh, 1964; Mortola, 2004). i.e., neonates do not appear to have a compromised ventilatory response to hypoxia. The magnitude of this depression in $\dot{V}O_2$ is proportional to the resting metabolic rate, i.e. smaller animals or those studied below their thermoneutral zone with a higher resting $\dot{V}O_2$ have larger decreases in $\dot{V}O_2$ during hypoxia (Barros et al., 2001; Dzal and Milsom, 2021; Frappell et al., 1991; Mortola and Dotta, 1992; Saiki et al., 1994). This is consistent in newborn animals that have a higher resting $\dot{V}O_2$ (Dzal et al., 2020;

Moore and Underwood, 1963; Mortola and Dotta, 1992). Generally, neonates that have smaller $HVR_{\dot{V}E}$ exhibit greater reductions in metabolism during hypoxia compared to adults (Cross et al., 1958; Frappell et al., 1991; Hill, 1959; Mortola, 1999; Mortola et al., 1989). Thus, a majority of data from multiple species indicate that hypoxia evokes a sustained increase in $\dot{V}E/\dot{V}O_2$ at all ages; i.e., neonates do not appear to have a compromised ventilatory response to hypoxia (Dzal et al., 2020; Frappell et al., 1992, 1991; Mortola, 1999; Mortola and Dotta, 1992; Mortola et al., 1989; Waters and Gozal, 2003).

These data, however, have their own limitations. Most significant is that the developmental window examined in these studies did not start at birth, sometimes including animals as old as 2 weeks in the neonatal group (Fahey and Lister, 1989; Frappell et al., 1991; Mortola et al., 1989; Rohlicek et al., 1998). Rodent studies did not include neonates before P2. The few studies in rodents that have measured $\dot{V}E$ and $\dot{V}O_2$ from P0 or premature infants suggest that hypoxia does not depress $\dot{V}O_2$ at these very early stages (Cross et al., 1958; Liu et al., 2009; Liu and Wong-Riley, 2013). For example, premature infants examined a few days after premature delivery show smaller decreases in $\dot{V}O_2$ during hypoxia than when at two-weeks post birth. Premature infants in general do not depress metabolic rate in hypoxia as much as full-term newborns (Cross et al., 1958). Recent data from rats show that P0–1 rats do not respond to hypoxia with a fall in metabolic rate (Liu et al., 2009; Liu and Wong-Riley, 2013). These results challenge the hypothesis that all neonates depress $\dot{V}O_2$ in hypoxia, and that the magnitude of hypoxic hypometabolism decreases monotically with development. Instead, these data suggest that the capacity to depress metabolic rate in response to hypoxia changes biphasically during development (Cross et al., 1958). During early development, including fetal life, hypoxia does not decrease metabolism. Then, at some point during the early postnatal period the capacity to decrease metabolism in response to hypoxia emerges very quickly before gradually decreasing or disappearing in adulthood. In Chapter 4, I will explore this possibly by measuring on a daily basis the $\dot{V}E$ and $\dot{V}O_2$ responses of different rodents from birth until hypoxia depressed $\dot{V}O_2$.

1.4 Specific Aims

In summary, the literature review presented in Section 1.2 describes literature underlying my hypothesis that postnatal changes in the purinome within CNS respiratory networks contribute to

developmental changes in the HVR. Purinergic signaling in other brain regions may contribute to this reflex, but our discussion has focused on the preBötC because it is within this region that we have the strongest evidence that P2 and P1 receptor signaling and ectonucleotidase activity shape the HVR$\dot{V}_E$. Of particular interest, the preBötC inspiratory network is sensitive to the excitatory actions of astrocyte-released ATP during hypoxia and the inhibitory actions of ADO that accumulates in the brain during hypoxia. The modulatory actions of ATP and ADO in the brain, including within the preBötC network, affect breathing during the secondary phase of the HVR$\dot{V}_E$ (Angelova et al., 2015; Funk, 2013; Funk and Gourine, 2018b; Gourine and Funk, 2017; Rajani et al., 2017; Reklow et al., 2019). Less is known about the impact of ATP and ADO in modulating the HVR$\dot{V}_E/\dot{V}_{O_2}$, since $\dot{V}O_2$ was not consistently measured in vivo. Section 1.3 details the importance of measuring $\dot{V}E$ and $\dot{V}O_2$ in studies of the HVR, since the reduction of O_2 consumption in response to hypoxia is another adaptive strategy to counteract hypoxia, particularly in young mammals. It is also the basis of the argument that the HVR$\dot{V}_E/\dot{V}_{O_2}$ is not compromised in the neonatal mammals (Mortola et al., 1989). However, closer scrutiny shows that analysis of rodents did not include animals younger than P2 and other species were not examined immediately after birth (Mortola et al., 1989). In addition, more recent data suggest that both the HVR$\dot{V}_E$ and HVR$\dot{V}_E/\dot{V}_{O_2}$ are immature in newborn rodents younger than P2 (Liu et al., 2009; Liu and Wong-Riley, 2013). Therefore, the overall objective of my research is to explore in vitro how purinergic signaling in the preBötC inspiratory network changes during postnatal development and how these changes contribute to the postnatal development of the ventilatory and metabolic responses to hypoxia. I describe three specific aims designed to help achieve this objective.

Specific Aim 1. To characterize during postnatal development how different components of the purinome affect baseline inspiratory-related preBötC rhythm and its modulation by ATP and ADO and whether these changes underlie a shift in the ATP–ADO balance from inhibitory ADO signaling at birth to excitatory ATP/$P2Y_1$ signaling (Chapter 2).

I will test the following hypotheses:

(i) Excitatory actions of ATP and $P2Y_1$Rs in the preBötC inspiratory network increase postnatally (in vitro, Chapter 2);

(ii) Inhibitory actions of ADO via P1Rs in the preBötC inspiratory network decrease postnatally (in vitro, Chapter 2), and;

(iii) Postnatal changes in the activity of different elements of the purinome, including ECTOs, ENTs, and ADK, contribute to developmental changes in the overall effect of purinergic signaling in the preBötC inspiratory network

Specific Aim 2. To test the hypothesis that postnatal changes in purinergic signaling identified in vitro contribute to the postnatal changes in the HVR in vivo; i.e., the inability to produce a sustained increase in ventilation during hypoxia ($HVR_{\dot{V}E}$ and $HVR_{\dot{V}E/\dot{V}O_2}$) (Chapter 3).

Specific Aim 3. To challenge the concept that although the $\dot{V}E$ response of neonatal mammals to hypoxia ($HVR_{\dot{V}E}$) is immature, showing only a transient increase in $\dot{V}E$ during hypoxia (i.e., a greater hypoxic respiratory depression), the $\dot{V}E/\dot{V}O_2$ response ($HVR_{\dot{V}E/\dot{V}O_2}$) is mature/adult-like comprising a sustained increase throughout hypoxia; i.e., the hypoxic response of newborns is not compromised compared to adults (Chapter 4).

I will test the following hypotheses:

(i) Hypoxia does not evoke a decrease in metabolic rate ($\dot{V}O_2$) at birth;

(ii) The lack of a hypoxia-induced decrease in metabolism is an important factor for the immature $HVR_{\dot{V}E/\dot{V}O_2}$ in rodents, and;

(iii) The time course over which the ability of hypoxia to cause a decrease in $\dot{V}O_2$ emerges and the $HVR_{\dot{V}E/\dot{V}O_2}$ matures varies between rodent species.

Chapter 2. Characterizing postnatal changes of the purinome that modulates preBötzinger Complex inspiratory network activity in mice, in vitro.

2.1 Introduction

The central respiratory network is responsive to chemosensory feedback from the periphery (mainly the carotid body in humans) and the central nervous system that adjust breathing in proportion to metabolic rate, maintaining homeostatic control over arterial blood and CSF gases and pH; e.g., if PaO_2 decreases or $PaCO_2$ increases, a negative feedback loop causes ventilation to increase, thereby restoring homeostasis. Oxygen is very plentiful in the atmosphere so under most conditions in mammals (non-diving; non-burrowing) blood Hb is fully saturated even with falls in PaO_2 in the 5–10 mmHg range. In contrast, ventilation is very sensitive to small changes in $PaCO_2$, which is the primary variable important in determinant $\dot{V}E$ on a moment-to-moment basis (Guyenet et al., 2010). Extremely powerful reflexes, however, have evolved to protect blood and brain oxygen levels when PaO_2 falls to the point where desaturation significantly impairs O_2 delivery. One of the most important is the biphasic HVR, the reflex relevant to the studies in this thesis. In adult mammals, this involves an initial increase in breathing during the first 1–2 minutes of hypoxia, followed by a secondary hypoxic respiratory depression (HRD) where breathing falls during the subsequent 2–3 minutes, reaching a new steady-state. In adults, ventilation during this steady state phase remains above baseline; i.e., mature mammals produce a sustained increase in ventilation throughout hypoxia. The magnitude of the secondary depression varies during development (Bonora et al., 1984; Mortola, 1999; Moss, 2000). Premature and newborn mammals respond to hypoxia with an initial increase in ventilation (often smaller than in adults), but this is followed by a much greater HRD during which ventilation can fall to, or even well below baseline levels, which can cause further reductions on PaO_2 (Bonora et al., 1984; Carroll and Bureau, 1987; Cross and Oppe, 1952). The degree to which ventilation falls varies depending on species and developmental stage (e.g., a P0 rodent is not the same a P0 lamb) (Frappell et al., 1992; Mortola, 1999, 1996; Mortola et al., 1989), but premature/newborn mammals do not mount a sustained increase in ventilation when acutely exposed to hypoxia.

There are clinical implications of this immature HVR. For example, mammals including human infants, born prematurely often produce a breathing rhythm that includes frequent apneas, reflecting immaturity of the central networks that produce and control breathing. Apneas reduce blood PaO_2, evoking the HVR which can depress breathing below baseline levels, exacerbating the hypoxia leading to secondary apneas and the initiation of a life-threatening positive feedback

loop requiring rapid intervention. Caffeine is used clinically to stimulate breathing in premature infants with AOP to reduce the incidence of apneas. However, alternate therapies are required because ~20% of infants with AOP do not respond, or respond negatively, to caffeine, and these infants are more likely to require prolonged ventilator support and face greater rates of lung pathology, cognitive delay and cerebral palsy (Schmidt et al., 2012, 2007).

Mechanistic control of the HVR is not fully known. The initial increase in ventilation is mediated by peripheral chemoreceptors, especially the carotid bodies, in mammals (Martin-Body et al., 1985; Serra et al., 2001). These chemoreceptors sense low arterial oxygen and quickly send signals via the carotid sinus nerve and nucleus tractus solitarius to brainstem regions that control breathing, including the retrotrapezoid nucleus (RTN, chemosensory site) and the preBötC (site of inspiratory rhythm generation) (Angelova et al., 2015; Funk, 2013; Gray et al., 2001; Johnson et al., 2001; Schwarzacher et al., 2011; Smith et al., 1991; Vandam et al., 2008; Wang et al., 2014). This signaling mediates an increase in breathing. If this increase in breathing does not immediately restore arterial oxygen levels, ventilation starts to fall (roll-off) (Rajani et al., 2017; Reklow et al., 2019). This secondary inhibition or depression is largely attributed to central mechanisms that are not completely understood (Bissonnette, 2000; Moss, 2000), but GABAergic mechanisms and especially purinergic signaling via ADOe at adenosine receptors is strongly implicated (Fiore et al., 2013; Herlenius et al., 2002; Koos et al., 1997; Paolillo and Picone, 2013; Reklow et al., 2019). The greater secondary depression in premature/newborn mammals is attributed, in part, to the greater inhibitory actions of ADOe at birth (Reklow et al., 2019).

Until recently, it was thought that the only role of the CNS in the HVR was in the depression of breathing (via increases in extracellular GABA or ADOe) (Funk, 2013). However, this view has been challenged over the last decade by evidence that the secondary phase is also shaped by a slow onset, central, ATP-mediated excitation. Our current working model proposes that during hypoxia, preBötC astrocytes sense low oxygen and release ATP, which excites inspiratory neurons via metabotropic $P2Y_1$ receptors, increases breathing and attenuates the secondary depression (Fig. 1.2) (Angelova et al., 2015; Rajani et al., 2017). At the same time, ADOe increases in the CNS, including respiratory regions of the brainstem (Mayer et al., 2006), during hypoxia through the rapid breakdown of extracellular ATP (including ATP released by astrocytes) by ectonucleotidases

(ECTOs), and the direct release of ADO from sources that are not fully known (Dale and Frenguelli, 2009). ADO antagonists, such as caffeine, attenuate the HRD (Darnall, 1985; Easton and Anthonisen, 1988; Kawai et al., 1995). ADOe acts at metabotropic presynaptic inhibitory A_1 receptors on preBötC neuron synapses and postsynaptic excitatory A_{2A} receptors on brainstem GABAergic inhibitory neurons to inhibit of breathing (Mayer et al., 2006; Rajani et al., 2017; Zwicker et al., 2011). Thus, during hypoxia, breathing is determined in part by a dynamic balance between excitatory actions of ATP and inhibitory actions of ADOe within regions of the central nervous system, including the preBötC.

The balance between the actions of ATP and ADOe in the brain are determined not just by their actions at their respective P2 and P1 receptors, but by a complex signaling system, collectively referred to as the purinome. This includes of course the types and levels of P2 and P1 receptors present in a specific brain region, but also the subtype and amount of ECTOs present and the proteins involved in removing ADOe from its sites of action. ECTOs hydrolyze ATP to ADP, AMP, and finally ADOe, which, as mentioned above, is strongly implicated in the secondary respiratory depression. In other words, ECTOs not only stop the actions of ATP signaling, they initiate the signaling actions of ADO. Additional members of the purinome are involved in the clearance of ADOe. ENTs transport ADO bidirectionally across cell membranes down its concentration gradient (Anderson et al., 1999; Wall and Dale, 2013; Young et al., 2008; Zhang et al., 2011). Intracellular enzymes, including ADK that converts ADOi into AMPi (Nguyen et al., 2015; Otsuguro et al., 2015; Sandau et al., 2016), facilitate ENT-mediated clearance of ADOe by maintaining the concentration of ADO inside cells lower than that outside (i.e. $[ADO]_e > [ADO]_i$). The developmental trajectory of each component of the purinome will influence the developmental trajectory of how purinergic signaling affects the activity of local neuronal networks once it is released. In hypoxia, ATP is released in the preBötC where its excitatory actions attenuate the secondary roll-off, however, ADO also contributes to the secondary depression. Understanding how components of the purinergic signaling system in the preBötC change during development and affect inspiratory activity is an important research question that could identify novel targets for therapeutic to stabilize breathing in a variety of clinical conditions where disruptions in purinergic signaling are implicated, including AOP (Fiore et al., 2013; Funk, 2013; Paolillo and Picone, 2013) and SUDEP (Boison, 2016; Devinsky et al., 2016; Richerson et al., 2016).

The overall goals of this chapter are therefore to advance our understanding of the purinome in the preBötC and determine how during development its different components modulate baseline inspiratory-related activity, as well as the responses of the preBötC to ATP and ADO. I use rhythmically-active medullary slices from mice ranging in age from P0–12 in which agonists/antagonists are applied specifically to the preBötC to directly measure effects within this network. I use purinergic agonists rather than hypoxia since hypoxic stimuli in vitro actually comprise changes from hyperoxia to anoxia at different depths within a rhythmic slice and responses to hypoxic stimuli in vitro have questionable relevance to physiological responses that contribute to homeostatic control of breathing (Funk, 2013; Funk and Greer, 2013). A series of specific aims are addressed in this chapter. Over the first two weeks of postnatal development, I specifically characterized changes in i) $P2Y_1R$-mediated excitation; ii) ADO-mediated inhibition; and iii) the actions of ATP, which involve activation of both $P2Y_1$ and ADO mechanisms if ECTO are active, on preBötC inspiratory frequency in mice. Furthermore, I utilized both pharmacological and transgenic tools to assess how ADOe clearance, mediated by ENT and ADK activity, influences basal preBötC activity and impacts the network's response to adenosinergic signaling during the first two weeks of development.

2.2 Methods

2.2.1 Animals

All animal experiments were reviewed in accordance with the guidelines of the Canadian Council on Animal Care and were approved by the University of Alberta's Health Sciences Animal Care and Use Committee. Four different genotypes of mice were used for this study including two wild-type (WT) strains, FVB/NCrl (FVB, Strain Code 207, Charles River, Wilmington, MA, USA) and C57BL/6J mice (Jackson Laboratories, Bar Harbor, ME, USA), as well as ENT1/2 knockout (KO) under an FVB background and the homozygous ADK transgenic (ADKtg) under the C57BL/6 background. Each mouse strain was separately bred to establish local colonies that were housed with the University of Alberta's Health Sciences Laboratory Animal Services and maintained on a 12-h light/dark schedule with *ad libitum* access to food and water. ENT1/2 KO mice were originally obtained from the laboratories of Dr. James Young and Dr. Carol Cass. Briefly, this genetic knockout was achieved using a viral gene trap insertion between exon 2 and 3 of each gene

(Altaweraqi et al., 2020). ADK transgenic (Adktg) mice were obtained from a different collaborator, Dr. Detlev Boison. Adktg mice were made from Adktm1$^{-/-}$ mice lacking the endogenous *Adk* gene. A 1865bp full length Adk cDNA homologous to human *Adk-S* gene was inserted into the genome via a transgene expression vector, resulting in ubiquitous (over) expression of ADK-S from conception (Fedele et al., 2005; Li et al., 2007).

2.2.2 Rhythmically-active medullary slice preparation

Rhythmically-active medullary slices were prepared from neonates, ranging in age from P0–12, similar to protocols previously described previously (Funk et al., 1994; Ruangkittisakul et al., 2011; Smith et al., 1991). First, the brainstem-spinal cord (BSSC) was isolated in cold (4°C) artificial cerebrospinal fluid (aCSF) containing (in mM): 120 NaCl, 3 KCl, 1.25 NaH_2PO_4, 1 $CaCl_2$, 2 $MgSO_4$, 26 $NaHCO_3$, 20 D-Glucose (all from Fisher Scientific, Hampton, NH, USA) and bubbled with 95% O_2–5% CO_2. For P9–12 mice, tissue was dissected in choline chloride aCSF, which replaced NaCl with choline chloride (120 mM, Sigma-Aldrich, St. Louis, MO, USA) to reduce excitotoxicity and improve the viability of this older tissue. All experiments, however, took place under the standard aCSF conditions described above. The BSSC was pinned to a wax chuck with the ventral surface upward and serial 100–200 μm sections were cut in the rostral to caudal direction using a vibrating microtome (VT1200S; Leica, Nussloch, Germany). Sections were trans-illuminated to identify anatomical landmarks, until the structure of the subnuclei of the inferior olive was identified in the slice. Then, a 550 (P0–8) or 600 μm (P9–12) rhythmic transverse slice containing preBötC was obtained. Rhythmic slices were pinned rostral surface up on Sylgard resin in a 5 mL recording chamber and perfused with 100 mL of recirculating standard aCSF (25 ± 1°C) at a flow rate of 8 mL min^{-1}. The concentration of K^+ in the aCSF was raised from 3 to 9 mM at least 30 min before the start of data collection to produce prolonged stable rhythm. Rhythmic inspiratory-related motor output was recorded through suction electrodes (A-M Systems, Carlsborg, WA, USA) placed on the hypoglossal (XII) nerve rootlets or the sites on the rostral surface overlying the XII motor nucleus or preBötC. Signals were amplified, bandpass filtered (100 Hz to 5 kHz), full-wave rectified, integrated using a leaky integrator (τ = 25 or 50 ms), and displayed using Axoscope 9.2 (Molecular Devices, Sunnyvale, CA, USA). Data were displayed and acquired to computer using a Digidata 1322 A/D board (acquisition rate = 1 kHz)

and AxoScope 9.2 software (Molecular Devices, Sunnyvale, CA, USA) for off-line analysis.

2.2.3 Medullary Tissue Punches

Brainstem tissue punches were obtained from 600 µm preBötC-containing transverse slices that were prepared as described above, except tissue was dissected in phosphate-free aCSF containing (in mM): 124 NaCl, 4.5 KCl, 2.5 $CaCl_2$, 1.3 $MgSO_4$, 20 $NaHCO_3$, and 20 D-Glucose. A rostral 600 µm medullary tissue slices was also taken from each animal. The rostral surface of the rostral slice was 1.2–1.5 mm rostral to rostral border of the preBötC slice. Tissue punches were obtained using 21-G needles that were cut, sharpened and mounted on 4-axis micromanipulator (SD Instruments, San Diego, CA, USA) for precise control. Slices were pinned on sylgard and visualized under a dissecting microscope (Zeiss, Oberkochen, Germany). A total of 4 punches were taken from slices containing the preBötC, 2 from the ventrolateral column including the preBötC bilaterally, as described previously (Huxtable et al., 2009), and two from the XII nucleus (1 punch from each side). Two punches were taken from the ventrolateral medulla of rostral slices. The punches were digitally imaged using a camera (EOS, Canon, Tokyo, Japan) mounted on the dissecting scope equipped with a trinocular head (Zeiss, Oberkochen, Germany). Punches were not perfectly columnar as tissue compression resulted in their having a wider diameter on the rostral compared to the caudal surface. Images were therefore used to calculate the volume of each tissue punch in order to calculate PO_4 production in relation to tissue volume.

2.2.4 Phosphate Assay

ECTO activity in the different brainstem regions was assessed by measuring the rate at which known volumes of tissue converted extracellular ATP into PO_4. Single punches were transferred to individual 2 mL microfuge tubes containing 130 µL phosphate-free HEPES aCSF (in mM: 124 NaCl, 4.5 KCl, 2.5 $CaCl_2$, 1.3 $MgSO_4$, 20 HEPES, and 20 D-Glucose) incubation solution as well as 150 µM ATP. An additional microfuge tube was included that contained incubation solution and ATP but no tissue punch to control for non-tissue-mediated degradation of ATP. To control for ATP-independent PO_4 production, previous control experiments in which the incubation solution ATP showed that tissue punches alone produced undetectable PO_4 levels (Huxtable et al., 2009). Microfuge tubes (6 with tissue punches plus one control with ATP and no slice) were mounted in a Thermomixer (Eppendorf, Hamburg, Germany) maintained at 31°C and 600 rpm.

Microfuge tubes were incubated for 60 mins. Duplicate 50 µL samples were taken from each microfuge tube and transferred to 14 wells of a 96-well plate. A standard curve was simultaneously generated in duplicate on the same microplate using wells containing PO_4 at concentrations of 0, 4, 8, 12, 16, 24, 32, and 40 µM. A colorimetric PO_4 assay (PiBlue Phosphate Assay Kit, BioAssay Systems, Hayward, CA, USA) was used to quantify PO_4. 100 µL of PiBlue reagent was added to each well and incubated for 40 mins at room temperature. Absorbance was measured at 630 nm using a microplate reader (VERSAmax, Molecular Devices, Sunnyvale, CA, USA) and the phosphate concentration produced from the incubated samples was calculated in reference to the standard curve. The phosphate concentration was converted to amount (nmol PO_4) and PO_4 production reported relative to the tissue volume.

2.2.5 ENT1/2 KO Mice Genotyping

DNA was isolated from FVB (WT) and ENT1/2 KO mouse tail snips using a DNeasy Blood & Tissue Kit (Qiagen, Hilden, Germany). As per the instructions of the kit, the mouse tail clippings were first finely sliced using a clean razor, then vortexed with 180 µL Buffer ATL and 20 µL Proteinase K solution and incubated at 56°C overnight to further lyse the tissue. Then, 200 µL of Buffer AL was added, the solution was vortexed and 200 µL of EtOH (96–100%) was added to the solution. The lysate was pipetted into a DNeasy Mini spin column placed inside a 2 mL collection tube and centrifuged at 6000 x *g* for 1 min. Flow-through was discarded and the spin column was placed back into the collection tube. Then 500 µL Buffer AW1 was added to the column, centrifuged again at 6000 x *g* for 1 min and flow-through was discarded. Finally, the spin column was placed in another 2 mL collection tube and 500 µL Buffer AW2 was added to the column, then centrifuged at 20,000 x *g* for 3 mins to dry the DNeasy membrane. The dried spin column was then placed in a clean 2 mL centrifuge tube, 200 µL Buffer AE was added directly onto the membrane and then incubated at room temperature for 1 min and finally centrifuged at 6000 x *g* for 1 min to elute the DNA.

Genomic DNA was amplified using GoTaq Green Mastermix (Promega, Wisconsin, USA) according to the manufacturer's instructions, and 0.5 µM Forward and Reverse oligos (Integrated DNA Technologies, Coralville, Iowa, USA; primer sequences 5' to 3': **ENT1_SY_F**: CACCGTCCTGCCAACATCGAGTC; **ENT1_SY_R**: TTCTCAGTCCAAGGCCACTAAC;

ENT2_F: CCACGAGCCTTTGAATTCCC; **ENT2_R**: ACAGGAAGGAGTTGAGGAGC; **LTR**: AAATGGCGTTACTTAAGCTAGCTTGC) in an Eppendorf thermocycler. The PCR cycle was set up as follows: an initial 2-minute denaturation at 95°C, and 30 cycles consisting of a 30 s denaturation at 95°C, an annealing step of 30 seconds at 55°C, and extension at 72°C for 2 minutes, and a final extension at 72°C for 5 minutes. DNA was separated on a 2% (w/v) agarose gel containing RedSafe (Froggabio, Concord, ON) and imaged on a ChemiDoc imaging system (Bio-rad, Hercules, CA, USA).

2.2.6 Adenosine Kinase Western Blot

Postnatal day 0–3 (P0–3), P6–8, P12–14, P20–23 (young adult), and P49+ (adult) WT and Adktg mice were use. Animals were anesthetized via inhalation of isoflurane (cat# CP0406V2, Fresenius Kabi, ON, Canada). P0–14 mice were decerebrated and P20+ mice were decapitated to ensure quick retrieval of brain tissue. Brains were pinned anterior side down in a Sylgard-coated chamber with cold, artificial CSF (pH 7.4, in mM: 218 sucrose, 3.0 KCl, 1.0 $CaCl_2$, 2.0 $MgSO_4$, 26 $NaHCO_3$, 1.25 NaH_2PO_4, and10 D-glucose) and tissue from the cortex, cerebellum, and medulla was extracted. Tissue was lysed in RIPA buffer (cat# 89900, Thermo Fisher Scientific, MA, USA) and protein stability was maintained by adding proteinase and phosphatase inhibitors (one tablet in 10 mL RIPA, cat# A32861, Thermo Fisher Scientific, Waltham, MA, USA). 150 µl of buffer was added per 10 mg of brain tissue, then samples were incubated for 1 hour on ice. Tissue was mechanically homogenized using a pipette and insulin syringe, centrifuged at 12,000 g for 10 minutes, and the supernatant containing the protein was stored at -20ºC. Protein concentrations were determined with a BCA Protein Assay kit (cat# 23227, Pierce Biotechnology, Waltham, MA, USA). Protein samples were diluted to the lowest sample concentration so that each tube contained the same protein concentration. Laemmeli that was 4x more concentrated than the working concentration (cat# 161-0747. BIO-RAD, Hercules, CA, USA) and β-mercaptoethanol (cat# M3148, Millipore Sigma, Burlington, MA, USA) were added to each protein sample to improve protein visualization/movement on the gel and protein denaturation, respectively. Proteins were separated on a 10% sodium dodecyl sulphate/polyacrylamide gel at 150 V for 60–70 minutes, with each well/lane containing the same amount of protein (29–31 µg depending on the experiment). Proteins were then transferred from the gel to the polyvinylidene difluoride (PVDF) membrane using a current of 400 mA for 1 hour. Membranes were incubated for with Intercept blocking buffer

(cat# 927-60001, LI-COR, Lincoln, NE, USA) for 1–2 hours at room temperature to prevent non-specific antibody binding. Membranes were then probed with a polyclonal rabbit anti-ADK antibody (1:4500, cat# A304-280A-M Bethyl Laboratories, Montgomery, TX, USA) at 4°C overnight. After washing the membranes with 1x tris buffer saline and tween (TBS-T), a IRDye 800CW donkey anti-rabbit secondary antibody (1:10000, cat# 926-32213, LI-COR, Lincoln, NE, USA) was added for 1 hour at RT. All incubations occurred on a shaker. For the loading control, a monoclonal mouse anti-β-actin antibody (1:10000, cat# 3700, Cell Signaling Technology, Danvers, MA, USA) and a IRDye 680RD donkey anti-mouse secondary antibody (1:10000, cat# 926-68072, LI-COR, Lincoln, NE, USA) were used, following the same incubation and washing steps. This control confirmed that equal amounts of protein were loaded into each gel lane. Membranes were washed in 1x TBS-T then 1x TBS and imaged with an Odyssey scanner (LI-COR, NE, USA). ImageJ (NIH, Bethseda, MD, USA) was used to quantify ADK-S, ADK-L, and β-actin band optical densities. ADK-S and ADK-L values were divided by the loading control to normalize them. One mouse sample from each age group was used for a single Western-Blot experiment. Three separate experiments were conducted for both WT and ADKtg mice strains, creating 3 sets of experimental data to analyze for each mouse group.

2.2.7 Drugs and Drug Application

ATP (100 μM), ADO (500 μM), 2-Phenylaminoadenosine (CV 1808, 0.1 and 1 mM), and 1,3-Dipropyl-8-cyclopentylxanthine (DPCPX, 2 μM) were obtained from Sigma-Aldrich (St. Louis, MO, USA). Substance P (1 μM), MRS 2365 (100 μM), 6-*S*-[(4-Nitrophenyl)methyl]-6-thioinosine (NBMPR, 100 μM), and 5-(3-Bromophenyl)-7-[6-(4-morpholinyl)-3-pyrido[2,3-*d*]byrimidin-4-amine hydrochloride (ABT 702, 10 μM) were obtained from Tocris Bioscience (Bristol, UK). Drugs were prepared as stock solutions in aCSF and frozen in aliquots, except for ATP and ADO which were prepared fresh before each experiment. CV 1808 (local application via drug-pipette) required EtOH for complete solubility at 100 μM (0.5%) and 1 mM (5%). DMSO was used to dissolve DPCPX (bath applied: 0.2%; drug-pipette: 0.02%), ABT 702 (bath applied, 0.1%), and NBMPR (bath-applied, 0.1%). For drugs locally-applied via drug-pipette, the final $[K^+]$ equaled the bath aCSF concentration. For experiments that used control vehicle solutions, these contained the same concentration of solvent as the experimental drug solutions.

Drugs were locally microinjected into the preBötC using a triple-barreled glass pipette (5–6 µm per barrel, outer diameter) using a picospritzer (~12 psi, Spritzer4 Pressure Micro-Injector; Bioscience Tools, San Diego, CA, USA) controlled by a programable stimulator (Master-8; AMPI, Jerusalem, Israel). The preBötC injection site was initially located first using a surface electrode to define the region that produces the greatest inspiratory-related signal. It was then functionally confirmed by mapping responses to local injections of Substance P (NK1R agonist, 1 µM, 10 s) to define a region that elicited at least a doubling of the baseline preBötC frequency (Gray et al., 1999; Lorier et al., 2007; Rajani et al., 2017; Zwicker et al., 2011). All injections were made at least 15 mins apart to ensure the network returned to its basal state. Our previous work suggests that responses evoked by injections repeated at this interval are highly reproducible (Huxtable et al., 2009; Lorier et al., 2008, 2007; Zwicker et al., 2011). For bath application experiments, appropriate volumes of stock solutions were aliquoted into the reservoir containing the recirculating aCSF and allowed to gradually wash-in to the recording chamber for at least 30 mins. Network activity was recorded during this wash-in period to observe any acute changes in preBötC rhythm.

2.2.8 Data Analysis and Statistical Comparisons

Inspiratory-related activity recorded from the XII nerve, XII nucleus (XIIn), and preBötC surface (VRC) from rhythmic slices was analyzed using Clampfit (Version 9.2) and Microsoft Excel. Effects of P2 agonists (i.e. ATP and MRS 2365) on preBötC frequency were calculated in 10 s time bins for the first min and then 30 s time bins for the next 2–4 mins. Effects of ADO on preBötC frequency were calculated in 30 s time bins from the onset of the drug-application. Effects of bath-applied drugs were calculated in 5 min time bins. All data was reported relative to a 1 min (local drug injections) or 5 min (bath-applied drugs) control period preceding drug application. The maximum peak frequency of the P2 agonist injections was defined as the maximum 10 s binned frequency of the initial 30 s following the injection onset. The maximum nadir frequency of the P1 agonist injections was defined as the minimum frequency observed in the initial 3 mins post-injection obtained from the rolling average (based on 5 consecutive bursts) of the instantaneous frequency time series. The duration of the ADO-mediated inhibition of preBötC frequency was calculated by measuring the 5-burst nadir frequency and measuring the time it took for frequency to recover by 90% of baseline frequency for at least three consecutive bursts and

subtracted this time value from the time of the onset of the ADO injection (i.e. if ADO evoked a depression in rhythm from 20 bpm to 10 bpm, then the duration was calculated using the timepoint that frequency returned to at least 18 bpm for at least 3 consecutive bursts subtracted from timepoint at the onset of the ADO injection).

All statistical comparisons were made using Prism, version 7 (GraphPad Software Inc., La Jolla, CA, USA). Raw data from all groups was first tested for normality using a Shapiro-Wilk normality test to determine whether parametric or nonparametric analysis was appropriate. For comparisons of relative effects across age groups or strains, nonparametric analyses were used. For comparison of two groups, means were compared using either paired or unpaired *t* tests (parametric) or Mann-Whitney tests (nonparametric). For comparison for 3 or more groups, one-way ANOVA (parametric) or Kruskal-Wallis test (nonparametric) were employed with either a Tukey or Dunn's *post hoc* multiple comparison test, respectively. Two-way ANOVA was used in conjunction with Sidak's (or Dunnett's for repeated-measures two-way ANOVA analyses) *post hoc* multiple comparison test when comparing mean differences between groups with two independent variables. $P < 0.05$ was considered significant for all tests. Time-course graphs showing the mean and S.E.M were created using Excel. Box plots were created using Prism and the five whiskers represent the lowest sample value, first quartile, median, third quartile, and greatest sample value. The points within the boxes show individual data points.

2.3 Results

2.3.1 Developmental changes in the actions of ATP and $P2Y_1R$ activation on preBötC during the first two postnatal weeks

The interaction between P2 and P1 systems determines the overall actions of ATP in the preBötC following its release during hypoxia, therefore changes in that interaction during development, which is determined by all components of the purinome, are implicated in developmental changes in the HVR. While the actions of MRS 2365 solely reflect the impact of $P2Y_1R$ modulation, the effects of ATP will be determined by multiple components of the purinome, including the rate at which ATP is degraded by ECTOs which also determines the rate of ADO production, the actions of ADO via diverse P1Rs, and the rate at which ADOe is removed. Characterizing differences in the responses evoked by ATP and MRS 2365 is the first step toward defining which factors account

for the differences in the responses evoked by ATP and MRS 2365, as this will define which purinergic components shape responses of the preBötC to ATP.

My first objective was to characterize differences in the excitatory actions of ATP vs MRS 2365 on preBötC rhythm during the first two weeks of development, irrespective of postnatal age, as well as the contribution to those differences of A_1R activation secondary to ATP degradation by extracellular ECTOs. I hypothesized that the excitatory actions of ATP via $P2Y_1R$ activation would be reduced or attenuated by its rapid degradation and/or activation of A_1Rs subsequent (Huxtable et al., 2009; Zwicker et al., 2011). To distinguish between these possibilities, i.e., assess whether differences between the effects of ATP and $P2Y_1R$ activation were due solely to the degradation of ATP, or ATP degradation and other factors listed above (A_1Rs, ADO clearance), I locally injected drugs directly into the preBötC in medullary slices from mice ranging from P0–12 and compared the local response of the network to ATP alone (100 μM, 10 s), ATP following DPCPX (A_1R antagonist, 2 μM, 90 s), or MRS 2365 (a $P2Y_1R$ agonist that does not degrade to produce ADO, 100 μM, 10 s) (Fig. 2.1A, B). I predicted that if the difference between ATP and $P2Y_1R$ effects were entirely due to the ATP degradation, then the effects of ATP = DPCPX/ATP < MRS 2365. However, if the difference was due to a combination of ATP degradation and ADO actions that could include its clearance, then the effects of ATP < DPCPX/ATP < MRS 2365. For this initial analysis, data from all experiments were included, meaning that data are not paired and the sample size varies between groups.

Baseline frequency prior to the injections was not significantly different between groups (Baseline ATP: 13 ± 1 bpm vs. DPCPX/ATP: 15 ± 1 bpm, $p = 0.43$; or vs. MRS 2365, 12 ± 1 bpm, $p = 0.97$, MRS2365 vs. ATP/DPCX: $p = 0.38$). The peak frequency evoked by ATP (20 ± 1 bpm) was smaller than both ATP following DPCPX (27 ± 2 bpm, $p = 0.0001$) and MRS 2365 (28 ± 2 bpm, $p < 0.0001$), but there were no differences between the peak evoked by DPCPX/ATP and MRS 2365 ($p = 0.78$, two-way ANOVA, Tukey's *post hoc* test) (Fig. 2.1C). Additionally, the duration of the excitatory effect of ATP (16 ± 2 s) was shorter than ATP applied after DPCPX (33 ± 5 s, $p = 0.002$), while MRS 2365 evoked a longer response than ATP alone (96 ± 9 s, $p < 0.0001$) and DPCPX/ATP ($p = 0.006$, Kruskal-Wallis test, Dunn's *post hoc* comparison) (Fig. 2.1D). In other

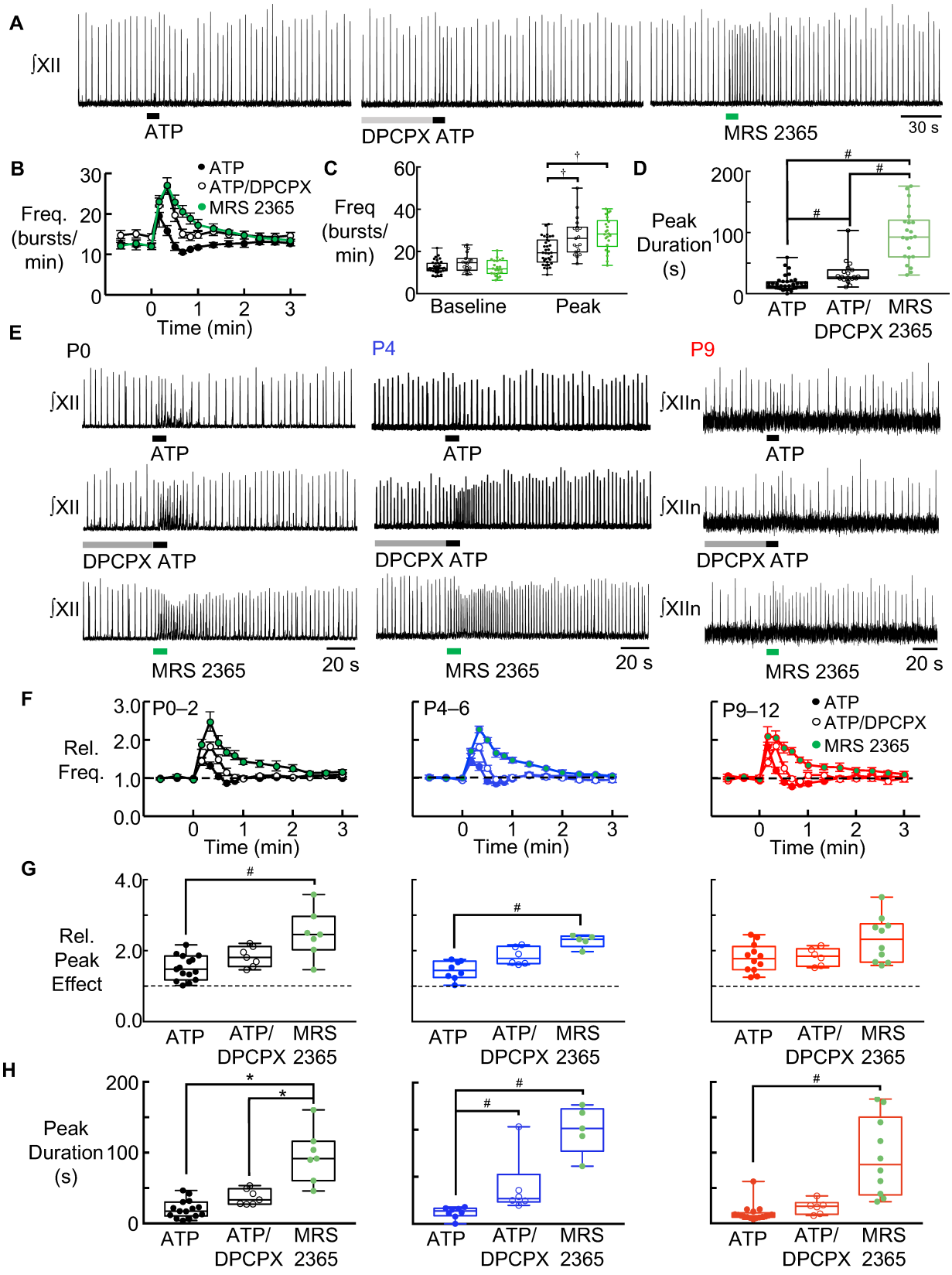
A
∫XII
ATP
DPCPX ATP
MRS 2365
30 s
B
Freq. (bursts/ min)
ATP
ATP/DPCPX
MRS 2365
Time (min)
C
Freq (bursts/ min)
Baseline
Peak
D
Peak Duration (s)
ATP
ATP/ DPCPX
MRS 2365
E
P0
P4
P9
∫XII
∫XIIn
ATP
DPCPX ATP
MRS 2365
20 s
F
Rel. Freq.
P0–2
P4–6
P9–12
Time (min)
G
Rel. Peak Effect
H
Peak Duration (s)

Figure 2.1: Characterization of ATP and P2Y1R excitation on preBötC activity in slices from P0–12 FVB mice.

A) Representative traces and B) summary time-course plots show the effect ATP (10 μM, 10 s, n = 35), ATP following DPCPX (2 μM, 90 s, n = 19), and MRS 2365 (100 μM, 10 s, n = 22) locally-applied to the preBötC of P0–12 FVB mice. C) Summary box and whisker plots show the frequency of the preBötC network before and during the peak effect of each injection as well as the D) duration of the excitatory effects of each injection. E) Representative traces and F) summary time-course graphs show the effect of locally-applied ATP, ATP following DPCPX, and MRS 2365 on the preBötC network in P0–2 (left, black panels), P4–6 (middle, blue panels), and P9–12 mice (right, red panels). Summary data show the G) relative peak and H) duration of the excitatory effect of each injection in each age window. For P0–2, N for ATP = 15; ATP/DPCPX = 7; and MRS 2365 = 7. For P4–6, N for ATP = 8; ATP/DPCPX = 6; and MRS 2365 = 5. For P9–12, N for ATP =12; ATP/DPCPX = 6; and MRS 2365 = 10. †signifies difference ($P < 0.05$) between effect of each injection on preBötC frequency determined by two-way ANOVA with Tukey's *post hoc* comparison. #signifies differences between injection effects determined using a Krukal-Wallis comparison with Dunn's *post hoc* test. *signifies differences between injection effects determined using a one-way ANOVA with Tukey's *post hoc* comparison.

words, the effects of ATP < DPCPX/ATP < MRS 2365. These data support my hypothesis, suggesting that the excitatory effect of ATP activation via $P2Y_1Rs$ is reduced and shortened by the rapid breakdown of ATP and A_1R-mediated inhibition/ADO clearance.

I next sought to determine whether the relative contributions of ATP degradation and ADO actions/clearance to differences between the excitatory effects of ATP and $P2Y_1R$ activation change during the first two postnatal weeks. I predicted that the difference between the actions of ATP, DPCPX/ATP and MRS 2365 would decrease with development because in SD rats the ADO-mediated inhibition of preBötC activity disappears by P3 (Herlenius et al., 1997; Huxtable et al., 2009). In addition, the greater hypoxic respiratory depression, which is attributed in part to ADO, is strongest in neonate mammals (Bonora et al., 1984; Mortola, 1999; Moss, 2000). While the ADO mediated inhibition of preBötC activity is much stronger in P0–4 Swiss CD mice compared to P0–4 SD rats (Zwicker et al., 2011), the developmental time course of the ADO-mediated effect is not known in Swiss CD mice, nor the FVB mice under examination here.

To test my prediction, I repeated the same experimental protocol and analysis performed in Fig. 2.1A and B, separately on slices from P0–2, P4–6 and P9–12 mice. The relative peak frequency evoked by ATP (100 μM, 10 s) was not significantly greater following the application of DPCPX (2 μM, 90 s) at P0–2 (ATP: 51 ± 9%; DPCPX/ATP: 83 ± 11%, $p = 0.35$,), at P4–6 (ATP: 45 ± 9%; DPCPX/ATP: 85 ± 10%, $p = 0.36$) or at P9–12 (ATP; 79 ± 12%; DPCPX/ATP: 82 ± 10%, $p > 0.99$, all ages analyzed using Kruskal-wallis, Dunn's *post hoc* test). However, the effect of MRS 2365 (100 μM, 10 s), a $P2Y_1R$ agonist that is not degraded by ECTOs, was significantly greater than that of ATP at P0–2 (147 ± 25%, $p = 0.002$) and P4–6 (127 ± 8%, $p = 0.002$). Importantly, at P9–12, differences in the effects of ATP (79 ± 12%) and MRS 2365 (132 ± 20%, $p = 0.10$) on peak frequency were no longer significant (Fig. 2.1E–G), which appeared to reflect an increase in the excitatory effects of ATP compared to younger age groups.

At P0–2, the duration of the peak increase evoked by ATP (20 ± 3 s) was numerically but not significantly increased by pre-application of DPCPX (37 ± 4 s, $p = 0.20$) (Fig. 2.1H). In contrast the duration of increase evoked by MRS 2365 (96 ± 15 s) was much greater than that evoked by ATP alone ($p < 0.0001$) and following DPCPX ($p < 0.0001$, one-way ANOVA, Tukey's *post hoc*

test). A similar story was observed at the two older age groups where DPCPX caused variable increases in the duration of the ATP-evoked increase, while the response evoked by MRS 2365 lasted much longer than that ATP response. At P4–6, the ATP-evoked increase lasted 12 ± 2 s, the increase following DPCPX lasted 40 ± 13 s ($p = 0.04$) and that following MRS 2365 lasted 100 ± 11 s ($p = 0.0006$, Kruskal-Wallis test, Dunn's *post hoc* comparison). At P9–12, the duration of the frequency increase evoked by ATP was 14 ± 3 s, by ATP after DPCPX was 23 ± 4 s ($p = 0.24$), while that evoked by MRS 2365 lasted 94 ± 18 s ($p < 0.0001$, Kruskal-Wallis test, Dunn's *post hoc* comparison). In contrast to their effect in P0–2 slices, the duration of the DPCPX/ATP and MRS 2365 peaks were not different at P4–6 ($p = 0.58$) and P9–12 ($p = 0.15$). In summary, the analysis of individual age groups revealed that at P0–2 and P4–6 the actions of ATP, ATP/DPCPX and MRS 2365 were still very different, while at P9–12 their actions were similar. These data suggest that between P6 and P9–12, there are changes with respect to the processing and actions of ATP by different elements of the purinome; i.e., in older animals either the degradation of ATP was reduced (which would increase ATP excitation and reduce ADO inhibition), the excitatory effects of $P2Y_1Rs$ increased, the inhibitory effect of ADO at A_1Rs was reduced, or the mechanisms that clear ADOe were more effective (which would reduce A_1R mediated inhibition and increase ATP actions at $P2Y_1Rs$).

Having established that the purinergic signaling system that shapes the actions of ATP in the preBötC changes between P6 and P9–12, data from P0–2 and P4–6 mice were pooled. All subsequent experimental analyses compared data from P0–6 and P9–12 to identify developmental mechanisms underlying my observation that between P0–6 the actions of ATP < MRS 2365 while at P9–12 the difference disappears. Given that the excitatory component of the HVR increases developmentally due to increased excitation and a reduced secondary hypoxic depression, and that ATP/$P2Y_1R$ mediated excitation contributes to the excitation in adults, I was particularly interested in changes in the purinome that might contribute to maturation of the HVR.

I first tested the hypotheses that the excitatory responses evoked by ATP or $P2Y_1R$ activation increase developmentally. Indeed, while the duration of the frequency increase evoked by ATP was similar between age groups (Fig. 2.2C) (P0–6: 17 ± 2 s; P9–12: 14 ± 3 s, $p = 0.97$), the peak frequency evoked by ATP at P9–12 (83 ± 12%) was significantly greater than at P0–6 (43 ± 8%,

Mann-Whitney test, p = 0.002) (Fig. 2.2B). In contrast, the peak frequency increases evoked by MRS 2365 at P0–6 (139 ± 15%) and P9–12 (132 ± 20%, Mann-Whitney test, p = 0.99) were similar. Response durations evoked by MRS 2365 were also similar between age groups (P0–6: 97 ± 9 s; P9–12: 94 ± 17 s, p = 0.92, Mann-Whitney test) (Fig. 2.2C).

I next tested the hypothesis that the difference in the ATP response between P0–6 and P9–12 is due to secondary inhibitory actions of ATP through an A_1R-mediated inhibition of frequency, which decrease developmentally. The duration of frequency increases evoked by DPCPX/ATP at P0–6 (38 ± 6 s) and P9–12 (23 ± 4 s) were not different (p = 0.74, Mann-Whitney test) (Fig. 2.2C), however application of DPCPX prior to ATP eliminated the peak frequency difference between P0–6 (84 ± 7%) and P9–12 age groups (82 ± 10%, p = 0.83, Mann-Whitney test), which were similar to the 83 ± 12% frequency increase evoked by ATP alone in P9–12 mice (Fig. 2.2B). Overall, these results suggest that the excitatory effect of ATP in preBötC increases in the first week of life due to developmental reductions in the inhibitory actions associated with ATP application.

2.3.2 Mechanisms underlying developmental increases in the ATP-mediated, but not the $P2Y_1$R-mediated, excitation of preBötC frequency.

At least three different mechanisms, acting alone or in combination, could explain the above observations that the excitatory effect of selective $P2Y_1$R activation on preBötC rhythm was similar between age groups while the ATP-mediated excitation increased developmentally to match the effects of ATP (and MRS 2365) in the older animals. These include that: i) the inhibitory actions of ADO decrease developmentally; ii) the degradation of ATP into ADO by ECTOs is decreases developmentally; and, iii) the clearance of ADO becomes more efficient with age. Subsequent sections describe results of experiments designed to examine the development of these different elements and/or developmental changes in their effects on baseline inspiratory rhythm or their effects on baseline inspiratory rhythm or the adenosinergic modulation of preBötC rhythm.

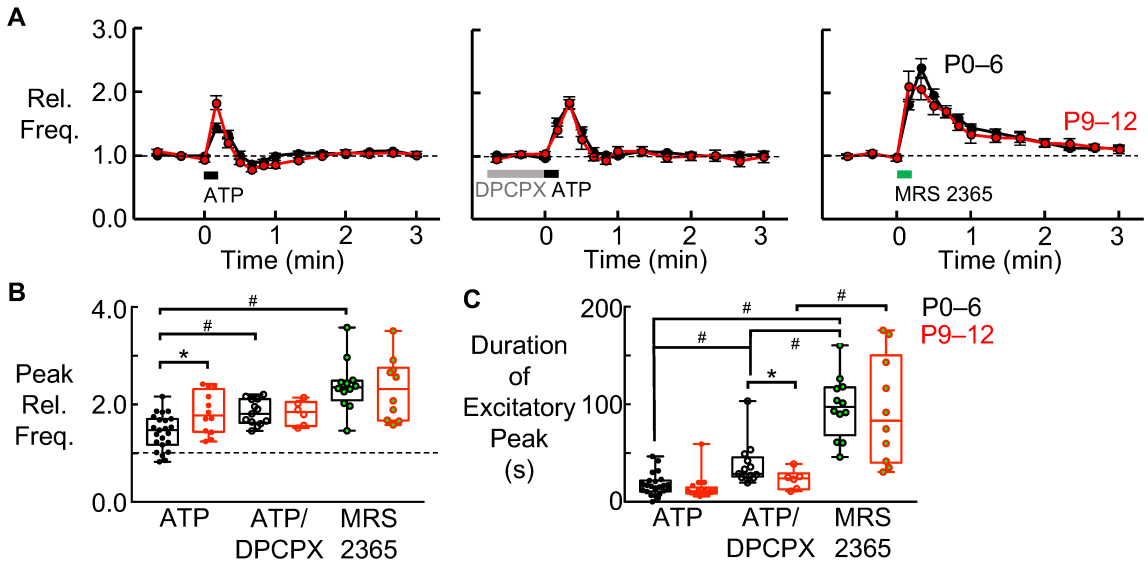

Figure 2.2. Comparing preBötC responses of ATP and P2Y$_1$R stimulation in early development between P0–P12.

A) Time-course graphs show the effect of locally-applied ATP (10 µM, 10 s, left panel), ATP following DPCPX (2 µM, 2 s, middle panel) and MRS 2365 (100 µM, 10 s, right panel) on preBötC frequency in slices taken from P0–6 (black symbols) and P9–12 (red symbols) FVB mice. Summary box and whisker plots show differences in the B) peak relative frequency evoked by each injection and C) the duration of the excitatory effect in P0–6 and P9–12 slices. For P0–6, N for ATP = 23; ATP/DPCPX = 13; and MRS 2365 = 12. For P9–12, N for ATP = 17; ATP/DPCPX = 6; and MRS 2365 = 10. *signifies differences ($P < 0.05$) between the age groups determined using a Mann-Whitney analysis. #signifies differences between injection effects within a specified age group determined using a Krukal-Wallis comparison with Dunn's *post hoc* test.

2.3.2i Inhibitory actions of ADO at A1Rs in the preBötC in vitro do not change in the first two postnatal weeks

Since ADO is implicated in the stronger hypoxic respiratory depression in neonates and A_1R inhibition depresses the ATP-mediated excitation in P0–6 mice, I hypothesized that the sensitivity of the preBötC network to ADO was greatest at birth. I compared the inhibitory actions of exogenously-applied ADO (500 μM, 30 s) in the preBötC network in P0–6 and P9–12 mice, which is a high concentration used to ensure maximal activation of ADO receptors (Fig. 2.3A–D). The maximum decrease in frequency was reported relative to pre-drug control values based on the lowest 5-burst frequency recorded in the first 3 mins of ADO application, referred to as the nadir frequency. The maximum inhibition evoked by ADO did not change developmentally between P0–6 and P9–12 (Fig. 2.3C). In P0–6 slices, baseline frequency fell from 13 ± 0.5 bpm at baseline to 9 ± 0.3 bpm reaching a relative nadir frequency that was 32 ± 3% of control, which was not different than the effect in P9–12 slices where frequency reached a nadir that was 29 ± 3% below baseline ($p = 0.53$, Mann-Whitney test) after fall from 11 ± 0.5 bpm at baseline to 8 ± 0.4 bpm. However, the duration of inhibitory action decreased significantly between P0–6 (226 ± 24 s) and P9–12 (136 ± 27 s; Student's t-test, $p = 0.02$, Fig. 2.3D). These data suggest that the increase in the excitatory effect of ATP between P0–6 and P9–12 to match the excitatory effects of MRS 2365, which are the same at both age groups, is either due to reduced breakdown of ATP or improved clearance of ADOe rather than a reduction in the efficacy of A_1Rs to inhibit rhythm.

The ADO-mediated inhibition of preBötC rhythm frequency is primarily reported to occur through an A_1R mechanism (Bissonnette et al., 1991; Herlenius and Lagercrantz, 1999; Huxtable et al., 2009; Lagercrantz et al., 1984; Zwicker et al., 2011). An $A_{2A}R$-mediated excitation of GABAergic neurons outside the preBötC (and not contained in slices used in this study) contribute to the ADO mediated inhibition in more intact mammalian preparations, including sheep, piglets and rats (Koos and Chau, 1998; Koos et al., 2002; Mayer et al., 2006; Wilson et al., 2004). The source of this $A_{2A}R$-mediated GABAergic inhibition is most likely suprabulbar as it has never been seen in reduced preparations lacking suprbulbar structures (Herlenius and Lagercrantz, 1999; Mayer et al., 2006; Mironov et al., 1999; Wilson et al., 2004). Nevertheless, given the potential for species differences, that the effects of ADO on preBötC rhythm have not previously been examined in FVB mice, the remote possibility that GABAergic terminals in the preBötC could be activated by

A_{2A}Rs in the slice and that the effects of A_{2B}Rs is not known, I tested for the presence in the preBötC of an A_2R inhibitory mechanism. I compared the effects of locally applying into the preBötC a general A_2R agonist, CV 1808 (0.1 and 1 mM, 30 s) and ADO (500 μM, 30 s) on frequency (Fig. 2.3E, F). Frequency of preBötC activity was not significantly affected by either concentration of CV 1808 (0.1 mM: -13 ± 4% p = 0.07; 1 mM: -12 ± 7%, p = 0.19) while ADO injected at the same site caused a significant, 36 ± 4% decrease in preBötC frequency (p = 0.002, two-way ANOVA, Sidak's *post hoc* test) (Fig. 2.3F), indicating that in the FVB mouse there is no A_2R inhibitory mechanism in the preBötC; i.e., the ADO inhibition in FVB mice is mediated by A_1Rs.

2.3.2ii Metabolism of ATP by ectonucleotidases in the preBötC increases developmentally

Since the sensitivities of the preBöC network to $P2Y_1$R and A_1R sensitivity do not appear to change during development, I next tested the hypothesis that developmental reductions in the activity of enzyme systems that degrade ATP (ECTOs) might contribute to the greater ATP response in older mice. Contrary to my hypothesis, ECTO activity in the preBötC increases approximately 2-fold between E10 and P0–4 in SD rats, but postnatal changes are not known. In addition, compared to the preBötC of P0–5 SD rat, ATP is converted much more rapidly into ADO in the preBötC of P0–4 Swiss CD mice where it almost completely obscures the excitatory actions of ATP (Zwicker et al., 2011). Thus, it is conceivable that developmental reductions in preBötC ECTO activity could enhance ATP excitation in the FVB mouse.

In addition to testing whether ECTO activity in the preBötC decreases with development, I was also interested in how ECTO activity in the preBötC compared with other brainstem regions less critical in generating inspiratory rhythm. Given the significance of the preBötC in rhythm generation, the adaptive nature of the ATP-mediated excitation in counteracting the secondary hypoxic depression of breathing and the negative consequences of ADO-mediated inhibition during hypoxia, I hypothesized that the preBötC might be unique compared to other brainstem regions in having lower levels of ECTO that, when ATP is released, would favour ATP excitation over ADO inhibition. To test these two hypotheses, I compared the rate at which tissue punches

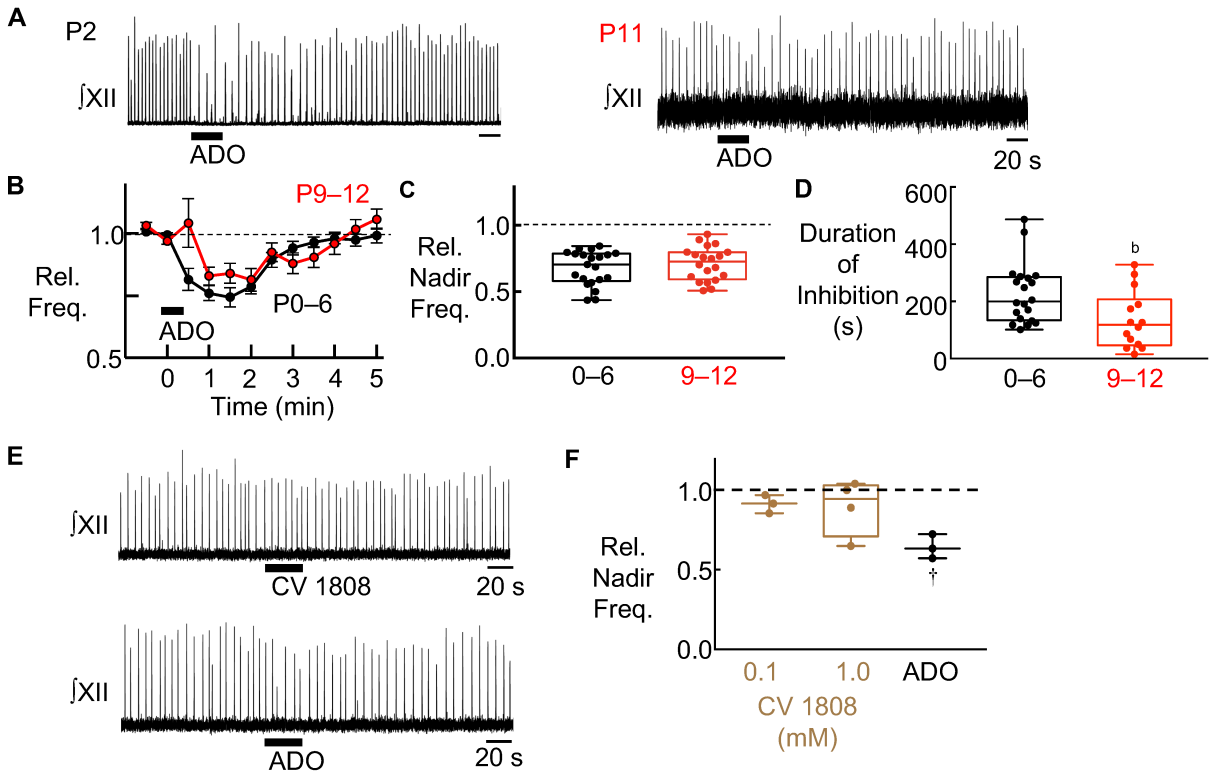

Figure 2.3. Characterization of ADO actions on preBötC activity in slices from P0–6 and P9–12 FVB mice.

A) Representative XII nerve recordings and B) summary time-course graphs show the effect of locally-applied ADO (500 µM, 30 s) on preBötC frequency in slices taken from P0–6 (black symbols) and P9–12 FVB mice (red symbols). Summary box and whisker plots show differences in the C) relative nadir frequency evoked by ADO and D) the duration of the inhibitory effect in P0–6 (N = 21) and P9–12 slices (N = 20). E) Representative traces and F) summary data show differences in the effect of locally-applied CV 1808 (A_2R agonist, 100 µM (N = 3) or 1 mM (N = 4), 30 s) and ADO (500 µM, 30 s, N = 3). [b]signifies differences ($P < 0.05$) in ADO effects between the age groups determined using a Student's t-test. [†]signifies differences between injection effects from baseline determined a two-way ANOVA with Sidak's *post hoc* test.

taken from various regions at P1–5 and P10–12 produced PO_4 when incubated for 60 min in PO_4-free aCSF containing 150 μM ATP. Tissue punches were taken from the preBötC, the XII nucleus and a ventral lateral punch from a rostral medullary slice whose rostral edge was 1.2–1.5 mm above the rostral edge of the preBötC slice.

In contrast to my hypotheses, PO_4 production in the preBötC increased by ~50% between P1–5 and P10–12 from 41 ± 2 to 61 ± 4 nM PO_4/hr/mm^3, respectively ($p < 0.0001$). Moreover, the rate of PO_4 production at P1–5 was similar in all brainstem regions and increased similarly with development. In the XII nucleus, PO_4 production increased from 42 ± 2 nM to 54 ± 3 nM PO_4/hr/mm^3 ($p = 0.03$) at P1–5 and P10–12, respectively, while in the rostral medulla, PO_4 production increased from 45 ± 3 to P10–12: 62 ± 4 nM PO_4/hr/mm^3 ($p = 0.0009$, two-way ANOVA, Sidak's *post hoc* test) (Fig. 2.4). There were no differences in the PO_4 production between regions of either age group. My observation that PO_4 production, which reflects ECTO activity, increases developmentally in the preBötC, it is highly unlikely that developmental changes in ECTO activity contribute to the developmental increase in the excitatory actions of ATP on preBötC rhythm. I therefore test my final hypothesis that developmental increases in the efficiency of ADOe clearance mechanisms contribute to developmental increases in ATP-mediated excitation.

2.3.3 Postnatal development of two mechanisms involved in clearing ADOe and their impact on basal preBötC rhythm and purinergic signaling

ADOe is an important modulator of synaptic transmission in the CNS and endogenous levels of ADOe are believed sufficient to exert a tonic inhibitory influence on neuronal activity (Ballarín et al., 1991). Baseline levels of ADOe and the spatiotemporal profile of changes in ADOe that are produced following the direct release of ADO or the release and subsequent degradation of ATP, as occurs in hypoxia, are determined by a host of processes that vary between brain region and change with development, including transport and ADO metabolism. Transporters fall in two main classes, concentrative NTs (CNTs) that consume energy to transport ADO against its concentration gradient, and ENTs that transport ADO across membranes passively and bidirectionally down the concentration gradient between intra- (ADOi) and extracellular (ADOe) compartments. The direction of this gradient is not constant as ADOi and ADOe are constantly changing as a function

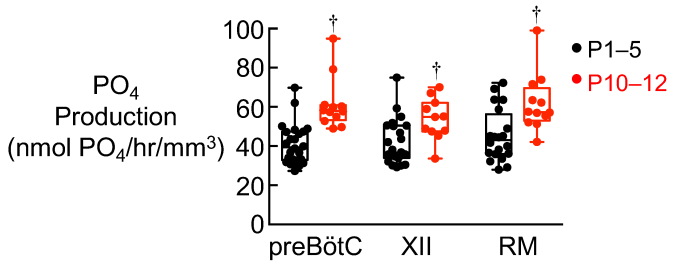

Figure 2.4. Characterization of ectonucleotidase activity by measuring phosphate production in brainstem regions from P1–5 and P10–12 FVB mice.
Summary box and whisker plot shows the amount of phosphate (PO_4) produced by tissue punches incubated in solution with 150 µM ATP from the preBötC (N: P1–5 = 22; P10-12 = 11), the hypoglossal (XII) nucleus (from the same slice as the preBötC punch) (N: P1–5 = 23; P10–12 = 11), and a punch taken from a rostral medullary (RM) slice whose rostral edge was 1.2–1.5 mm above the rostral edge of the preBötC slice (N: P1–5 = 20; P10–12 = 11). †signifies difference ($P < 0.05$) of PO_4 production of each region between age groups determined using a two-way ANOVA with Sidak's *post hoc* test.

of metabolic rate, the energy status of local neurons, ADO transport and enzymes like Adenosine Deaminase that converts ADOi or ADOe into inosine and Adenosine Kinase (ADK) that converts ADOi into AMP (Nguyen et al., 2015; Parkinson et al., 2011, 2005). I focus on developmental changes in the two main forms of ENT in the CNS, ENT1 and 2, because unlike ENT3, 4 and CNTs, they appear to underlie the majority of ADO transport across the plasma membrane in the brain under physiological conditions (Chu et al., 2013; Parkinson et al., 2011; Young et al., 2008). My focus on the enzyme ADK reflects its key role in determining ADOi but especially because in other regions of the brain the activity of the ADK isoform, ADK-S, that affects ADOi and the ADO concentration gradient is very low at birth and increases postnatally. ADK is very important in facilitating clearance of ADOe because it reduces ADOi levels and helps keep ADOi < ADOe and supports removal of ADOe via ENTs.

2.3.3i The effect of ENT activity on basal preBötC rhythm and its influence on the actions of ADO on preBötC rhythm increase developmentally

Developmental changes in ENT activity would only contribute to the developmental increase in the excitatory actions of ATP if ENT activity, and therefore ADOe clearance, increases developmentally. To test the hypothesis that effects of ENT activity on basal preBötC frequency increases with development I compared the effects of bath-applied NBMPR, an ENT blocker, on baseline frequency of P0–5 and P9–12 mouse slices. Under baseline conditions (standard aCSF at 9mM [K+]), NBMPR (100 μM, bath-applied) had no effect on baseline frequency at P0–5 (frequency increased 5 ± 5%, $p = 0.70$) but significantly decreased frequency by 31 ± 5% in P9–12 slices, presumably by increasing ADOe ($p = 0.0007$, two-way ANOVA, Sidak's *post hoc* test,) (Fig. 2.5A–C). Note that this developmental change could reflect that ENT activity is very low in young mice or that under baseline conditions in P0–5 mice, ADOi and ADOe are in equilibrium; i.e., there is no ADOi – ADOe gradient, and blocking ENTs will not affect ADOe.

I next tested whether the role of ENT activity in shaping preBötC frequency responses to large ADOe loads, as might occur during hypoxia, increases with development. I compared in P0–5 and P9–12 slices the responses evoked by local injection of ADO into the preBötC (to crudely simulate a high ADOe load) in the absence or presence of bath applied NBMPR. As seen in Fig. 2.5B, C, NBMPR significantly depressed baseline frequency only in P9–12 slices (Fig. 2.5E).

Thus, for P0–5 slices, the effects of ADO on frequency in control and NBMPR conditions were measured from similar baseline frequencies. For P9–12 slices however, the effects of ADO on baseline frequency were assessed from different baseline frequencies under control and NBMPR conditions. For this reason, I report the nadir frequency evoked by ADO relative to the baseline for that trial.

NBMPR had no effect on the relative nadir frequency evoked by ADO injected into preBötC at either age (Fig. 2.5D–G). At P0–5, the ADO-mediated nadir frequency was 25 ± 3% below baseline under control conditions, whereas the ADO depressed the preBötC frequency by 19 ± 1% with NBMPR in the bathing solution ($p = 0.64$). At P9–12, the nadir frequency evoked by ADO was 42 ± 2% and 36 ± 10% in control and NBMPR conditions, respectively ($p = 0.70$, two-way ANOVA, Sidak's *post hoc* test, Fig. 2.5G). Surprisingly, NBMPR did not affect the duration of the ADO-mediated inhibition at P0–5 or P9–12 (Fig. 2.5H). At P0–5, the ADO-mediated inhibition lasted 121 ± 27 s and 144 ± 17 s in control and NBMPR conditions ($p = 0.93$), respectively. Meanwhile, NBMPR had no effect on the duration of ADO-evoked inhibition at P9–12, which was 204 ± 36 s in control conditions and 290 ± 62 s with NBMPR in the bath ($p = 0.41$, two-way ANOVA, Sidak's *post hoc* test, Fig. 2.5H). While NBMPR has some effect at the concentrations used; i.e., it reduced baseline preBötC frequency in the P9–12 slices, and I expected relatively complete block at these concentrations (Miller et al., 2020), incomplete block of ENT activity might contribute to my inability to detect an effect of NBMPR on the duration of the ADO. In summary, the impact of ENT activity on baseline frequency increases with development. However, this could reflect that ENT activity is very low in young mice or that under baseline conditions in P0–5 but not P9–12 mice, ADOi and ADOe are in equilibrium; i.e., there is no ADOi – ADOe gradient, and blocking ENTs will not affect ADOe.

2.3.3ii Genetic knockout of ENTs does not influence the sensitivity of inspiratory rhythm to ATP or $P2Y_1R$ or ATP metabolism within the preBötC network.

To explore the importance of ENT-mediated ADOe clearance in shaping preBötC responses to ADOe loads during development, I adopted a transgenic approach where I could be certain that ENT activity was completely absent. I used an ENT1/2 double KO mouse (ENT1/2 KO) to

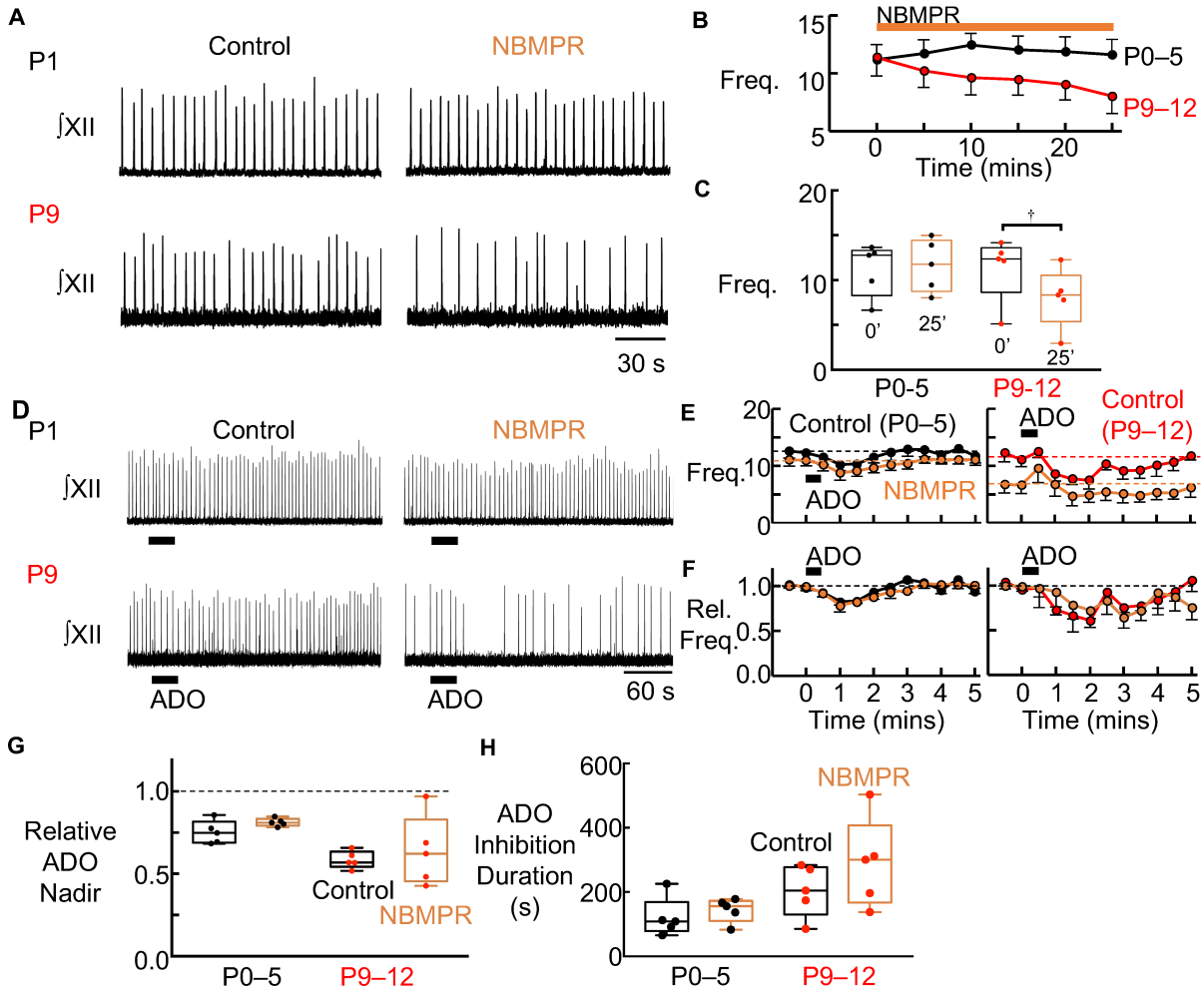

Figure 2.5. Effect of pharmacological inhibition of ENT activity on baseline rhythm and adenosinergic modulation of preBötC in P0–5 and P9–12 mouse slices.

A) Representative XII recordings, B) time-course and C) group data show the effect of blocking ENTs activity using NBMPR (100 µM, bath-applied) on preBötC frequency in slices from P0–5 (black) and P9–12 mice. D) Representative XII recordings and E) absolute and F) relative time-course graphs show the effect of locally-applied ADO (500 µM, 30 s) in the preBötC in control conditions and in the presences of NBMPR in slices from P0–5 and P9–12 mice. The G) depressive nadir and H) duration of the inhibitory effects evoked by ADO under baseline and in the presences of NBMPR at each age are shown in the box and whisker summary graphs. For each age, N = 5. †signifies a difference ($P < 0.05$) from baseline determined using a two-way ANOVA with Sidak's *post hoc* test.

examine the impact that the complete lack of ENT1/2-mediated transport would have on the responses evoked by ADO in the preBötC through development. First, I confirmed the genetic phenotype of the transgenic mice via PCR analysis of DNA extracted from tail clippings from WT FVB and ENT1/2 KO animals. The gel shown in Fig. 2.6A shows that in contrast to the WT FVB mice, the endogenous genes encoding for ENT1 or ENT2 were not detected in ENT1/2 KO animals (Fig. 2.6A).

I was concerned that complete lack of ENT1/2 throughout life and potentially altered level of ADOe/ADOi could alter development of multiple components of the purinergic signaling system, including the expression of P2Rs, ADORs and ECTOs in the ENT KO mice. Therefore, before examining the impact of ENT1/2 KO on ADO responses, I functionally assessed the degree to which ENT1/2 KO affected other components of purinergic signaling system in the preBötC.

To functionally assess the impact of ENT KO on P2R signaling, I first compared at P0–6 and P10–12 the sensitivity of WT and ENT1/2 KO mice to ATP and the $P2Y_1R$ agonist MRS 2365. The excitatory actions of ATP on preBötC frequency had a similar effect in WT and ENT KO mice at both P0–6 (WT: 50 ± 6%; ENT KO: 47 ± 13%, $p = 0.96$) and P9–12 (WT: 80 ± 11%; ENT KO: 117 ± 16%, two-way ANOVA, Sidak's *post hoc* test, $p = 0.15$) (Fig. 2.6B, C). The peak excitatory effect of ATP was significantly higher at P9–12 compared to P0–6 in both the WT ($p = 0.05$) and ENT1/2 KO mice ($p = 0.004$, two-way ANOVA, Sidak's *post hoc* test). The duration of the excitatory ATP-evoked peak was similar between P0–6 and P9–12 groups (data not shown). MRS 2365 also had similar excitatory actions in both strains of the P0–6 (WT: 132 ± 8%; ENT KO: 121 ± 13%, $p = 0.81$) and P9–12 groups (WT: 143 ± 21%; ENT KO: 121 ± 12%, two-way ANOVA, Sidak's *post hoc* test, $p = 0.65$) (Fig. 2.6B, D). The excitatory effect of MRS 2365 was not different between P0–6 and P9–12 WT ($p = 0.85$) or ENT KO mice ($p > 0.99$, two-way ANOVA, Sidak's *post hoc* test). Collectively, these data suggest that postnatal development of the ATP and $P2Y_1R$ responses were not disrupted by the loss of ENT activity in the KO mice.

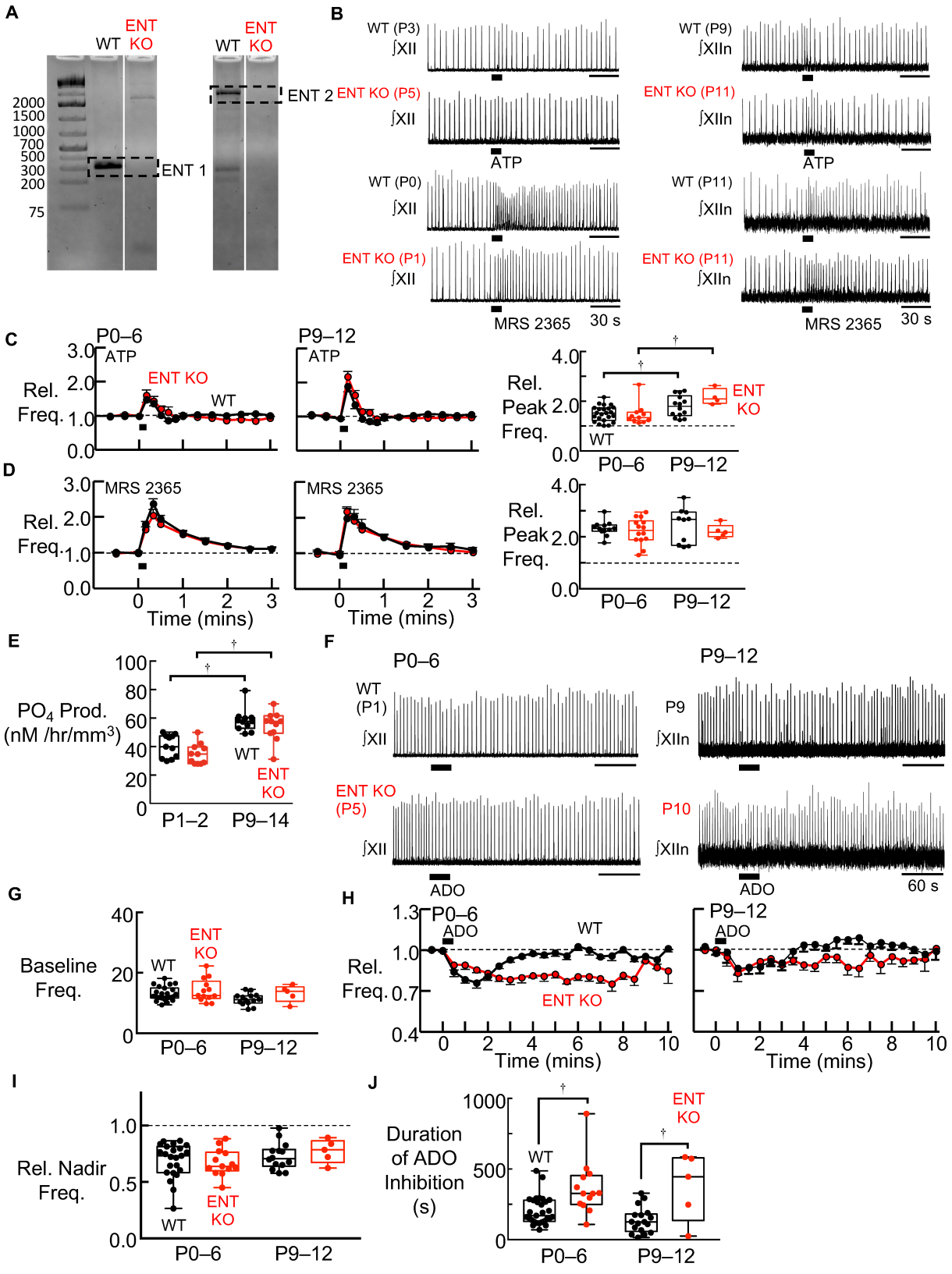
A
WT
ENT KO
2000
1500
1000
700
500
300
200
75
ENT 1
ENT 2
B
WT (P3)
∫XII
ENT KO (P5)
ATP
WT (P0)
ENT KO (P1)
MRS 2365
30 s
WT (P9)
∫XIIn
ENT KO (P11)
C
P0–6
P9–12
Rel. Freq.
Rel. Peak Freq.
D
Time (mins)
E
PO4 Prod. (nM /hr/mm3)
P1–2
P9–14
F
WT (P1)
P9
P10
ADO
60 s
G
Baseline Freq.
H
Rel. Freq.
I
Rel. Nadir Freq.
J
Duration of ADO Inhibition (s)

Figure 2.6. Characterizing the effect of genetic ENT 1/2 knockout on purinergic modulation of preBötC activity in P0–6 and P9–12 mice.
A) Southern-blot images show ENT 1 (~350 kDa) and ENT 2 DNA bands (~2000 kDa) from isolated tissue samples of WT (FVB) and ENT 1/2 KO mice. B) Representative XII and XII nucleus recordings show the effect of locally-applied ATP (100 μM, 10 s) and MRS 2365 (100 μM, 10 s) on preBötC frequency in slices from P0–6 and P9–12 WT (black) and ENT 1/2 KO (red) mice. Summary time-course and box and whisker plots show differences in the effect of C,D) ATP and E,F) MRS 2365 in the WT and transgenic animals at P0–6 and P9–12. N for ATP P0–6 WT = 23; ENT 1/2 KO = 11; N for P9–12 WT = 14; ENT 1/2 KO = 4. N for MRS 2365 P0–6 WT = 12; ENT 1/2 KO = 14; N for P9–12 WT = 10; ENT 1/2 KO = 5. E) Summary box and whisker plot shows the amount of phosphate (PO_4) produced by preBötC tissue punches incubated in solution with 150 μM ATP from P0–6 and P9–12 WT and ENT 1/2 KO mice (N = 11 for punches of both ages and strains). F) Representative XII traces and summary data show how ENT 1/2 KO affects G) baseline preBötC frequency and H) time-course, I) nadir frequency and J) duration of the inhibitory effects of locally-applied ADO (500 μM, 30 s) on preBötC frequency compared to age-matched P0–6 and P9–12 WT mice. For P0–6 N for WT = 29; ENT 1/2 KO = 13; and for P9–12 WT = 17; ENT 1/2 KO = 5. †signifies a difference ($P < 0.05$) between age group or strain determined using a two-way ANOVA with Sidak's *post hoc* test.

I next assessed the impact of ENT KO on the development of ECTO activity. preBötC punches isolated from P1–2 and P10–14 WT and ENT KO mice were incubated in ATP and PO_4 production compared as described previously. PO_4 production increased significantly with development and was similar in WT (P1–2: 40 ± 2 nM PO_4/hr/mm^3; P10–14: 58 ± 2 nM PO_4/hr/mm^3 $p < 0.0001$) and ENT KO (P1–2: 34 ± 2 nM PO_4/hr/mm^3; P10–14: 54 ± 3 nM PO_4/hr/mm^3, $p < 0.0001$, two-way ANOVA, Sidak's *post hoc* test) strains at both developmental time points (Fig. 2.6E). Between strains, there was no difference at P1–2 ($p = 0.25$) or P10–14 ($p = 0.51$, two-way ANOVA, Sidak's *post hoc* test). These functional data suggest that KO of ENT1/2 did not globally disrupt the postnatal development of the purinergic system in the preBötC.

2.3.3iii ENT activity shortens the ADO-evoked inhibitory response in the preBötC network.

Finally, I compared the inhibitory effect evoked by ADO in WT and KO mice. The ADO-mediated reduction in instantaneous frequency, reported relative to baseline, were similar in P0–6 WT (-31 ± 3%) and ENT1/2 KO mice (-32 ± 3%, $p = 0.90$) and P9–12 mice (WT: -27 ± 3%; ENT1/2 KO: -23 ± 5%, $p = 0.78$, two-way ANOVA, Sidak's *post hoc* test) (Fig. 2.6F, H, I), indicating that the sensitivity of the preBötC to A_1R-mediated inhibition, and likely A_1R expression, were not affected by ENT KO. However, the duration of the inhibition evoked by ADO was significantly longer in the ENT1/2 KO mice at both P0–6 (WT: 207.2 ± 18.5 s; ENT1/2 KO: 367.0 ± 53.0 s, $p = 0.001$) and P9–12 (WT: 138.0 ± 22.2 s; ENT1/2 KO: 375.3 ± 106.5 s; $p = 0.002$, two-way ANOVA, Sidak's *post hoc* test) (Fig. 2.6J). These data suggest that under high ADOe loads, as occurs during hypoxia, ENT1 and ENT2 play an important role in removing ADOe and shaping the time course of the preBötC response to ADOe from the time of birth.

2.3.3iv ADK expression and its impact on preBötC activity change postnatally

ENT KO experiments clearly demonstrate that from the time of birth ENTs are expressed at some level in the preBötC where they influence preBötC activity and ADO responses. The impact of ENT activity (and ENT inhibition) on preBötC activity at any moment in time, however, will depend on the concentration gradient for ADO. Data indicate that in my experimental conditions ADOe was typically greater than ADOi such that ENTs were transporting ADOe into cells such that inhibition of ENTs either reduced basal frequency or slowed recovery from an ADO bolus. Key determinants of the ADO gradient are intra- and extracellular enzymes, such as adenosine

deaminase and adenosine kinase (ADK), for both of which ADO is a substrate. I focused on the intracellular enzyme, ADK, that phosphorylates ADOi to produce AMP, because its reduction of ADOi favours the ENT-mediated transport of ADOe into the cytoplasm. Moreover, ADK distribution and activity changes dramatically during postnatal development. ADK exists as a long, nuclear isoform (ADK-L) and a cytoplasmic short (ADK-S) isoform that reduces ADOi and alters the ADOe–ADOi to favor ADOe clearance. In the cerebral cortex and hippocampus, ADK-S expression is very low at birth and matures over the first 2–3 postnatal weeks; neuronal and network excitability in these regions increases in parallel with ADK-S expression (Gebril et al., 2021; Studer et al., 2006). Basal neuronal and network excitability increase in parallel with ADK-S expression. In other words, one of the major enzymes important in ADOe clearance in the cortex and hippocampus is very immature at birth. If the same holds true in the brainstem, I speculated that the reduced capacity to clear ADO from respiratory networks could be a factor in the inability of neonatal mammals to mount a sustained increase in breathing when exposed to hypoxia.

I began by using Western Blot to assess the developmental profiles of ADK-L (top band) and ADK-S (bottom band) expression in the brainstem compared to the cerebral cortex and cerebellum in FVB mice (Fig. 2.7A, B). ADK-S and ADK-L from the different regions and ages are reported relative to the OD of Actin. At P0–3, the signal for ADK-L was more prominent than ADK-S, which was very low in all brain regions. ADK-S expression then increased dramatically, reaching adult levels at different times depending on region. In the medulla, ADK-S expression (relative to Actin) increased significantly from 0.08 ± 0.01 a.u. at P0–3 to 0.57 ± 0.06 a.u. by P20–22 ($p = 0.004$), levels that were similar in adult (0.58 ± 0.03 a.u., $p = 0.004$, one-way ANOVA, Dunnett's *post hoc* test, Fig. 2.7B). I observed similar trends in higher regions of the brain. In the cortex, ADK-S expression similarly increased significantly from birth (0.17 ± 0.04) to reach levels similar to the adult by P20–23 (0.71 ± 0.17; $p = 0.01$, one-way ANOVA, Dunnett's *post hoc* test). The developmental increase in ADK-S expression appeared to happen earlier in cerebellum where levels increased significantly from 0.06 ± 0.04 at P0–2 to 0.35 ± 0.09 by P8 ($p = 0.03$, one-way ANOVA, Dunnett's *post hoc* test).

I next used the ADK-inhibitor, ABT 702, to assess the functional consequences of these developmental changes in the brainstem ADK-S expression for preBötC behaviour. If ADK-S is

important in modulating rhythm by reducing ADOe levels, inhibition of ADK-S with ABT-702 should produce an ADOe-mediated decrease in frequency. To address possible off-target actions, I first confirmed that the inhibitory effects of ABT 702 on rhythm are sensitive to the A_1R antagonist, DPCPX. Fig. 2.**7**C–E show that bath application of ABT 702 to P0–11 slices caused a significant dose-dependent decrease in basal frequency from 17 ± 1 bpm to 15 ± 1 bpm ($p = 0.01$) at 1 μM and 14 ± 1 bpm ($p = 0.02$; repeated-measures two-way ANOVA, Dunnett's *post hoc* test) at 10 μM. After DPCPX was added to the bath, however, preBötC rhythm increased to 16 ± 1 bpm, which restored frequency to levels not significantly different from baseline ($p = 0.64$; repeated-measures two-way ANOVA, Dunnett's *post hoc* test, Fig. 2.7E)

I next tested the hypothesis that the sensitivity of baseline preBötC rhythm to ADK increases developmentally by comparing the effects of bath-applied ABT 702 on the rhythm produced by medullary slices from P0–5 and P9–12 FVB mice. ABT 702 (10 μM) depressed baseline rhythm of P9–12 slices by 13 ± 9%, which was significantly greater than its effects in P0–5 slices, which only decreased frequency by 3 ± 2% ($p = 0.03$, Mann-Whitney test) suggesting that ADK activity in the preBötC network increases in the second week of life (Fig. 2.7F–H). ADK inhibition did not impact the ADO-mediated (500 μM, 30 s) nadir of preBötC frequency compared to baseline at P0–5 (Control: -21 ± 3%; ABT 702: -19 ± 4%, $p = 0.86$) and P9–12 (Control: 26 ± 4%; ABT 702: 41 ± 8%, $p = 0.06$, two-way ANOVA, Sidak *post hoc* test) (Fig. 2.7I–L), nor the duration of the ADO-mediated inhibition at either age (P0–5 Control: 179 ± 35 s; ABT 702: 120 ± 28 s, $p = 0.47$; P9–12 Control: 149 ± 59 s; ABT 702: 199 ± 29 s, $p = 0.82$, two-way ANOVA, Sidak *post hoc* test) (Fig. 2.7M). The absence of an ABT 702-mediated increase in the duration of the ADO inhibition was surprising, similar to the experiments in which pharmacological inhibition affected baseline rhythm in older slices but did not affect response duration. As then, the challenge of achieving complete pharmacological block of ADK activity (an intracellular enzyme) must be considered.

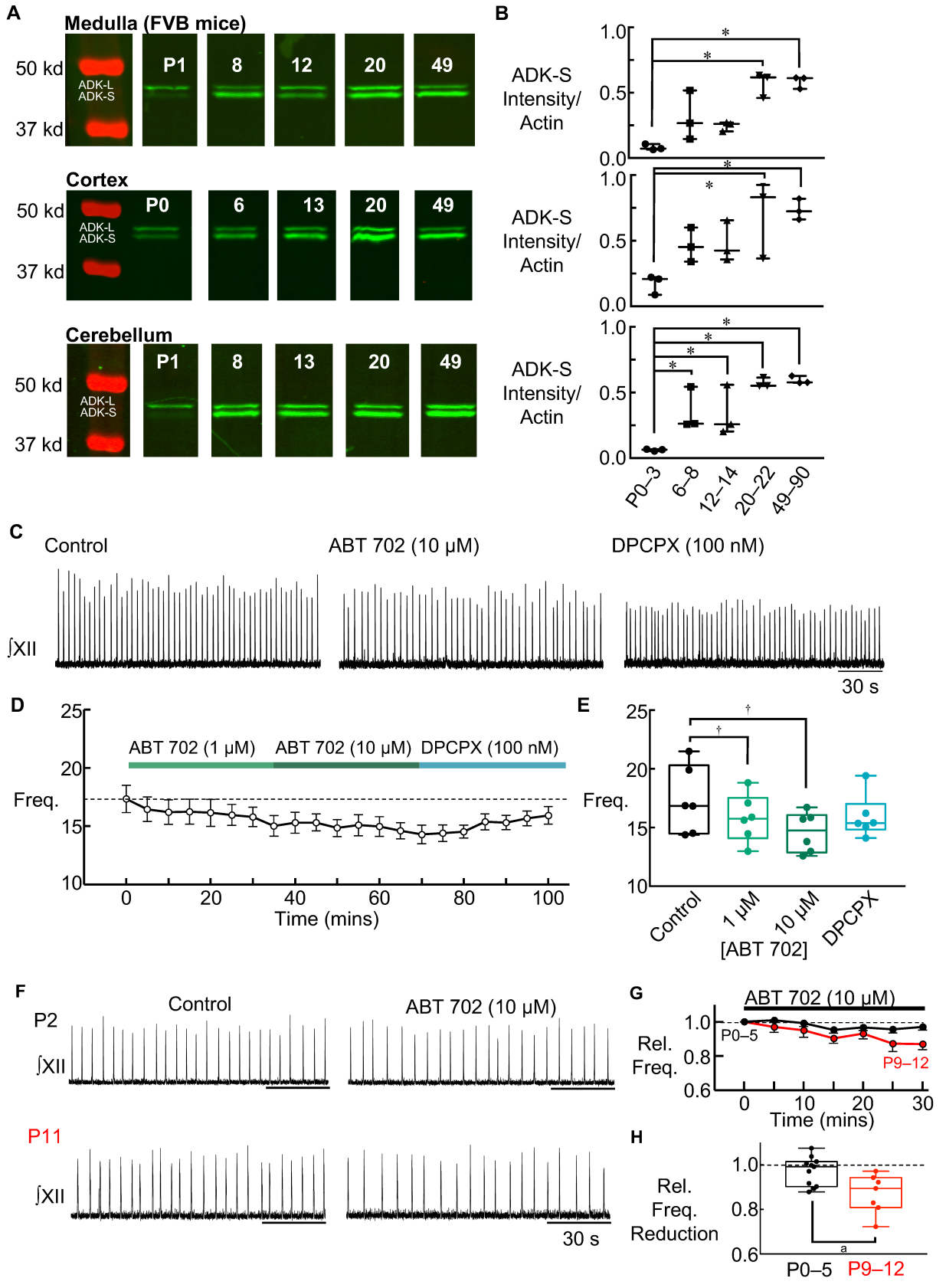
A
Medulla (FVB mice)
50 kd
37 kd
ADK-L
ADK-S
P1
8
12
20
49
Cortex
P0
6
13
Cerebellum
B
ADK-S Intensity/ Actin
1.0
0.5
0.0
P0–3
6–8
12–14
20–22
49–90
C
Control
ABT 702 (10 μM)
DPCPX (100 nM)
∫XII
30 s
D
ABT 702 (1 μM)
ABT 702 (10 μM)
DPCPX (100 nM)
Freq.
Time (mins)
E
[ABT 702]
Control
1 μM
10 μM
DPCPX
F
P2
P11
G
ABT 702 (10 μM)
Rel. Freq.
P0–5
P9–12
H
Rel. Freq. Reduction

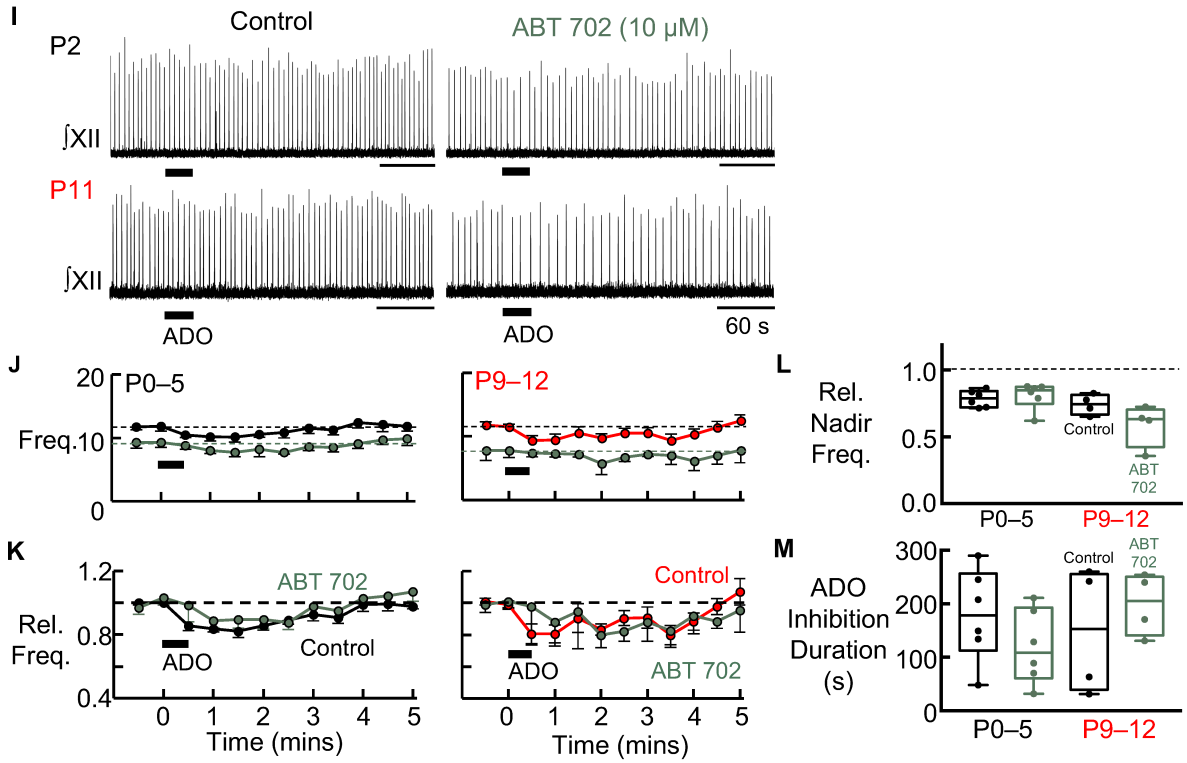

Figure 2.7. Characterizing developmental changes in ADK expression in FVB mice from P0–P90 and the effect of ADK inhibition using ABT 702 on baseline preBötC activity and adenosinergic modulation of the network in young mice from P0–P12.
A) Western Blot images and B) summary graphs show developmental changes in expression of the long (top band) and short (bottom band) isoforms of ADK in the medulla, cortex, and cerebellum of P0–P90 FVB mice. C) Representative XII recordings, D) time-course, and E) summary box and whisker plots show the effect of ABT 702 (1 and 10 µM, bath-applied) alone and with DPCPX (100 nM, bath-applied) on preBötC frequency in P0–11 slices (N = 6). F) Representative traces, G) time-course, and H) summary graphs show the developmental effect of ABT 702 (10 µM, bath-applied) on preBötC frequency in P0–5 (N = 11) and P9–12 slices (N = 7). I) Representative XII recordings, J) absolute and K) relative time-course graphs show the effect of ABT 702 on locally-applied ADO (500 µM, 30 s) effects on preBötC frequency at P0–5 (N = 6) and P9–12 (N = 4). Summary box and whisker plots show the L) nadir frequency relative to baseline and M) the duration of the inhibition evoked by ADO injection in the two developmental groups. *signifies a difference ($P < 0.05$) in ADK-S expression from P0–3 in each brain region determined using one-way ANOVA with Dunnett's *post hoc* comparison. †signifies a difference between experimental conditions determined using a two-way ANOVA with Dunnett's *post hoc* comparison. [a]signifies a difference between age groups determined using a Mann-Whitney test.

2.3.3v The capacity of endogenous ADK to modulate preBötC activity in response to adenosine increases postnatally

An additional limitation to the experiment in Fig. 2.7 that tests whether the effect of ADK inhibition on the preBötC response to ADO increases developmentally is that basal rhythm was significantly depressed by ABT 702 in juveniles, most likely through increases in ADOe. Thus, the application of ADOe in older slices incubated in ABT 702 likely occurred on an elevated baseline of endogenous ADOe, which could mask developmental increases in the effect of ADK on the ADO response in juveniles.

ADK KO strategies are not appropriate in this case because ADK-S levels are very low at birth (Fig. 2.7A, B), and complete ADK KO is lethal after birth (Boison et al., 2002) Instead, to further functionally assess whether development of endogenous ADK modulates the preBötC response to ADO, I used ADK transgenic (ADKtg) mice that constitutively overexpress ADK-S throughout the CNS at adult levels birth, to test whether the role of ADK-S in shaping preBötC responses to ADO loads increases developmentally. I predicted that at birth, the ADO mediated inhibition will last much longer in WT than the ADKtg mouse due to enhanced ADOe clearance and that with development the difference will diminish as endogenous ADK-S expression increases along its normal developmental trajectory.

ADKtg mice were produced on a C57BL/6J background strain. Thus, I first used Western Blot to assess whether the developmental profile of ADK-S expression in C57BL/6J mice was similar to that of FVB mice and to assess the degree of ADK-S overexpression in the ADKtg mice. Western blots showing ADK-L and ADK-S expression from C57BL/6J and ADKtg mice at 5 different ages reveal a developmental trajectory similar to that of FVB mice. ADK-S expression in the medulla, reported relative to Actin, increased steadily from P0–2 levels (0.08 ± 0.05 a.u.) to become significantly greater by P20–23 (0.85 ± 0.14, one-way ANOVA, Dunnett's *post hoc* test, $p = 0.003$, Fig. 2.8A, B). The developmental increase occurred earlier in cortex (P0–3: 0.06 ± 0.05 a.u.; P12–14: 0.37 ± 0.06 a.u., one-way ANOVA, Dunnett's *post hoc* test, $p = 0.03$). Larger variability in measurements from cerebellum precluded detection of a potential significant increase but the trend suggests increased developmental expression of ADK-S in the cerebellum as well. Important for the purposes of my experiments, ADK-S was overexpressed in the medulla, cerebellum and cortex

of ADKtg mice from birth (Fig. 2.8A, B). While levels in each area were similar across all ages, the level of overexpression decreased because endogenous ADK-S levels increased developmentally.

I compared the preBötC response to ADO in P0–4 and P9–12 WT and ADKtg mice (Fig. 2.8C–F). ADO (500 μM, 30 s) evoked a similar 35 ± 3% and 26 ± 5% depression in baseline frequency in P0–4 WT and ADKtg mice, respectively ($p = 0.30$, Fig. 2.8E). Similarly, at P9–12, preBötC rhythm of ADKtg mice was depressed 35 ± 6% by ADO, which was not different than the 32 ± 4% depression evoked by ADO in WT slices ($p = 0.84$, two-way ANOVA, Sidak's *post hoc* test). That saturating concentrations of ADO evoked similar frequency decreases in WT and ADKtg mice suggests the overexpression of ADK-S did not alter the peak ADOe levels reached but more importantly, that ADOR expression within the preBötC was not affected by the transgenic introduction of ADK-S. In contrast, the duration of the inhibition evoked by 500 μM, but not 50 μM (50 μM ADO: WT: 69 ± 8 s vs. ADKtg: 56 ± 14 s, $p = 0.89$), ADO was reduced significantly in P0–4 ADKtg mice compared to WT. At P0–4, the inhibition evoked by 500 μM ADO lasted 213 ± 22 s in WT compared to 134 ± 28 s in ADKtg mice ($p = 0.02$, Fig. 2.8F). By P9–12, these strain differences in the duration of ADO-evoked inhibition disappeared. ADO evoked an inhibiton that lasted 174 ± 25 s in WT slices compared to an inhibition that lasted 149 ± 43 s in slices from ADKtg mice ($p = 0.89$, two-way ANOVA, Sidak's *post hoc* test, Fig. 2.8F). These data suggest that compared to the youngest WT mice that have low levels of endogenous ADK-S, overexpression of ADK-S in preBötC of the ADKtg mouse at this age facilitates clearance of an ADOe load, shortening the ADO mediated inhibition. That the difference in ADO response duration between ADKtg and WT mice disappeared by P9–12 suggests that endogenous ADK-S expression has increased to a level in the WT mice that its effect on ADO response duration is not distinguishable from ADKtg mice – i.e., the role of endogenous ADK-S in shaping the response of the respiratory network to ADO loads increases developmentally.

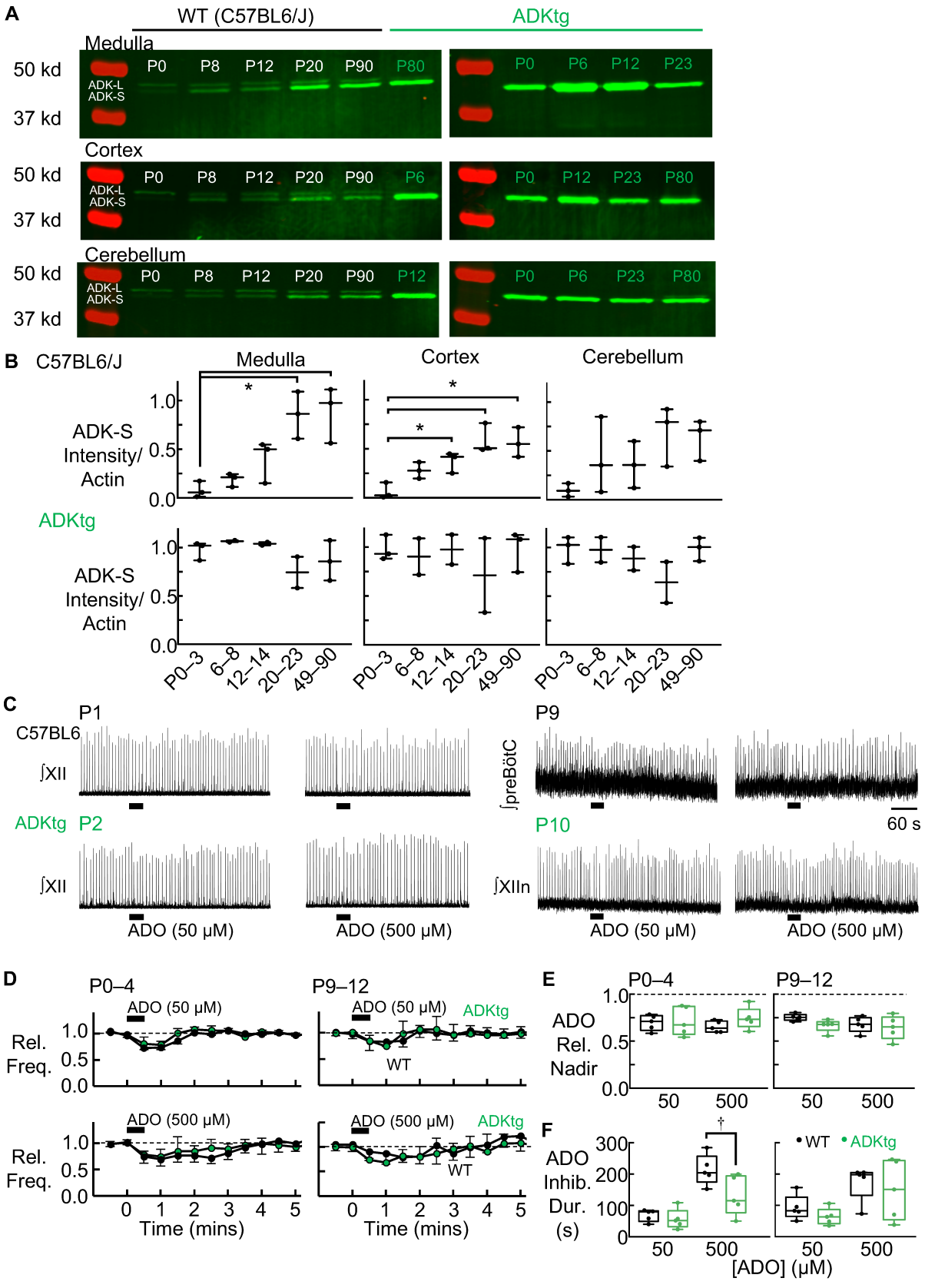
A
WT (C57BL6/J)
ADKtg
Medulla
50 kd
37 kd
ADK-L
ADK-S
P0
P8
P12
P20
P90
P80
P6
P23
Cortex
Cerebellum
B
C57BL6/J
ADKtg
ADK-S Intensity/ Actin
1.0
0.5
0.0
P0–3
6–8
12–14
20–23
49–90
C
P1
C57BL6
∫XII
P9
∫preBötC
60 s
ADKtg
P2
P10
∫XIIn
ADO (50 μM)
ADO (500 μM)
D
P0–4
P9–12
Rel. Freq.
WT
Time (mins)
E
ADO Rel. Nadir
F
ADO Inhib. Dur. (s)
300
200
100
0
†
[ADO] (μM)

Figure 2.8. Assessing the effect of transgenic introduction of the mature ADK-S isoform in the brain on ADO effects in the preBötC of developing C57BL/6J mice from P0–12.
A) Western Blot images and B) summary graphs show developmental changes in expression of the immature, long (top band) and mature, short (bottom band) isoforms of ADK in the medulla, cortex, and cerebellum of P0–P90 C57BL/6J and ADKtg mice. C) Representative recordings and D) summary time-course graphs show the effect of transgenic introduction and overexpression of ADK-S from birth on preBötC frequency responses to locally-applied ADO (500 μM, 30 s) in P0–4 and P9–12 C57BL/6J (WT, black symbols) and ADKtg mice (green symbols). Summary box and whisker plots show the E) nadir frequency relative to baseline and F) duration of the inhibitory responses evoked by ADO injection in the preBötC of both strains. For each strain at each age, N = 5. *signifies a difference ($P < 0.05$) in ADK-S expression between ages in specified brain region determined using one-way ANOVA with Dunnett's *post hoc* test. †signifies a difference ($P < 0.05$) between the WT and ADKtg strain determined using two-way ANOVA with Sidak's *post hoc* test.

2.4 Discussion

Purinergic signaling in the brainstem, specifically within the preBötC, is implicated in shaping the secondary phase of the biphasic hypoxic ventilatory response via both excitatory ATP- and inhibitory ADOR-mediated actions. The excitatory component of the HVR of adults includes not only a carotid body-mediated, initial rapid increase in ventilation, but a slower central excitation mediated by astrocyte-derived ATP that activates $P2Y_1Rs$ on preBötC inspiratory neurons, increasing ventilation and attenuating the secondary hypoxic respiratory depression. ATP, however, is rapidly broken down in the CNS to ADO, which inhibits breathing via P1Rs and is strongly implicated in the hypoxic respiratory depression that is much more pronounced in premature and neonatal mammals. Our lab has shown previously in Sprague-Dawley (SD) rats that the preBötC network is sensitive to ATP and adenosinergic modulation from the moment the network first becomes active at E17. Moreover, the complement and activity of local ECTOs plays a profound, species-specific role in shaping the interaction between ATP and ADO signaling in the preBötC at birth (P0–4) (Huxtable et al., 2009). Here, I extend this work by determining during the first two postnatal weeks how purinergic ($P2Y_1R$- and A_1R-mediated) signaling and additional elements of the purinome, including ECTOs, ENTs and ADK, impact the basal behaviour of the preBötC network and shape its responses to ATP and ADO. I was particularly interested in identifying mechanisms/processes that could contribute to the greater hypoxic respiratory depression in early development; i.e., the inability of newborns to produce a sustained increase in $\dot{V}_E$ during hypoxia.

To summarize the most significant observations, these data demonstrate that ATP is a potent excitatory modulator of the preBötC inspiratory network throughout the first two postnatal weeks in mice where its potentiation of frequency is attenuated by the actions of ECTOs and A_1R-mediated inhibition, particularly at birth. With development, the efficacy of the ATP excitation increased, but this did not reflect increased efficacy of the $P2Y_1R$-mediated excitatory mechanism or decreased ADO sensitivity as the preBötC responses to both agonists did not change postnatally. The possibility that a reduction in ECTO activity contributed to the increased ATP sensitivity was also excluded. PO_4 production from ATP by preBötC tissue actually increased ~50% over the same window.

The element most responsible for the developmental increase in the excitatory actions of ATP was the maturation of ADOe clearance mechanisms. The ADK isoform that affects intracellular ADO levels (ADK-S) is minimally expressed at birth but expression increases thereafter reaching adult levels by the third week of life in the medulla, cerebellum, and cortex. Pharmacological inhibition of ENTs and ADK did not affect baseline preBötC rhythm until P9–12, suggesting that the role of ENTs and ADK in setting preBötC ADOe tone, a key factor in establishing local network excitability, increases developmentally. In addition, ENTs from birth and ADK at P9–12 shorten the inhibitory actions of ADOe in the preBötC, suggesting that these clearance systems limit the inhibitory actions of ADO as mice mature. Overall, our data suggest that the actions of ATP in the preBötC of FVB mice are determined by a dynamic interaction between developmentally stable $P2Y_1R$ excitatory and A_1R inhibitory mechanisms. Developmental increases in the excitatory actions of ATP likely reflect that, despite increased ECTO activity, there is a shift in the ATP-ADOe interaction due to enhanced ADOe clearance. A likely contributor to the enhanced clearance is elevated ADK-S expression, which converts ADOi into AMP, facilitating ENT-mediated intracellular transport of ADOe and termination of its inhibitory actions. Whether developmental changes in ENT activity/expression contributes to the enhanced clearance is uncertain.

2.4.1 Postnatal changes in ATP sensitivity; alterations in the balance between $P2Y_1$ excitation and A_1 inhibition.

The preBötC network of the SD rat is sensitive to $P2Y_1R$ excitation and A_1R inhibition from the moment the network first becomes active at E17. Moreover, from this embryonic stage to the early postnatal period (P0–4), the net effect of ATP in the preBötC is determined by an interaction between the actions of ATP at $P2Y_1Rs$ and the ATP metabolite, ADO at A_1Rs (Huxtable et al., 2009). Data presented here in FVB mice show that this holds true through at least the first two postnatal weeks. Data also show that the balance between $P2Y_1R$ excitation and A_1R inhibition evoked by ATP changes in favor of excitation over the same time window; i.e., the effects of ATP on preBötC frequency of FVB mice were smaller in the first week (P0–6) compared to second postnatal week (P9–12). This shift may contribute to development changes in the HVR and the ability of mature mammals to respond to hypoxia with a sustained increase in ventilation.

The objective of this study is to identify candidates within the purinergic signaling system that could account for this developmental shift, however data rule out an increased sensitivity of the FVB preBötC to $P2Y_1R$ excitation. As seen between E17 and P0–4 in SD rat (Huxtable et al., 2009), $P2Y_1R$ activation in the preBötC of FVB mice more than doubled inspiratory frequency and these effects were consistent during the first two weeks. Direct comparisons of preBötC sensitivity to $P2Y_1R$ activation between P12 and adults are not available, but the sensitivity of the preBötC to $P2Y_1R$ excitation persists into adulthood, as demonstrated by the MRS 2279-mediated ($P2Y_1$ antagonist) attenuation of the HVR in anesthetized, adult rats following its injection into the preBötC (Rajani et al., 2017). $P2Y_1R$ expression has been characterized throughout the brainstem, including central respiratory networks, which suggests that it may have an important role throughout life influencing neural activity (Alvares et al., 2014; Fong et al., 2002; Gourine et al., 2010; Lorier et al., 2007; Rajani et al., 2017, 2016). Previous results also suggest that $P2Y_1R$ expression is detected as early as E14 in the CNS of rats (Franke and Illes, 2006), and increases by E18 (Cheung et al., 2003). While there are likely differences between rats and mice, which were used in this study, data are consistent that the newborn rodent preBötC network is sensitive to $P2Y_1R$ stimulation, confirming $P2Y_1$ expression in the network from birth. Given data also suggest sensitivity remains stable through the first two weeks of life, this could reflect that expression of $P2Y_1Rs$ is also unchanged during this time.

The developmental increase in the excitatory actions of ATP is also not due to a reduction in preBötC sensitivity to ADO inhibition. ADO has wide-spread inhibitory actions in the brain by activating P1Rs, which includes respiratory control regions of most mammals (Herlenius et al., 1997; Koos et al., 2001; Mironov et al., 1999). ADO is strongly implicated in determining the time course and magnitude of the hypoxic respiratory depression since there is a buildup of ADO levels in brainstem respiratory networks during hypoxia (Koos et al., 1997; Mayer et al., 2006; Winn et al., 1981) and ADOR antagonists can attenuate the hypoxic respiratory depression, including in humans (Darnall, 1985; Easton and Anthonisen, 1988; Kawai et al., 1995). In other brain regions, developmental changes in synaptic sensitivity to ADO appears region-specific, as data suggests sensitivity may increase as observed in the cerebellum (Atterbury and Wall, 2009), remain constant as seen in the hippocampus (Psarropoulou et al., 1990), or decrease over time, as occurs within the auditory system at the calyx of Held (Kimura et al., 2003).

Regarding receptor mechanism, my data is consistent with numerous observations in rat and mice (Mironov et al., 1999; Vandam et al., 2008; Zwicker et al., 2011), that the only ADO-mediated inhibition of rhythm operating in the brainstem is via A_1Rs. A_{2a}Rs are present in the medulla of rat (Rosin et al., 1998; Zaidi et al., 2006), but our observation that CV 1808, an A_2 agonist, had no depressive effect on preBötC rhythm, further confirms the absence of an A_2R-mediated inhibition in the brainstem. This is consistent with data showing that A_2 agonists have no effect on rhythmic activity of the medullary slice (Mironov et al., 1999) and brainstem-spinal cord preparation (Brockhaus and Ballanyi, 2000). A central A_{2a}R-mediated excitation of inhibitory GABAergic neurons that inhibits ventilation during hypoxia has been described in lambs (Koos et al., 2004), piglets (Wilson et al., 2004) and rats (Mayer et al., 2006) in vivo, but as of now there are no data supporting an A_2R-mediated inhibition of breathing rhythm in the brainstem.

As mentioned above, my data in FVB mice indicate that the inhibitory effects of ADO on preBötC frequency by ADO do not change in the first two weeks. This was perhaps surprising given in vitro data in SD or Wistar rat that preBötC sensitivity to ADO disappears between P0 and P3 (Herlenius et al., 2002; Huxtable et al., 2009; Zwicker et al., 2011) and in vivo data from multiple species that sensitivity of the respiratory network to ADO-mediated inhibition decreases developmentally (Bissonnette et al., 1990; Lagercrantz, 1987; Lagercrantz et al., 1984; Mayer et al., 2006; Runold et al., 1986). However, the development of purinergic signaling in mouse may differ substantially from rat and even between mouse strains. For example, in the outbred Swiss CD mouse, the rapid accumulation of ADO from degradation of ATP potently activates A_1Rs such that ATP has no excitatory effect – the excitatory actions of ATP at $P2Y_1$Rs and inhibitory actions of ADO cancel each other out, whereas blocking A_1Rs reveals a rat-like $P2Y_1$R-mediated ATP excitation (Zwicker et al., 2011). The potent ADO inhibition and $P2Y_1$R excitation in the Swiss CD mouse persist until P5. The A_1R mediated inhibition associated with ATP application in FVB mice is not as potent as that seen in Swiss CD mice. In fact, the ATP response of FVB mice more closely resembles the rat than the Swiss CD response. Most importantly, these data highlight the potential for interspecies and even strain differences in purinergic signaling. Thus, my observations that ADO effects are constant through development, and that the excitatory actions of ATP at P0–6, but not P9–12, are limited by A_1R-mediated inhibition (i.e., at P0–6, pre-application of DPCPX increased the effects of ATP on frequency to match those seen at P9–12, that also matched the excitation

evoked by $P2Y_1R$ activation at both ages) suggests that developmental changes in ATP efficacy are due to changes in how ATP and its metabolites are processed. Consistent with this possibility, the sensitivity of the preBötC to ADO (the reduction in frequency) was constant from P0–12 in FVB mice, but the duration of the ADO-mediated inhibition lasted much longer in neonates, suggesting changes in ADOe clearance.

2.4.2 Impact of developmental changes in ATP degradation and metabolite clearance mechanisms in the preBötC on inspiratory rhythm and purinergic signaling.

ATP Degradation, Reflecting Ectonucleotidase Activity, Increases Postnatally

Data showing that excitatory $P2Y_1$ and inhibitory A_1R mechanisms have consistent effects on the preBötC network during the first two weeks after birth in FVB mice suggest that purinergic components that control the spatiotemporal pattern of each agonist play key roles in shaping developmental responses to ATP, ADO and possibly hypoxia. A key contributor to the balance between competing ATP and ADO actions are ECTOs, which degrade ATP. There are four groups of ECTOs, which are membrane-bound enzymes that catalyze the breakdown of ATP and its metabolites ultimately into ADO. Three of the 4 groups are differentially expressed in the CNS, specifically, ectonucleotidase triphosphate diphoshohydrolases (ENTPDase 1–3), tissue non-specific alkaline phosphatase (TNAP), and ecto-5'-ectonucleotidase (Langer et al., 2008; Robson et al., 2006). A comparison of responses evoked by ATP in SD rat and Swiss CD mouse demonstrates that the complement of ECTOs are profoundly important in determining the interaction between $P2Y_1R$ and A_1R signaling that evolves following ATP application (Zwicker et al., 2011) In the preBötC of neonate SD rats, ENTPDase-2 is the predominant ECTO. It preferentially hydrolyzes ATP into ADP (a stronger $P2Y_1$ agonist), which excites network activity. In contrast, in the preBötC of neonate Swiss CD mice TNAP predominates, which rapidly metabolizes ATP directly to inhibitory ADO. While I did not examine the complement of ECTOs expressed developmentally, my data from medullary and preBötC tissue punches suggests that ATP metabolism, and indirectly ECTO activity, increases in P10–14 mice compared to newborns. Greater metabolism of ATP did not substantially shorten the duration of ATP-mediated excitation in P9–12 slices compared to P0–6 slices, which could reflect that greater capacity for ATP breakdown in older tissue does not impact the acute temporal profile of ATP effects in the preBötC through P0–12. For developmental changes in ECTO activity to contribute for the developmental

increase in ATP sensitivity, I expected ECTO activity would have to decrease with development, contrary to much of the previous literature. ECTO activity appears to increase during postnatal development throughout the brain, including the hippocampus (Grkovic et al., 2014), hypothalamus (Grković et al., 2016), and cerebellar cortex (Yoshioka and Tanaka, 1989). Regulation of basal ATP and ADO levels is crucial for normal CNS development; ATPe impairs axon growth (Cheung et al., 2005), whereas TNAP activity, which increases ADOe, promotes neuronal elongation and growth in vitro (Abbracchio et al., 1989; Díez-Zaera et al., 2011). ECTO activity, and therefore regulation of ATPe, appears to increase postnatally during normal development in other regions of the CNS, therefore these data support my observation that ATP metabolism in the preBötC of FVB mice also increases during development. Characterization of which ECTOs are expressed will be useful to showing if ATP is preferentially broken down to ADP or ADO at different periods of development, however my data showing increases in ATP metabolism does not support the developmental increase in ATP-mediated excitation of preBötC network.

ADOe Clearance via ENT and ADK Activity is Immature at Birth

Any mechanism that clears ADOe will help terminate its inhibitory signaling actions and therefore influence the balance between P2 and P1 signaling systems. Of the four reported ENT isoforms, ENT1 and ENT2 are expressed on the outer cell membrane and are responsible for moving ADO down its concentration gradient (Parkinson et al., 2011). My data indicates that ENT1/2 KO reduces the duration of ADO-mediated inhibition of preBötC activity from birth, while inhibition of ENTs has greater depressive effects on preBötC activity, presumably from the buildup of ADOe, in P9–12 slices compared to those from P0–5 mice. This suggests that ENT1 or ENT2 transport ADO across cell membranes down its concentration gradient in the preBötC. The difference in effects on basal preBötC rhythm by ENT inhibition between P0–5 and P9–12 could reflect that there is a developmental increase in ENT activity/expression. However, the increased impact of ENT inhibition on basal rhythm in older slices could also reflect developmental changes in the ADOe–ADOi concentration gradient or an indirect effect associated with increased ADK-S expression that facilitates ENT activity. The lack of an NBMPR effect in P0–6 slices suggests that ADOe and ADOi are very similar at this age, while in P9–12 slices ADOe > ADOi. Whether this represents a true physiological difference is not clear. It could simply reflect that the

metabolic/energy status of neurons neurons/glia in brain slices from older mice is compromised compared to slices from young animals. However, ADO release under hypoxic conditions in vitro appears to be conditionally related to age and temperature in spinal cord preparations, as those from P5–8 rats released ADO and inosine, whereas those from P0–3 did not unless the bathing solution was raised from 27°C to 33°C (Otsuguro et al., 2011). Still, data are limited with respect to whether development influences basal ADO gradients in the brain in vivo. Since the activity intracellular enzymes that metabolize ADO, such as ADK, increase developmentally, I would speculate that the intracellular gradient for ADO will increase in most of the brain (i.e. ADOe > ADOi in older subjects). Furthermore, dysfunction in adenosinergic signaling systems are implicated in Alzheimer's and Parkinson's disease, as well as depression (Liu et al., 2019), therefore an enhanced ADO gradient in older mammals may also prevent the onset of pathophysiological conditions typically associated with aging. I did not test whether *ENT1* and *ENT2* expression increases postnatally, however previous data suggest that *ENT1* expression, and its effects on ADOe levels, are developmentally important in the striatum (Roberts et al., 2022) and somatosensory cortex (Matyash et al., 2017) and ENT1 is abundant in the rat spinal dorsal horn in both neonates and adults (Ackley et al., 2003). Characterization of changes in *ENT2* expression through development is less complete. Deletion of *ENT2* increased ADOe levels in the brain of 8–10 week-old mice compared to fully intact animals, suggesting that ENT2 activity is at least present in the brain of young adult mice (Wu et al., 2020). ENT2 is also robustly expressed throughout the human body, including the brain (Crawford et al., 1998). An analysis of 247 ethnically-diverse human subjects demonstrated genetic and functional variation of ENT1 and ENT2 was significantly lower than 22 other membrane transport proteins studied (Leabman et al., 2003; Osato et al., 2003; Owen et al., 2006), suggesting that these transporters are under higher selective pressure and may highlight their importance in the body. While it is not clearly demonstrated that both ENT1 and ENT2 are expressed in respiratory networks from birth, functional data showing that ENT1/2 KO prolongs the inhibitory effects of ADO in mice from P0–12 suggest there is some activity/expression of these transporters in the preBötC network even from birth.

Genetic manipulation can cause unpredicted impacts on other genes or systems as a result of mechanisms that compensate to maintain/replace the physiological functioning affected by the

altered gene, therefore data is not necessarily translatable to normal physiological conditions. Data, however, suggests that global transgenic removal of ENT1/2 did not impact the preBötC response to ATP or MRS 2365 compared to WTs, nor was the sensitivity to ADO impacted. While the loss of these transporters did not affect the sensitivity of the network to $P2Y_1R$ or ADOR activation, ENT1/2 KO prolonged the ADO-mediated inhibition. Surprisingly, I did not see the same effect when ENTs were acutely inhibited using NBMPR. NBMPR had a bigger depressive effect on basal rhythm in P9–12 slices, therefore the absolute nadir evoked by ADO reached a lower point than control injections, however the relative change from baseline was not different. The duration of the ADO-evoked inhibition in P9–12 slices trended higher than control injections. This difference was not significant, however, possibly due to a low sample size (n = 5) as well as larger variability in this data set caused by the depressive and irregular bursting pattern of older slices in the presence of the ENT inhibitor. NBMPR has typically been used to differentiate the effects of ENT1 from ENT2, since ENT2 is insensitive to its pharmacological effects at nanomolar levels (Baldwin et al., 2004; Parkinson et al., 2011). The concentration of NBMPR used here (100 μM), however, has been shown to inhibit both ENT1 and ENT2 activity (Crawford et al., 1998). The lack of effects on adenosinergic signaling by pharmacological inhibition of ENTs may reflect that ENT2 activity, which is less sensitive to NBMPR inhibition than ENT1, is not completely blocked and facilitates removal of ADOe by itself thereby eliminating any differences compared to control ADO injections. While possible, it would be surprising that the likely-complete block of ENT1 activity by NBMPR, which significantly depressed basal rhythm, did not affect the preBötC temporal response to ADO. Given that NBMPR had depressive effects on preBötC rhythm in P9–12 slices, the applied concentration and diffusion within the preBötC network did not appear to be limiting factors.

A more likely explanation for this difference was that intracellular mechanisms that affect ADOe transport through ENTs, such as ADK, are immature at birth, therefore inhibiting limited ENT activity in young mice as little effect on the response of the network to exogenous ADO. In P9–12 mice, intracellular mechanisms that support ENT activity increase its transport of ADO under baseline conditions, which explains why ENT inhibition depresses preBötC rhythm likely by elevated ADOe. If ADOe is acutely increased by NBMPR, unlike ENT KO where a different steady state for ADOe levels is likely established, injecting maximal concentrations of ADO into

the preBötC under acute ENT inhibition may have little effect on an already saturated adenosinergic system. I expected that ADOe would remain elevated for a longer period of time following inhibition of ENTs in older slices. If the ADOe concentration following local injection is supramaximal, the NBMPR-mediated reduction in ENT clearance of ADO may have been too small to detect at the level of preBotC frequency. Whether ENT activity is important in shaping ventilatory responses to natural stimuli that evoke large loads of endogenous ADOe is not clear – as I do not know whether the ADO profile produced by injection simulates endogenous release. Under basal conditions, ADO levels are estimated between 40–460 nM (Ballarín et al., 1991), however hypoxia can induce significant increases in brain ADO measuring up to 5 μM (Gourine et al., 2002; Winn et al., 1981). Previous experiments established that local injections to the preBötC slice must be ~10-fold greater than bath-applied concentrations, as the concentration of drug will decrease exponentially from the injection site (Liu et al., 1990; Nicholson, 1985). Therefore, these experiments used high (500 μM) concentrations of ADO, although the levels of ADO spreading throughout the preBötC would be closer to physiological levels (5 μM) recorded during hypoxia. Data produced from using microinjections of ATP or ADO to replicate hypoxia in vitro will not perfectly replicate hypoxia in vivo. Nonetheless, my results provide evidence that ENTs affect basal preBötC activity, presumably through its effects setting ADO tone in the network, but further experiments will be needed to determine if ENTs influence the HVR in a whole animal.

Adenosine Kinase Activity Influences ADO Actions in the preBötC and Increases Postnatally

At birth, ADK is primarily expressed as a nuclear isoform in neurons (Studer et al., 2006). Within two to three weeks, ADK expression shifts to a cytoplasmic isoform in astrocytes that influences ADOe levels (Fedele et al., 2005; Studer et al., 2006). The upregulation of ADK-S appears to occur in most regions of the brain, although ADK-L levels may persist into adulthood in regions undergoing neurogenesis including the cerebellum (Gebril et al., 2021) and hippocampus (Fábera et al., 2022) Here, data from FVB and C57BL/6J mice confirms that the cytoplasmic isoform of ADK, ADK-S, is expressed at its lowest at birth but increases significantly by the third week of life in the medulla, cerebellum, and cortex. Similar to when ENTs were blocked, ADK inhibition had a greater depressive effect on basal preBötC activity in P9–12 slices compared to P0–5 mice, suggesting that the activity of ADK in the medullary slice, which can increase ENT transport of

ADOe, increases developmentally. Additionally, the effects of ABT 702 on basal preBötC rhythm can be attenuated by bath-applying the A_1R inhibitor, DPCPX. As with NBMPR, ABT 702-mediated inhibition of endogenous ADK activity had no effect on the nadir or duration of the ADO-mediated inhibition. Again, this could reflect that ADK-S levels, which ultimately influence ADOe concentration, are low at birth therefore its inhibition as little effect on basal preBötC activity or its response to exogenous ADO in P0–5 slices. In P9–12 slices, ADK inhibition may acutely increase ADOe levels (reflected by the larger depressive effect of ABT 702 in these slices) however, injecting maximal concentrations of ADO into the network masks differences in slices under pharmacological inhibition relative to control injections. The relative nadir and absolute duration of inhibition of evoked by ADO injection appeared numerically in the P9–12 slices in the presence of ABT 702 compared to control injections, however statistical significance may have been affected by the smaller sample size (n = 5) for this experiment.

In ADKtg mice, which overexpress the ADK-S throughout the CNS from birth, the overall nadir evoked by ADO was unchanged in both groups, suggesting P1 sensitivity was not impacted in the transgenic mice. ADK-S activity, however, shorted the duration of inhibition evoked by a 500 μM ADO injection in P0–4 slices. By P9–12, the preBötC response to ADO was similar in WT and ADKtg mice, suggesting increases in endogenous ADK-S expression reduced the duration of ADO-mediated effects in the network. There was no difference in the responses of either strain to 50 μM ADO injections, which could reflect that endogenous ADOe clearance mechanisms, including minimal ADK-S levels present at birth, can effectively clear a smaller bolus of ADO that is closer to physiological levels during hypoxia, but these become saturated with higher ADO concentrations. Nonetheless, data indicate that endogenous ENT and ADK activity increases developmentally and influences basal preBötC activity, likely by reducing ADOe levels. Genetic, but not pharmacological, manipulation of ADK activity affected the response of the network to high (500 μM) levels of exogenously-applied ADOe, which was chosen to replicate hypoxic conditions. While it is possible that ADK-S activity is important for supporting removal of high ADO concentrations, previous results suggest ADK activity is more important for regulating basal levels of ADO (Boison et al., 2010). In my ADKtg experiments, enzyme activity was introduced in neonates whereas transporter and enzyme activity were reduced by pharmacological inhibition using NBMPR and ABT 702, meaning the expected effect on ADO responses is different and will

be constrained differently. Future experiments may answer whether pharmacological manipulation of ADOe clearance mechanisms will affect preBötC responses under smaller ADO loads, however, the lack of effect in this study does not detract from my conclusions that ADK activity i) increases developmentally; ii) influences basal ADO tone in the preBötC network; and iii) introduction of the functional ADK-S isoform shortens the inhibitory effects of ADO in neonate mice.

2.4.3 Physiological Significance

The purpose of this study was to investigate developmental changes in elements that influence P2 and P1 signaling in the preBötC inspiratory network, collectively known as the "purinome". My data suggest that network sensitivity to ATP increases in the second week of life. The A_1R-mediated inhibition evoked by ATP degradation decreased developmentally, but this was not a result of increased $P2Y_1R$ sensitivity, decreased A_1R sensitivity or decreases in ATP metabolism by ECTOs. Rather, data suggest that enhanced clearance mechanisms for ADOe, namely ENTs and ADK, may contribute to a developmental shift favouring P2 excitation of the network following ATP release. ADO is strongly implicated in the secondary hypoxic respiratory depression, therefore immature ADOe clearance mechanisms in breathing networks such as the preBötC may partially underlie the enhanced hypoxic respiratory depression in premature and neonate infants. My data suggests that ENT and ADK activity sets baseline ADO tone in the preBötC, which is important in establishing network excitability. This role increases developmentally as does their influence on responses to ADOe, as might occur during hypoxia. If so, enhanced ADOe clearance with development could contribute to developmental differences in the HVR, and partially explain the inability of neonates to mount a sustained response. In vitro data can provide important information regarding underlying physiological mechanisms, however this approach does not conclusively demonstrate what will happen under hypoxic conditions in the whole animal in vivo. Injections of ATP and ADO were used to replicate "hypoxic" conditions, since this approach allowed me to directly measure the effect of purinergic molecules that have been previously demonstrated to influence the preBötC network during hypoxia. The rhythmic slice is bathed in a hyperoxic solution, however the partial pressure of O_2 in the core of the slice is held at approximately physiological levels under these conditions (Hill et al., 2011; Mulkey et al., 2001). Oxygenation and pH already differ throughout the slice, therefore exposing the slice to a hypoxic bathing solution will exacerbate non-physiological conditions, varying from slice-to-

slice as a function of tissue age, thickness, and neuronal activity (Funk and Greer, 2013). Injecting ATP and ADO at calculated concentrations that will diffuse throughout the preBötC at approximate hypoxic physiological levels (~3 μM for ATP (Gourine et al., 2005); ~5 μM for ADO (Gourine et al., 2002; Winn et al., 1981) reduces experimental variability compared to directly applying hypoxic solutions to the slice, especially since responses of the network were compared during the first two weeks of rapid, dynamic development of the mice. A caveat to this approach is demonstrated by differences in the response to ADO in WT and ADKtg slices at only high (500 μM) concentrations. This could reflect that the spatial distribution of ADO (and ATP) following their injection into the preBötC may be very different compared to endogenous conditions, when these molecules are released or metabolized in close proximity to enzymes and transporters that affect signal termination.

Experiments using transgenic mice suggest that ENT activity, which is supported by developmental increases in ADK-S activity, shorten the preBötC response to ADO. Reducing central ADO actions may have important implications in reducing the magnitude the secondary hypoxic respiratory depression, which is strongest in newborn and premature infants. However, these data showing the effect of ENT and ADK activity on ADO responses were not replicated using pharmacological inhibitors. As discussed above, this may reflect a number of issues that arise from attempting to replicate hypoxic conditions in a slice using injections of purinergic agents. Future in vivo experiments are needed to test the contribution that both ENT and ADK activity have on influencing the developmental changes in the HVR. Data from this study support my prediction that both mechanisms that support ADOe clearance will i) reduce the magnitude or ii) delay the onset of the secondary depression of the HVR. While ENT data suggests activity is present at birth, developmental increases in ADK activity may be important in reducing of ADOe buildup throughout the CNS, which is strongly implicated in the secondary depression of the HVR.

Finally, these data also highlight substantial species and strain differences in the development of the purinergic signaling system in the preBötC. Data from two strains of mice (Swiss CD and FVB) and the SD rat demonstrate that the preBötC is sensitive to $P2Y_1R$ excitation from the time of birth (and likely earlier) and that ATP responses in all neonate mice tested are impacted by ATP degradation and A_1R actions (Huxtable et al., 2009; Lorier et al., 2007; Zwicker et al., 2011). Data

also show that the balance between elements influencing P2 and P1 actions varies. The ATP–ADO interaction described here for the FVB mouse bears a much greater similarity to the interaction in SD rat compared to the outbred Swiss CD mouse in which the degradation of ATP is so rapid and ADO action so potent that ATP alone has no excitatory effect – the actions of ATP and ADO cancel each other out. ECTO enzymes expressed in the Swiss CD mouse favour more rapid accumulation of ADO from ATP, while only SD rats become insensitive to ADO after birth. Therefore, overall ATP effects in rodents appears to be determined by the same main players that are expressed at different levels, resulting in significant developmental and species differences. This variability between species and strains may be more reflective of diversity observed in human populations. From a clinical perspective, it is important to know how to manipulate specific components and then, on a patient-by-patient basis, figure out which component of their purinome is most amenable to manipulation to address central disorders that affect breathing. My study provides fundamental information on the role of purinergic signaling in these responses during development. Understanding all the different ways that these purinergic elements can modulate homeostatic control processes during development may eventually create new opportunities to implement personalized medicine and underpin novel successful interventions for pathophysiological conditions arising from maladaptive functioning in this system.

Chapter 3. Role of equilibrative nucleoside transporters (ENTs) and adenosine kinase (ADK) in shaping the hypoxic ventilatory response during development.

3.1 Introduction

Breathing is regulated to maintain homeostatic control of arterial blood and CSF gases and pH Discrete mechanisms mediate responses to elevated $PaCO_2$/decreased pH vs reduced PaO_2. When PaO_2 falls, mammals respond with a rapid (Phase I) increase in $\dot{V}E$ that is largely driven by increased activity in peripheral, carotid body chemoreceptors (Martin-Body et al., 1985; Serra et al., 2001) that increase ventilation via projections to the nucleus tractus solitarius (NTS) (Guyenet, 2014; Nurse and Piskuric, 2013), which relays to multiple sites in the ventral respiratory column (VRC) including the RTN (CO_2 chemosensory site) and preBötC (Anderson and Ramirez, 2017; Funk, 2013; Gray et al., 2001; Johnson et al., 2001; Del Negro et al., 2018; Smith et al., 1991; Vandam et al., 2008; Wang et al., 2014). If PaO_2 is not restored in the first 1–2 minutes, $\dot{V}E$ will fall to a lower steady-state level (Phase II), which varies depending on developmental stage (Rajani et al., 2017; Reklow et al., 2019). In adults, the steady-state Phase II level of $\dot{V}E$ normally remains elevated above baseline, but in premature and neonate mammals $\dot{V}E$ falls to or below baseline, causing further reductions in PaO_2, potentially exacerbating the respiratory depression (Bissonnette, 2000; Mortola, 1996; Moss, 2000). Without intervention, this positive feedback loop can be life threatening. Hypoxia is not uncommon in newborns, and especially premature infants, when immature respiratory networks are unstable and apneas are more common. This is especially true in premature infants; nearly all infants born at < 29 weeks gestation suffer from AOP (Eichenwald, 2016; Fiore et al., 2013; Paolillo and Picone, 2013). Caffeine therapy is commonly used as a respiratory stimulant in AOP to reduce incidence of apneas. It is associated with earlier discontinuation from ventilator support in premature infants, reduced rates of lung pathology, cognitive delay and cerebral palsy (Schmidt et al., 2012, 2007). While highly effective, caffeine is ineffective in ~20% of infants with AOP so alternate treatments are needed (Schmidt et al., 2012, 2007). A primary action of caffeine is blocking the activation of adenosine (ADO) receptors. While the mechanisms that cause $\dot{V}E$ to fall during the secondary phase of the HVR are not fully understood, inhibitory actions of ADO on breathing via the A_1 subtype of P1Rs are strongly implicated (Fiore et al., 2013; Herlenius et al., 2002; Koos et al., 1997; Paolillo and Picone, 2013; Reklow et al., 2019).

As discussed in Chapters 1 and 2, purinergic signaling and the balance between the excitatory actions of ATP via $P2Y_1Rs$ and inhibitory actions of ADO in the preBötC shape the secondary

phase of the HVR. A shift in this balance from ADO to $P2Y_1R$ dominance during development could contribute to the developmental changes in the HVR and the greater hypoxic respiratory depression in neonates. Hence the goal of Chapter 2 was to define the components of the purinome most likely to account for such a shift. Those experiments demonstrated that the main factors accounting for the developmental increase in the excitatory effects of ATP in the preBötC under in vitro conditions were those involved in clearing ADOe, specifically transport involving ENTs, which is affected by the intracellular enzyme adenosine kinase (ADK).

ADO is transported across cell membranes via two classes of nucleoside transporters, equilibrative (ENTs) and concentrative (CNTs). Three isoforms of CNTs have been characterized the CNS; they are all Na^+-coupled and indirectly consume ATP to move ADO against its concentration gradient, but there is currently no evidence that CNTs regulate ADOe under normal physiological conditions (Chu et al., 2013; Parkinson et al., 2011). There are four ENT isoforms, but the ENT1 and ENT2 isoforms are expressed on extracellular membranes in the brain and are responsible for the majority of ADO transport across these membranes (Parkinson et al., 2011; Young et al., 2008). ENTs transport ADO down its concentration gradient, therefore removal of ADOe requires that the concentration of intracellular ADO (ADOi) is lower than the extracellular concentration. Data presented in Chapter 2 showing that the duration of ADOe-mediated reduction in frequency is much longer in ENT1/2 KO mice (P0–12) compared to WT mice (Fig. 2.6) suggest that ENT1 and ENT2 are important in clearing ADOe from the preBötC in mice until at least 12 days of age (oldest age tested). In addition, the observation that pharmacological inhibition of ENT activity has greater inhibitory effects on basal preBötC frequency in P9–12 mice compared to P0–5 animals suggests that the gradient for ENTs to remove ADOe increases developmentally.

ENT-mediated transport of ADOe is influenced by intracellular ADOi metabolism which is accomplished through enzymatic activity of adenosine kinase (ADK). ADK is expressed in two isoforms. The long isoform, (ADK-L), is expressed primarily in the nuclei of neurons where it is implicated in neurogenesis and CNS development, including development of the cerebrum and cerebellum (Gebril et al., 2021, 2020; Studer et al., 2006). The short isoform, ADK-S, is expressed in the cytoplasm primarily in astrocytes where it reduces ADOi levels by converting it into AMP (Gebril et al., 2021; Kiese et al., 2016; Studer et al., 2006) (Fig. 2.7, 2.8). ADK-S expression in

the cerebellum and cortex (Gebril et al., 2021; Studer et al., 2006), as well as the brainstem (Fig. 2.7, 2.8), is very low at birth, increases significantly by the second postnatal week and reaches adult levels by the third week of life (Fig. 2.7, 2.8). Consistent with these anatomical data, pharmacological inhibition of ADK leads to a gradual decrease in baseline preBotC frequency in slices from P9–12 mice but not neonatal slices. Moreover, the inhibition can be reversed by blocking A_1 ADO receptors (Fig. 2.7). Furthermore, transgenic overexpression of ADK-S in newborns shortens the inhibitory effects of ADO exogenously applied into the preBötC network in vitro (Fig. 2.7). Together, these results suggest that both the expression and activity of ADK-S increase postnatally in the preBötC where it has a progressively greater ability to attenuate the inhibitory modulation of preBotC network activity by ADOe.

Based on the in vitro data from Chapter 2 that pointed to ENTs and ADK as important in shaping the developmental changes in the effects of ATP and ADO in the preBötC, the objective of this chapter was to determine the role of ENTs and ADK in shaping the development of the HVR in vivo during development; i.e., are low ENT or low ADK activity at birth factors in the inability of neonatal mice to produce a sustained increase in $\dot{V}E$ ($HVR_{\dot{V}E}$) or $\dot{V}E/\dot{V}O_2$ ($HVR_{\dot{V}E/\dot{V}O_2}$) during hypoxia. My first aim was to test how ENT1 and ENT2 activity affects the development of the ventilatory and metabolic responses to hypoxia by comparing responses of WT mice to mice lacking the genes for ENT1 and ENT2 (ENT1/2 KO). My second aim was based on the exciting observation in Chapter 2 that ADK-S expression in the brainstem is very low at birth and increases to adult levels by three weeks of age. This suggested that lack of ADK activity might be a key factor in the immature HVR – i.e., in the inability of neonatal mice to produce a mature $HVR_{\dot{V}E}$ or $HVR_{\dot{V}E/\dot{V}O_2}$ in which both $\dot{V}E$ and $\dot{V}E/\dot{V}O_2$ remain elevated throughout the hypoxic exposure. I first tested this via pharmacological inhibition of ADK. I reasoned that if ADK function is minimal at birth and increases developmentally, ADK-S inhibition will progressively attenuate the magnitude and/or duration of the hypoxia-induced increase in $\dot{V}E$ as animals get older. My second test of the role of ADK-S in development of the HVR was based on the rationale that if the lack of ADK-S accounts for the immature $HVR_{\dot{V}E}$, then mice engineered to express adult levels of ADK-S at birth should have a mature $HVR_{\dot{V}E}$ and $HVR_{\dot{V}E/\dot{V}O_2}$. I tested this using a transgenic mouse, ADKtg, engineered to express adult levels of ADK-S at birth. I predicted that at birth ADKtg mice would have an adult-like $HVR_{\dot{V}E}$ and $HVR_{\dot{V}E/\dot{V}O_2}$. With development and increased expression of

endogenous ADK-S in the WT mice, the differences between the ADKtg and WT mice would gradually disappear.

3.2 Methods

3.2.1 Ethics Approval

Experimental procedures were approved by the Animal Care and Use Committee (ACUC) of the University of Alberta (AUP #256) in compliance with the Canadian Council on Animal Care Standards.

3.2.2 Animals

Mice aged from postnatal day (P)0–56 were obtained from colonies housed with the University of Alberta's Health Sciences Laboratory Animal Services and maintained on a 12-h light/dark schedule with *ad libitum* access to food and water.

Double ENT1/2 knockout (KO) mice were obtained from Dr. James Young and Dr. Carol Cass at the University of Alberta and the Cross Cancer Institute in Edmonton, AB, CAN. The mENT1 and mENT2 genes were disrupted using a retroviral gene trap insertion method and backcrossed into FVB mice, as described in (Altaweraqi et al., 2020). The mENT1 homozygous and mENT2 homozygous mice were crossed to generate the mENT1/mENT2 double knockout (KO) mouse, which was confirmed using genotyping (Fig. 2.5). FVB/NCrl (Strain Code 207, Charles River, Wilmington, MA, USA) mice were used as wild-type (WT) controls for the ENT1/2 KO mice, and to test the effects of pharmacologically inhibiting ADK activity on preBötC rhythm (see below).

Adktm$^{-/-}$-transgenic (ADKtg) mice were obtained from Dr. Detlev Boison at Rutger's University in New Brunswick, NJ, USA and a colony established at the University of Alberta. These mice were made from Adktm1$^{-/-}$ mice lacking the endogenous *Adk* gene. A 1865bp full length *Adk* cDNA homologous to human ADK-S gene was inserted into the genome via a transgene expression vector, resulting in ubiquitous (over) expression of ADK-S from conception throughout the brain (Fedele et al., 2005; Li et al., 2007). ADK-S is the mature short-isoform of ADK which is expressed in the cytoplasm of astrocytes primarily. ADK-S levels are low in the CNS, including the brainstem, at birth but increase to adult levels by the third week of life in mice (Gebril et al.,

2020; Studer et al., 2006). ADKtg mice were generated using C57BL/6J mice (abbreviated C57BL/6J). Therefore, a colony of C57BL/6J mice was established at the University of Alberta for use as WT controls using mating pairs purchased from Jackson Laboratories (Bar Harbor, ME, USA).

3.2.3 Head-Out Plethysmography; P0–14 mice

All plethysmography experiments (head-out and whole-body) took place between 0900–1800 hrs. Baseline ventilatory and metabolic parameters and responses to hypoxia of unanesthetized P0–14 mice were measured using a head-out plethysmograph that was custom-designed to minimize problems associated with the neck seal (Robinson et al., 2002, 2000). The Perspex plethysmograph consisted of separate head (8 ml) and body (40 ml) chambers that were separated by a flexible latex seal (Coltene, Altstätten, Switzerland) attached to the back of the head chamber. The head chamber consisted of threaded inner and outer cylinders. The rear edge of the inner cylinder contacted a spacer that in turn contacted the latex seal. Rotation of the inner cylinder moved it forward or backward relative to the outer cylinder, shrinking or expanding a hole in the latex seal for the animals' heads. Animals were placed in the body chamber, and the hole in the latex seal was expanded. Animals were positioned with their heads through the hole into the head chamber, and then the edges of the latex sheet were coated with a thin layer of vacuum grease. To establish a seal without restricting respiratory airflow, the inner cylinder of the head chamber was rotated and the diameter of the hole was gradually reduced until the body/plethysmograph chamber was able to maintain constant positive pressure when air was injected into the plethysmograph chamber (after outflow through the pneumotachograph was blocked). Integrity of the seal was verified before and after each experiment. Data were excluded if the seal was not maintained throughout the trial. Head-out plethysmography was used to measure ventilation and $\dot{V}_{O_2}$ in the youngest animals to avoid limitations associated with obtaining accurate measurements of V_T and $\dot{V}_E$ from young rodents using whole-body plethysmography (Mortola and Frappell, 2013). Inspired gases were mixed using a GSM-3 (CWE Inc., Ardmore, PA, USA) and delivered to the head chamber at a flow-rate of 40 ml/min (flowmeter, Fischer & Porter Co., Warminster, PA, USA).

3.2.4 Whole-Body Plethysmography

For mice older than P19, baseline ventilatory and metabolic parameters and responses to hypoxia were recorded using either a 65 ml (P19–23) or 350 ml (P43–56) whole-body plethysmograph chamber. Rectal temperature was measured using the PhysioSuite probe (Kent Scientific, Torrington, CT, USA) prior to placing the mice into the chamber and then again after recording 1 minute of breathing during the normoxic recovery period. The inspired air mixture was delivered at a set rate of twice the chamber volume per minute, therefore flowrate was 130 ml/min and 700 ml/min for the smaller and larger chambers, respectively (Matheson Tri-Gas Inc., Montgomeryville, PA, USA).

3.2.5 Protocols

P0–14 mice were placed into the head-out plethysmograph with air (21% O_2 and N_2 balance) flowing through the head chamber and allowed at least 15 min to acclimate before recording began. Once a stable period of stable breathing of at least 2 min duration was recorded in normoxic conditions (21% O_2 and N_2 balance) inspired gas composition was rapidly (≤ 10 s) changed via a manual valve to hypoxia (10% or 8% O_2 and N_2 balance) for 10 minutes and then rapidly returned to normoxia for a 10 min recovery period. The plethysmograph chamber was located in an incubator maintained at 32 ± 0.5°C to mimic the nest temperature recorded in the home cage.

Mice > P19 were allowed at least 30 min to acclimate in the whole-body plethysmograph and remained in normoxic conditions for up to 60 minutes until at least 2 minutes of stable, quiescent breathing was recorded, at which point the gas composition was rapidly (< 25 s) changed to hypoxia (10% O_2 and N_2 balance) via a manual valve and mice exposed to hypoxia for 10 minutes before quickly returning to normoxia (21% O_2 and N_2 balance). Recovery was monitored for only 1 min when animals were removed from the chamber and T_B measured. The whole-body plethysmograph experiments were completed at room temperature between 23–26°C.

3.2.6 Calculation of ventilatory and metabolic parameters

In both the head-out and whole-body plethysmograph systems, the pressure deflections produced by rhythmic inspiration and expiration were detected using a differential pressure transducer (Validyne Engineering, Northridge, CA, USA) attached to a port on the body chamber or whole-

animal chamber, respectively. Pressure transducer output was passed through a CD15 carrier demodulator (Validyne Engineering), digitized using a PowerLab System (ADInstruments, Sydney, Australia) and visualized using the LabChart data analysis software (version 7, ADInstruments).

The head-out system was calibrated using the average increase in the recorded signal produced by three 0.2 ml injections of air into the sealed body chamber. The whole-body system was calibrated by averaging the differential signal produced by 0.25 ml injections of air delivered at 200 injections/min, which approximately matched the breathing rate of the mice in control conditions. For the head-out system, tidal volume (V_T) was calculated using the formula: $V_T = V_K \times (P_T / P_K)$, where V_K is the calibration volume (0.2 ml), P_T is the pressure deflection of each inspired breath, and P_K is the pressure deflection of standardized injection. For the whole-body plethysmograph system, V_T was calculated using the formula described by (Drorbaugh and Fenn, 1955):

$$V_T = V_K \times (P_T / P_K) \times Tb \times (P_B - P_C) / Tb \times (P_B - P_C) \times T_A \times (P_B - P_R),$$

where Tb is body temperature (in Kelvin), P_B is barometric pressure, P_C is the measured water vapour pressure in the chamber (RH-300 analyzer, Sable Systems International, North Las Vegas, NV, USA), T_A is the air temperature within the chamber (BioTherm13 PIT tag, Biomark, Boise, ID, USA), and P_R is the water vapour pressure at specific Tb based on tables from (Dejours, 1981). $\dot{V}_E$ was calculated as the product of V_T and respiratory frequency. For both the head-out and whole-body plethysmography experiments, O_2 and CO_2 fractions of the inflow and outflow gas were passed through a drying column (Drierite, Sigma-Aldrich, St Louis, MO, USA) and sampled using a gas-analyzer (ADInstruments, Sydney, Australia). Gases were sampled from the inflow and outflow ports of the head chamber or the whole-body chamber for head-out or whole-body experiments, respectively. Metabolic rate ($\dot{V}_{O_2}$) was determined using the formula:

$$\dot{V}_{O_2} = [FR \times (FiO_2 - FeO_2) - FiO_2 \times (FeCO_2 - FiCO_2)] / 1 - FiO_2,$$

where FR is the flowrate of gas through the chamber (ml/min), FiO_2 is the inflow O_2 fraction, FeO_2 is the outflow O_2 fraction, $FiCO_2$ is the inflow CO_2 fraction and $FeCO_2$ is the outflow CO_2 fraction.

V_T, $\dot{V}_E$, and $\dot{V}_{O_2}$ were normalized to the body weight of the mice (kg) and data presented in standard conditions of temperature, pressure and dry air.

3.2.7 Drugs and Drug Application

5-(3-Bromophenyl)-7-[6-(4-morpholinyl)-3-pyrido[2,3-d]byrimidin-4-amine hydrochloride (ABT 702, 10 mg/kg) was dissolved in 0.6% DMSO and 0.9% saline, then injected interperitoneally to acutely inhibit ADK activity in FVB mice at P0–2, P11–12, and P20. Six FVB mice from two different litters were split into two groups; the test group was injected with the drug while the control group was injected with vehicle (0.6% DMSO in 0.9% saline, 10 mg/kg, i.p.). Injections were made 30 minutes prior to starting the acclimation process. From that point on, the protocol was the same as described above for the head-out plethysmography experiments.

3.2.8 Data Analysis and Statistical Comparisons

Ventilatory parameters were analyzed using LabChart 8 software, specifically using the blood pressure add-on (ADInstruments). Breathing frequency and P_T (pressure deflection of each breath) were measured using the heart rate and pulse pressure functions, respectively. Calculations to determine V_T, $\dot{V}_E$, and $\dot{V}_{O_2}$ were completed in Microsoft Excel (Redmond, WA, USA). Variables reported along the response time course represent values averaged during each time bin and are as follows: (t = 0, baseline averaged from 2 min of calm breathing prior to onset of hypoxia; t = 0.33: average of first 10-20 sec of hypoxia when the measured chamber O_2 was < 20% and > 11%); t = 1: average from 0.33 – 1.0 min of hypoxia; t = 2: 1–2 min of hypoxia; t = 4: 3–4 min of hypoxia; t = 10: average from 7–10 min of hypoxia; t=11: 0–1 min of recovery beginning when O_2 in the chamber measured > 20%).

All statistical comparisons were made using Prism, version 7 (GraphPad Software Inc., La Jolla, CA, USA). Two-way ANOVA was used in conjunction with Sidak's post hoc multiple comparison test when comparing mean differences between groups with two independent variables. Developmental changes in weight in wild-type and transgenic mice were compared using linear regression. The Kruskal-Wallis test (nonparametric) was employed to compared relative changes from baseline between age groups in Figure 1. $P < 0.05$ was considered significant for all tests. Time-course graphs showing the mean and S.E.M. were created using Excel. Box plots were

created using Prism where the five whiskers represent the lowest sample value, first quartile, median, third quartile, and greatest sample value. Points within the boxes show individual data points.

3.3 Results

3.3.1 Development of hypoxic ventilatory and metabolic responses in WT FVB mice

Given the variability in hypoxic responses between mouse strains (Tankersley et al., 1994), my first objective was to describe the postnatal development of the ventilatory and metabolic responses of WT FVB mice to hypoxia. Using head-out and whole-body barometric plethysmography, I measured breathing frequency, tidal volume (V_T), minute ventilation ($\dot{V}_E$), metabolic rate ($\dot{V}_{O_2}$), and the air convection requirement ($\dot{V}_E/\dot{V}_{O_2}$) at rest (21% inspired O_2, average of 2 min) and during acute exposure to hypoxia (10% O_2, 10 min) in FVB mice; the latter three parameters are reported in Fig. 3.1. FVB mice were tested at five stages of development: P2; P7–8; P13–14; P20–22; and P49–57. Note, to improve clarity, details of the statistical analyses are provided in the figure captions.

Acute hypoxia evoked a biphasic $\dot{V}_E$ response in FVB mice at all ages tested (Fig. 3.1Ai). $\dot{V}_E$ increased to its peak in the first minute of hypoxia and then fell to a lower steady-state Phase II level that varied depending on the developmental stage. The time course data in Fig. 3.1Ai and box plot data in Fig. 3.1Aii, which plots the value of $\dot{V}_E$ at the end of hypoxia relative to the baseline pre-hypoxia levels, show that in the three youngest age groups, P2, P7–8 and P13–14, $\dot{V}_E$ fell back to baseline levels by the end of the hypoxic period (Fig. 3.1Ai, Aii). In contrast, $\dot{V}_E$ remained significantly above baseline throughout hypoxia in the oldest groups and by the end of hypoxia was 35 ± 6% and 84 ± 18% greater than baseline in P20–22 ($p < 0.0001$) and P49–57 mice ($p < 0.0001$), respectively (Fig. 3.1Aii). In addition, the steady-state level of $\dot{V}_E$ in P20–22 mice was significantly greater than P2 ($p = 0.008$) and P13–14 mice ($p = 0.0007$), while the steady-state level of $\dot{V}_E$ in P49–57 mice was significantly greater than P2 ($p = 0.0002$), P7–8 ($p = 0.003$), and P13–14 mice ($p < 0.0001$) (Fig. 3.1Aii).

In contrast, hypoxia caused a reduction in $\dot{V}_{O_2}$ in all groups. Time course data show that in all but the oldest animals, this fall comprised a relative rapid fall in the first two min followed by a gradual

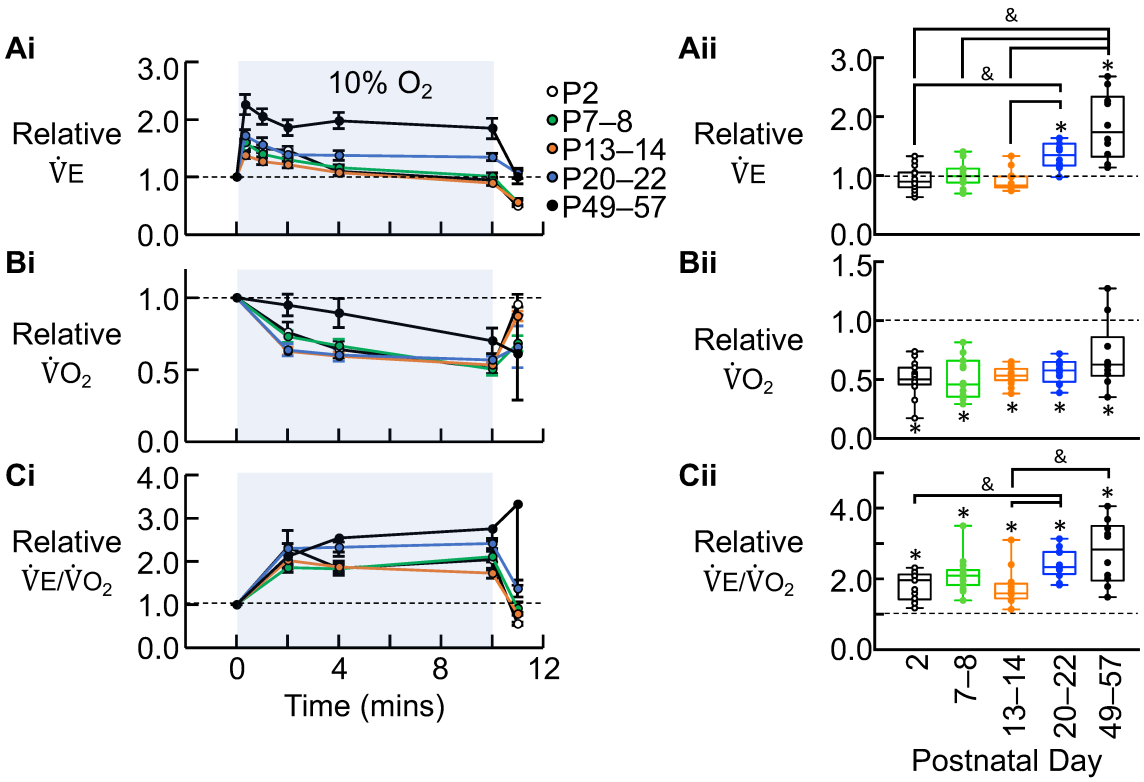

Figure 3.1 Postnatal development of ventilatory and metabolic responses to hypoxia in FVB mice.

Time-course plots showing relative Ai) minute ventilation ($\dot{V}_E$), Bi) metabolic rate ($\dot{V}O_2$), and Ci) air convection requirement ($\dot{V}_E/\dot{V}O_2$) changes from baseline in response to a 10-minute, 10% O_2 exposure in developing FVB mice. In the right-hand column, summary data shows relative changes at the end of hypoxia (average of minute 7–10) from baseline for Aii) $\dot{V}_E$, Bii) $\dot{V}O_2$ and Cii) $\dot{V}_E/\dot{V}O_2$. Measurements were made in P2 (n = 15), P7–8 (n = 15), P13–14 (n = 16), P20–22 (n = 12) and P49–57 mice (n = 10). *indicates for each age group a significant difference ($P < 0.05$) from its own baseline (in absolute terms) determined using a two-way ANOVA with Sidak's *post hoc* test. &indicates a difference between age groups in the relative average of each parameter at 10 mins of hypoxia assessed using a Kruskal-Wallis test with Dunn's *post hoc* comparison.

decline to ~50% of baseline by the end of hypoxia (P2-P23: $p \leq 0.0001$). P49–57 mice showed only a modest decrease in $\dot{V}O_2$ in the first 2 min that reached a maximum inhibition of 30 ± 8% by the end the hypoxic period (P49–57: $p = 0.04$). The hypoxic reduction of $\dot{V}O_2$ at the end of hypoxia, while numerically greater in the 4 youngest age groups, was not significantly different ($p > 0.26$) between age groups (Fig. 3.1Bii).

These hypoxic changes in $\dot{V}E$ and $\dot{V}O_2$ were responsible for a sustained increase in $\dot{V}E/\dot{V}O_2$, a hyperventilation, throughout hypoxia in all age groups (Fig. 3.1Ci, Cii). At 10 minutes of acute hypoxic exposure, $\dot{V}E/\dot{V}O_2$ was 82 ± 10% above baseline in P2 animals ($p = 0.007$). Similar increases were seen in P7–8 and P13–14 age groups. The magnitude of the increase then increased developmentally. At P20–22, $\dot{V}E/\dot{V}O_2$ was 141 ± 12% above baseline and significantly greater than the values at P2 ($p = 0.04$) and P13–14 ($p = 0.002$) while the 175 ± 28% increase at P49–57 was greater than that at P13–14 ($p = 0.003$). It is noteworthy that the hypoxia-induced increase in $\dot{V}E/\dot{V}O_2$ in the three youngest age groups was due exclusively to the hypoxia-induced metabolic depression while in the two oldest groups it reflected both the hypoxia-induced increase in $\dot{V}E$ and metabolic depression (Fig. 3.1Cii).

3.3.2 Equilibrative nucleoside transporters (ENTs)

Minimal impact of ENT KO on baseline beathing behaviour during postnatal development.

Before comparing how the loss of ENTs affected ventilatory and metabolic responses to hypoxia, I first confirmed that ENT1/2 KO did not alter physical development compared to WT mice. I performed a linear regression analysis of body weight as a function of age for the two strains (Fig. 3.2A). The slope of the relationship between body weight and age was similar in WTs (slope=0.48 ± 0.02) and ENT1/2 KO mice (0.44 ± 0.01, $p = 0.46$), suggesting that growth over the first two months was unaffected by the KO and of ENT1/2. I then compared ventilatory and metabolic parameters of WT and ENT1/2 KO under baseline conditions to assess the impact of ENT1/2 KO on baseline behaviour. There were very few differences. In all age groups, $\dot{V}E$ and $\dot{V}E/\dot{V}O_2$ in WT and ENT1/2 KO mice were similar across all groups (Fig. 3.2B, F). The only differences were that: i) baseline frequency was significantly lower in P6–8 (214 ± 7 bpm) and P49–57 WTs (186 ± 15 bpm) compared to the ENT1/2 KO mice of the same age (P6–8: 249 ± 6 bpm, $p = 0.05$;

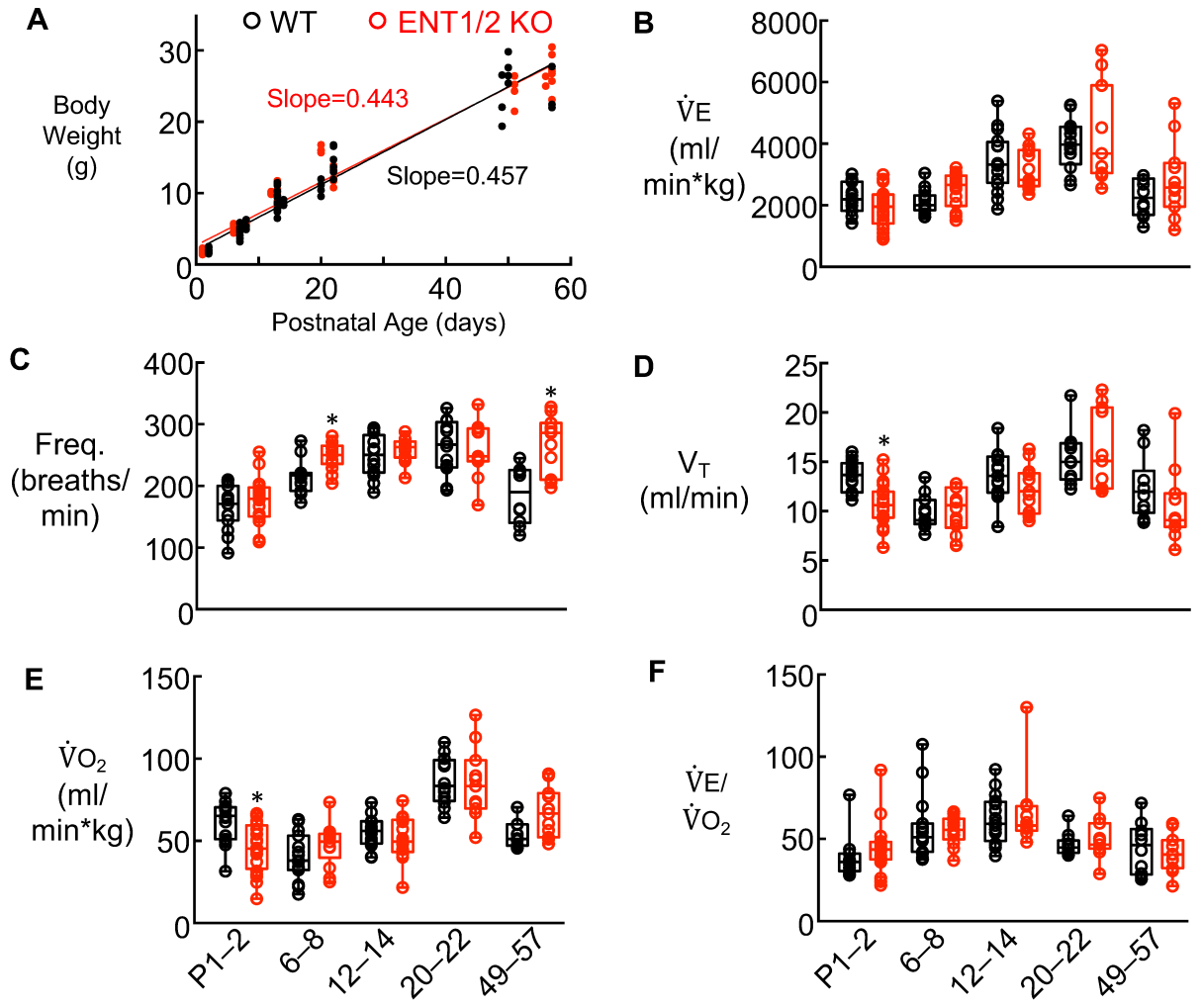

Figure 3.2. Comparison of baseline ventilatory and metabolic parameters between FVB (WT) and ENT1/2 KO mice during early development.

A) Linear regression comparing the body weight of WT FVB mice (black) and ENT1/2 KO mice (red) from P1 until P57. Summary box and whisker graphs compare the basal measurements of B) minute ventilation ($\dot{V}_E$), C) ventilatory frequency, D) tidal volume (V_T), E) metabolic rate ($\dot{V}O_2$), and F) the air convection requirement ($\dot{V}_E/\dot{V}O_2$) between WT and ENT1/2 KO mice at P1–2 (WT: n = 15, ENT1/2 KO: n = 20), P6–8 (WT: n = 15, ENT1/2 KO: n = 14), P12–14 (WT: n = 16; ENT1/2 KO: n = 13), P20–22 (WT: n = 12, ENT1/2 KO: n = 11), and P49–57 (WT: n = 10, ENT1/2 KO: n = 11). *indicates significant difference ($P < 0.05$) between strains at each age, as determined by one-way ANOVA with a Sidak's *post hoc* test.

P49–57: 268 ± 14 bpm, $p < 0.0001$) (Fig. 3.2C); ii) baseline tidal volume (V_T) was greater in the WT mice (13.6 ± 0.4 ml/min) than ENT1/2 KO at P2 (10.8 ± 0.5 ml/min, $p = 0.007$) (Fig. 3.2D), and; iii) metabolic rate in WT mice (62 ± 3 ml/min/kg) was greater than the ENT1/2 KO mice at P2 (47 ± 3 ml/min/kg, $p = 0.007$) (Fig. 3.2E).

Knockout of ENT1 and 2 alters breathing pattern responses of newborn mice to hypoxia and reduces the duration of hypoxia-induced excitation of frequency, $\dot{V}_E$ and $\dot{V}_E/\dot{V}_{O_2}$.

My next objective was to test the hypothesis that ENT1/2 activity is important in shaping the ventilatory and metabolic responses to hypoxia and that its role increases with postnatal development. The prediction of this hypothesis is that removal of ENT1/2 should reduce the duration of hypoxia induced increase in $\dot{V}_E$, and that if the role of ENTs increases developmentally, the difference between the responses of WT and ENT1/2 KO mice should increase with age.

To test these hypotheses, I compared the ventilatory and metabolic responses to hypoxia of WT and transgenic mice lacking ENT1/2 (ENT1/2 KO) at P1–2, P6–8, P12–14, P20–22 and P49–57. I measured frequency, tidal volume (V_T), minute ventilation ($\dot{V}_E$), metabolic rate ($\dot{V}_{O_2}$), and $\dot{V}_E/\dot{V}_{O_2}$ at rest (21% inspired O_2, 5 min), during an acute exposure to hypoxia (10% O_2, 10 min) and during recovery (21% O_2). Outcome measures, plotted as mean ± S.E.M., were first compared between strains to assess differences (*) in each parameter throughout the hypoxic exposure. Data were also compared within each strain to determine the time points when parameters were significantly different from baseline (pre-hypoxia) values. Note that the hash symbol (#) signifies timepoints when both groups were statistically different from baseline, whereas the black section (§) and red double cross (‡) symbol highlight differences from pre-hypoxic values in the WT or ENT1/2 KO group, respectively. All statistical comparisons were made using absolute data. Note, however, that time-course responses are plotted first in both absolute and relative to baseline. Significance symbols in the absolute time course plots (Fig. 3.3Ai, Bi, Ci, Di, Ei) indicate differences between strains. Significance symbols in the relative time course plots (Fig 3Aii, Bii, Cii, Dii, Eii) indicate within strain differences between that time point and the pre-hypoxia baseline value. Since the hypothesis being tested is that the duration of the hypoxia evoked increase in ventilation will be attenuated in the ENT1/2 KO mice, I illustrate the interval when each parameter is significantly

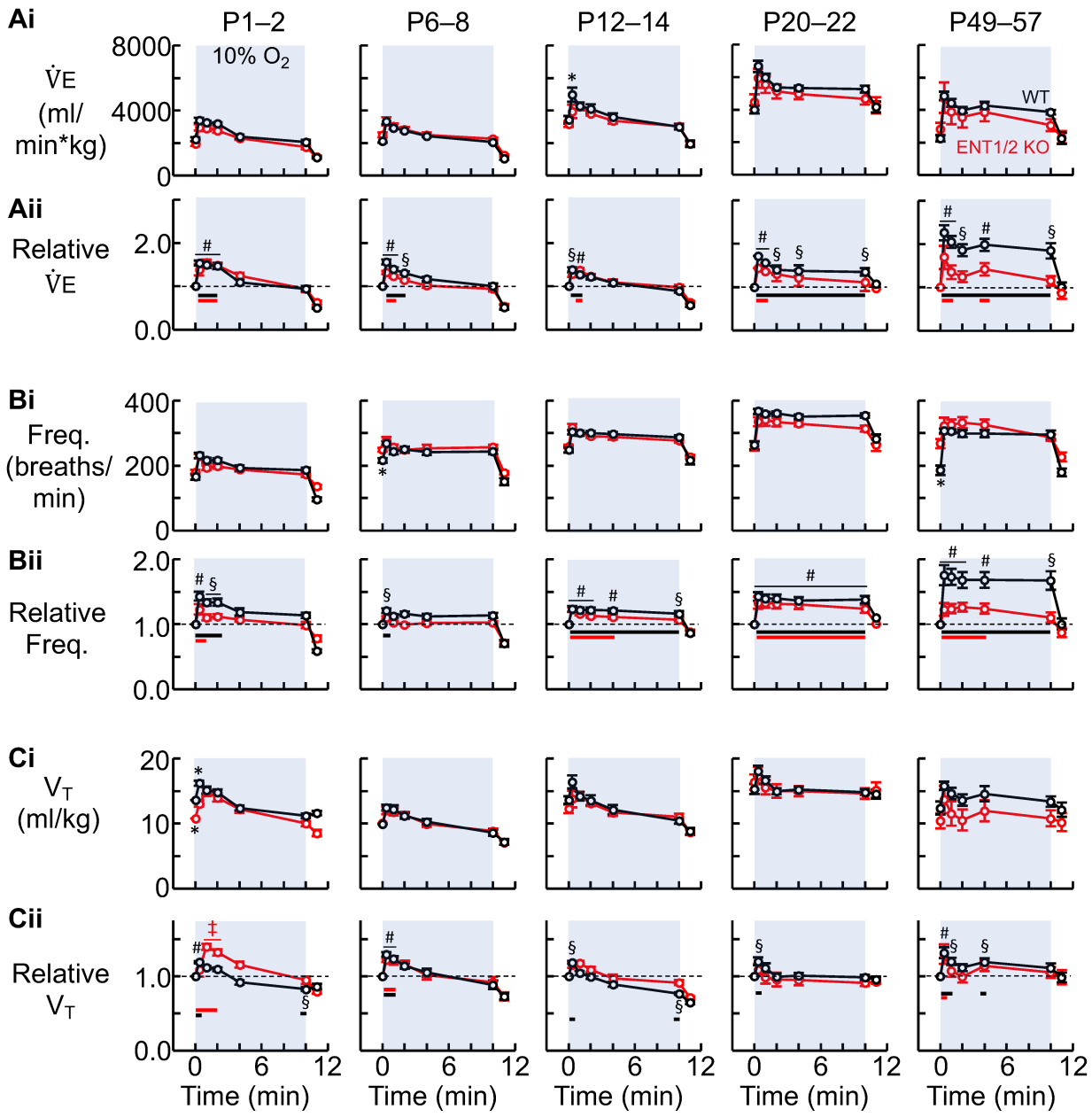
Ai
P1–2
P6–8
P12–14
P20–22
P49–57
10% O2
WT
ENT1/2 KO
V̇E (ml/ min*kg)
8000
4000
0
Aii
Relative V̇E
2.0
0.0
Bi
Freq. (breaths/ min)
400
200
0
Bii
Relative Freq.
2.0
1.0
0.0
Ci
VT (ml/kg)
20
10
0
Cii
Relative VT
1.0
0.0
0
6
12
Time (min)

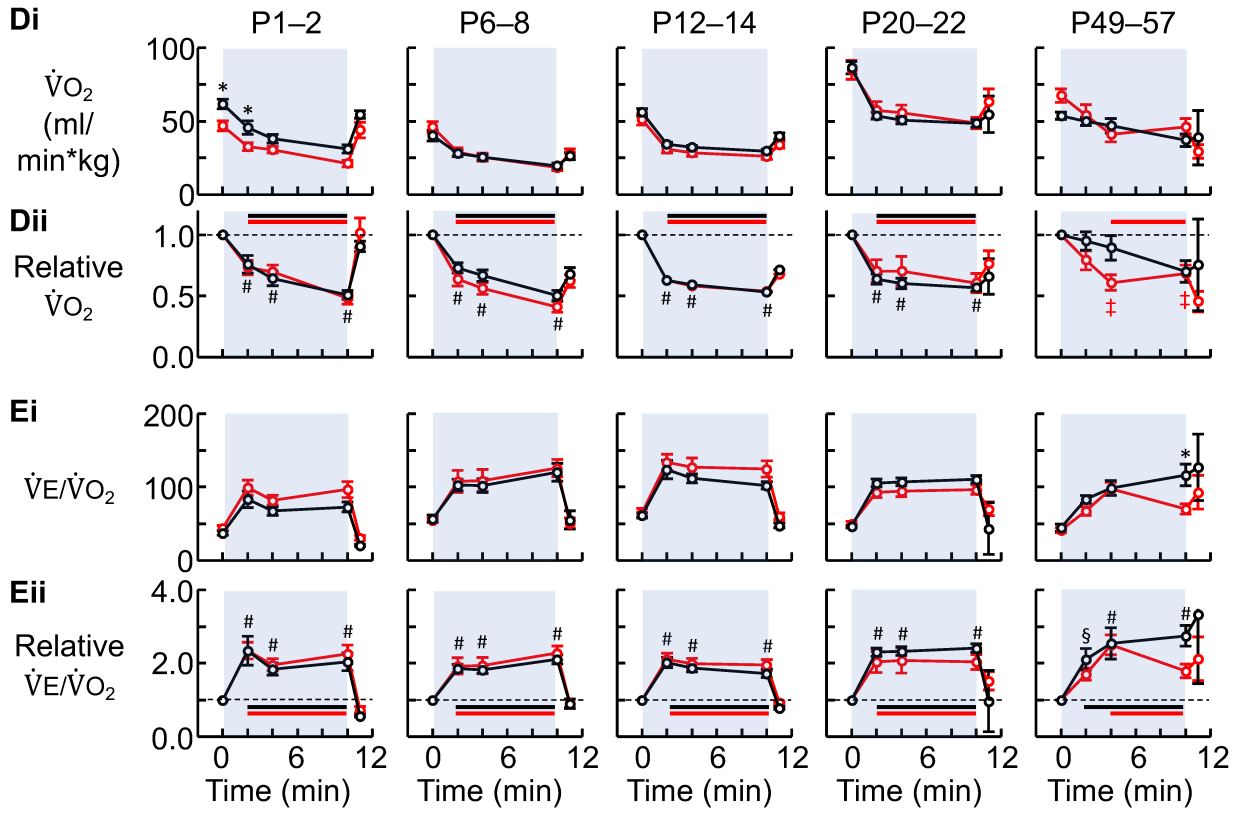

Figure 3.3. The effect of global ENT1/2 KO on ventilatory and metabolic responses to hypoxia through development from P1 until P57 compared to WT-FVB mice.
Time-course plots showing differences in the absolute (i) and relative (ii) changes in A) minute ventilation ($\dot{V}_E$), B) frequency, C) tidal volume (V_T), D) metabolic rate ($\dot{V}O_2$), and E) the air convection requirement ($\dot{V}_E/\dot{V}O_2$) measured using head-out (P1–P14) and barometric whole-body (P20–P57) plethysmography in WT and ENT1/2 KO mice in response to a 10-minute, 10% O_2 hypoxic stimulus. Developmental comparisons were made at P1–2 (WT: n = 15, ENT1/2 KO: n = 20), P6–8 (WT: n = 15, ENT1/2 KO: n = 14), P12–14 (WT: n = 16; ENT1/2 KO: n = 13), P20–22 (WT: n = 12, ENT1/2 KO: n = 11), and P49–57 (WT: n = 10, ENT1/2 KO: n = 11). All statistical tests were performed on absolute data using a two-way ANOVA with Sidak's post hoc comparison. For clarity, significant differences between strains are shown on the plots of absolute data (Ai, Bi, Ci, etc); *signifies a difference ($P < 0.05$) between the strains. Significant differences from absolute baseline values within a strain are shown on the plots of relative data (Aii, Bii, Cii, etc) with the following symbols: §indicates a significant difference from baseline in the FVB group; ‡indicates a difference from baseline in the ENT1/2 KO group; and #indicates significant difference from baseline in both groups. Black and red bars in relative time-course graphs designate periods when each parameter is significantly different from baseline in the WT or ENT1/2 KO groups, respectively.

different from baseline in the WT and ENT1/2 KO groups using black and red bars, respectively in relative time-course graphs.

Minute Ventilation ($\dot{V}_E$)

As seen with the baseline $\dot{V}_E$ in the two strains (Fig. 3.2), I found only one difference across all age groups in the absolute values of $\dot{V}_E$ during hypoxia. At P12–14, $\dot{V}_E$ of WTs at the onset (20 sec) of hypoxia was significantly greater than in ENT1/2 KO mice (vs. WT, 4973 ± 437 ml/min/kg; ENT1/2 KO, 3944 ± 411 ml/min/kg; $p = 0.05$) (Fig. 3.3Ai).

I then compared within each strain when during hypoxia $\dot{V}_E$ differed from baseline values. During the transition period when O_2 levels in the chamber fell from 21% to 10%, $\dot{V}_E$ increased 54 ± 6% ($p < 0.0001$) above baseline in P1–2 WTs and 55 ± 8% ($p < 0.0001$) above baseline in ENT1/2 KOs. $\dot{V}_E$ remained elevated above baseline through the first two minutes of hypoxia (for both strains: $p < 0.0001$) before returning to baseline at the 4-minute timepoint of hypoxia in both strains (Fig. 3.3Aii). P6–8 WT mice increased $\dot{V}_E$ by 60 ± 6% ($p < 0.0001$) at the onset of hypoxia, by 40 ± 4% throughout the first minute ($p < 0.0001$), and by 30 ± 4% through the second minute ($p = 0.003$) (Fig. 3.3Aii). In contrast, $\dot{V}_E$ of P6–8 ENT1/2 KO mice initially increased 32 ± 4% ($p < 0.0001$) during the transition to hypoxia and 23 ± 3% ($p = 0.01$) in the first minute but was not significantly different than baseline during the second minute of the hypoxic challenge (14 ± 3%, $p = 0.32$) (Fig. 3.3Aii). At P12–14, WTs quickly increased $\dot{V}_E$ above baseline at the onset of hypoxia (40 ± 7%, $p < 0.0001$) (Fig. 3.3Aii). $\dot{V}_E$ remained elevated above baseline in the WT mice at the end of the first minute of hypoxia when the increase in ENT1/2 KO mice also reached significance (WT, 28 ± 6%, $p = 0.05$; ENT1/2 KO, 44 ± 11%, $p = 0.01$). $\dot{V}_E$ then returned to baseline in both strains by the end of the second minute (Fig. 3.3Aii). At P20–22, both strains significantly increased $\dot{V}_E$ relative to baseline at the onset of hypoxia by ~60% (WT, $p < 0.0001$; ENT1/2 KO, $p = 0.0003$) (Fig. 3.3Aii) and it remained elevated at the end of the first minute of hypoxia (WT, 56 ± 13% $p < 0.0001$; ENT1/2 KO, 37 ± 19% $p = 0.01$). $\dot{V}_E$ remained elevated in P20–22 WTs during the 2nd (39 ± 8%, $p = 0.0005$), 4th (38 ± 8%, $p = 0.0009$) and 10th min of hypoxia (35 ± 6%, $p = 0.0014$), but fell to baseline in ENT1/2 KOs before the end of minute two (29 ± 21%, $p = 0.28$) (Fig. 3.3Aii). Finally, $\dot{V}_E$ in P49–56 adult WT mice increased relative to

baseline at the onset of hypoxia (WT, 126 ± 17%, $p < 0.0001$) and remained elevated throughout the hypoxic period (minute 1; 105 ± 14%, $p < 0.0001$; minute 2, 86 ± 14%, $p < 0.0001$; minute 4, 98 ± 14%, $p < 0.0001$; minute 10, 84 ± 17%, $p < 0.0001$). In contrast, $\dot{V}_E$ in the adult ENT1/2 KO mice increased relative to baseline at the onset of hypoxia (ENT1/2 KO, 69 ± 27% $p < 0.0001$) and during the first minute (ENT1/2 KO, 35 ± 16% $p = 0.005$), fell to baseline in minute 2, increased in the fourth minute (ENT1/2 KO, 42 ± 14%, $p = 0.006$) and fell once again to baseline levels by minute 10 (Fig. 3.3Aii). In summary, similar to the frequency responses, at every age the duration of the $\dot{V}_E$ increase was reduced in ENT1/2 KO mice; in addition, the reduction in the duration of the $\dot{V}_E$ increase in ENT1/2 KO mice appeared to increase with development.

Respiratory Frequency

To assess whether knockout of ENT1/2 had any effect on breathing pattern responses to hypoxia during development, I first compared frequency responses between the WT and ENT1/2 KO mice, at the five time points. Between strains, I compared the absolute frequency at every timepoint during hypoxia but found no significant differences in any of the developmental stages studied (Fig. 3.3Bi), other than baseline differences at P6–8 and P49–57 discussed earlier (Fig. 3.2C).

I then examined within each strain when the frequency in hypoxia differed from the baseline values. In P1–2 mice, frequency increased significantly in both WTs (43 ± 7% ($p < 0.0001$) and ENT1/2 KOs (30% ± 4%, $p < 0.0001$) at the onset of hypoxia (Fig. 3.3Bii). In P1–2 WTs, frequency remained elevated throughout the first two minutes of hypoxia (1 min: 34 ± 5%, $p = 0.0001$; 2 min: 34 ± 6%, $p = 0.0001$), while frequency of the ENT1/2 KOs returned to baseline during the first minute of the hypoxic stimulus (11% ± 5%, $p = 0.58$). At P6–8, breathing frequency in WTs increased by 19 ± 3% ($p = 0.001$) at the onset of hypoxia, while breathing rate was not elevated above baseline at any point in the ENT1/2 KO group. In P12–14 mice, frequency of WTs was significantly increased at least 17 ± 4% throughout the duration of hypoxia (all timepoints: $p < 0.0001$) (Fig. 3.3Bii). In contrast, breathing frequency of P12–14 ENT1/2 KOs remained significantly increased at the onset (23 ± 3%, $p < 0.0001$), during the first (16 ± 2% $p < 0.0001$), second (13 ± 2%, $p = 0.0004$) and fourth minutes (11 ± 3%, $p = 0.002$) before falling to baseline by end of the 10-minute hypoxic exposure (Fig. 3.3Bii). At P20–22, frequency was increased by ~30–40% throughout hypoxia in both strains (all timepoints, both groups: $p < 0.0001$) (Fig. 3.3Bii).

In the final developmental P49–57 window, frequency was increased by ~70% in WT mice from the onset of hypoxia through the final 10-minute timepoint ($p < 0.0001$). On the other hand, ENT1/2 KO increased breathing frequency by 23 ± 10% ($p = 0.001$) at the onset of hypoxia, 24 ± 7% ($p = 0.0007$) during the first minute, 26 ± 7% ($p = 0.0001$) in the second minute, and 24 ± 8% ($p = 0.0008$) in the fourth minute of hypoxia, but frequency was not significantly elevated by the end of hypoxia (10 ± 8%, $p = 0.69$) (Fig. 3.3Bii). Thus, at every age except P20–22 where the frequency increase was sustained through hypoxia, the duration of the frequency increase was reduced in ENT1/2 KO mice and the reduction in the duration of the response between the WT and ENT1/2 KO mice appeared to increase with development.

Tidal Volume

I next compared how changes in tidal volume (V_T) in hypoxia differed between WT mice and ENT1/2 KO animals during developmental. In absolute terms, there were only a few differences between the groups at each period of development. The only difference was detected in the P1–2 mice, in which V_T of WTs was significantly greater than ENT1/2 KOs during baseline and at the onset (20 sec) of hypoxia (WT, 16 ± 1 ml/kg; ENT1/2 KO, 13 ± 1 ml/kg, $p = 0.0001$) (Fig. 3.3Ci).

Relative to pre-hypoxic values, V_T of P1–2 WTs was only significantly increased at the onset of hypoxia (19 ± 2%, $p = 0.003$) and fell 17 ± 3% below baseline at 10 minutes of the hypoxic stimulus ($p = 0.007$), whereas in ENT1/2 KOs, V_T was elevated significantly during the transition period (22 ± 4%, $p = 0.004$), 1st minute (40 ± 4%, $p < 0.0001$) and 2nd minute (32 ± 4%, $p < 0.0001$,) of hypoxia (Fig. 3.3Cii). In P6–8 mice, V_T was elevated above baseline levels in both WT and ENT1/2 KOs at the onset (WT, 36 ± 6%, $p < 0.0001$; ENT1/2 KO, 22 ± 3%, $p = 0.03$) and during the first minute of hypoxia (26 ± 3%, $p = 0.0004$; ENT1/2 KO, 20 ± 5%, $p = 0.03$). Unlike WT mice between P12–14, who initially increased V_T by 20 ± 2% ($p = 0.02$) at the onset of hypoxia before V_T significantly decreased 23 ± 2% below baseline by minute 10 of hypoxia ($p = 0.002$), V_T did not significantly change from baseline during hypoxia in P12–14 ENT1/2 KO animals (Fig. 3.3Cii). At P20–22, V_T was only significantly increased from baseline in WT mice at the onset of hypoxia (20 ± 5%, $p = 0.002$) (Fig. 3.3Cii). In mice tested between P49–57, WTs exhibited a longer duration increase in V_T that began at the onset of hypoxia (32 ± 7%, $p < 0.0001$), extended to the first minute of hypoxia (20 ± 4%, $p = 0.01$) and then increased significantly again in the fourth

minute of hypoxia (19 ± 5%, p = 0.01). In contrast, V_T only increased at the onset of hypoxia (30 ± 13%, p < 0.0001) in the KO mice and fell back to baseline by the end of the first minute (8 ± 8%, p = 0.39) (Fig. 3.3Cii). Overall, there were few differences in the magnitude or the duration of the V_T response to hypoxia between strains during development.

Metabolic Rate ($\dot{V}O_2$)

There were very few differences in metabolic responses of WT and ENT1/2 KOs mice to hypoxia. The only difference in absolute $\dot{V}O_2$ values between the two strains was seen at P1–2 when WT mice had higher levels of $\dot{V}O_2$ at baseline and after 2 min of hypoxia (WT, 48 ± 5 ml/min/kg; ENT1/2 KOs, 33 ± 3 ml/min/kg, p = 0.04) (Fig. 3.3Di).

In every age group between P1–2 and P20–22, both WT and ENT1/2 KO mice significantly reduced $\dot{V}O_2$ between ~30–40% from control levels in the 2nd and 4th minute of hypoxia (all ages: p ≤ 0.002) before falling to ~50% relative of baseline by the 10th minute of hypoxia (all ages: p < 0.0001) (Fig. 3.3Dii). At P49–57 however, the metabolic responses differed between strains. $\dot{V}O_2$ was not different from baseline at any time point during hypoxia in the WT mice (p > 0.07), while the hypoxic depression of $\dot{V}O_2$ in the ENT1/2 KO mice also took longer to develop than in younger age groups. The decrease in $\dot{V}O_2$ was not significantly different from baseline until the fourth (39 ± 6%, p = 0.0008) and tenth minute (32 ± 7%, p = 0.008) of hypoxia. Thus, loss of ENT1/2 produced a hypoxic hypometabolic response through adulthood, which was not seen in WT mice with endogenous ENT activity.

Air Convection Requirement ($\dot{V}E/\dot{V}O_2$)

Finally, I compared changes in $\dot{V}E/\dot{V}O_2$ during hypoxia between the two strains. I found no differences in absolute $\dot{V}E/\dot{V}O_2$ values between strains during hypoxia in any age group, except for P49–57 mice, where $\dot{V}E/\dot{V}O_2$ was significantly increased in the WTs (117 ± 15 a.u) compared to ENT1/2 KOs at the 10-minute point of hypoxia (70 ± 7 a.u, p = 0.0005) (Fig. 3.3Ei).

Relative to baseline, $\dot{V}E/\dot{V}O_2$ increased in both strains similarly between P1–P22. In P1–2 mice, $\dot{V}E/\dot{V}O_2$ increased > 130% in the second minute of hypoxia (WT, p = 0.0002; ENT1/2 KO, p < 0.0001), dropping slightly in the fourth minute (WT, 84 ± 17%, p = 0.03; ENT1/2 KO, 96 ± 17%,

p = 0.0006) but increasing to more than double by the 10th minute (WT, 104 ± 24%, p = 0.006; ENT1/2 KO, 126 ± 24%, p < 0.0001) (Fig. 3.3Eii). In both strains of P6–8 mice, $\dot{V}_E/\dot{V}_{O_2}$ increased by ~90% in the 2nd minute and 4th minute of hypoxia before increasing further to 111 ± 12% (WT) and 128 ± 19% (ENT1/2 KO, all timepoints of both strains: p < 0.0001) by the 10th minute (Fig. 3.3Eii). In P12–14 mice, $\dot{V}_E/\dot{V}_{O_2}$ approximately doubled in the second (WT, 102 ± 14%; ENT1/2 KO: 87 ± 12, both strains p = 0.0001) and fourth minute of hypoxia (WT, 87 ± 11%, p = 0.0002; ENT1/2 KO, 98 ± 15%, p = 0.0001), remaining > 70% above baseline at the end of hypoxia (WTs, p = 0.003; ENT1/2 KO, p = 0.0001) (Fig. 3.3Eii). Likewise, P20–22 mice increased $\dot{V}_E/\dot{V}_{O_2}$ more than double throughout the 10% O_2 exposure (both stains, each timepoint: p < 0.0001) (Fig. 3.3Eii). There were differences $\dot{V}_E/\dot{V}_{O_2}$ response at P49–57 as only WT mice increased $\dot{V}_E/\dot{V}_{O_2}$ by 110 ± 29% at 2 minutes in hypoxia (p = 0.005), whereas the increase of $\dot{V}_E/\dot{V}_{O_2}$ was not significant in ENT KOs (p = 0.07). By the fourth minute of hypoxia, $\dot{V}_E/\dot{V}_{O_2}$ increased by 154 ± 43% in WTs and 150 ± 27% in ENT1/2 KOs above baseline (p < 0.0001) and remaining elevated by 175 ± 28% and 79 ± 18% at 10 minutes of hypoxia in WT (p < 0.0001) and KOs (p = 0.03), respectively (Fig. 3.3Eii).

In summary, despite differences between strains in terms of their relative hypoxic $\dot{V}_E$ responses, both strains of mice at all ages responded to hypoxia with a sustained increase in $\dot{V}_E/\dot{V}_{O_2}$; the only difference was a modest reduction in the duration of the increase in $\dot{V}_E/\dot{V}_{O_2}$ in the oldest group of ENT1/2 KO mice.

3.3.3 Adenosine Kinase (ADK)

Pharmacological inhibition of ADK has greater depressive effects on baseline ventilation and metabolism in older mice

My next objective was to explore the hypothesis that postnatal maturation of ADK-S is an important factor in the maturation of the HVR$_{\dot{V}_E}$; i.e., the lack, or low level of ADK-S in the brain at birth is a key contributor the inability of neonates to produce a sustained increase in $\dot{V}_E$ during hypoxia. For reasons described previously, I focused on ADK-S because its expression is very low at birth and reaches adult levels by third week of life in the cortex, cerebellum (Gebril et al., 2021; Studer et al., 2006) and brainstem (Fig. 2.7, 2.8). In addition, the conversion of ADOi into AMPi by ADK-S supports ENT-mediated clearance of ADOe. Thus, lack of ADK-S at birth will

compromise ADOe clearance and attenuate the hypoxic excitation of $\dot{V}_E$. I utilized a pharmacological approach to acutely inhibit ADK using intraperitoneal injections of ABT 702 (10 mg/kg). The rationale for this experiment was that if ADK function is minimal at birth and increases with development, pharmacological inhibition of ADK should have minimal effect on ventilatory parameters at birth. With development, ADK inhibition should progressively attenuate the magnitude and/or duration of the hypoxic increase in $\dot{V}_E$. I could not predict the effects of ADK inhibition on the $\dot{V}_{O_2}$ response because the developmental role of ADK-S in metabolic regulation is not known.

Before testing whether pharmacological inhibition of ADK affected the ventilatory and metabolic responses to hypoxia, I first tested the effects of ABT 702 on baseline $\dot{V}_E$ and $\dot{V}_{O_2}$ in WT mice (Fig. 3.4). I compared drug-injected animals to vehicle-injected (0.6% DMSO in 0.9% saline, i.p.) controls at P0–2, P11–12, and P20. When ADK-S expression in the brainstem reaches adult levels (Fig. 2.7, 2.8). At P0–2, the only significant effect of ABT 702 was a reduction in respiratory frequency from 161 ± 24 bpm in the vehicle group to 95 ± 20 bpm ($p = 0.04$) in the ABT 702 group (Fig. 3.4B**)**. $\dot{V}_E$, V_T, $\dot{V}_{O_2}$, and $\dot{V}_E/\dot{V}_{O_2}$ were not significantly affected ABT 702 at this age. In contrast, at P11–12 and P20 ABT 702 caused a significant reduction in all parameters except $\dot{V}_E/\dot{V}_{O_2}$. At P11–12, ABT 702 caused $\dot{V}_E$ to decrease to almost one third of normal baseline levels from 3535 ± 416 ml/min/kg in vehicle to 1280 ± 136 ml/min/kg in ABT 702 ($p = 0.0009$) (Fig. 3.4A). Frequency fell ~25% from 248 ± 10 bpm in vehicle to 175 ± 13 bpm ($p = 0.03$) in ABT 702 (Fig. 3.4B), while V_T fell almost 50% from 14.2 ± 1.5 ml/kg in vehicle to 7.3 ± 0.6 ml/kg ($p = 0.0009$) in ABT 702 (Fig. 3.4C). Like $\dot{V}_E$, $\dot{V}_{O_2}$ fell ~67% from 68 ± 7 ml/min/kg in vehicle or 22 ± 1 ml/min/kg ($p = 0.004$) in ABT 702 (Fig. 3.4D). Similarly, in P20 mice, $\dot{V}_E$ was depressed by more than half in ABT 702-treated mice (3218 ± 628 ml/min/kg) relative to vehicle treated mice (6581 ± 467 ml/min/kg, $p < 0.0001$) (Fig. 3.4A). Respiratory frequency fell by one-third in ABT 702 from 363 ± 21 bpm to 238 ± 13 bpm ($p = 0.0001$) (Fig. 3.4B), as did V_T from 18.3 ± 1.2 ml/min in vehicle-treated mice to 13.2 ± 1.8 ml/min in ABT 702 ($p = 0.02$) (Fig. 3.4C). In P20 mice, ABT 702 caused similar reductions in $\dot{V}_{O_2}$ as $\dot{V}_E$, reduced by half (56 ± 10 ml/min/kg) relative to vehicle controls (118 ± 14 ml/min/kg, $p = 0.0001$) (Fig. 3.4D). Notably, $\dot{V}_E/\dot{V}_{O_2}$ was not affected by ABT 702 at any age (Fig. 3.4E).

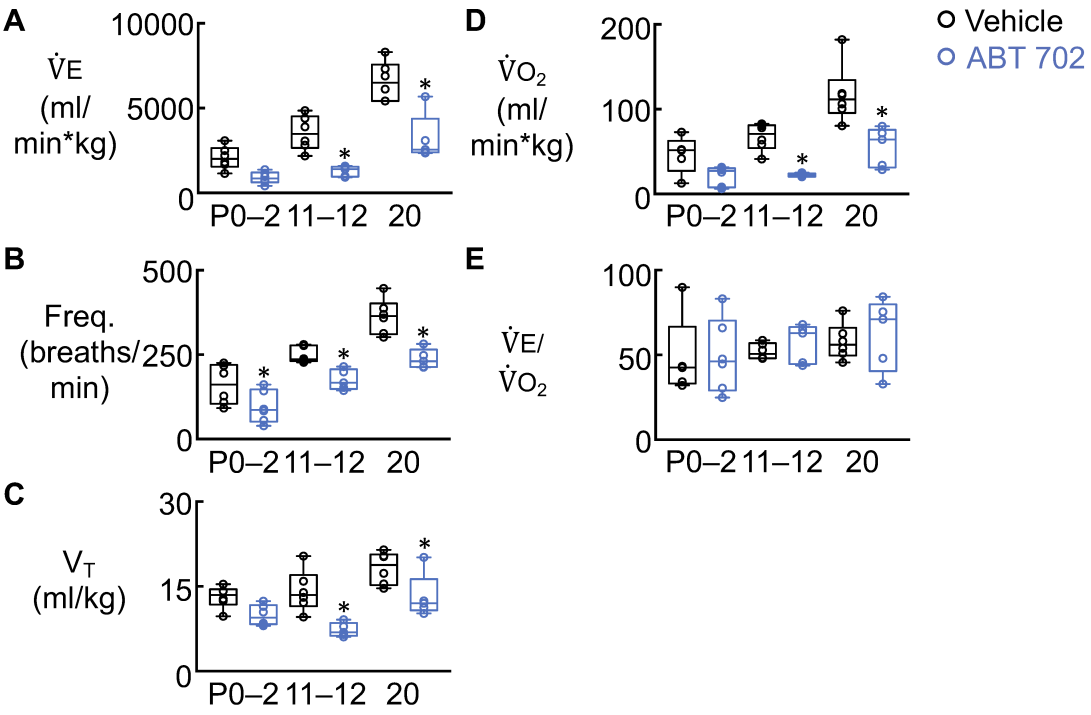

Figure 3.4. The effect of ADK inhibition using ABT 702 (10 mg/kg, i.p.) on baseline ventilatory and metabolic parameters in P0 to P20 FVB mice.

Summary box and whisker plots compare the basal measurements of A) minute ventilation ($\dot{V}_E$), B) ventilatory frequency, C) tidal volume (V_T), D) metabolic rate ($\dot{V}_{O_2}$), and E) the air convection requirement ($\dot{V}_E/\dot{V}_{O_2}$) between vehicle- (0.6% DMSO in 0.9% saline, 10 mg/kg, i.p.) and ABT 702-treated (ADK inhibitor, 10 mg/kg, i.p.) mice at P0–2 (Vehicle: n = 6, ABT 702: n = 6), P11–12 (Vehicle: n = 6, ABT 702: n = 5), and P20 (Vehicle: n = 6, ABT 702: n = 5) *indicates significant difference ($P < 0.05$) between treatment groups at specific ages, as determined using one-way ANOVA with Sidak's *post hoc* test.

Two key observations are first that the effects of ABT 702 on ventilation and metabolic rate emerged between P0–2 and P11–12, providing functional corroboration of expression data and indicates ADK-S activity is low at birth and matures thereafter. Second, the observation that ABT 702 had no effect on $\dot{V}_E/\dot{V}_{O_2}$ at any age indicates that the changes in $\dot{V}_E$ were proportional to reductions in $\dot{V}_{O_2}$. This, in turn suggests that the primary effect of ABT 702 was to inhibit $\dot{V}_{O_2}$, that all changes in $\dot{V}_E$, frequency and V_T were subsequent to drop on metabolic rate and that homeostatic reflexes responsible for matching $\dot{V}_E$ to $\dot{V}_{O_2}$ were not affected by ABT 702.

Effect of ADK inhibition on ventilatory and metabolic responses to hypoxia

Minute Ventilation ($\dot{V}_E$)

I then tested the effects of ABT 702 on the ventilatory and metabolic responses to hypoxia in WT mice during the first three weeks of development. Data in Fig. 3.5 are presented using the same format and conventions used in Fig. 3.3 to show significance between strains and then within each strain to show differences between the value of specific parameter during hypoxia compared to baseline. In P0–2 mice, $\dot{V}_E$ was significantly greater in vehicle-treated mice throughout the first 2 minutes of hypoxia. During the 10 s transition and at 1 min and 2 min of hypoxia, $\dot{V}_E$ in vehicle and ABT 702 groups, respectively was 2223 ± 294 ml/min/kg vs 958 ± 224 ml/min/kg ($p = 0.03$); 2846 ± 438 ml/min/kg vs 1320 ± 295 ml/min/kg ($p = 0.004$) and 2741 ± 362 ml/min/kg vs. 1442 ± 425 ml/min•kg, ($p = 0.03$) (Fig. 3.5Ai). After 10 minutes in hypoxia, $\dot{V}_E$ fell in the vehicle group back to control levels that were similar to the ABT 702 group. In P11–12 mice, $\dot{V}_E$ of ABT 702-treated animals was significantly lower than controls throughout hypoxia including through the transition to 10% O_2 (Vehicle: 3766 ± 433 ml/min/kg vs. ABT 702: 1403 ± 146 ml/min/kg, $p < 0.0001$), as well as through the first (Vehicle: 5044 ± 441 ml/min/kg vs. ABT 702: 2259 ± 296 ml/min/kg, $p < 0.0001$), second (Vehicle: 4685 ± 375 ml/min/kg vs. ABT 702: 2455 ± 322 ml/min/kg, $p = 0.0001$) and tenth minute of the stimulus (Vehicle: 3295 ± 171 ml/min/kg vs. ABT 702: 1825 ± 241 ml/min/kg, $p = 0.02$) (Fig 3.5Ai). At P20, $\dot{V}_E$ was significantly greater in vehicle-treated mice but only through the first minute and after 10 minutes of hypoxia. During the transition and at 1 min, $\dot{V}_E$ in vehicle and ABT 702 groups, respectively was 9165 ± 1019 ml/min/kg vs. 5296 ± 1150 ml/min/kg ($p = 0.005$) and 8378 ± 995 ml/min/kg vs. 5136 ± 909

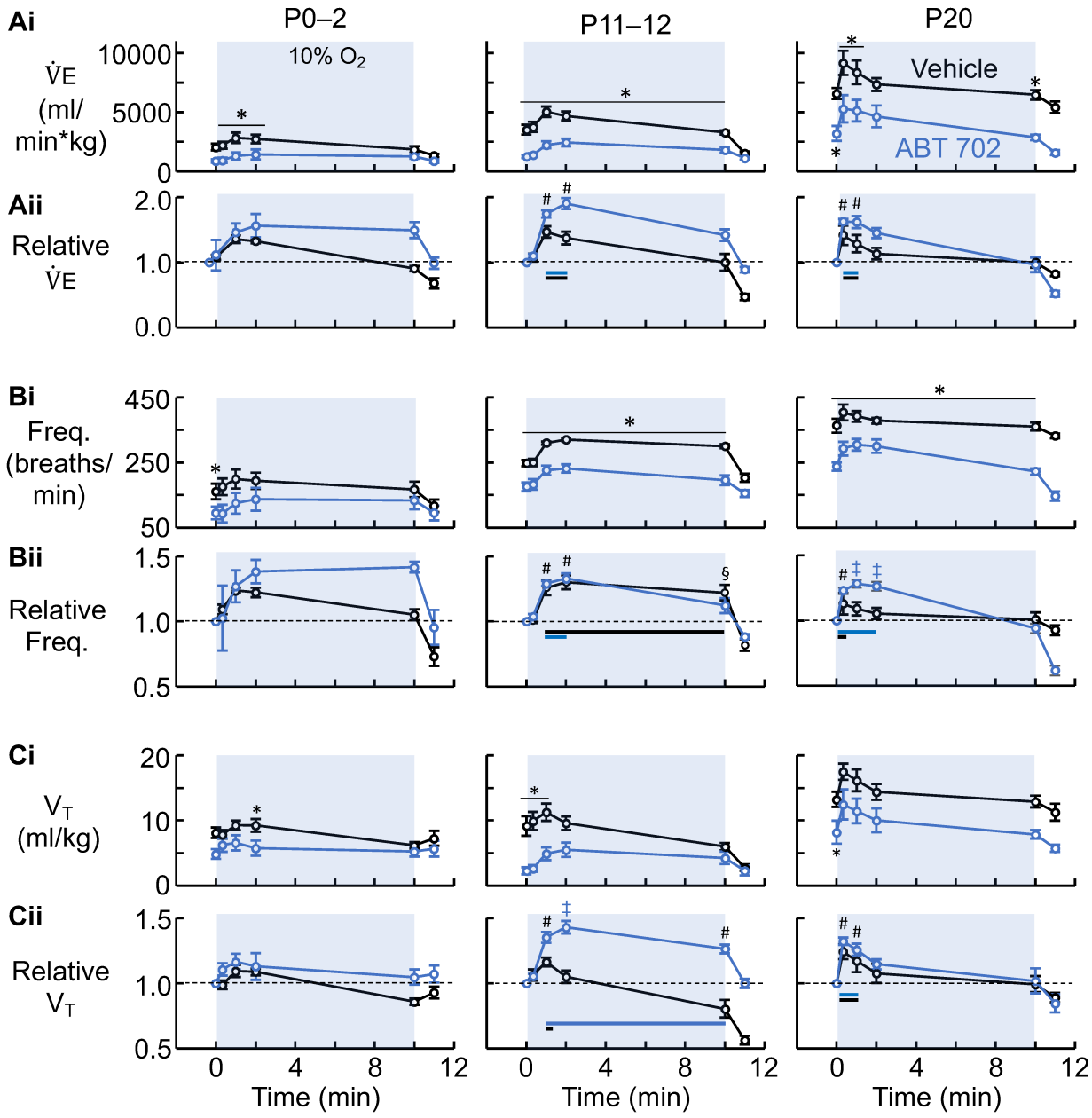
Ai
P0–2
P11–12
P20
10% O2
Vehicle
ABT 702
V̇E (ml/ min*kg)
10000
5000
0
Aii
Relative V̇E
2.0
1.0
0.0
Bi
Freq. (breaths/ min)
450
250
50
Bii
Relative Freq.
1.5
1.0
0.5
Ci
VT (ml/kg)
20
10
0
Cii
Relative VT
1.5
1.0
0.5
0
4
8
12
Time (min)

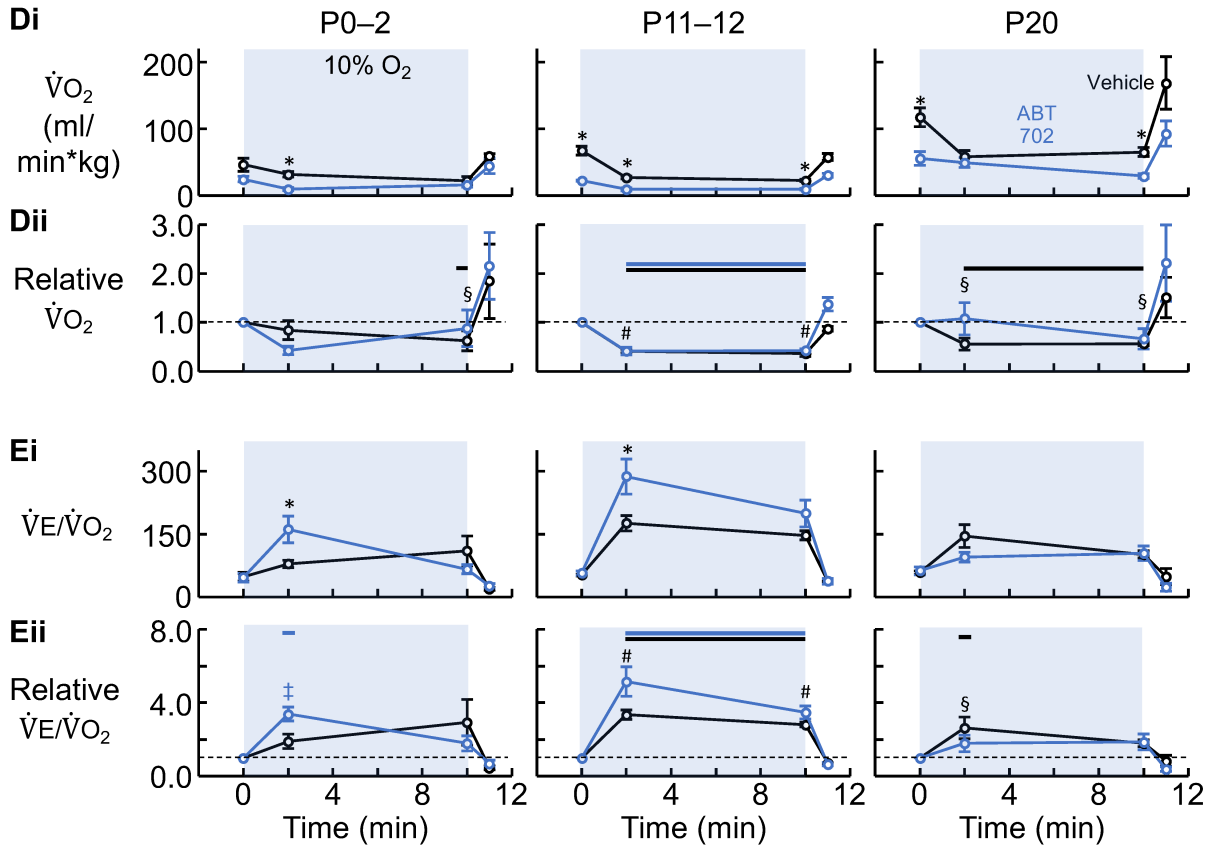

Figure 3.5. The effects of blocking ADK activity using ABT 702 (i.p.) on the kinetics of the ventilatory and metabolic responses to hypoxia during development between P0 and P20 in FVB mice.

Time-course plots showing the absolute (i) and relative (ii) changes in A) minute ventilation ($\dot{V}_E$), B) frequency, C) tidal volume (V_T), D) metabolic rate ($\dot{V}_{O_2}$), and E) the air convection requirement ($\dot{V}_E/\dot{V}_{O_2}$) measured using head-out (P0–P12) and barometric whole-body (P20) plethysmography in vehicle (0.6% DMSO in 0.9% saline, i.p.) (black) and ABT 702-treated mice (10 mg/kg, i.p.) (blue) in response to a 10-minute, 10% O_2 hypoxic stimulus. Developmental comparisons were made at P0–2 (Vehicle: n = 6, ABT 702: n = 6), P11–12 (Vehicle: n = 6, ABT 702: n = 5), and P20 mice (Vehicle: n = 6; ABT 702: n = 5). All statistical tests were performed using a two-way ANOVA with Sidak's *post hoc* comparison. Significant differences between strains are shown on the plots of absolute data (Ai, Bi, Ci, etc.); *indicates significant differences ($P < 0.05$) between the groups. Significant differences from absolute baseline values within each group are shown on the plots of relative data (Aii, Bii, Cii, etc) with the following symbols: §signifies a significant change from baseline in the vehicle-treated group; ‡signifies a difference from baseline in the ABT 702-treated group; and $^{\#}$signifies significant differences from baseline in both groups. Black and blue bars over relative time-course graphs designate periods which each parameter is significantly different from baseline in the vehicle or ABT 702 treated groups, respectively.

ml/min/kg ($p = 0.03$). Then at the end of hypoxia, $\dot{V}_E$ was 6463 ± 488 ml/min/kg in the vehicle group but 2870 ± 235 ml/min/kg in ABT 702-treated mice ($p = 0.01$) (Fig 3.5Ai).

Relative to their baseline values, $\dot{V}_E$ was not increased in vehicle-treated or ABT 702-treated mice at P0–2 (Fig. 3.5Aii). At P11–12, $\dot{V}_E$ increased in both groups for the first (Vehicle: 47 ± 9%, $p < 0.0001$; ABT 702: 75 ± 6%, $p = 0.003$) and second minute of hypoxia (Vehicle: 37 ± 10%, $p = 0.0001$; ABT 702: 90 ± 9%, $p = 0.0003$). In the third age group (P20), there were no differences in the time that $\dot{V}_E$ was elevated relative to baseline. $\dot{V}_E$ was increased 41 ± 15% and 63 ± 4% relative to baseline through the transition to 10% O_2 in vehicle and ABT 702, respectively. $\dot{V}_E$ remained throughout the first minute of hypoxia (Vehicle: 29 ± 13%, $p = 0.03$; ABT 702: 62 ± 9%, $p = 0.03$) but fell to baseline thereafter (both groups: $p > 0.16$) (Fig. 3.5Aii).

Respiratory Frequency

Respiratory frequency was significantly greater in vehicle-treated P0–2 mice compared to ABT 702 mice in normoxia (Fig. 3.4) but this difference was lost upon exposure to hypoxia (Fig. 3.5Bi). At P11–12, the reduction in baseline frequency observed in ABT 702-treated mice persisted throughout the hypoxic period including during the 10 s transition (Vehicle: 250 ± 12 bpm vs. ABT 702: 183 ± 16 bpm, $p = 0.0005$), at 1 min (Vehicle: 310 ± 5 bpm vs. ABT 702: 226 ± 15 bpm, $p < 0.0001$) and 2 min of hypoxia (Vehicle: 320 ± 5 bpm vs. ABT 702: 232 ± 13 bpm, $p < 0.0001$). By the end of hypoxia, frequency remained elevated (300 ± 6 bpm) in the vehicle-treated group relative to ABT 702-treated mice (195 ± 15 bpm, $p < 0.0001$). Similarly, in the third age group (P20), the depression of baseline frequency by ABT 702 continued through the hypoxic exposure. During the transition to 10% O_2 and at 1 min, 2 min and 10 min of hypoxia, frequency in vehicle and ABT 702 groups, respectively was 403 ± 24 bpm vs. 293 ± 21 bpm ($p = 0.0003$); 391 ± 17 bpm vs. 305 ± 18 bpm ($p = 0.005$); 378 ± 9 bpm vs. 300 ± 21 bpm ($p = 0.02$); and 360 ± 12 bpm vs. 222 ± 10 bpm ($p < 0.0001$) (Fig. 3.5Bii).

In relative terms, at P0–2 neither vehicle- nor ABT 702-treated mice increased frequency at any point during hypoxia (Fig. 3.5Bii). At P11–12, frequency was increased ~30% ($p < 0.0001$) for the first and second minutes of hypoxia in both groups, but by the end of hypoxia, only vehicle-treated mice showed a sustained increase in frequency above baseline (Vehicle: 22 ± 6%, $p < 0.0001$;

ABT 702: 12 ± 6%, p = 0.18). P20 mice from both treatment groups increased breathing frequency at the onset of hypoxia (Vehicle: 13 ± 8%, p = 0.04; ABT 702: 23 ± 2%, p = 0.007), although frequency fell immediately after back to baseline in vehicle-treated mice (1 min: 9 ± 5%, p = 0.23), while frequency in ABT 702 mice was sustained above baseline through the first (28 ± 3%, p = 0.0008) and second minute of hypoxia (26 ± 3%, p = 0.002).

Tidal Volume

Next, I examined the effect of ABT 702-mediated ADK inhibition of hypoxic changes in V_T. I found that there were very little differences between the vehicle and drug treatment group at P0–2, V_T was decreased in the second minute of hypoxia in the ABT 702 group (Vehicle: 14.3 ± 1.0 ml/min/kg vs. ABT 702: 10.8 ± 1.2 ml/min/kg, p = 0.04). In P11–12 mice, the reduction in V_T in normoxia persisted through the transition to 10% O_2 and the first minute of hypoxia, as V_T was 14.9 ± 1.4 ml/min/kg vs. 7.7 ± 0.5 ml/min/kg (p = 0.0001) and 16.3 ± 1.3 ml/min/kg vs. 9.9 ± 1.0 ml/min/kg (p = 0.0009) in the vehicle and ABT 702-treated groups, respectively (Fig. 3.5Ci). While baseline V_T was depressed by ABT 702 in P20 mice, there were no differences between treatment groups throughout hypoxia (each timepoint: p > 0.1) (Fig. 3.5Ci).

At P0–2, V_T was not different from baseline throughout hypoxia in either vehicle (p > 0.4) or ABT 702 group (p > 0.5) (Fig. 3.5Cii). At P11–12, V_T was increased in both groups during the first minute of hypoxia (Vehicle: 16 ± 3%, p = 0.008; ABT 702: 35 ± 4%, p = 0.002), but fell to baseline by the second minute in the vehicle-treated group (p = 0.76). V_T was elevated 43 ± 5% (p = 0.0002) and 26 ± 3% (p = 0.03) above baseline at 2 and 10 minutes of hypoxia in ABT 702, while V_T of vehicle-treated mice depressed 19 ± 7% below baseline after 10 minutes (p < 0.0001) (Fig. 3.5Cii). In the third age window (P20), hypoxia evoked 24 ± 6% (p = 0.0014) and 32 ± 3% (p = 0.004) increases in V_T during the transition to 10% O_2 and 17 ± 9% (p = 0.04) and 26 ± 5% (p = 0.03) through the first minute in vehicle and drug-treated mice, respectively. V_T was not significant from baseline in either group thereafter.

Metabolic Rate ($\dot{V}O_2$)

At P0–2, $\dot{V}O_2$ was reduced by two-thirds at 2 minutes in hypoxia in ABT 702 (10 ± 2 ml/min/kg) relative to the vehicle group (32 ± 3 ml/min/kg, p = 0.03), however $\dot{V}O_2$ in the control group fell

to similar levels by the end of hypoxia (p = 0.8) (Fig. 3.5Di). The significant reduction in basal $\dot{V}O_2$ in P11–12 ABT 702-treated mice relative to vehicle controls continued throughout hypoxia. $\dot{V}O_2$ at 2 min and 10 min in the vehicle and drug-treatment group, respectively was 27 ± 2 ml/min/kg vs. 10 ± 2 ml/min/kg (p = 0.003) and 23 ± 2 ml/min/kg vs. 10 ± 1 ml/min/kg (p = 0.03) (Fig. 3.5Di). In the P20 groups, while baseline $\dot{V}O_2$ was significantly reduced by ABT 702, the difference between groups disappeared in the second minute of hypoxia (Vehicle: 58 ± 9 ml/min/kg vs. ABT 702: 50 ± 7 ml/min/kg, p = 0.89). At the end of hypoxia, $\dot{V}O_2$ in vehicle (65 ± 7 ml/min/kg) was again higher than in ABT 702 (30 ± 4 ml/min/kg, p = 0.04) (Fig. 3.5Di).

Relative to baseline, $\dot{V}O_2$ responses differed in the vehicle and ABT 702-treated mice in the youngest mice and at P20. At P0–2, hypoxia evoked a 37 ± 20% depression in $\dot{V}O_2$ at the end of hypoxia (p = 0.009), however $\dot{V}O_2$ was different from baseline at any point in the neonate ABT 702 group (p > 0.1) (Fig. 3.5Dii). At P11–12, $\dot{V}O_2$ was reduced ~60% during hypoxia in both groups. At 2 minutes, $\dot{V}O_2$ fell to 58 ± 4% (Vehicle, p < 0.0001) and 58 ± 8% (ABT 702: p = 0.03) relative to baseline, remaining depressed at 10 minutes by 63 ± 6% (Vehicle: p < 0.0001) and 58 ± 4% (ABT 702, p = 0.03). In contrast, differences in the relative response of each group appeared again at P20. Hypoxia depressed $\dot{V}O_2$ by ~45% at 2 minutes (p = 0.001) and 10 minutes (p = 0.003) in vehicle-treated mice, whereas mice injected with ABT 702 did not depress $\dot{V}O_2$ at any point during hypoxia (2 min: +8 ± 33%, p = 0.90; 10 min: -33 ± 21%, p = 0.20) (Fig. 3.5Dii).

Air Convection Requirement ($\dot{V}E/\dot{V}O_2$)

The final parameter compared in this experiment was the air convection requirement, $\dot{V}E/\dot{V}O_2$. In normoxia, ABT 702 did not affect $\dot{V}E/\dot{V}O_2$ at any age (Fig. 3.4), however during hypoxia in P0–2 and P11–12 mice, $\dot{V}E/\dot{V}O_2$ was elevated in the ABT 702 treatment group (P0–2: 161 ± 32 a.u.; P11–12: 287 ± 42 a.u.) relative to vehicle controls (P0–2: 85 ± 10 a.u., p = 0.007; P11–12: 175 ± 18 a.u., p = 0.004) at 2 minutes before returning to a similar level by 10 minutes (p = 0.4) (Fig. 3.5Ei). At P20, there were no differences in $\dot{V}E/\dot{V}O_2$ between either group at 2 minutes (vehicle: 145 ± 27 a.u.; ABT 702: 95 ± 12 a.u., p = 0.09) or 10 minutes of hypoxia (vehicle: 102 ± 9 a.u.; ABT 702: 104 ± 17 a.u., p > 0.99) (Fig. 3.5Ei).

At P0–2, unlike the vehicle-treated mice that did not significantly increase $\dot{V}_E/\dot{V}_{O_2}$ at any point in hypoxia ($p > 0.08$), $\dot{V}_E/\dot{V}_{O_2}$ was increased 239 ± 38% ($p = 0.0002$) above baseline in ABT 702 treated mice at 2 minutes in hypoxia before falling back to pre-hypoxic levels by 10 minutes ($p = 0.8$) (Fig. 3.5Eii). Between 2 minutes and 10 minutes in hypoxia, $\dot{V}_E/\dot{V}_{O_2}$ fell 59% in the P0–2 ABT 702 treated mice ($p = 0.002$), a significant decrease which was not observed in vehicle controls ($p > 0.99$) (Fig. 3.5Eii). In the second age group (P11–12), hypoxia caused $\dot{V}_E/\dot{V}_{O_2}$ to increase 235 ± 26% (Vehicle) and 415 ± 80% (ABT 702, both groups: $p < 0.0001$) relative to baseline at 2 minutes and by 182 ± 13% (Vehicle, $p = 0.002$) and 247 ± 35% (ABT 702, < 0.0001) at 10 minutes (Fig. 3.5Eii). $\dot{V}_E/\dot{V}_{O_2}$ decreased 31% from 2 minutes to 10 minutes of hypoxia in the ABT 702 group ($p = 0.006$) but this intial increase in $\dot{V}_E/\dot{V}_{O_2}$ was sustained until the end of hypoxia in vehicle-treated mice ($p = 0.52$). In P20 mice, $\dot{V}_E/\dot{V}_{O_2}$ increased 163 ± 59% from baseline in vehicle treated mice at 2 minutes ($p = 0.003$), returning to pre-hypoxic levels at 10 minutes ($p = 0.19$). In the P20 ABT 702-treated mice $\dot{V}_E/\dot{V}_{O_2}$ was not elevated above baseline at any point ($p > 0.3$) (Fig. 3.5Eii).

Effects of ADK-S overexpression on growth, development of baseline ventilatory and metabolic parameters

I next examined the role of ADK-S in the development of the HVR using a transgenic model engineered to express in newborn mice adult levels of ADK-S. My rationale was that if low levels of ADK-S are responsible for the immature $HVR_{\dot{V}_E}$ in which mice cannot produce a sustained increase in $\dot{V}_E$ during hypoxia, neonatal mice that express adult levels of ADK-S at birth should have a mature $HVR_{\dot{V}_E}$ and $HVR_{\dot{V}_E/\dot{V}_{O_2}}$. I also predicted that the differences between the transgenic mice and WT mice would gradually disappear during development as the expression of endogenous ADK-S in WT mice gradually increased to match the levels in the transgenic mice.

To achieve this, I obtained a transgenic mouse from Dr. Boison at Rutgers University which was produced by inserting into the *Adk*$^{-/-}$ mouse that lacks the endogenous *Adk* gene, a transgene that ubiquitously expresses from conception, the mature short-isoform of ADK (ADK-S) specifically in the brain (Shen et al., 2012). The transgenic ADK (ADKtg) mice, were generated on a C57BL/6J background, thus all experiments were performed using these mice as the WT control.

Prior to testing the main hypothesis that introduction of ADK-S into the brains of neonatal mice

would produce mice with an adult like HVR, I first assessed whether introduction of the transgene for human ADK-S, and deletion of the endogenous *Adk*-gene (which also codes for ADK-L) affected growth or the baseline respiratory and metabolic behaviour of WT C57BL/6J mice. I plotted body weight vs age for both strains of mice from P0 and adulthood and performed linear regressions on data from the two strains. The slopes of the lines of best-fit line of the body weight vs. age relationship was similar for WT (0.38 ± 0.01) and ADKtg mice (0.40 ± 0.01, p = 0.22) (Fig. 3.6A). I then compared baseline ventilatory and metabolic parameter in the two strains in 5 different age groups P0–3, P6–7, P12–14, P19–23, and P43–56 mice.

At the earliest developmental time points, P0–3 and P6–7, ventilatory and metabolic parameters were all similar in WT and ADKtg mice (Fig. 3.6B-F). Breathing frequency remained similar between strains throughout the remainder of development and into adulthood (Fig. 3.6C). However, from P12–14 to adulthood, $\dot{V}_E$ (Fig. 3.6B) and V_T (Fig. 3.6D) were significantly reduced in ADKtg compared to WT mice.

At P12–14, $\dot{V}_E$ in WT was 3769 ± 185 ml/min/kg compared to 2741 ± 162 ml/min/kg (p = 0.0005), in Adktg mice; at P19–23 $\dot{V}_E$ was 3624 ± 338 ml/min/kg compared to 2482 ± 179 ml/min/kg (p < 0.0001) in ADKtg while at P43–56 $\dot{V}_E$ was 2868 ± 283 ml/min/kg vs. 1985 ± 134 ml/min/kg (p = 0.003) in ADKtg mice (Fig. 3.6B). The reduced $\dot{V}_E$ in ADKtg mice in the oldest three groups of mice was entirely due to reduced V_T. At P12–14, 20-23 and P43–55, V_T in WT and ADKtg mice, respectively was 16.9 ± 0.8 ml/kg vs. 11.1 ± 0.5 ml/kg (p < 0.0001), 15.7 ± 0.7 ml/kg vs. 11.7 ± 0.4 ml/kg (p < 0.0001) and 12.9 ± 0.4 ml/ kg vs. 10.1 ± 0.4 ml/kg (p = 0.002) (Fig. 3.6D). Like $\dot{V}_E$, baseline metabolic rate was reduced in ADKtg (46 ± 3 ml/min/kg) compared to WT mice (64 ± 3 ml/min/kg, p = 0.01) (Fig. 3.6E) at P12–14. $\dot{V}_{O_2}$ in ADKtg mice remained numerically lower that WT at P19–23 and P43–56, but these differences were not significant. As a result, baseline $\dot{V}_E/\dot{V}_{O_2}$ was similar in the two strains across all age groups, with the exception that at P6–7, $\dot{V}_E/\dot{V}_{O_2}$ in ADKtg mice 62 ± 4 a.u.) was increased relative to WT mice (45 ± 4 a.u., p = 0.005).

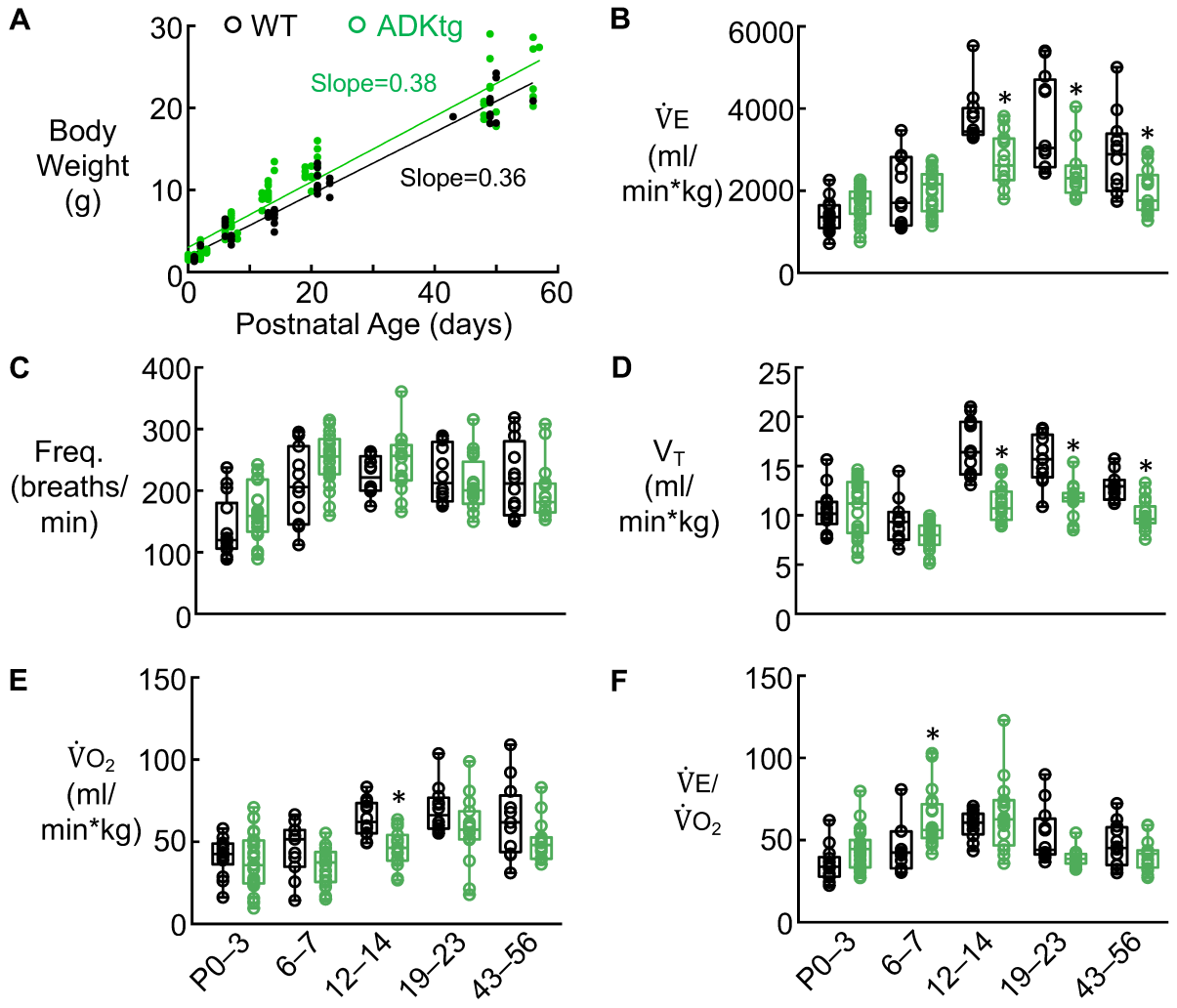

Figure 3.6. Comparison of baseline ventilatory and metabolic parameters between WT (C57BL/6J) and ADKtg mice during the first two months of development.
A) Linear regression comparing the body weight of WT C57BL/6J mice (black) and ADKtg mice (green) from P0 until P56. Summary box and whisker graphs compare the basal measurements of B) minute ventilation ($\dot{V}E$), C) ventilatory frequency, D) tidal volume (V_T), E) metabolic rate ($\dot{V}O_2$), and F) the air convection requirement ($\dot{V}E/\dot{V}O_2$) between WT and ADKtg mice at P0–3 (WT: n = 14, ADKtg: n = 27), P6–7 (WT: n = 11, ADKtg: n = 23), P12–14 (WT: n = 12; ADKtg: n = 16), P19–23 (WT: n = 12, ADKtg: n = 16), and P43–56: WT: n = 12, ADKtg: n = 17).*indicate significant difference ($P < 0.05$) between strains of a particular age group as determined by one-way ANOVA with Sidak's post hoc test.

ADK-S overexpression produces neonatal mice with an adult-like sustained, hyperventilatory ($HVR_{\dot{V}E/\dot{V}O_2}$) response to hypoxia due to an enhanced hypometabolic rather than enhanced ventilatory response to hypoxia.

Air Convection Requirement ($\dot{V}E/\dot{V}O_2$)

I report first the effects of ADK-S overexpression on development of $\dot{V}E/\dot{V}O_2$ response to hypoxia as this provides the most direct test of the primary hypothesis that the lack of ADK-S at birth and its postnatal development are critical in the maturation of the HVR. With ADKtg mice, I test the hypothesis that neonatal mice that express adult levels of ADK-S at birth will have a mature $HVR_{\dot{V}E}$ and $HVR_{\dot{V}E/\dot{V}O_2}$ and that the differences between the hypoxic responses of ADKtg and WT mice during development will parallel differences in the expression of ADK-S between transgenic vs WT mice.

As predicted, P0–3 ADKtg mice responded to hypoxia with a significant sustained, adult-like increase in $\dot{V}E/\dot{V}O_2$ that was significantly greater than the response of WT animals in which $\dot{V}E/\dot{V}O_2$ remained at or below baseline throughout the hypoxic exposure. At 2, 4 and 10 min of hypoxia, $\dot{V}E/\dot{V}O_2$ in the ADKtg mice was at 81 ± 9 a.u., 93 ± 12 a.u., and 81 ± 9 a.u., $p < 0.0001$), respectively, which was significantly greater than WT mice at the same time points (30 ± 3 a.u., $p = 0.0004$; 31 ± 3 a.u., $p < 0.0001$; and 30 ± 3 a.u.., $p < 0.0001$) (Fig. 3.7Ai). The differences are even more obvious when comparing the $\dot{V}E/\dot{V}O_2$ hypoxic responses relative to pre-hypoxic baseline values. In P0–3 ADKtg mice, $\dot{V}E/\dot{V}O_2$ increased relative to baseline by 80 ± 31% ($p = 0.03$), 98 ± 35% ($p = 0.005$) and 100 ± 38% ($p = 0.01$) at 2, 4 and 10 min of hypoxia above baseline in the ADKtg mice ($p = 0.01$) (Fig. 3.7Aii). $\dot{V}E/\dot{V}O_2$ in newborn WT mice (P0–3) did not change significantly at any time during hypoxia.

Differences between the $\dot{V}E/\dot{V}O_2$ responses to hypoxia of ADKtg and WT mice remained in P6–7 and P12–14 mice but they were much less dramatic and as both strains at these ages increased $\dot{V}E/\dot{V}O_2$ in response to hypoxia. At P6–7, $\dot{V}E/\dot{V}O_2$ was significantly greater in the ADKtg group (123 ± 10 a.u.) at 4 minutes in hypoxia compared to the WT strain (85 ± 14 a.u., $p = 0.05$), while at P12–14, $\dot{V}E/\dot{V}O_2$ was greater in ADKtg mice (162 ± 14 a.u.) at 10 mins compared to WTs (118 ± 9 a.u, $p = 0.03$). At P19–23, the differences increased again with ADKtg mice showing a

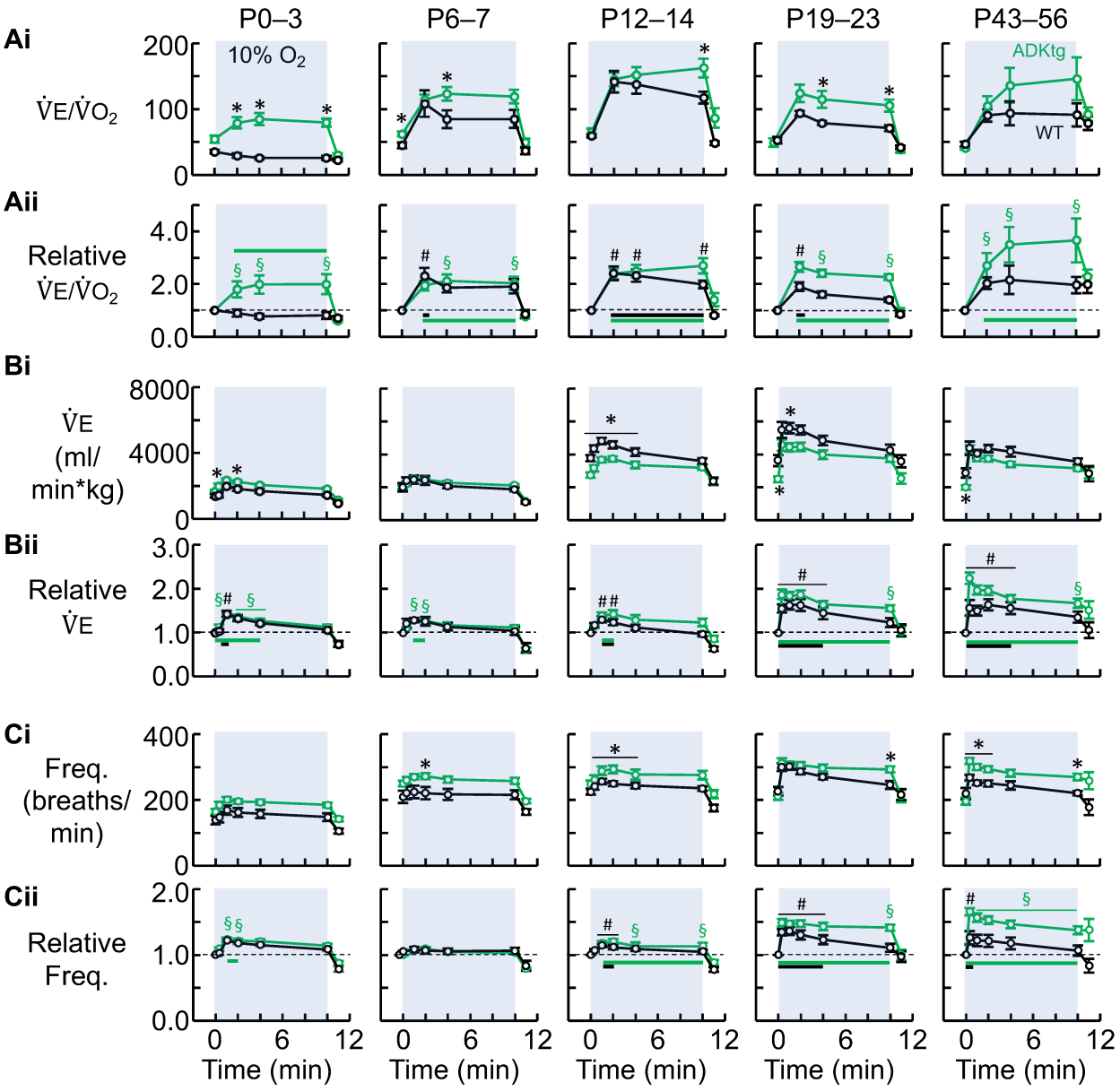
P0–3
P6–7
P12–14
P19–23
P43–56
Ai
10% O2
ADKtg
WT
V̇E/V̇O2
200
100
0
Aii
Relative V̇E/V̇O2
4.0
2.0
0.0
Bi
V̇E (ml/ min*kg)
8000
4000
0
Bii
Relative V̇E
3.0
2.0
1.0
0.0
Ci
Freq. (breaths/ min)
400
200
0
Cii
Relative Freq.
2.0
1.0
0.0
0
6
12
Time (min)

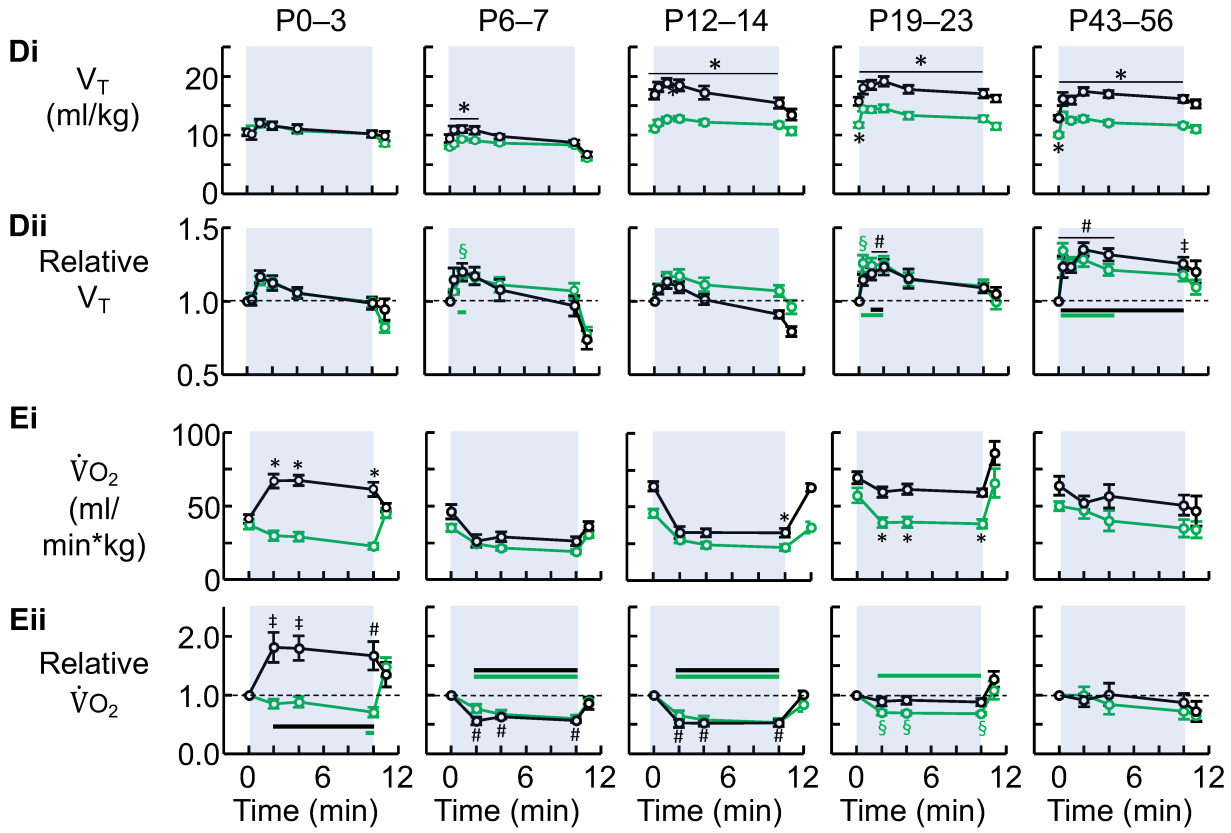

Figure 3.7. The effect of ADK-S transgenic overexpression on the development of ventilatory and metabolic responses to hypoxia (10% O_2) in WT (C57BL/6J) and ADKtg mice.
Time-course plots showing differences in the absolute (i) and relative (ii) changes in A) the air convection requirement ($\dot{V}E/\dot{V}O_2$), B) minute ventilation ($\dot{V}E$), C) frequency, D) tidal volume (V_T), and E) metabolic rate ($\dot{V}O_2$) measured using head-out (P0–P14) and barometric whole-body (P19-P56) plethysmography in WT and ADKtg mice in response to a 10-minute, 10% O_2 hypoxic stimulus. Developmental comparisons were made at P0–3 (WT: n = 14, ADKtg: n = 27), P6–7 (WT: n = 11, ADKtg: n = 23), P12–14 (WT: n = 12; ADKtg: n = 16), P19–23 (WT: n = 12, ADKtg: n = 16) and P43–56 (WT: n = 12, ADKtg: n = 17) Statistical differences analyzed using two-way ANOVA with Sidak's *post hoc* comparison. Significant differences between strains are shown on the plots of absolute data (Ai, Bi, Ci, etc.); *signifies a difference ($P < 0.05$) between the strains. Significant differences from absolute baseline values within a strain are shown on the plots of relative data (Aii, Bii, Cii, etc.) with the following symbols: §signifies a significant change from baseline in the FVB group; ‡signifies a difference from baseline in the WT group; and #signifies significant differences from baseline in both groups. Black and green bars on relative time-course graphs designate period which each parameter was significantly different from baseline in the WT or ADKtg groups, respectively.

greater $\dot{V}_E/\dot{V}_{O_2}$ response at 4 (115 ± 13 a.u. vs 79 ± 3 a.u, p = 0.03) and 10 min of hypoxia (105 ± 9 a.u. vs 71 ± 4 a.u., p = 0.04). There were no differences in the absolute values of $\dot{V}_E/\dot{V}_{O_2}$ during hypoxia between the ADKtg and WT mice at P43–56.

Comparing $\dot{V}_E/\dot{V}_{O_2}$ changes during hypoxia relative to each strain's pre-hypoxic baseline value, clarified that the strain differences in the $\dot{V}_E/\dot{V}_{O_2}$ responses to hypoxia diminished between P0–3 and P6–7, diminished further by P12–14 but then appeared to increase again in the two oldest groups. For example, at P6–7 both strains similarly elevated $\dot{V}_E/\dot{V}_{O_2}$ at 2 minutes in hypoxia (WT, 131 ± 31%, p = 0.0005; ADKtg: 94 ± 18%, p = 0.0001), but at 4 (112 ± 24%, p = 0.0001) and 10 minutes only the ADKtg strain maintained $\dot{V}_E/\dot{V}_{O_2}$ above baseline (ADKtg: 103 ± 25%, p < 0.0001). At P12–14 there was little difference between strains; both WT and ADKtg mice increased $\dot{V}_E/\dot{V}_{O_2}$ ~140% above baseline during the 2nd (WT, 141 ± 26%, p < 0.0001; ADKtg: 139 ± 20%, p < 0.0001) and 4th minute (WT, 133 ± 24%, p < 0.0001; ADKtg: 149 ± 24%, p < 0.0001), however by the 10th minute of hypoxia, $\dot{V}_E/\dot{V}_{O_2}$ fell slightly in WT mice (99 ± 15%, p = 0.0027) but elevated to 169 ± 29% (p < 0.0001) in the ADKtg strain (Fig. 3.7Aii). Then at P19–23, strain differences became more apparent again. Both showed increases in $\dot{V}_E/\dot{V}_{O_2}$ relative to baseline at 2 minutes in hypoxia (WT, 90 ± 16%, p = 0.01; ADKtg: 165 ± 19%, p < 0.0001), but by 4 min $\dot{V}_E/\dot{V}_{O_2}$ was only elevated in the ADKtg mice (WT, 60 ± 12%, p = 0.2; ADKtg: 141 ± 14%, p < 0.0001) and remained elevated at 10 min in the transgenic mice (127 ± 11%, p < 0.0001; WT, 40 ± 8%, p = 0.5). In adult P43–56 mice, while both WT and ADKtg mice appeared to increase $\dot{V}_E/\dot{V}_{O_2}$ above baseline, the increase was only statistically significant for the ADKtg mice at 2 min (171 ± 47%, p = 0.03), 4 min (250 ± 67%, p = 0.0007), and 10 min (266 ± 83%, p = 0.0002). While $\dot{V}_E/\dot{V}_{O_2}$ in P43–56 WT mice was nearly doubled at 2 min (104 ± 22%), 4 min (116 ± 54%) and 10 min of hypoxia (96 ± 31%), these differences were not significant from baseline (p > 0.3) (Fig. 3.7Aii).

In summary, expression ADK-S at adult levels in neonatal mice produces neonates that respond to hypoxia with an adult-like hyperventilatory response markedly different from WT mice who show no increase in $\dot{V}_E/\dot{V}_{O_2}$ during hypoxia. Differences between ADKtg and WT mice decrease with development as predicted and are very similar at P12–14 but then start to diverge again such that by adulthood the $\dot{V}_E/\dot{V}_{O_2}$ of ADKtg mice is once again more sustained than in WTs.

Minute Ventilation

Having shown that the $\dot{V}E/\dot{V}O_2$ response to hypoxia is greatly enhanced in ADKtg mice, the next step is to test the prediction that this will result from an enhanced ventilatory response to hypoxia; i.e. reduced ADO accumulation in the preBötC of ADKtg mice will result in a sustained, rather than biphasic $HVR_{\dot{V}E}$ in neonatal mice. Surprisingly, this was not the case. The $\dot{V}E$ responses of WT and ADKtg mice were remarkably similar, especially in the youngest age groups when both strains showed a biphasic response in which $\dot{V}E$ increased but then returned to baseline by the end of the hypoxia (Fig. 3.7B). However, there were modest changes suggesting a potentiated $\dot{V}E$ response to hypoxia in ADKtg mice. During hypoxia in P0–3 animals, absolute $\dot{V}E$ of WT mice was less than the ADKtg mice at the onset (WT, 1325 ± 197 ml/min/kg vs. ADKtg, 2007 ± 133 ml/min/kg, $p = 0.008$) and during the second minute of hypoxia (WT, 1698 ± 166 ml/min/kg vs. ADKtg, 2249 ± 99 ml/min/kg, $p = 0.03$).

Comparing the magnitude of the $\dot{V}E$ response to 10% O_2 of each strain to their baseline measurements at each age (Fig. 3.7Bii) revealed that compared to WTs, ADKtg mice sustained $\dot{V}E$ significantly above baseline longer at almost every developmental timepoint examined. As with the $\dot{V}E/\dot{V}O_2$ response, responses of the two strains became more similar between P0–3 and P12–14 but then the $\dot{V}E$ response became more sustained with maturation. At P0–3, only the ADKtg mice elevated $\dot{V}E$ by 13 ± 5% ($p = 0.05$) above baseline at the beginning of hypoxia (Fig. 3.7Bii). $\dot{V}E$ was greater than baseline in both strains at 1 min of hypoxia (WT, 41 ± 4%, $p = 0.007$; ADKtg, 43 ± 7%, $p < 0.0001$), remained elevated at 2 (32 ± 6%, $p < 0.0001$) and 4 min (27 ± 5%, $p = 0.03$) in ADKtg mice, but fell back to baseline in WT by the 2nd minute (22 ± 6%, $p = 0.09$) (Fig. 3.7Bii).

At P6–7, there were no absolute differences in $\dot{V}E$ during hypoxia between the strains, however relative to baseline (Fig. 3.7Bi), only the ADKtg mice significantly increased $\dot{V}E$ in the first (29 ± 3%, $p = 0.02$) and second minute of hypoxia (26 ± 5%, $p = 0.04$). During the first minute of hypoxia, WT mice raised $\dot{V}E$ by 28 ± 5%, but this change was significantly different from baseline ($p = 0.3$) (Fig 3.7Bii).

Beginning at P12 and continuing through P56, baseline $\dot{V}_E$ was reduced in the ADKtg animals compared to WTs. In P12–14 mice, this pattern persisted as absolute $\dot{V}_E$ was greater in WT (4348 ± 199 ml/min/kg) compared to ADKtg from the onset of hypoxia (3153 ± 193 ml/min/kg, $p < 0.0001$) and through the first (WT, 4813 ± 191 ml/min/kg vs. ADKtg, 3665 ± 158 ml/min/kg, $p = 0.0002$), second (WT, 4575 ± 224 ml/min/kg vs. ADKtg, 3722 ± 166 ml/min/kg, $p = 0.01$), and fourth minute of hypoxia (WT, 4140 ± 236 ml/min/kg vs. ADKtg: 3360 ± 204 ml/min/kg, $p = 0.02$) (Fig. 3.7Bi). Relative to baseline however, both WT and ADKtg mice elevated $\dot{V}_E$ during the first (WT, 17 ± 5%, $p = 0.002$; ADKtg: 38 ± 8%, $p = 0.001$) and second minute hypoxia (WT, 23 ± 7%, $p = 0.03$; ADKtg: 42 ± 9%, $p = 0.0005$) before falling back to baseline by the fourth minute (WT, 11 ± 6%, $p = 0.65$; ADKtg, 29 ± 11%, $p = 0.06$) (Fig. 3.7Bii).

At P19–23, $\dot{V}_E$ in the WT mice (5593 ± 317 ml/min/kg) was greater than ADKtg mice (4428 ± 256 ml/min/kg, $p = 0.04$) only in the first minute of hypoxia. Both WT and ADKtg mice increased $\dot{V}_E$ above baseline at the onset of hypoxia (WT: 55 ± 9%, $p = 0.0003$; ADKtg, 87 ± 11%, $p < 0.0001$) and through the first four minutes. The relative increases for the WT and ADKtg mice at 1 min, 2 min and 4 min, respectively were 63 ± 11% ($p = 0.0001$) vs. 84 ± 9% ($p < 0.0001$); 63 ± 14% ($p = 0.0003$) vs. 86 ± 10% ($p < 0.0001$); and 45 ± 15% ($p = 0.04$) vs. 64 ± 8% ($p = 0.001$). However, only the ADKtg animals sustained $\dot{V}_E$ above baseline (55 ± 7%, $p = 0.007$) by the end of hypoxia (WT, 23 ± 10%, $p = 0.63$) (Fig. 3.7Bii)

In the last age group at P43–56, there were no differences in absolute $\dot{V}_E$ between the groups during the hypoxic challenge (Fig. 3.7Bi). Comparing $\dot{V}_E$ relative to baseline however, revealed only one difference. $\dot{V}_E$ was raised ~55% above baseline in WTs through the first four minutes of hypoxia ($p < 0.005$), whereas in ADKtg mice, $\dot{V}_E$ was increased 124 ± 13% at the onset of hypoxia ($p < 0.0001$) then 97 ± 11%, 96 ± 10%, and 77 ± 8% through the first, second and fourth minute of hypoxia, respectively ($p < 0.0001$) (Fig. 3.7Bii). At the end of hypoxia, however $\dot{V}_E$ was not different from baseline in the oldest WT mice (23 ± 10%, $p = 0.63$) but remained 67 ± 11% above baseline ($p=0.0004$) in the ADKtg adults (Fig. 3.7Bii)

Frequency

Next, I began comparing the breathing pattern responses to hypoxia in WT and ADKtg, starting with changes in respiratory frequency (Fig 3.7C). In neonates between P0–3, there were not differences in frequency between WT and ADKtg mice throughout the 10-minute hypoxic stimulus (Fig. 3.7Ci). ADKtg mice increased their respiratory rate by 25 ± 3% in the first minute ($p = 0.01$) and 22 ± 3% in second minute of hypoxia ($p = 0.05$), whereas frequency was not different from baseline at any point during hypoxia in P0–3 WT mice ($p > 0.3$).

During hypoxia at P6–7, ADKtg mice exhibited a greater breathing rate (272 ± 9 bpm) in the second minute hypoxia compared to WT mice (220 ± 19 bpm, $p = 0.03$), although there were no other differences throughout hypoxia (Fig. 3.7Ci). Relative to baseline values, frequency was not significantly changed in P6–7 WT ($p > 0.9$) or ADKtg mice ($p > 0.4$) during hypoxia (Fig. 3.7Cii)

Frequency of P12–14 WT mice (241 ± 10 bpm) was reduced compared to ADKtg animals at the onset of hypoxia (261 ± 14 bpm, $p < 0.0001$), and through the first 4 minutes of hypoxia. Frequency of WT and ADKtg animals at 1 min, 2 min and 4 min of hypoxia, respectively were 256 ± 8 bpm vs. 289 ± 13 bpm ($p = 0.0002$); 249 ± 8 bpm vs. 293 ± 12 bpm ($p = 0.01$); and 243 ± 9 bpm vs. 277 ± 16 bpm, ($p = 0.02$) (Fig. 3.7Ci). Despite these differences, breathing rate was increased ~15% above baseline during the first two minutes of hypoxia in both WT ($p < 0.003$) and ADKtg mice ($p = 0.04$). For the remainder of hypoxia, only ADKtg mice sustained the increase in frequency above baseline at 4 min (13 ± 6%, $p = 0.001$ vs. WT, 9 ± 3%, $p = 0.17$) and 10 min (13 ± 5%, $p = 0.002$ vs. WT, 5 ± 3%, $p = 0.8$) (Fig. 3.7Cii).

Breathing frequency was only different between groups at the end of hypoxia in P19–23 WT mice (245 ± 12 bpm), which breathed at a slower rate than the transgenic mice (293 ± 9 bpm, $p = 0.02$) (Fig. 3.7Ci). In P19–23 mice, frequency of WT (34 ± 5%, $p = 0.0001$) and ADKtg mice (49 ± 6%, $p < 0.0001$) was increased above baseline at the onset of hypoxia. The enhanced frequency persisted through the first (WT, 36 ± 6%, $p < 0.0001$; ADKtg: 48 ± 4%, $p < 0.0001$), second (WT, 30 ± 7%, $p = 0.002$; ADKtg: 48 ± 5%, $p < 0.0001$), and fourth minute of hypoxia (WT, 23 ± 7%, $p = 0.005$; ADKtg: 43 ± 6%, $p < 0.0001$), but at the ten-minute timepoint, only ADKtg mice sustained their breathing frequency 41 ± 5% above baseline ($p < 0.0001$) (Fig. 3.7Cii).

In the last age window, P43–56 WT mice was depressed relative to ADKtg mice at the onset of hypoxia (268 ± 9 bpm vs. 318 ± 9 bpm, p = 0.007). The trend continued during the first (WT, 252 ± 7 bpm vs. ADKtg: 300 ± 9 bpm, p = 0.009) and second minutes (WT, 250 ± 7 bpm vs. ADKtg: 293 ± 9 bpm, p = 0.03), but was not different again until the end of the 10-minute hypoxic challenge (WT, 220 ± 7 bpm vs. ADKtg: 270 ± 10 bpm, p = 0.007). Adult WT mice, only significantly elevated frequency by 26 ± 10% (p = 0.02) at the onset of hypoxia, whereas ADKtg increased frequency 66 ± 5% at this point, sustaining the increase through hypoxia at minute 1 (57 ± 6%), minute 2 (53 ± 6%), minute 4 (46 ± 6%) and the end of hypoxia (38 ± 6%, all points: p < 0.0001).

Tidal Volume (V_T)

Continuing with my investigation as to whether breathing pattern was affected by ADKtg, I then measured hypoxic changes in V_T throughout development. Similar to baseline, tidal volume of the neonate P0–3 mice was not different between the WT and ADKtg group throughout hypoxia (p > 0.9) (Fig. 3.7Di). Furthermore, hypoxia did not evoke changes in V_T in either WT (p > 0.3) nor ADKtg mice (p > 0.2) during the hypoxic exposure (Fig. 3.7Dii).

At P6–7, I began to observe a pattern that persisted throughout development in the experimental age groups, as WT mice had a greater V_T than the ADKtg mice. At the onset of 10% O_2, V_T was 10.9 ± 0.7 ml/kg in WTs but 8.4 ± 0.3 ml/kg in ADKtg (p = 0.0003) (Fig. 3.7Di). The difference persisted through the first minute (WT, 11.0 ± 0.6 ml/kg vs. ADKtg, 9.3 ± 0.3 ml/kg, p = 0.01) and second minute of hypoxia (WT, 10.8 ± 0.7 ml/kg vs. ADKtg, 9.0 ± 0.3 ml/kg, p = 0.01). Relative to their pre-hypoxic values, ADKtg elevated V_T by 18 ± 2% (p = 0.01) in the first minute of hypoxia, while the largest difference in V_T of WTs at 1 min (20 ± 6%) was not different from baseline (p > 0.06) (Fig. 3.7Dii).

Again, at P12–14, WT mice had a greater V_T than ADKtg mice throughout hypoxia, however starting at this age and continuing until adulthood, V_T was depressed in the transgenic mice at baseline (Fig. 3.6D). V_T of WT mice (18.2 ± 0.8 ml/kg) was greater than ADKtg at the onset of hypoxia (12.1 ± 0.5 ml/kg, p < 0.0001) and during the first minute (18.9 ± 0.7 ml/kg vs. 12.8 ± 0.3 ml/kg (p < 0.0001). In the second, fourth, and tenth minutes, V_T of WT mice and ADKtg,

respectively was 12.8 ± 0.4 ml/kg vs. 9.0 ± 0.3 ml/kg ($p < 0.0001$); 17.2 ± 1.1 ml/kg vs. 12.2 ± 0.4 ml/kg ($p < 0.0001$); and 15.4 ± 0.9 ml/kg vs. 11.8 ± 0.4 ml/kg ($p = 0.0006$) (Fig. 3.7Di). Despite differences between strains, V_T did not significantly change during hypoxia in either P12–14 WT ($p > 0.21$) or ADKtg mice ($p > 0.23$) (Fig. 3.7Dii).

The pattern that V_T of WTs was significantly greater than ADKtg mice throughout hypoxia continued at P19–23. V_T of WTs at the onset of hypoxia was 18.0 ± 1.1 ml/kg, then 18.5 ± 0.8 ml/kg in the first minute, raising slightly to 19.1 ± 0.8 ml/kg in the second, before falling to 17.8 ± 0.7 ml/kg and 17.0 ± 0.7 ml/kg in the fourth and tenth minute, respectively (Fig. 3.7Di). At the onset of hypoxia V_T in ADKtg mice was significantly lower (14.5 ± 0.4 ml/kg, $p = 0.001$), continuing to be depressed relative to WTs in the first (14.4 ± 0.5 ml/kg), second (14.5 ± 0.6 ml/kg), fourth (13.3 ± 0.6 ml/kg) and tenth minutes of hypoxia (12.8 ± 0.5 ml/kg ($p < 0.0001$). Mice older than P19–23 showed more sustained increases in V_T during hypoxia, but there were differences in the response of the WT and ADKtg mice. Specifically, at P19–23, V_T of ADKtg animals increased 26 ± 6% at the onset of hypoxia ($p = 0.008$) while V_T of WTs was not significantly different ($p = 0.08$). In the first minute of hypoxia however, both WT (19 ± 4%, $p = 0.03$) and ADKtg mice (24 ± 5%, $p = 0.01$) elevated V_T, which persisted through the second minute of hypoxia (WT, 23 ± 5%, $p = 0.003$; ADKtg: 25 ± 5%, $p = 0.005$) (Fig. 3.7Dii).

In the adult age group, V_T was elevated in the P43–56 WT mice relative to ADKtg mice throughout hypoxia. At the onset, V_T of WTs measured 16.1 ± 1.1 ml/kg vs. 13.4 ± 0.5 ml/kg in ADKtg mice ($p = 0.005$). At the end of the 1st, 2nd, 4th, and 10th minute, V_T of WTs and ADKtg mice, respectively were 15.9 ± 0.7 ml/kg vs. 12.5 ± 0.5 ml/kg ($p = 0.0002$); 17.4 ± 0.7 ml/kg vs. 12.8 ± 0.5 ml/kg ($p < 0.0001$); 7.0 ± 0.6 ml/kg vs. 12.1 ± 0.4 ml/kg ($p < 0.0001$); and 16.2 ± 0.6 ml/kg vs. 11.7 ± 0.4 ml/kg ($p < 0.0001$) (Fig. 3.7Di). Relative to baseline, V_T increased in WTs by 23 ± 7% at the onset of hypoxia ($p = 0.002$) and 23 ± 4% during the first minute ($p = 0.003$), before increasing 35 ± 5% above pre-hypoxic levels in the second minute ($p < 0.0001$), 32 ± 4% in the fourth minute ($p < 0.0001$) and 25 ± 4% at the end of hypoxia ($p = 0.001$). Adult ADKtg mice increased V_T by 34 ± 5% at the onset of hypoxia ($p < 0.0001$), but the response steadily fell during the rest of the stimulus. In the first minute, V_T was raised 26 ± 4% ($p = 0.003$), then 28: ± 5% ($p = 0.001$) in the

second and 21± 4% (p = 0.02) in the fourth minute. At the end of hypoxia, V_T of ADKtg mice was not different than baseline (p = 0.11) (Fig. 3.7Dii).

Metabolic Rate ($\dot{V}O_2$)

I did not predict how transgenic animals would respond to hypoxia in terms of $\dot{V}O_2$ compared to the WT mice. While I expected significant enhancement of the $\dot{V}E$ response in ADKtg mice, I observed that overexpression of the mature isoform of ADK in the brain had varied effects on ventilatory parameters in mice throughout development. In general, ADKtg appeared to promote greater respiratory frequency and higher minute ventilation during hypoxia compared to WTs but these were minor compared to the transformation of the $\dot{V}E/\dot{V}O_2$ response in P0–3 ADKtg mice to an adult-like $\dot{V}E/\dot{V}O_2$ response (Fig 3.7A). Thus, the major contributor must be an enhanced hypoxic depression of $\dot{V}O_2$, or at least a reduced increase in $\dot{V}O_2$ in the ADKtg mice compared to WT. Indeed, whereas P0–3 WT mice unexpectedly increased during hypoxia, ADKtg adaptively reduced $\dot{V}O_2$ by 30 ± 8% (p = 0.001) at the end of the 10-minute hypoxic stimulus (Fig. 3.7Eii). Unlike in normoxia, $\dot{V}O_2$ was reduced in ADKtg mice relative to WTs throughout hypoxia (all timepoints between strains: p < 0.0001). At 2 min, WTs raised $\dot{V}O_2$ by 81 ± 25% (p < 0.0001) to 67 ± 5 ml/min/kg compared to ADKtg that maintained $\dot{V}O_2$ at pre-hypoxic levels (30 ± 4 ml/min/kg) (Fig. 3.7Ei). By 4 mins, WTs sustained the 80 ± 21% increase (p < 0.0001) in $\dot{V}O_2$ (67 ± 4 ml/min•kg) unlike ADKtg mice that remained a baseline (29 ± 3 ml/min/kg). By the end of the 10th minute, $\dot{V}O_2$ of WTs was 61 ± 5 ml/min/kg which represented an increase of 67 ± 24% relative to baseline (p = 0.002), whereas $\dot{V}O_2$ of ADKtg mice fell to 23 ± 2 ml/min/kg (Fig. 3.7Eii).

By P6–7 however, differences in absolute $\dot{V}O_2$ between strains disappeared (Fig 3.7Ei), as both similarly depressed $\dot{V}O_2$ in hypoxia. In WTs, $\dot{V}O_2$ fell by 44 ± 7%, 37 ± 4%, and 43 ± 3% in the second, fourth, and tenth minute, respectively (p > 0.0001). Similarly, in ADKtg mice at 2 mins $\dot{V}O_2$ fell by 23 ± 7% (p = 0.003), falling by 37 ± 4% at 4 mins (p = 0.0004), and 40 ± 6% at the end of hypoxia (p > 0.0001) (Fig. 3.7Eii).

In the next age group (P12–14), there was one difference between strains, as $\dot{V}O_2$ of WTs (32 ± 3 ml/min/kg) was elevated relative to ADKtg mice (22 ± 2 ml/min/kg, p = 0.05) at 10 minutes in

hypoxia (Fig. 3.7Ei). Similar to the P6–7 groups, $\dot{V}O_2$ was significantly depressed by >45% in P12–14 WTs ($p < 0.0001$) and >34% ADKtg mice ($p < 0.0001$) throughout hypoxia (Fig. 3.7Eii).

At P19–23, $\dot{V}O_2$ of WTs was increased relative to ADKtg mice during hypoxia. In the 2nd min, $\dot{V}O_2$ of WTs was 59 ± 4 ml/min/kg vs. 39 ± 3 ml/min/kg in transgenic mice ($p = 0.0009$). At 4 min, $\dot{V}O_2$ of WTs elevated slightly to 61 ± 4 ml/min/kg, while ADKtg was 39 ± 4 ml/min/kg ($p = 0.0003$). At the end of 10 min, $\dot{V}O_2$ of WTs was 59 ± 3 ml/min/kg, which was greater than 38 ± 3 ml/min/kg observed in ADKtg mice ($p = 0.0006$). In P19–23 ADKtg mice, $\dot{V}O_2$ was depressed from baseline levels by 30 ± 4% ($p < 0.0001$) during the second minute of hypoxia and remained significantly depressed by 31 ± 4% in the fourth minute ($p < 0.0001$) and by 32 ± 3% at the end of hypoxia ($p < 0.0001$). In contrast, $\dot{V}O_2$ of P19–23 WT mice did not significantly change in hypoxia.

In the final age window (P43–56), there were no differences between the strains in $\dot{V}O_2$ at any point in hypoxia (3.7Ei), nor was $\dot{V}O_2$ different from baseline in either WT ($p > 0.38$) or ADKtg strain ($p > 0.17$) during hypoxia (Fig. 3.7Eii)

Effects of ADK-S overexpression on ventilatory and metabolic responses to hypoxia are similar at 10% and 8% O2.

In the previous experiment, most surprising was that the $\dot{V}O_2$ of P0–3 WT C57BL/6J mice did not fall during hypoxia (but even increased), while that of the ADKtg mice remained constant or decreased. It is widely accepted that the magnitude of the hypoxic depression of $\dot{V}O_2$ is largest in the youngest animals and then decreases with development (Mortola, 1996). Close scrutiny of the literature reveals that this may reflect that the developmental studies of this response in rodents does not include animals younger than P2 (Liu et al., 2009). Regardless, our data in FVB mice (Fig. 3.1) suggest that neonate FVB and C57BL/6J mice differ in their metabolic response to hypoxia.

Air Convection Requirement ($\dot{V}E/\dot{V}O_2$)

To eliminate the possibility that ventilatory and especially the unexpected metabolic responses of neonatal C57BL/6J mice to hypoxia were not due to an insufficient hypoxic stimulus in this strain,

I repeated the comparison of young WT and ADKtg mice (P0–14) to a more severe hypoxic challenge of 8% O_2 challenge. Indeed, P1–3 WT mice failed to elicit a significant change in $\dot{V}E/\dot{V}O_2$ in response to 8% O_2, whereas ADKtg neonates with functional ADK-S significantly increased $\dot{V}E/\dot{V}O_2$ by 219 ± 91% in the second minute of hypoxia (p = 0.0009), maintaining this increase by 207 ± 80% (p = 0.006) and 178 ± 46% (p = 0.0009) at the fourth and tenth minute of hypoxia, respectively (Fig. 3.8Aii).

As seen in the previous 10% O_2 experiment, differences between the WT and ADKtg strains in terms of the $\dot{V}E/\dot{V}O_2$ response to hypoxia disappeared at P6–8. Between strains, there was no difference in the absolute values of $\dot{V}E/\dot{V}O_2$ during hypoxia (Fig. 3.8Ai). 8% O_2 hypoxic stimulus evoked a significant increase in $\dot{V}E/\dot{V}O_2$ throughout hypoxia in both strains. WTs responded by increasing $\dot{V}E/\dot{V}O_2$ by 213 ± 34% (p = 0.0002) in the second minute, before falling slightly to 159 ± 21% (p = 0.001) but remaining 142 ± 16% above baseline at the end of hypoxia (p = 0.003). ADKtg mice significantly increased $\dot{V}E/\dot{V}O_2$ by 254 ± 62% (p = 0.0001) in the second minute of hypoxia, also falling slightly to 205 ± 64% in the fourth minute (p = 0.008) but stabilizing 209 ± 47% above baseline at the end of hypoxia (p = 0.001) (Fig. 3.8Aii).

At P12–13, absolute measurements of $\dot{V}E/\dot{V}O_2$ again did not differ throughout the 8% O_2 hypoxic stimulus (Fig. 3.8Ai). Similarly, 8% O_2 evoked significant increases in $\dot{V}E/\dot{V}O_2$ throughout hypoxia (Fig. 3.8Aii). At 2 mins, 4 mins and 10 mins, $\dot{V}E/\dot{V}O_2$ relative to baseline in WT and ADKtg mice, respectively was 267 ± 33% (p = 0.009) vs. 253 ± 34% (p = 0.002); 315 ± 65% (p < 0.0001) vs. 327 ± 72% (p < 0.0001); and 288 ± 48% (p = 0.0001) vs. 340 ± 41% (p < 0.0001) (Fig. 3.8Aii).

Minute Ventilation ($\dot{V}E$)

I then sought to determine if the difference in $\dot{V}E/\dot{V}O_2$ response between WT and ADKtg mice was again due to changes in $\dot{V}O_2$ or if the stronger hypoxic stimulus also depressed the $\dot{V}E$ response to WT mice. In absolute terms, $\dot{V}E$ of P1–3 WT (2201 ± 137 ml/min/kg) was significantly greater than the ADKtg mice (1575 ± 94 ml/min/kg) only at 4 minutes in 8% O_2 (p = 0.007) (Fig. 3.8Bi).

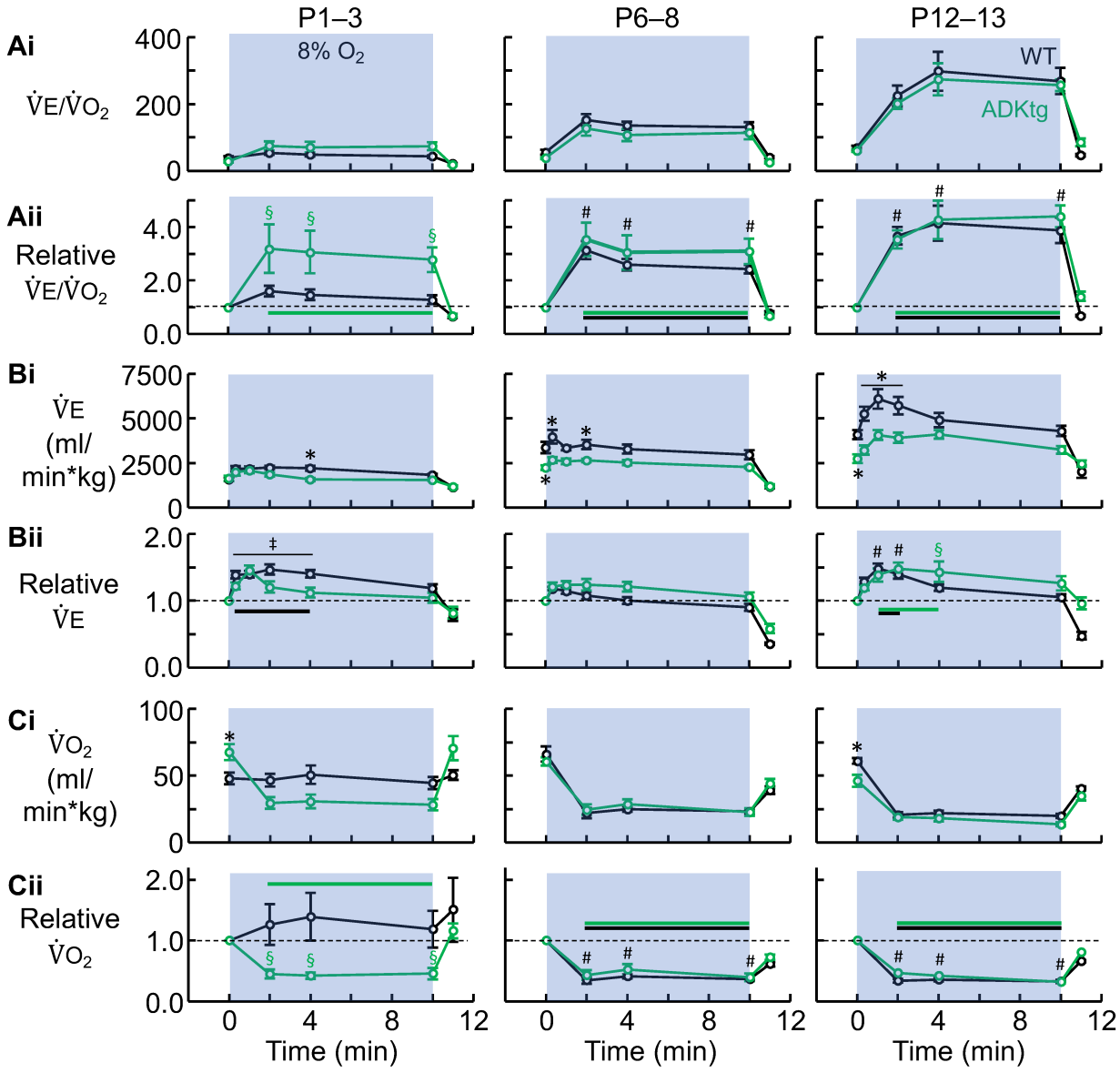
P1–3
P6–8
P12–13
8% O2
WT
ADKtg
Ai
V̇E/V̇O2
400
200
0
Aii
Relative V̇E/V̇O2
4.0
2.0
0.0
Bi
V̇E (ml/min*kg)
7500
5000
2500
0
Bii
Relative V̇E
2.0
1.0
0.0
Ci
V̇O2 (ml/min*kg)
100
50
0
Cii
Relative V̇O2
2.0
1.0
0.0
0
4
8
12
Time (min)

Figure 3.8. The effect of ADK-S transgenic overexpression on the development of ventilatory and metabolic responses to hypoxia (8% O_2) in WT (C57BL/6J) and ADKtg mice.
Time-course plots showing differences in the absolute (i) and relative (ii) changes in A) the air convection requirement ($\dot{V}_E/\dot{V}_{O_2}$), B) minute ventilation ($\dot{V}_E$), C) metabolic rate ($\dot{V}_{O_2}$) in WT and ADKtg mice in response to a 10-minute, 8% O_2 hypoxic stimulus. Measurements made in P1–3 (WT: n = 14, ADKtg: n = 16), P6–8: (WT: n = 14, ADKtg: n = 11) and P13–14 (WT: n = 14; ADKtg: n = 10) mice. Statistical differences analyzed using two-way ANOVA with Sidak's *post hoc* test. Significant differences between strains are shown on the plots of absolute data (Ai, Bi, Ci, etc.); *signifies a difference ($P < 0.05$) between the strains. Significant differences from absolute baseline values within a strain are shown on the plots of relative data (Aii, Bii, Cii, etc.) with the following symbols: §signifies a significant change from baseline in the FVB group; ‡signifies a difference from baseline in the WT group; and #signifies significant differences from baseline in both groups. Black and green bars on relative time-course graphs designate periods which each parameter was significantly different from baseline in the WT or ADKtg groups, respectively.

Relative to their baseline levels, only the WT mice significantly increased $\dot{V}_E$ in severe hypoxia. At the onset of hypoxia, $\dot{V}_E$ was 39 ± 6% above baseline (p = 0.009). In the two minutes, WT $\dot{V}_E$ was 40 ± 5% (p = 0.006) and 47 ± 8% above baseline (p = 0.002), respectively, and 47 ± 8% in the fourth minute (p = 0.004) before falling back to baseline (Fig. 3.8Bii).

P6–8 WTs also had greater $\dot{V}_E$ measurements first at the onset of hypoxia (WT, 3975 ± 380 ml/min/kg vs. ADKtg, 2669 ± 167 ml/min/kg, p = 0.0002), then during the second minute of 8% O_2 (WT, 3543 ± 263 ml/min/kg vs. ADKtg, 2638 ± 96 ml/min/kg, p = 0.02) (Fig. 3.8Bi). Neither WT nor ADKtg mice at this age group had a significant change in $\dot{V}_E$ throughout the 8% O_2 stimulus (Fig. 3.8Bii).

As seen in the other ages, $\dot{V}_E$ of P12–13 WT mice was greater than ADKtg mice first at the onset of 8% hypoxia (WT, 5265 ± 390 ml/min/kg vs. ADKtg: 3228 ± 275 ml/min/kg, p = 0.0001) then through the first (WT, 6098 ± 548 ml/min/kg vs. ADKtg: 4076 ± 276 ml/min/kg, p = 0.0005) and second minute of hypoxia (WT, 5721 ± 491 ml/min/kg vs. ADKtg: 3919 ± 293 ml/min/kg, p = 0.0009) (Fig. 3.8Bi). Unlike the younger age groups both P12–14 WT and ADKtg mice elevated $\dot{V}_E$ above baseline during 8% O_2 hypoxia. In the first minute, WT raised $\dot{V}_E$ 48 ± 7% above baseline (p = 0.0003), while ADKtg mice raised $\dot{V}_E$ by 39 ± 10% (p = 0.03). Through the second minute of hypoxia, $\dot{V}_E$ relative to baseline of WT and ADKtg mice was 40 ± 6% (p = 0.006) and 48 ± 9% (p = 0.04), respectively. After this, only ADKtg mice maintained $\dot{V}_E$ above baseline in the 4th minute of 8% O_2, (44 ± 15%, p = 0.02; WT, 16 ± 4%, p = 0.4) before falling to baseline by the end of hypoxia (p = 0.8) (Fig. 3.8Bii).

Metabolic Rate ($\dot{V}_{O_2}$)

Newborn WT mice responded with a stronger relative $\dot{V}_E$ response compared to ADKtg mice, thus the difference between their $\dot{V}_E/\dot{V}_{O_2}$ must be due to an attenuated hypometabolic response to hypoxia as seen in the 10% O_2 experiments. Indeed, while absolute values of $\dot{V}_{O_2}$ during hypoxia were similar between strains (Fig. 3.8Ci), P1–3 WT mice showed no change in $\dot{V}_{O_2}$ in response to 8% O_2, whereas neonate ADKtg mice significantly depressed $\dot{V}_{O_2}$ by 54 ± 7% in the second minute

($p < 0.0001$), 58 ± 5% in the fourth minute ($p < 0.0001$), and 56 ± 11% at the end of hypoxia ($p < 0.0001$) (Fig. 3.8Cii).

By P6–8, there were no differences in absolute $\dot{V}O_2$ measurements between strains (Fig. 3.8Ci), and both strains depressed $\dot{V}O_2$ during hypoxia by approximately half throughout hypoxia. Relative to baseline, measurements of $\dot{V}O_2$ at 2 min, 4 min and 10 min between the WT and ADKtg strains, respectively measured 65 ± 5% vs. 57 ± 8%; 59 ± 3% vs. 48 ± 9%, and 63 ± 3% vs. 60 ± 6% (all comparisons: $p < 0.0001$) (Fig. 3.8Cii).

The trend continued in P12–13 mice, with no differences in absolute $\dot{V}O_2$ measurement between the strains at any timepoint during hypoxia (Fig. 3.8Ci). Both strains of P12–13 mice depressed $\dot{V}O_2$ by > 50% throughout hypoxia. At 2 min, $\dot{V}O_2$ of WTs was reduced 66 ± 3% and 53 ± 6% in ADKtg mice. Then at 4 min, metabolic rate of WTs was reduced 64 ± 3% similar to ADKtg mice that fell 57 ± 8%. At the end of hypoxia, $\dot{V}O_2$ was reduced 67 ± 3% and 68 ± 4% in WT and ADKtg mice, respectively. (Fig. 3.8Cii)

3.4 Discussion

Developmental analysis of purinergic signaling in the preBötC in vitro (Chapter 2) established that elements involved in ADOe clearance, specifically ENTs and the ADK-S, are immature at birth suggesting that reduced ability to clear ADOe early in postnatal life is an important contributor in the immature HVR – i.e., the inability to produce a sustained increase in $\dot{V}E$ in response to hypoxia. The main objective of this study was therefore to explore in vivo the importance in the brain of ENTs and ADK in shaping the ventilatory and metabolic responses to hypoxia during development in mice using pharmacological and transgenic approaches.

The main contributions of this work include the demonstration that complete removal of ENT1 and 2 has little impact on baseline breathing, breathing pattern or metabolic rate throughout postnatal development, suggesting either that under baseline conditions ADOi ≈ ADOe or more likely that the loss of ENT1/2-mediated ADO transported has somehow been compensated.

Given the role attributed to ADOe in the secondary hypoxic respiratory depression, I predicted that the impact of ENT1/2 KO on the HVR$_{\dot{V}E}$ would be much more obvious than its impact on basal ventilation. Indeed, because ADOe and its inhibitory actions are believed to accumulate during hypoxia, I predicted that loss of ENT-mediated ADO transport would cause a progressive increase in ADO-mediated inhibition and a reduction in the duration of any hypoxia-induced excitation; i.e., the hypoxia-induced increase in $\dot{V}_E$ that is only transient at birth and becomes sustained with development would be attenuated in the ENT1/2 KO mice.

Indeed, while perhaps smaller than expected, ENT1/2 KO had the predicted effects on the ventilatory response to hypoxia, confirming a role for ENT-mediated ADO transport in shaping the HVR. The duration of hypoxia-induced increase in frequency and $\dot{V}_E$ was attenuated in the ENT1/2 KO mouse and the impact increased developmentally. In other words, ENT activity enhances/prolongs the hypoxia-induced excitation of frequency and $\dot{V}_E$. Interestingly, in the younger ages, ENT activity appears more important in controlling rapid dynamics of the breathing pattern responses to hypoxia (i.e. frequency and V_T) since the final levels of frequency and $\dot{V}_E$ attained at the end of the hypoxic period were the same between strains. The attenuated frequency response to hypoxia in the ENT KO mice is consistent with a site of action in the preBötC. Indeed, ATP release and subsequent production of ADO in the preBötC during hypoxia shape the HVR (Angelova et al., 2015; Rajani et al., 2017; Reklow et al., 2019). In vitro data also establish that ENT1/2 are active and modulate preBötC rhythm during the first two postnatal weeks (Chapter 2). However, the actual site where the KO of ENT activity causes the differences in responses of WT and ENT1/2 KO mice remain to be determined.

In addition, ENTs and their impact on ADOe or ADOi do not appear to be part of the pathway via which hypoxia depresses metabolism. ENT1/2 KO had little effect on metabolic responses to hypoxia. $\dot{V}_{O_2}$ was not affected at any age and, compared to the hypoxia induced changes in $\dot{V}_{O_2}$, the relatively small changes in $\dot{V}_E$ in ENT1/2 KO mice were such that homeostatic control, best assessed via the relationship between $\dot{V}_E/\dot{V}_{O_2}$, was not impacted by ENT1/2 KO. Finally, while the impact of the ENT1/2 KO on $\dot{V}_E$ increased with development, it remains unclear whether this is a direct result of increased ENT activity or indirect via developmental increases in ADK activity, which would indirectly enhance ENT activity.

Previous observations that ADK-S expression and activity in the brainstem is very low at birth (Fig. 2.7, 2.8) led to the exciting hypothesis that the associated reduction in capacity to clear ADOe could be a major factor in the immature HVR of premature and neonatal mammals; i.e., that greater accumulation of ADOe during hypoxia was responsible for the greater respiratory depression and the inability of young mammals to mount a sustained increase in $\dot{V}_E$ during hypoxia. Efforts to test this via pharmacological inhibition of ADK activity were greatly confounded by the profound effects of ABT 702 on basal $\dot{V}_E$ and $\dot{V}_{O_2}$. Evaluation of this hypothesis was therefore based on comparing the HVR of WT mice that have low levels and low activity of ADK-S at birth with mice engineered to express adult levels of ADK-S in the brain from birth. My hypothesis was that neonatal ADKtg mice would produce an adult-like sustained ventilatory and $\dot{V}_E/\dot{V}_{O_2}$ response to hypoxia and that with development, differences in the ADKtg mice and WT mice would disappear as endogenous ADK-S in WT mice increased to adult levels. Data supported this hypothesis. Neonatal ADKtg mice responded to hypoxia with a sustained, adult-like increase in $\dot{V}_E/\dot{V}_{O_2}$ while WT equivalents showed no increase in $\dot{V}_E/\dot{V}_{O_2}$. The differences in the $HVR_{\dot{V}_E/\dot{V}_{O_2}}$ were largely gone by P6–8 and by P13–14 responses of the two strains were indistinguishable. With additional maturation, the $HVR_{\dot{V}_E/\dot{V}_{O_2}}$ of the P19–23 and adult ADKtg mice once again exceeded that of WT in that it was more sustained. To my surprise, the adult like response in neonatal ADKtg mice was due to a minor increase in the duration of the hypoxia-induced increase in $\dot{V}_E$, but primarily arose from a much lower $\dot{V}_{O_2}$ in the transgenic mice. The metabolic depression was then very similar at P6–7 and 12-14 but more sustained again at P19–23. In adult mice, overexpression of ADK-S in ADKtg mice did not impact metabolic responses to hypoxia but enhanced the increased in $\dot{V}_E$. Thus, there is a developmental transition in the impact of ADK-S overexpression. At birth, ADK-S overexpression enhances the $HVR_{\dot{V}_E/\dot{V}_{O_2}}$ through reductions in metabolism, which is one adaptive strategy to prolong survival in low O_2 conditions. In contrast, in adults the enhanced $\dot{V}_E/\dot{V}_{O_2}$ response reflects an increase in $\dot{V}_E$, which is another adaptive strategy to prolong survival in hypoxic conditions. Similar responses to the greater hypoxic challenge of 8% confirmed that this was not due to unusually low hypoxic sensitivity of the C57BL/6J mice used in the ADKtg study.

An additional, unexpected observation was that, in contrast to the established view in neonatal mammals that the depression of metabolic rate by hypoxia is greatest at the earlier stages of development and decreases, often disappearing by adulthood, is not uniform across species or even

strains of mice. While FVB mice showed a consistent reduction in the magnitude of the hypoxic metabolic depression between P2 and adulthood, $\dot{V}O_2$ did not fall in P1–2 C57BL/6J mice exposed to hypoxia – in fact $\dot{V}O_2$ increased in response to 10% O2 and did not change in response to 8% O_2. After one week of development, both strains showed the expected hypoxic depression of metabolic rate. While the mechanisms underlying the strain differences in metabolic responses to hypoxia are not known, these data suggest that additional scrutiny is required to assess the uniformity of the adaptive strategies employed by newborn mammals to increase hypoxia tolerance.

3.4.1 ENT activity modulates breathing pattern and $\dot{V}E$ responses to hypoxia throughout development

This study tested the contribution of ENTs to the development of the ventilatory and metabolic responses to hypoxia by comparing WT (FVB) and transgenic knockout mice lacking genes for both ENT1 and 2. My results suggest that postnatal growth (weight gain) is unaffected by ENT activity. Similarly, lack of ENT1 and 2 did not have any major impact on postnatal changes in baseline metabolism or breathing behaviour. Importantly, $\dot{V}E/\dot{V}O_2$ was similar between strains throughout development, suggesting that at least under baseline conditions, lack of ENT1/2 activity does not alter homeostatic control of breathing.

Before discussing this data, I must address a caveat of these experiments (and others in this chapter), as mice < P14 were recorded using a restrained, head-out plethsmograph technique, whereas mice three-weeks and older were allowed to freely move inside a whole-body chamber. Head-out measurements afforded direct assessment of both respiratory volume and rate in the youngest mice, however stress and greater movement caused by restraint in the head chamber could increase metabolic rate. Previous experiments characterizing the developmental analysis of ENT mice using the whole-body technique yielded similar results in that frequency and relative $\dot{V}E$ (calculated from respiratory rate multiplied by relative tidal volume) fell more rapidly in hypoxia (partially shown in Fig. 1.4). Thus, while I cannot exclude that restraint caused increased stress in mice tested using the head-out plethysmograph, this technique allowed me to accurately measure $\dot{V}E$ and $\dot{V}O_2$ in mice from birth. Furthermore, comparison of developmental changes between each strain were measured using identical plethysmograph setups, therefore any

confounding variables from using either the head-out or whole-body chambers should have equally affected each strain similarly at each age.

Given that ENT1 and 2 provide the primary mechanism via which ADO is transported across extracellular membranes (Chu et al., 2013; Parkinson et al., 2011), and clear evidence that long-term disruption of ADOe tone following changes in ADK expression have severe consequences for network excitability; i.e., epilepsy (Boison, 2013b, 2012a), the finding the $\dot{V}_E$ and $\dot{V}_{O_2}$ were so minimally affected in ENT1/2 KO mice was surprising. One interpretation is that under baseline conditions ADOe and ADOi are very similar and there is minimal ENT-mediated transport of ADO. However, this seems unlikely. It is indeed possible that ADOe and ADOi are similar under baseline conditions in WT animals in which ENT-mediated transport is available to restore ADOe tone following disruptions. However, the ENT1/2 KO mice lack the major transporters necessary to establish normal ADO tone.

Based on the assumption that reduced clearance of ADOe in neonatal mammals results in greater ADOe accumulates during hypoxia in the young and that this contributes to the greater hypoxic respiratory depression, I expected differences in $\dot{V}_E$ between ENT1/2 KO and WT to increase as the hypoxia progressed; i.e. the duration of the hypoxia-induced increase in ventilation would be reduced in the ENT1/2 KO mice due to greater accumulation of ADOe. I also hypothesized that ENT activity is greater in older mice, in which case the hypoxia-induced increase in $\dot{V}_E$ would be most significantly reduced in the oldest ENT1/2 KO mice; i.e., the hypoxic $\dot{V}_E$ response of adult KO mice would resemble the neonatal response in which the hypoxia-induced increase in $\dot{V}_E$ is not sustained and $\dot{V}_E$ returns back to baseline levels during the hypoxic exposure. As predicted, the impact of ENT KO on the ventilatory response to hypoxia increased with development. The $\dot{V}_E$ response was very similar in the youngest animals, differing only in pattern with frequency falling back to baseline more rapidly in KO mice compared to WTs. With further development from P6–8 through P12–14, the duration of the hypoxia-induced increase in $\dot{V}_E$ was reduced in the KO animals. $\dot{V}_E$ remained significantly above baseline for between 1-2 min in WTs but for only one minute in KO mice. The greatest difference in $\dot{V}_E$ was observed in three-week old juveniles and adults where $\dot{V}_E$ remained above baseline throughout the hypoxic period in WTs but fell to

baseline within 1-2 min in the KO animals. The differences in $\dot{V}_E$ largely reflected that the duration of the hypoxia-induced frequency increase was reduced in KO mice, consistent with the inhibition of frequency by ADOe in the preBötC. These data demonstrate that the duration of the hypoxia induced increase in $\dot{V}_E$ (and frequency), which increases with development, is reduced in a developmentally dependent manner in mice that lack ENT1 and 2, primarily through attenuated frequency responses. Results also suggest that the normal function of ENTs in the HVR is to increase the duration of the hypoxic $\dot{V}_E$ response by removing ADOe. The observation that the effect is primarily mediated through changes in frequency is consistent with my working model that during hypoxia ATP is released in the preBötC, the primary site of rhythm generation. The primary actions of ATP, ADO and other modulators in the preBötC are mediated through changes in frequency (Funk, 2013; Rajani et al., 2017; Reklow et al., 2019).

Whether the developmental increase in the effects of ENT KO reflect developmental increases in ENT activity or are secondary to developmental increases in ADK activity, which will impact ENT transport by increasing the concentration gradient that favours ENT-mediated clearance of ADOe, remains unclear. To date, there are no studies which detail if ENT activity or its expression in the brain, and particularly in respiratory networks, changes developmentally. My previous in vitro work suggests that ENTs in the preBötC are present at birth and contribute to ADOe clearance. In fact, the observation that the inhibitory effects on frequency of locally applying ADO into the preBötC are prolonged equivalent amounts at P0–6 and P9–12 ENT1/2 KO mice (Fig. 2.6) suggests that ENT1/2 expression/activity is similar in the first two postnatal weeks. The observation that ENT inhibition depressed basal preBötC rhythm in slices from P9–12 mice but had no effect on P0–5 slices, might indicate a developmental increase in ENT activity. However, the problem with that interpretation is that a change in baseline frequency following block of ENT activity depends on much more that ENT expression levels. ENT transport of ADO depends on the concentration gradient of ADO across the extracellular membrane. The failure to see an effect of ENT inhibitors on frequency at P0–5 could simply indicate that at this age in vitro the concentration of ADOe is the same as ADOi. Likewise, a greater effect of ENT inhibition in older slices could indicate greater ENT activity but it could also indicate that in older slices, there is a greater difference in the concentration of ADOe vs ADOi, which could be physiological or an artifact of in vitro preparations prepared from animals of different ages. A further limitation in

making conclusions about whether ENT expression or ENT activity levels change developmentally based on the effects of inhibitors is that the ADOe–ADOi concentration gradient, which determines the amount of ADO transport is affected by a host of enzymes whose activity also change during development. A prominent example is ADK-S that increases its expression and activity in the brainstem during development. ADK-S activity supports ADOe clearance so greater effects of ENT inhibition on frequency in older slices could simply reflect increased ADK activity. Nonetheless, my data shows that ENT1 or 2 activity affects preBötC responses to ADO from birth, which support my observation that differences in the hypoxic $\dot{V}_E$ response between WT and ENT KO mice throughout development largely reflects reduced breathing frequency during hypoxia in the transgenic mice.

I am unaware of data characterizing the expression of ENT1 or ENT2 in the brainstem of rodents during development. ENT expression varies between brain regions and between species. In rats, ENT1 and ENT2 are expressed in neurons, astrocytes, as well as blood vessels in the brain and the choroid plexus (Anderson et al., 1999). ENT1 levels are highest in the rat brainstem compared to other brain regions including the hippocampus, cerebellum, and cerebral cortex (Alanko et al., 2006), but how its expression changes developmentally is not known. Moreover, while information about the distribution of ENTs and their activities is abundant in rats, caution is required when extrapolating these data to other species. For example, ENT1 mRNA expression is higher in the brains of male rats compared to female rats, but there are no sex differences in mice (Lu et al., 2004; Parkinson et al., 2011). In addition, while ENT2 expression and activity are higher than ENT1 in rat brain cells, the opposite is true humans, mice and guinea pigs where ENT1 dominates (Parkinson et al., 2011, 2005). Finally, ENT1 expression correlates strongly with A_1R expression in humans and is highest in the frontal and parietal cerebral cortex (Jennings et al., 2001), but this correlation is not observed in rats or mice. Additional experiments that directly quantified ENT expression were unsuccessful due to lack of selective antibodies for ENT1 and 2. Alternative approaches include in situ hybridization or RT-PCR, however these assays do not quantify functional protein levels. Therefore, further work is required to determine how ENT expression and activity changes in specific respiratory networks and to assess the importance of ENTs in these regions in shaping the development of ventilatory and metabolic responses to hypoxia. My data,

however, support that ENT1 or 2 are functional in the preBötC at birth, as their activity shortens the duration of the response to ADO (Fig. 2.6).

In summary, the primary impact of ENTs is in shaping breathing pattern and $\dot{V}_E$ responses to hypoxia, although homeostatic control processes are not affected. Aside from adults, $\dot{V}_{O_2}$ responses in hypoxia were similar between WT and KO mice suggesting that ENT1 and 2 are not involved in shaping the metabolic response to hypoxia, at least in early development. The result is that animals of both strains at all ages responded to hypoxia with an adaptive hyperventilation; i.e., an increase in $\dot{V}_E/\dot{V}_{O_2}$ above baseline. As seen previously in multiple species, the factors contributing to the hyperventilation change developmentally. With development the increase in $\dot{V}_E/\dot{V}_{O_2}$ typically shifts from reflecting more of a fall in $\dot{V}_{O_2}$ to being more dependent on an increase in $\dot{V}_E$ (Frappell et al., 1991; Hill, 1959; Mortola, 1999; Mortola et al., 1989). In my experiments, relative changes in $\dot{V}_E$ and $\dot{V}_{O_2}$ that contributed to the increased $\dot{V}_E/\dot{V}_{O_2}$ were very similar in both strains at all ages until adulthood when the hypoxic decrease in $\dot{V}_{O_2}$ was attenuated and the $\dot{V}_E$ increase was enhanced in WTs. It was also only in adults at the end of the hypoxic exposure that $\dot{V}_E/\dot{V}_{O_2}$ responses difference between WT and ENT KO mice. Whereas $\dot{V}_E$ decreased continuously during hypoxia in WT, $\dot{V}_E$ stabilized in the latter phase of hypoxia in ENT KO mice. These changes, in combination with a relatively stable level of $\dot{V}_E$ over the same time interval, meant that the hyperventilatory response of adult ENT KO mice was less robust than WT, which again supports an important role for ENTs in adaptive responses to hypoxia.

A limitation of these experiments was that ENT1/2 were removed throughout the brain and periphery. The more rapid decline in $\dot{V}_E$ and frequency in KO mice older than P2 is consistent with in vitro data suggesting that ADOe is cleared by ENT1/2, thus limiting ADO inhibitory effects on preBötC activity (Fig. 2.6). Yet, ADO modulates the HVR in sites outside the preBötC including rostral pontine regions (Koos et al., 1994) and carotid bodies in the periphery (Koos and Chau, 1998; Sacramento et al., 2019). Therefore, the site(s) of action where ENT activity affects the HVR cannot be conclusively determined by these in vivo results. Moreover, the relatively minor effects of ENT1/2 KO on $HVR_{\dot{V}_E/\dot{V}_{O_2}}$ are surprising. Since the ENT1/2 KO was global throughout life, compensatory mechanisms for the lack of ENT-mediated ADO transport may have developed in

these mice. Mechanisms underlying this compensation, however, are unclear. ENT3 and ENT4 are not normally involved in ADO transport between intra and extracellular compartments. In WT mice, ENT3 is located on the nuclear membrane (Baldwin et al., 2005; Li et al., 2013) so compensation via ENT3 would require much more than simple upregulation, as its spatial distribution would have to change. At physiological pH, ENT4 does not transport ADO (Barnes et al., 2006; Parkinson et al., 2011). Upregulation of CNTs could compensate for the loss of ADO transport, but CNT-mediated transport requires energy, which would be expected to have multiple consequences on the KO mice, including perhaps increased $\dot{V}_{O_2}$. The only difference in $\dot{V}_{O_2}$ between strains was at P0–2 when basal $\dot{V}_{O_2}$ was reduced and in adults when $\dot{V}_{O_2}$ fell below baseline values in the ENT1/2 KO mice, not increased as would be expected. I did not assess the expression pattern or levels of ENT3, 4 or CNTs in the KO mice, although previous results suggest that ENT1 KO does not change expression of other NTs in the brain (Parkinson et al., 2011). Further studies that target ENTs in central respiratory networks or directly manipulate their activity in the preBötC using genetic or pharmacological techniques will not only confirm whether ENT activity in the network is responsible for its effects of the HVR$_{\dot{V}_E}$, but also limit any compensatory mechanisms that may have masked the effect of ENTs on the HVR$_{\dot{V}_E/\dot{V}_{O_2}}$ in the whole-body ENT1/2 KO.

3.4.2 Modulatory effects of ADK activity on baseline ventilation and metabolic rate increase as ADK-S expression increases

Pharmacological inhibition and transgenic overexpression of ADK-S provided several new insights into the role of ADK in control of $\dot{V}_E$, metabolic rate and their responses to hypoxia during development. First, I demonstrated that ADK-S expression in the brainstem (Fig 2.7, 2.8), as seen previously on cortex and cerebellum (Gebril et al., 2021; Studer et al., 2006), is barely detectable at birth and reaches adult levels by the third postnatal week. Second, consistent with ADK-S expression, pharmacological inhibition of ADK activity revealed very little effect of ADK on baseline minute ventilation or metabolic rate at birth. However, small but significant reductions in breathing frequency of newborn mice suggests that at birth, there is some functional ADK activity that increases baseline frequency, presumably via reductions in ADOe in respiratory control centres such as the preBötC. Third, data show that ADK activity increases substantially by P11–12, and despite significant increases in ADK-S expression between P11–12 and P20, the impact

of ADK-S activity on baseline $\dot{V}_E$ and $\dot{V}_{O_2}$ is similar between P11 and P20. The reduction in baseline $\dot{V}_E$ and $\dot{V}_{O_2}$ associated with ADK inhibition was similar at these ages. These data show that ADK activity is important in setting baseline $\dot{V}_E$ and $\dot{V}_{O_2}$, perhaps through its influence on ADO tone. However, that $\dot{V}_E/\dot{V}_{O_2}$ was not affected in either strain either age group suggests that the primary effect of ADK inhibition occurs through inhibition of metabolism. Reductions in $\dot{V}_E$ are likely to simply reflect reduced metabolic demand that homeostatic feedback loops controlling PaO_2, $PaCO_2$ and arterial pH and match $\dot{V}_E$ and $\dot{V}_{O_2}$ are intact. Inhibition of $\dot{V}_E$ by ADOe is well-established, however, whether ADK-mediated reductions in ADOe similarly reduce baseline $\dot{V}_{O_2}$ is less clear.

When I tested ADK inhibition affected responses to hypoxia in developing mice, I predicted that because ADK activity increases postnatally, the ABT 702 mediated inhibition of hypoxic ventilatory and metabolic responses should also increase with age. Data interpretation, however, was confounded by the powerful inhibitory actions of ABT 702 on baseline ventilation and metabolism. For example, the absolute levels of $\dot{V}_E$, V_T, frequency and $\dot{V}_{O_2}$ during hypoxia were lower in ABT 702 than in control, which clearly reflects that that powerful inhibition of $\dot{V}_E$ and $\dot{V}_{O_2}$ by ABT 702. However, when trying to assess hypoxic sensitivity, reporting data relative to baseline suggests that the sensitivity to hypoxia is much greater after blocking ADK. A question remains whether this really reflects greater sensitivity or was simply a consequence of the very low levels of $\dot{V}_E$ and $\dot{V}_{O_2}$ in ABT 702; e.g., $\dot{V}_E$ and $\dot{V}_{O_2}$ in ABT 702 in normoxia were ~ one third of baseline levels in vehicle treated mice. Indeed, the profile of the responses in the two groups appear similar and parallel each other, suggesting that ABT 702 does not dramatically affect response profiles.

An important and not completely unexpected observation was the impact of ADK inhibition on $\dot{V}_{O_2}$. Increases in ADOe in the CNS during hypoxia or seizure have long been considered neuroprotective through the widespread A_1 receptor-mediated presynaptic inhibition, a reduction in brain activity and reduced oxygen demand (Boison, 2013b; Fedele et al., 2006; Richerson et al., 2016). My data showing inhibition of ADK reduces basal $\dot{V}_{O_2}$ is supported by previous observations that ADK activity is increased during periods of wakefulness when basal metabolic

rate is higher (Alanko et al., 2003; Mackiewicz et al., 2003). Whether the reduction in $\dot{V}_{O_2}$ I see here are due to actions of ABT 702 within the CNS alone, which could include reductions in CNS metabolism and CNS-mediated systemic effects, or also include actions of ABT 702 in the periphery is not known since the drug was administered globally. However, reductions in CNS metabolism alone seems unlikely given that ABT 702 caused baseline metabolic rate to fall by at least 40% in the P11–12 and P20 groups.

A confounding result that arose from this data were that hypoxic ventilatory and metabolic responses of vehicle-injected FVB mice appeared different than the untreated FVB mice used to measure the effect of ENT1/2 KO through development. In the latter experiments, neonates significantly increased $\dot{V}_E$ during the initial phase of hypoxia and sustain $\dot{V}_E/\dot{V}_{O_2}$ above baseline throughout hypoxia, which was not seen in the controls used to test the effect of ABT 702. This could reflect additional stress caused by intraperitoneal injection of DMSO causing $\dot{V}_E$ to rise such that hypoxia did not elicit further increases. The number of FVB mice used in the ENT1/2 KO experiments was also much higher, therefore increasing the sample size may reduce variability in the vehicle-treatment FVB group, however the rationale for further hypoxia experiments using i.p. vehicle/ABT 702 injections is weakened since whole body ADK inhibition had significantly larger depressive effects on baseline $\dot{V}_E$ and $\dot{V}_{O_2}$ in developing mice that confound observations that compare the effects of hypoxia to pre-hypoxic values.

3.4.3 Overexpression of ADK-S in C57BL/6J mice produces an adult-like HVR in newborns and enhances ventilatory responses in older mice

Pharmacological approaches are only as good as the specificity of drugs used. Other than its acute inhibitory effects on ADK-L and -S activity (Jarvis et al., 2000), ABT 702 can also elicit long-term cardioprotective effects by reducing cardiac ADK-L content through a proteasome-dependent mechanism in mice (Wölkart et al., 2022), but that does not exclude unidentified off-target actions. Transgenic and shRNA technologies to remove or reduce ADK activity were not initially pursued because ADK KO is lethal (Boison et al., 2002) and ADK-S expression in the brain is very low at birth; i.e., it is difficult to block or inhibit something that is not yet expressed or functional. As an alternative approach, I tested the hypothesis that neonatal mice engineered to express adult levels of ADK-S at birth, ADKtg mice, will have adult-like ventilatory responses to hypoxia; i.e.

sustained increased in $\dot{V}_E$ and $\dot{V}_E/\dot{V}_{O_2}$. I also hypothesized that with increased expression of endogenous ADK-S in WT mice, differences in the HVR between strains would diminish.

The first point to address is that while the transgenic approach indeed achieved a consistent high level of ADK-S expression in the brainstem of ADKtg mice throughout development, the degree of overexpression was greatest at birth and decreased progressively until P20–23 and adult hood when the ADK-S expression WT mice increased to match that in the ADKtg mice, as shown in Chapter 2 (Fig. 2.8). ADKtg did not impact overall growth, as assessed by body weight. However, ADK overexpression did impact development of breathing behaviour and metabolic rate. Interestingly, during the stages in early stages development when ADK-S levels were most different (P0–3 and 6-7), $\dot{V}_E$, frequency V_T, and $\dot{V}_{O_2}$, $\dot{V}_E/\dot{V}_{O_2}$ were all similar between strains. As the levels of ADK-S in WT and ADKtg mice converged with development, differences in $\dot{V}_E$, V_T emerged and persisted into adulthood when ADK-S expression was similar between strains. Baseline $\dot{V}_{O_2}$ was also significantly lower in ADKtg mice at P12–14 and trended lower in P20–22 and P43–56 ADKtg. As a result, there were no differences in baseline $\dot{V}_E/\dot{V}_{O_2}$ between strains during (except at P6–7). These data suggest that reductions in baseline $\dot{V}_E$, V_T and possibly $\dot{V}_{O_2}$ in the older ADKtg mice were due to long-term changes in CNS function that developed as a consequence of early overexpression of ADK-S or under expression of ADK-L.

In contrast, ADK-S-mediated enhancement of the $\dot{V}_E/\dot{V}_{O_2}$ response correlated with the degree of ADK-S overexpression. I hypothesized that the accumulation of ADOe during hypoxia, which is implicated in the secondary hypoxic depression of breathing, would be reduced in the neonatal ADKtg due to more effective ADOe clearance, and neonate ADKtg mice would respond to hypoxia with a larger and/or longer-lasting increase in $\dot{V}_E$ increase. The enhanced $\dot{V}_E$ response would in turn would cause a larger and more sustained hyperventilatory response (i.e., increased $\dot{V}_E/\dot{V}_{O_2}$) to hypoxia. As predicted, P0–3 mice that ADK-S overexpressed ADK-S showed a mature sustained increase in $\dot{V}_E/\dot{V}_{O_2}$ during hypoxia while WT C57BL/6J did not show even a transient increase in $\dot{V}_E/\dot{V}_{O_2}$. Surprisingly, however, the primary reason for this was not a more sustained increase in $\dot{V}_E$. While the $\dot{V}_E$ response was modestly more sustained in the ADKtg mice, the main factor in the enhanced $\dot{V}_E/\dot{V}_{O_2}$ response was an altered metabolic response. P0–3 ADKtg mice

showed a modest decrease in $\dot{V}O_2$ that was significant at 10 min of hypoxia. By P6–7, between strain differences were greatly reduced and they were gone by P12–14, reflecting modest improvement of the $\dot{V}E$ response but primarily reflecting that WT and ADKtg mice both showed a hypometabolic response to hypoxia. It is well-established that neonatal mammals respond to hypoxia with a fall and metabolic rate and that the reduction is greatest in the youngest animals (Mortola, 1999). Variability in hypoxic and hypercapnic responses between mouse strains is well-established (Tankersley et al., 1994) but absence of a hypoxia-induced fall in $\dot{V}O_2$ was surprising. Nevertheless, to ensure that the lack of a metabolic depression did not simply reflect a reduced hypoxic sensitivity in C57BL/6J mice, I repeated the experiment using 8% O_2. The responses were virtually identical – $\dot{V}O_2$ was still much higher during hypoxia in the WT vs ADKtg mice, but in this case the ADKtg showed much stronger fall in $\dot{V}O_2$. Moreover, the WT mice neither increased nor decreased $\dot{V}O_2$. Thus, the association in young mice between ADKtg overexpression and the capacity to reduce $\dot{V}O_2$ during hypoxia seems clear. Once again, the main differences between WT and ADKtg mice were gone by P6–8. In mice older than P19 when ADK-S levels were similar between strains, the $\dot{V}E$ response to hypoxia was progressively enhanced in the ADKtg mice and the hypoxic hypometabolism became less prominent. Together, these results point to a role in ADK-S in modulating both ventilatory and metabolic responses to hypoxia. In terms of dynamic ventilatory and metabolic responses to hypoxia, the main effect of ADKtg in neonatal mice is to facilitate reductions in metabolic rate. At this developmental stage, ADK-S levels are greater in the ADKtg mice so this could reflect direct actions of ADK-S on metabolism. In older mice, the main effect in ADKtg mice on $\dot{V}E$ is through more sustained increases frequency during hypoxia. At this stage, ADK-S levels are similar in the two strains to the enhanced $\dot{V}E$ response is not likely to reflect greater capacity to convert ADOi into AMP. Instead, changes in the adults are likely to reflect more permanent changes in respiratory control centres as a result of early overexpression of ADK-S or the lack of ADK-L. Mechanisms via which enhanced ADK-S could cause a greater hypoxic depression (or at least a smaller increase in $\dot{V}O_2$) in neonates is not clear. One possibility is through increases in the AMP/ATP ratio which activates AMP kinase (AMPK). One consequence of AMPK activation is metabolic depression. The relevance of this mechanism to the hypoxic responses of ADKtg mice, however, is not known. AMPK activity has also been shown to increase $\dot{V}E$ responses to hypoxia (MacMillan and Evans, 2023; Mahmoud et al., 2016). Thus,

further studies will need to consider the role of AMPK in mediating the effects of ADKtg on both hypoxic ventilatory and metabolic responses, as enhanced ADK-S activity could activate this protein by increasing the AMP/ATP ratio.

I expected that differences in the hypoxic responses between C57BL/6J and ADKtg mice would diminish in older animals as endogenous ADK-S levels rose toward those produced by the ADK-S transgene. However, even in adult mice, $\dot{V}_E$ responses to hypoxia were smaller in C57BL/6J mice reflecting ADKtg had compensatory changes as a result of overexpressed ADK-S from birth or lack of ADK-L in the brain. The largest effect of ADKtg on hypoxic responses, however, was its effect on metabolic rate in the youngest mice. Pharmacological and ADKtg data point to the importance of ADK in modulating metabolic rate under baseline conditions response to hypoxia, respectively. Inhibition of ADK with ABT 702 caused a substantial inhibition of metabolic rate in P11–12 and P20 mice but did not affect baseline $\dot{V}_{O_2}$ of newborns. Exogenous expression of ADK in ADKtg mice bestowed upon P0–3 C57BL/6J mice an ability to depress $\dot{V}_{O_2}$ during hypoxia, and mount a sustained, adult-like hyperventilatory response to hypoxia. The mechanism and central network by which ADK influences these responses is not currently known, therefore future studies are needed to expand upon these results.

3.4.4 Metabolic responses to hypoxia differ in neonate FVB and C57BL/6J mice

A serendipitous finding of this study, that arose simply the because the ENT1/2 KO and ADKtg mice used were developed in different background strains, is that two WT strains of mice commonly used in research, appear to differ significantly in how they respond to hypoxia during development. At birth, metabolic rate of C57BL/6J mice appears much less sensitive to hypoxic depression compared to FVB mice. The biphasic $\dot{V}_E$ response of FVB and C57BL/6J mice to hypoxia follows the classical developmental profile in which young mice do not produce a sustained increase in $\dot{V}_E$; after a rapid phase I increase that peaks within the first minute (at all ages) $\dot{V}_E$ falls back to or below baseline. As mice develop, the degree of this secondary depression diminishes and $\dot{V}_E$ remains above baseline throughout the hypoxic exposure. The main difference was the lack of a hypoxic depression of $\dot{V}_{O_2}$ in the youngest C57BL/6J mice, which meant that while FVB responded to hypoxia with a sustained increase in $\dot{V}_E/\dot{V}_{O_2}$, $\dot{V}_E/\dot{V}_{O_2}$ did not change during hypoxia in the C57BL/6J mice.

These data are consistent with the view, based on analysis of developmental responses to hypoxia in multiple mammalian species, that the expression of an adaptive hyperventilatory response throughout hypoxia depends in neonates more on a progressive reduction in $\dot{V}O_2$ (Frappell et al., 1992; Mortola, 1999; Mortola et al., 1989). In other words, the greater and progressive secondary depression of $\dot{V}E$ in neonates may simply reflect a greater, progressive metabolic depression. Indeed, the magnitude of the $\dot{V}E$ depression that follows the phase I increase correlates with the magnitude of metabolic depression, suggesting the $\dot{V}E$ may not be compromised in neonates. In contrast, the sustained hyperventilatory response in adults relies more on the production of a sustained increase in $\dot{V}E$ (Frappell et al., 1992; Mortola, 1999). My data show that even between two similarly sized strains of mice there is considerable variability in the development of ventilatory and metabolic responses to hypoxia, and possibly their ability to tolerate hypoxia. Importantly, the data from C57BL/6J mice challenge dogma that neonatal mammals respond to hypoxia with a decrease in $\dot{V}O_2$ that is largest in the youngest animals. In fact, closer examination of the literature underlying the hypothesis that the greater hypoxic respiratory depression in neonatal mammals simply reflects a greater metabolic depression reveals a somewhat variable definition of newborn. Of course, a uniform definition of "newborn" is challenging given large differences in CNS maturity at the time of birth in, for example, precocial compared to altricial species. However, in some cases neonatal groups include two week-old animals, such as dogs (Rohlicek et al., 1998), cats (Rohlicek et al., 1996), lambs (Fahey and Lister, 1989) and rats (Gozal et al., 2003; Mortola et al., 1986). In almost all species included in the analysis of Mortola et al. (1989), P0 animals were not included. Rodent literature did not include animals younger than P2 (Frappell et al., 1992; Mortola et al., 1989). Recent work of Wong-Riley on SD rats and now my analysis of C57BL/6J mice show that at birth hypoxia does not depress $\dot{V}O_2$ (Liu et al., 2009; Liu and Wong-Riley, 2013). Similarly, human data suggest that adaptive reductions in metabolism do not occur in youngest premature infants but appear in older full-term babies (Cross et al., 1958). Strain difference in ventilatory responses of mice to hypoxic and hypercapnic challenges are well documented (Tankersley et al., 1994). Thus, the data presented here in FVB and C57BL/6J mice indicate the importance of revisiting the established view that neonatal mammals respond to hypoxia with a decrease in $\dot{V}O_2$, the magnitude of which decreases monotonical with development.

3.4.5 Physiological Significance

My analysis of baseline ventilation and metabolic rate as well as ventilatory and metabolic responses to hypoxia in WT, ENT1/2 KO and ADKtg mice provides evidence that ENT and ADK activity modulate ventilatory responses to hypoxia and that these effects increase postnatally. A surprising outcome is the potential importance of ADK in metabolic control and in shaping metabolic responses to hypoxia. Data also show that in general, the actions of ENT and ADK enhance adaptive responses to hypoxia either causing a prolongation of the excitatory effects of hypoxia on $\dot{V}_E$, or in the case of ADK, a prolongation of the inhibitory actions of hypoxia on $\dot{V}_{O_2}$. ENT1 and 2, and presumptive changes in ADOe–ADOi that result from loss of these transporters did not impact metabolism. My focus on ENTs and ADK in these studies was based on in vitro data showing that in the preBötC limited capacity for ADOe clearance in neonates could account for the greater hypoxic respiratory depression in newborns. In vivo experiments performed here using mice in which levels of ENTs or ADK-S were altered globally, either in the entire body (ENT1/2 KO) or the brain (ADKtg), were designed as initial surveys to assess the potential importance of these proteins in shaping ventilatory and metabolic responses to hypoxia. A major limitation of course is that the in vivo data do not provide insight about the site(s) at which ENTs or ADK act to produce the observed actions. Given the positive outcome of these initial experiments, the next stage will be to identify site(s) of action. This includes directly manipulating ENTs and ADK in the preBötC, although effects on $\dot{V}_E$ and frequency as shown here are entirely consistent with an action in the preBötC (Fig. 3.3, 3.7–3.8), which are supported by in vitro results showing ENT and ADK activity influence basal excitability in the network in juvenile slices and limit the inhibitory effects of ADO (Fig. 2.5–2.8).

Despite the lack of spatial resolution that comes with global manipulation of ENT activity, a bonus of this manipulation is that data are provide valuable insight into the source of elevated ADOe that develops in the brain during hypoxia. This is a longstanding question in purinergic signaling (Brundege and Dunwiddie, 1996; Koos et al., 1997; Lloyd et al., 1993; Meghji et al., 1989). Historically, the view was that the elevation in ADOe during hypoxia was from ENT-mediated transport of ADOi that accumulates inside cells during hypoxia when lack of O_2 limits ATP production. An opposing view that emerged in the last 25 years is that the main source of ADOe in hypoxia is from the degradation of ATP released into the extracellular space. The depression of

$\dot{V}_E$ and frequency relative to WT mice was quicker in ENT1/2 KOs consistent with the view that inhibitory ADOe is produced by the breakdown of ATPe rather than transport from inside cells through ENTs. This is consistent with data showing A_1 receptor activation limits the excitatory effects of locally applied ATP within the preBötC network (Huxtable et al., 2009; Zwicker et al., 2011) (Fig. 2.1). A caveat is that ADOe accumulation is not the only contributor to the secondary depression of the $HVR_{\dot{V}E}$, as modulators such as GABA are also implicated (Ballanyi, 2004; Neubauer et al., 1990; Xiao et al., 2000). I cannot exclude that global ENT1/2 KO did not affect other systems throughout the brain that potentiated the $\dot{V}_E$ depression. Future experiments that locally inhibit ENT activity or eliminate its expression directly in the preBötC would eliminate these compensatory effects, providing more direct evidence that ENT-independent ADOe accumulation from extracellular sources in the inspiratory network contributes to the hypoxic respiratory depression. Nonetheless, my data suggests that limiting the breakdown of ATPe to reduce the accumulation of ADOe may stabilize or stimulate breathing under conditions where breathing is compromised including apnea of prematurity and pathophysiological conditions where ventilation is compromised including a host of neurodegenerative diseases where the preBötC network undergoes degeneration (Howell and Newman, 2017; Presti et al., 2014) and SUDEP.

SUDEP is of particular interest in the context of ADO signaling and ADK because a precipitating brain injury can trigger biphasic regulation of ADK expression with acute downregulation that increases ADOe, followed by upregulation that persists after ADOe levels are restored (Boison, 2013b, 2012a; Li et al., 2007). Upregulated ADK is tightly linked to the development of an epileptic brain, known as epileptogenesis (Aronica et al., 2011; Boison, 2013b; Gouder et al., 2004; Klein et al., 2018; Li et al., 2008; Weltha et al., 2019). Elevated ADK reduces ADOe tone in the brain, which contributes to network hyperexcitability and a predisposition to seizure. ADO is strongly implicated in the dynamics of epileptic seizures since ADOe increases during seizures, which is an endogenous mechanism to stop the event, reduce energy consumption and limit further neurological injury (Boison, 2013b; Fedele et al., 2006; Richerson et al., 2016). ADOe increases are important in terminating seizures, however it is hypothesized that if seizure spreads to the brainstem, elevated ADOe are causally related to terminal apneas (Devinsky et al., 2016; Jansen et al., 2019; Patodia et al., 2018; Richerson et al., 2016), which appear to be the primary cause of

death in SUDEP (Ryvlin et al., 2013). This presents a clinical challenge since to treat seizures, the goal is to reduce ADK overexpression, as this increases ADOe tone and prevents seizure from occurring, however ADOe increases induced by inhibiting ADK also inhibits breathing and increase risk of apnea. Indeed, inhibiting ADK activity increases fatal seizure events in mice (Shen et al., 2022).

My data suggest that both ENT and ADK activity, which contribute to ADOe clearance, can reduce the magnitude of the secondary $\dot{V}_E$ depression. This most likely result from a reduction in ADOe, which is elevated during hypoxia (Funk, 2013; Koos et al., 1994; Moss, 2000; Richter et al., 1999; Yan et al., 1995). Thus, while inhibiting ENT and ADK could be important in reducing risk of SUDEP, this also increases the risk of seizures. During pathophysiological conditions, respiratory networks may still be susceptible to excessive ADOe levels produced in the epileptic brain and require further support to reduce the actions of ADO and prevent fatal apnea. Further research is needed to determine if ADK expression also increases in respiratory networks away from the seizure location, which would prevent ADO-mediated apneas. In the NTS, which is a medullary region important for cardiorespiratory regulation, ADK is upregulated following hippocampal seizure and may help contribute to reduced incidences of SUDEP (Shen et al., 2022) Nonetheless, data suggest that alterations of adenosinergic signaling can contribute to pathophysiological outcomes across development. Research from the fields of central respiratory control and epilepsy may be instrumental for designing new therapies that prevent ADO-mediated hypoventilation in vulnerable populations. Therapies targeted to reduce ADK levels in cortical regions responsible for seizure generation are actively being explored for the treatment of epilepsy (Boison, 2013b). Indeed, since the best way to reduce SUDEP is to reduce seizures, efforts to downregulate ADK to prevent seizures are likely the best approach, even if this does lead to reduced ADK expression and elevated ADOe in respiratory networks. However, in the development of any approach designed to reduce cortical/hippocampal ADK expression to reduce seizure, thorough evaluation of the efficacy and potential risks of such treatment will require a better understanding of how reduced ADK and elevated ADOe tone in respiratory networks impacts cardiorespiratory control in both short and long term.

Chapter 4: Variability in the ventilatory and metabolic responses of neonatal rodents to hypoxia: a direct challenge to the hypothesis that hypoxic depression of $\dot{V}O_2$ is a ubiquitous adaptive response amongst neonatal mammals.

4.1 Introduction

Breathing functions primarily to deliver oxygen rich air from the atmosphere to the gas exchange surface, the alveoli, in the lungs where it is extracted into the pulmonary circulation and returned to the heart for distribution to the rest of the body to support oxidative metabolism. At the same time that oxygen is extracted from the air in the alveoli, CO_2 is delivered from the pulmonary circulation to the alveoli and then expired into the atmosphere. The amount we breathe is homeostatically-regulated to maintain arterial oxygen (PaO_2) and carbon dioxide ($PaCO_2$) at constant levels; i.e., ventilation is adjusted to match metabolic demand. Precise regulation of PaO_2 and a constant supply of oxygen is particularly important for hypoxia-sensitive organs like the brain, which reflects its high metabolic rate, minimal capacity to store energy substrates (Bélanger et al., 2011; Bouzier-Sore et al., 2002; Schurr et al., 1999) and almost complete dependence on aerobic metabolism. Indeed, the brain can only survive for a few minutes without O_2 before suffering permanent damage (Cronberg et al., 2020; Novak et al., 2018). A number of protective/adaptive reflexes have evolved to protect PaO_2. One of the most important in mammals is the biphasic hypoxic ventilatory response, $HVR_{\dot{V}E}$, that is triggered by reductions in PaO_2. The $HVR_{\dot{V}E}$ comprises a rapid (< 1min), carotid-body mediated increase in ventilation followed by a secondary depressive phase over the next 3–4 min when ventilation falls to varying degrees, depending on species and stage of development, to a new steady-state level (Bissonnette, 2000; Mortola, 1996; Moss, 2000). The magnitude of the secondary depression generally decreases with development in most mammals (Bonora et al., 1984; Mortola, 1999; Moss, 2000). Thus, $\dot{V}E$ remains above baseline throughout hypoxia in adults, while in newborns $\dot{V}E$ often falls to, or below, baseline levels. The greater depression, which is attributed in part to more powerful central inhibitory mechanism (Fiore et al., 2013; Herlenius et al., 2002; Koos et al., 1997; Paolillo and Picone, 2013; Reklow et al., 2019), can underlie a life-threatening positive feedback loop in premature infants and newborns; i.e. if the initial increase in $\dot{V}E$ does not immediately restore PaO_2, $\dot{V}E$ can fall below baseline, potentially causing greater hypoxemia, greater respiratory depression, further reductions in PaO_2 and so on until the feedback loop is interrupted or the newborn dies (Bonora et al., 1984; Carroll and Bureau, 1987; Cross and Oppe, 1952).

Whether the secondary depression of $\dot{V}E$ during hypoxia becomes life-threatening, however, depends on other adaptive responses, the most important being the hypoxic depression of $\dot{V}O_2$. Just

as increasing the delivery of air to the lungs, even air that is low in O_2, is one strategy that will enhance the ability to tolerate hypoxia. A second strategy is to reduce the need for oxygen by decreasing metabolic rate. Clearly an increase in $\dot{V}_E$ and decrease in $\dot{V}_{O_2}$ will prolong the ability to survive periods when O_2 availability falls. Both strategies (increased $\dot{V}_E$ and decreased $\dot{V}_{O_2}$) will contribute to a sustained increase in $\dot{V}_E/\dot{V}_{O_2}$; i.e., more air moved per unit of O_2 consumed, which is defined as a hyperventilatory response (Barros et al., 2001; Cross et al., 1958; Frappell et al., 1992; Gill and Pugh, 1964; Mortola, 2004). Whether the greater secondary fall in $\dot{V}_E$ that occurs during hypoxia is problematic depends on the magnitude of the metabolic depression. If the secondary fall in $\dot{V}_E$ is in direct proportion to hypoxia-induced reductions in $\dot{V}_{O_2}$ then the respiratory homeostatic control system is performing as expected and blood gases should remain constant. Whether the greater secondary depression of $\dot{V}_E$ during hypoxia in newborns is simply due to a greater decrease in $\dot{V}_{O_2}$ (i.e., the depression of $\dot{V}_E$ in newborns is proportionate to reductions in $\dot{V}_{O_2}$, homeostatic, and newborns are not at greater risk during hypoxia), or whether neonates express a more powerful, centrally-mediated depression of breathing that exceeds the fall in metabolism (i.e., the depression of $\dot{V}_E$ puts neonates at higher risk when exposed to hypoxia) has been a topic of debate for decades (Alvaro et al., 1992; Haddad et al., 1982; Mortola, 1996; Moss, 2000). That the secondary depression of $\dot{V}_E$ is greater in neonatal mammals is well-established. That hypoxia depresses $\dot{V}_{O_2}$ and that this depression tends to be greater in neonatal mammals and diminish with age is also well-established over the developmental windows studied. The degree to which the fall in $\dot{V}_E$ is secondary and precisely matched to the hypoxia-induced fall in $\dot{V}_{O_2}$ remains contentious. A large body of data comparing $\dot{V}_E$ and metabolic responses of neonates across multiple mammalian species pushed the scale toward the view that the greater decrease in $\dot{V}_E$ during hypoxia is not a sign of an inadequate or immature HVR (Frappell et al., 1992; Hill, 1959; Mortola, 1999, 1996). Indeed, they showed that the secondary fall in $\dot{V}_E$ during hypoxia in many neonatal species is approximately proportional to reductions in metabolic rate. This was the basis of the conclusion that the inability of neonates to produce a sustained increase in $\dot{V}_E$ during hypoxia is the appropriate homeostatic response; $\dot{V}_E$ falls more because $\dot{V}_{O_2}$ falls more; i.e., O_2 homeostatic control systems, while not fully mature, are fully functional and enable newborns to respond to hypoxia with a sustained, adaptive hyperventilation (a sustained increase in $\dot{V}_E/\dot{V}_{O_2}$). Thus, mammals at all ages respond to hypoxia with a sustained hyperventilation; in

young mammals the increase in $\dot{V}_E/\dot{V}_{O_2}$ is more dependent on a decrease in $\dot{V}_{O_2}$ while in more mature mammals the increase in $\dot{V}_E/\dot{V}_{O_2}$ results primarily from an increase in $\dot{V}_E$ (the hypoxic depression of $\dot{V}_{O_2}$ decreases with development and often disappears in adulthood).

The major limitation of these data is that the analyses did not fully explore postnatal development (Fahey and Lister, 1989; Frappell et al., 1992; Mortola et al., 1989; Rohlicek et al., 1998). Measurements are most difficult to obtain in the period immediately following birth, and measurements from the earliest postnatal periods were lacking in many species. Measurements in rodents, for example, did not start until after P3 (Gozal et al., 2003; Mortola et al., 1986; Peyronnet et al., 2000). Thus, the sweeping conclusion that neonatal mammals respond to hypoxia with a depression of $\dot{V}_{O_2}$ that decreases monotonically with development requires extrapolation from the youngest animals measured to the youngest animals. It assumes that the mechanisms responsible for the hypoxic depression of $\dot{V}_{O_2}$ are functional and most effective at birth and decrease thereafter.

My developmental analysis of the hypoxic responses of FVB and C57BL/6J mice in Chapter 3 directly challenges this assumption. While data from FVB mice appeared to fit the hypothesis that mammals at all stages of development respond to hypoxia with a sustained hyperventilation ($\dot{V}_E/\dot{V}_{O_2}$), data from C57BL/6J did not. P1–2 C57BL/6J mice showed the expected biphasic ventilatory response to hypoxia but did not depress $\dot{V}_{O_2}$ during hypoxia, nor did they hyperventilate ($\dot{V}_E/\dot{V}_{O_2}$ did not change), unless they were modified to express adult levels of ADK-S in the CNS (Fig. 3.7, 3.8). These data suggest that, in contrast to most published data, hypoxia does not induce adaptive reductions in $\dot{V}_{O_2}$ in all neonates, and that mechanisms via which hypoxia depresses $\dot{V}_{O_2}$ emerge at some point during postnatal development. Consistent with our observations in C57BL/6J mice, daily measurements of hypoxic responses in SD rats during postnatal development show that hypoxia does not depress metabolic rate in P0 or P1 rats – the metabolic depression did not emerge until P2 (Liu et al., 2009). Similarly, the hypoxic depression of $\dot{V}_{O_2}$ is very small in premature infants on their day of birth compared to two week-old premature infants and full-term infants (Cross et al., 1958).

Thus, the overarching objective of this study was to examine in two strains of mice and SD rats, the validity of the hypothesis that hypoxia inhibits $\dot{V}_{O_2}$ in neonatal mammals and that the

magnitude of this inhibition is inversely related to age – i.e., it is strongest in the youngest and decreases with development. I began by first fully characterizing the postnatal development of ventilatory and metabolic responses of C57BL/6J mice to hypoxia. My next objective was to assess whether C57BL/6J mice are unique amongst rodents in not responding to hypoxia with a decrease in $\dot{V}O_2$. To this end, I compared hypoxic responses of C57 and FVB mice during development. Finally, I tested the hypothesis that the ability for hypoxia to depress $\dot{V}O_2$ in rodents emerges postnatally. To this end, I analyzed the day-over-day the ventilatory and metabolic responses of C57BL/6J and FVB mice, and Sprague-Dawley rats to hypoxia using head-out plethysmography.

4.2 Methods

4.2.1 Ethics Approval

Experimental procedures were approved by the Animal Care and Use Committee (ACUC) of the University of Alberta (AUP #256) in compliance with the Canadian Council on Animal Care Standards.

4.2.2 Animals

Neonate (P0–3) FVB/NCrl (Strain Code 207, Charles River, Wilmington, MA, USA) and C57BL/6J mice (P0–8) (Jackson Laboratories, Bar Harbor, ME, USA) were obtained from local colonies developed from breeding pairs purchased from the indicated supplier. P0–3 Sprague-Dawley (SD) rats were obtained from timed-pregnant dams shipped monthly from Charles River Laboratories (Wilmington, ME, USA). All animals were housed in the University of Alberta's Health Sciences Laboratory Animal Services and maintained on a 12-h light/dark schedule with *ad libitum* access to food and water.

4.2.3 Head-Out Plethysmography

All plethysmograph experiments took place between 0900–1800 hrs and were performed as described in Chapter 3. I limit my methods description in this Chapter to procedures/analyses that differ from those described in Chapter 3. Animals were placed into the head-out plethysmograph and allowed to acclimate in the chamber for at least 15 minutes, then baseline ventilatory and metabolic measurements were recorded until at least 2 minutes of stable, quiescent data was collected. The inspired air was then quickly ($\leq$ 10 s) changed to a hypoxic mixture (10% or 8% O_2

and N_2 balance) for 10 minutes before returning to normoxic conditions. The animal and chamber were placed within an incubator maintained at 32 ± 0.5°C. Gas mixtures were delivered at a flow-rate of 40 ml/min to the head-chamber using a GSM-3 (CWE Inc., Ardmore, PA, USA) and flowmeter (Fischer & Porter Co., Warminster, PA, USA). As described below in Section 4.2.5, gases were sampled from the inflow and outflow ports of the head chamber in order to determine metabolic rate ($\dot{V}O_2$).

4.2.4 Metabolic Measurements using the whole-body plethysmograph

Metabolic measurements were recorded in FVB mice at birth (P0) and at P3 using whole-body chamber. Mice acclimated in the chamber for at least 15 minutes and remained in normoxic conditions for a 5-minute period to record baseline $\dot{V}O_2$. Then, there was a rapid (< 20 s) transition to hypoxia (10% O_2 and N_2 balance), which the mice were exposed to for 10 minutes before quickly returning to normoxia (21% O_2 and N_2 balance). The inspired air mixture was delivered at a set flowrate of 40 ml/min. Composition of inspired and expired gases were measured at the inflow and outflow ports identical to the head-out plethysmograph experiments, as described in the next section. The metabolic rate experiments were also conducted within an incubator at the same temperature (32 ± 0.5°C) as the head-out plethysmography experiments.

4.2.5 Measurement of Ventilatory and Metabolic Parameters

Rhythmic inspiration and expiration of the rodents in the head-out plethysmograph were detected using a differential pressure transducer (Validyne Engineering, Northridge, CA, USA) attached to a port on the body chamber. Pressure transducer output was passed through a CD15 carrier demodulator (Validyne Engineering), digitized using a PowerLab System (ADInstruments, Sydney, Australia) and visualized using the LabChart data analysis software (version 7, ADInstruments). Tidal volume (V_T) was calculated using the formula described in Chapter 3.

For both the head-out and metabolic rate measurement experiments, O_2 and CO_2 fractions of the inhaled and exhaled air were passed through a drying column (Drierite, Sigma-Aldrich, St Louis, MO, USA) and then sampled using a gas-analyzer (ADInstruments). Metabolic rate ($\dot{V}O_2$) was determined using the formula:

$$\dot{V}O_2 = [FR \times (FiO_2 - FeO_2) - FiO_2 (FeCO_2 - FiCO_2)] / 1 - FiO_2,$$

where FR is the flowrate of gas through the chamber (ml/min), FiO_2 is the inflow O_2 fraction, FeO_2 is the outflow O_2 fraction, $FiCO_2$ was the inflow CO_2 fraction and $FeCO_2$ was the outflow CO_2 fraction. V_T, $\dot{V}E$, and $\dot{V}O_2$ were normalized to the body weight of the mouse or rat (kg) and data are presented in standard conditions of temperature, pressure and dry air.

4.2.6 Data Analysis and Statistical Comparisons

Ventilatory parameters were analyzed using LabChart 8 software (ADInstruments). Variables reported along the response time course represent values averaged during each time bin and are as follows: (t = 0, baseline averaged from 2 min of calm breathing prior to onset of hypoxia; t = 0.33: average of first 10–20 sec of hypoxia when the measured chamber O_2 was < 20% and > 11%); t = 1: average from 0.33 – 1.0 min of hypoxia; t = 2: 1–2 min of hypoxia; t = 4: 3–4 min of hypoxia; t = 10: average from 7–10 min of hypoxia.

Statistical comparisons were made using Prism, version 7 (GraphPad Software Inc., La Jolla, CA, USA). Two-way ANOVA with Sidak's *post hoc* multiple comparison tests were used to test if the average of each parameter at a given timepoint was different than the pre-hypoxic value. Kruskal-Wallis test with Dunn's *post hoc* comparisons compared differences in the relative steady-state change from baseline (i.e. 7–10 min of hypoxia) between every age group through development within strains. Significance for all comparisons was designated when $P < 0.05$. Time-course graphs showing the mean and S.E.M. were created using Excel. Box plots were created using Prism and the five whiskers represent the lowest sample value, first quartile, median, third quartile, and greatest sample value. The points within the boxes show individual data points.

4.3 Results

4.3.1 Postnatal development of ventilatory and metabolic responses to hypoxia in C57BL/6J

Developmental changes in the ventilatory and metabolic responses to hypoxia in C57BL/6J mice were described in Chapter 3 where they were plotted to compare at each age, differences between the C57BL/6J and ADKtg mice. To more clearly illustrate how $\dot{V}E$, $\dot{V}O_2$, and $\dot{V}E/\dot{V}O_2$ change developmentally, data from C57BL/6J of all age groups are plotted together on the same graph, as

done for FVB data in Fig. 3.1.

As seen in FVB mice, acute hypoxia evoked a biphasic ventilatory response in C57BL/6J mice at all ages (Fig. 4.1, 4.2). $\dot{V}_E$ showed a rapid increase at the onset of hypoxia that increased numerically between P13–14 and the two oldest age groups (e.g., the phase 1 increase in $\dot{V}_E$ was greater in P20–23 and adults compared to the three youngest age groups. After 10 min of hypoxia, $\dot{V}_E$ in all groups had fallen back to levels that were not significantly different from baseline at (Fig. 4.1A, B); i.e., $\dot{V}_E$ responses of C57BL/6J to hypoxia were never sustained for the entire 10 min of hypoxia. This differed from FVB mice in which the increase $\dot{V}_E$ lasted throughout the hypoxic exposure in the oldest two age groups. Nevertheless, the $\dot{V}_E$ responses of FVB and C57BL/6J mice still showed similar developmental trends in that the overall magnitude/duration of the $\dot{V}_E$ response to hypoxia increased developmentally; similarly, the magnitude/duration of the secondary ventilatory depression decreased developmentally. This is evident in Fig. 4.2A, which shows that the duration of time during hypoxia that $\dot{V}_E$ was elevated above baseline increased with age (i.e., the magnitude and duration of the secondary hypoxic ventilatory depression decreased with age).

Plotting the metabolic ($\dot{V}_{O_2}$) responses to hypoxia of all age groups on the same graph (Fig. 4.1C), clearly illustrates the dramatic developmental changes in the $\dot{V}_{O_2}$ response of C57BL/6J mice to hypoxia. Most remarkable was the sustained, hypoxia-induced increase in $\dot{V}_{O_2}$ in P1–2 mice; $\dot{V}_{O_2}$ increased by 2 min of hypoxia and remained 48 ± 17% above baseline at 10 minutes ($p = 0.004$) (Fig. 4.1C-D). This increase was completely opposite to the sustained hypoxia-induced reduction in $\dot{V}_{O_2}$ seen in FVB mice (Figure 4.2B). The hypoxia-induced increase in $\dot{V}_{O_2}$ in P1–2 C57BL/6J mice then reversed by P6–8; both P6–8 and P13–14 responded to hypoxia with a sustained decrease in $\dot{V}_{O_2}$ (44 ± 3%, $p = 0.02$; 48 ± 6% $p < 0.0001$, respectively), similar to that seen in FVB mice. As in FVB mice, the magnitude of the hypoxic metabolic depression then decreased with further development. The only difference between strains in the oldest two age groups was that $\dot{V}_{O_2}$ still fell significantly during hypoxia in FVB mice whereas in C57BL/6J mice $\dot{V}_{O_2}$ did not fall

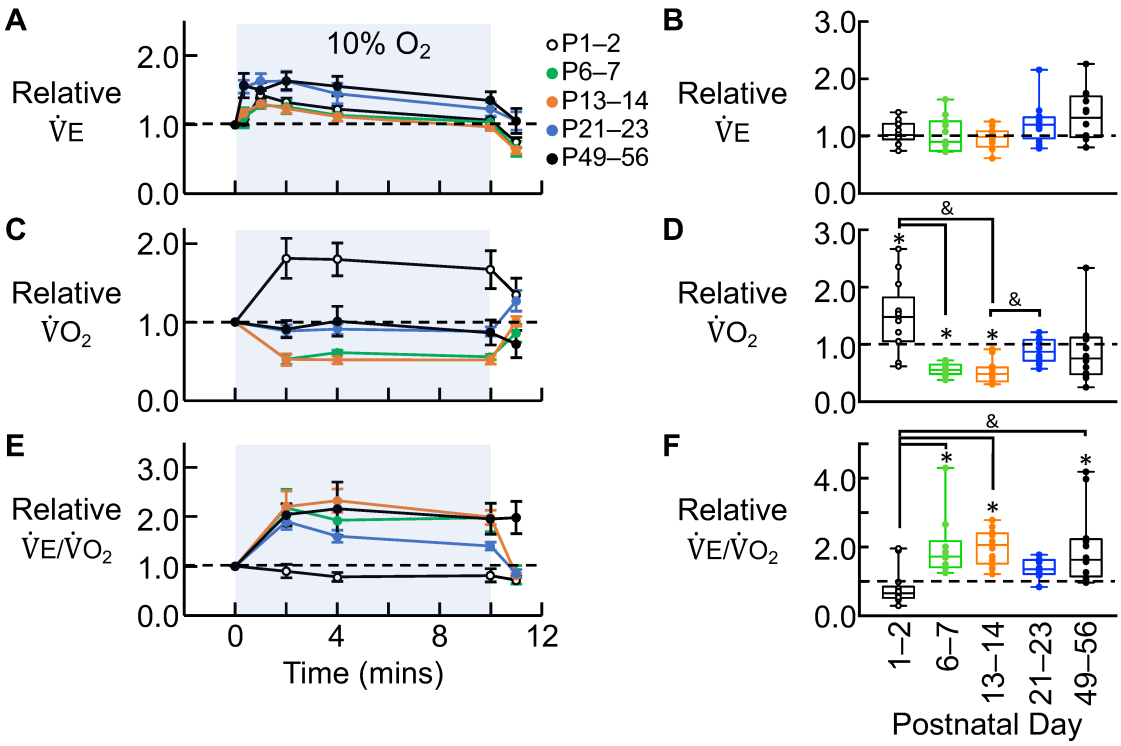

Figure 4.1. Development of ventilatory and metabolic responses to hypoxia in C57BL/6J mice.

Panels A–C plot, relative to pre-hypoxic baseline levels, the time course of changes in A) minute ventilation ($\dot{V}E$), C) metabolic rate ($\dot{V}O_2$) and E) the air convection requirement ($\dot{V}E/\dot{V}O_2$) that were evoked in C57BL/6J by hypoxia (10 minutes in 10% O_2). Box and whisker plots (B, D, F) show the value of each parameter at the end of hypoxia (averaged during minute 7–10 of hypoxia) relative to pre-hypoxic baseline levels for B) $\dot{V}E$, D) $\dot{V}O_2$, and F) $\dot{V}E/\dot{V}O_2$. Measurements were made in P1–2 (n = 14), P6–7 (n = 10), P13–14 (n = 12), P21–23 (n = 12) and P49–56 mice (n = 12). *indicates for each age group a significant difference ($P < 0.05$) from its own baseline (in absolute terms) determined using a two-way ANOVA with Sidak's *post hoc* test. &indicates significant difference between age groups in the relative value of each parameter recorded at the end of hypoxia (7–10 mins) as determined using a Kruskal-Wallis test with Dunn's *post hoc* comparison.

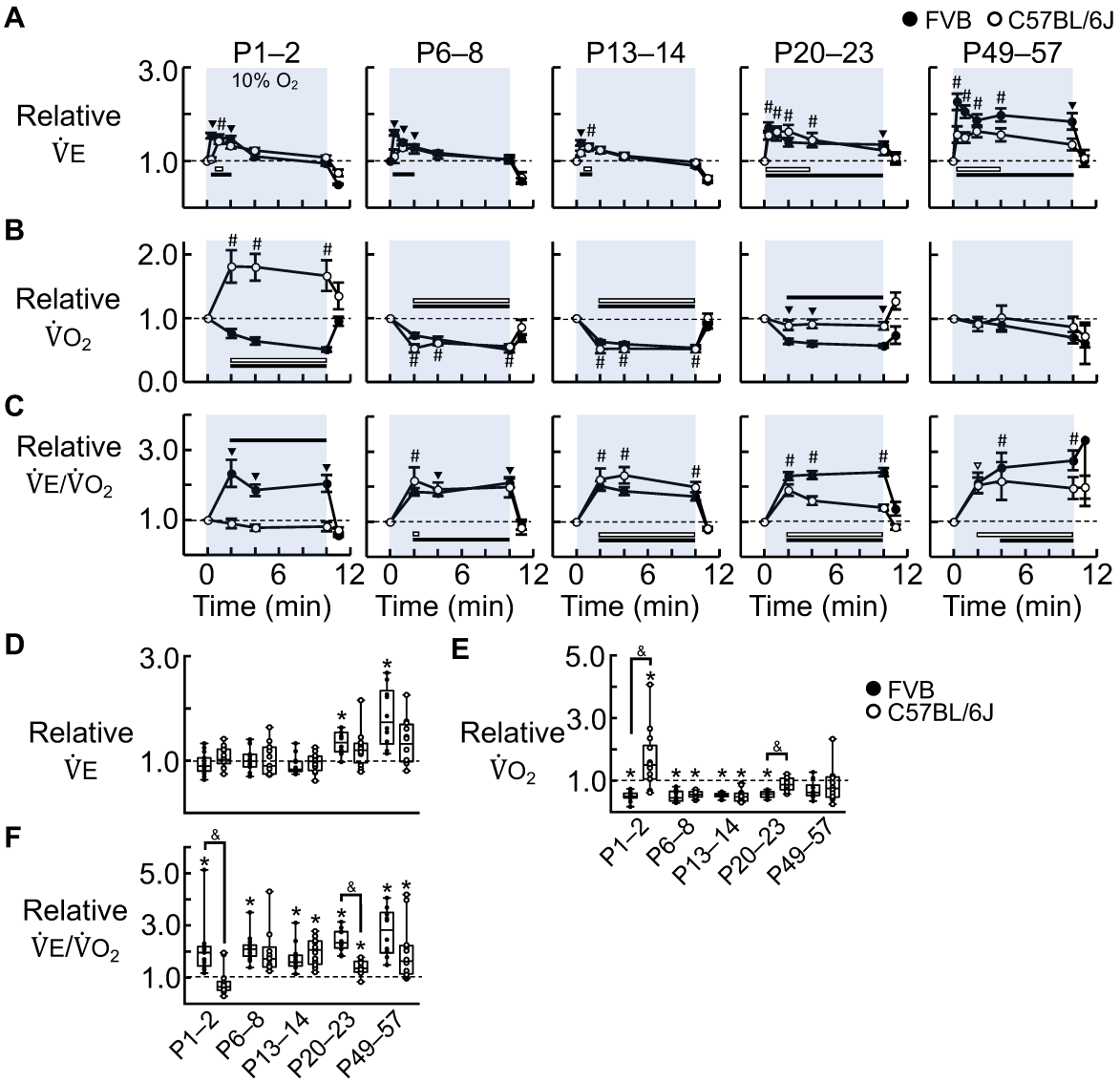
A
FVB
C57BL/6J
P1–2
P6–8
P13–14
P20–23
P49–57
10% O2
Relative V̇E
B
Relative V̇O2
C
Relative V̇E/V̇O2
Time (min)
D
E
F
P1–2
P6–8
P13–14
P20–23
P49–57

Figure 4.2. Developmental comparison of ventilatory and metabolic responses of FVB and C57BL/6J mice to hypoxia.

Panels A–C plot, relative to pre-hypoxic baseline levels, the time course of changes in A) minute ventilation ($\dot{V}_E$), B) metabolic rate ($\dot{V}_{O_2}$), and C) the air convection requirement ($\dot{V}_E/\dot{V}_{O_2}$) that were evoked by hypoxia (10 minutes in 10% O_2) at five stages during postnatal development in FVB (solid circles) and C57BL/6J mice (unfilled circles). Box and whisker plots show relative changes at the end of hypoxia (average of minutes 7–10) relative to pre-hypoxic baseline levels for D) $\dot{V}_E$, E) $\dot{V}_{O_2}$, and F) $\dot{V}_E/\dot{V}_{O_2}$. For A–C, statistical differences were assessed using two-way ANOVA with Sidak's *post hoc* test. For clarity, significant differences from absolute baseline values within a strain are shown in A–C; ▾ indicates a significant difference ($P < 0.05$) from baseline in the FVB group; ▿ indicates a significant difference from baseline in the C57BL/6J group; and $^{\#}$indicates a significant difference from baseline in both groups. Black and white horizontal bars on the relative time-course graphs designate periods when each parameter was significantly different from baseline in the FVB or C57BL/6J groups, respectively. For D–F, *indicates a significant difference from absolute baseline values within a strain as determined using a two-way ANOVA with Sidak's *post hoc* test, whereas $^{\&}$indicates a difference between strains at the indicated age in the relative value of each parameter recorded at the end of hypoxia (7–10 mins), as assessed using a Kruskal-Wallis test with Dunn's *post hoc* comparison.

significantly during hypoxia. So again, the main difference in the metabolic response between the two strains was that $\dot{V}O_2$ was not inhibited in the youngest C57BL/6J mice.

Given the relatively small $\dot{V}E$ response to hypoxia and the absence of a hypoxic metabolic depression in P1–2 C57BL/6J mice, it was not surprising that P1–2 C57BL/6J mice did not hyperventilate (ie., $\dot{V}E/\dot{V}O_2$ did not increase) in response to hypoxia (Fig. 4.1E, F). From that stage forward C57BL/6J mice of all ages showed a sustained hyperventilated during hypoxia. This sustained hyperventilation was significantly greater than baseline for all age groups (P6–7, $p = 0.005$; P13–14, $p < 0.0001$; P49–56, $p = 0.0007$) except P20–23.

4.3.2 Detailed quantification of differences in the ventilatory and metabolic responses of WT FVB and C57BL/6J mice to hypoxia during development

The major developmental differences in the ventilatory and metabolic responses of C57BL/6J and FVB mice to hypoxia are summarized in the preceding section. This section provides a detailed quantification and comparison between strains of the changes evoked by hypoxia (10% O_2) in $\dot{V}E$, $\dot{V}O_2$, and $\dot{V}E/\dot{V}O_2$ at 5 stages between birth and adulthood.

Minute Ventilation ($\dot{V}E$)

At the youngest stage examined, $\dot{V}E$ was greater than baseline at the onset of hypoxia (54 ± 6%, $p < 0.0001$) through the first (50 ± 7%, $p < 0.0001$) and second minutes (47 ± 7%, $p < 0.0001$) in P2 FVB mice (Onset: 54 ± 6%, $p < 0.0001$; 1 min: 50 ± 7%, $p < 0.0001$; 2 min: 47 ± 7%, $p < 0.0001$), while P1–2 C57BL/6J animals only increased $\dot{V}E$ above baseline during the first minute of hypoxia (43 ± 7%, $p = 0.006$) (Figure 4.2A).

In the second developmental window, $\dot{V}E$ raised above baseline in the P7–8 FVB, but not P6–7 C57BL/6J mice, beginning at the onset of hypoxia (60 ± 6%, $p < 0.0001$) and continuing through the through the first two minutes of 10% O_2 (1 min: 40 ± 4%, $p = 0.001$; 2 min: 30 ± 4%, $p = 0.02$).

In P13–14 mice, $\dot{V}E$ was elevated by 38 ± 6% ($p < 0.0001$) in FVB mice at the onset of hypoxia, and both strains increased $\dot{V}E$ above baseline during the first minute of hypoxia (FVB: 28 ± 6%, p

= 0.05; C57BL/6J: 30 ± 7%, p = 0.02). At the third week of development, $\dot{V}_E$ increased 72 ± 11% and 55 ± 9% in FVB (p < 0.0001) and C57BL/6J mice (p = 0.0001) at the onset of hypoxia, respectively.

P20–22 FVB mice sustained this increase in $\dot{V}_E$ through the remainder of the 10-minute hypoxic exposure. At 1 min, $\dot{V}_E$ increased 56 ± 13% (p < 0.0001) above baseline, falling slightly to 39 ± 9% at 2 min (p = 0.008), and stabilizing at 4 min (38 ± 8%, p = 0.01) and 10 min (35 ± 6%, p = 0.02). On the other hand, in P21–23 C57BL/6J mice, $\dot{V}_E$ was raised 63 ± 11% in the first minute (p < 0.0001) and 63 ± 14% in the second minute (p = 0.0001) before falling slightly to 45 ± 15% above baseline at 4 min (p = 0.02), after which, $\dot{V}_E$ then fell back to baseline.

Finally, in the oldest developmental window studied, P49–57 FVB and P49–56 C57BL/6J mice increased $\dot{V}_E$ above baseline at the beginning of hypoxia (FVB: 126 ± 17%, p < 0.0001; C57BL/6J: 56 ± 18%, p = 0.0002). At 1 min, 2 min and 4 min in FVB and C57BL/6J mice, respectively the relative increase in $\dot{V}_E$ was 105 ± 14% (p < 0.0001) vs. 50 ± 11% (p = 0.0002); 86 ± 14% (p < 0.0001) vs. 63 ± 13% (p = 0.005); and 98 ± 14% (p < 0.0001) vs. 56 ± 14% (p = 0.0013). At this age however, only FVB mice maintained $\dot{V}_E$ above baseline by the end of hypoxia (84 ± 18%, p = 0.0002).

These data show that the $\dot{V}_E$ response to hypoxia differs between FVB and C57BL/6J mice, in that FVB mice have more prolonged increases in $\dot{V}_E$ throughout development and the $HVR_{\dot{V}_E}$ matures such that $\dot{V}_E$ remains above baseline levels throughout hypoxia in FVB, but not C57BL/6J mice.

Metabolic Rate ($\dot{V}_{O_2}$)

Comparison of metabolic rate changes during hypoxia revealed that in newborns, P2 FVB mice depressed $\dot{V}_{O_2}$ by 24 ± 7% at 2 min (p = 0.008), by 36 ± 6% at 4 min (p < 0.0001) and by 49 ± 4%, by the end of hypoxia (p < 0.0001). In contrast, $\dot{V}_{O_2}$ rose above baseline throughout hypoxia in P1–2 C57BL/6J animals. $\dot{V}_{O_2}$ was 81 ± 25% above baseline at 2 min (p < 0.0001), increased 80 ± 21% at 4 min (p < 0.0001) and remained 67 ± 24% above baseline at 10 min (p = 0.001) (Fig. 4.2B).

One week later, both P7–8 FVB and P6–7 C57BL/6J mice depressed $\dot{V}O_2$ throughout hypoxia. For FVB mice, $\dot{V}O_2$ fell by 27 ± 4%, 33 ± 5% and 50 ± 4% at 2 min ($p = 0.001$), 4 min ($p = 0.002$) and 10 min ($p < 0.0001$), respectively. C57BL/6J mice reduced metabolic rate by 47 ± 6% ($p = 0.0002$), 39 ± 3% ($p = 0.002$) and 44 ± 3% ($p = 0.0002$) at these same time intervals.

Both strains again also depressed $\dot{V}O_2$ throughout hypoxia at P13–14. The reductions in FVB and C57BL/6J mice at 2 min, 4 min and 10 min, respectively were 37 ± 3% vs. 48 ± 7%; 41 ± 3% vs. -48 ± 5%; and 47 ± 2% vs. 48 ± 6% (all time points: $p < 0.0001$).

At three-weeks of age, $\dot{V}O_2$ fell significantly by ~40% during hypoxia only in the P20–22 FVB mice (2 min: -36 ± 4%; 4 min: -40 ± 4%; 10 min: -43 ± 3%, all time points: $p < 0.0001$), whereas $\dot{V}O_2$ of P21–23 C57BL/6J mice did not change at any point during hypoxia.

Then in the last age group, P49–57 FVB and P49–56 C57BL/6J adult mice did not depress $\dot{V}O_2$ from baseline during 10% O_2 hypoxia.

The largest difference between these strains occurs in neonates, when FVB mice elicit an adaptive $\dot{V}O_2$ depression, whereas metabolic rate of C57BL/6J significantly increases above baseline. By one week, however, differences between strains disappear and hypoxia evokes $\dot{V}O_2$ depression in both sets of mice until later in development when this response becomes attenuated.

Air Convection Requirement ($\dot{V}E/\dot{V}O_2$)

I then tested whether there were differences in the developmental $\dot{V}E/\dot{V}O_2$ responses from baseline during hypoxia in the FVB and C57BL/6J strains (Fig. 4.2C). In the youngest age group, P2 FVB mice, but not P1–2 C57BL/6J animals, hyperventilated above baseline levels throughout hypoxia. The increase in $\dot{V}E/\dot{V}O_2$ in neonate FVB mice was 133 ± 39% at 2 min ($p < 0.0001$), 84 ± 17% at 4 min ($p = 0.0008$) and 104 ± 24% by the end of hypoxia ($p < 0.0001$).

P7–8 FVB mice also hyperventilated 85 ± 11% relative to baseline at 2 min ($p = 0.0064$) then 83 ± 10% at 4 min ($p = 0.007$) and 111 ± 12% at 10 min ($p < 0.0001$), while P6–7 C57BL/6J mice

increased $\dot{V}_E/\dot{V}_{O_2}$ above baseline only during the second minute of hypoxia (118 ± 37%, p = 0.0010). These animals could not sustain the response through the rest of hypoxia.

At P13–14, both strains of mice hyperventilated above baseline levels at each timepoint analyzed during hypoxia. For FVB and C57BL/6J mice, the elevation of $\dot{V}_E/\dot{V}_{O_2}$ above baseline at 2 min, 4 min and 10 min, respectively was 102 ± 14% ($p < 0.0001$) vs. 121 ± 31% ($p < 0.0001$); 87 ± 11%, ($p = 0.0002$) vs. 133 ± 24% ($p < 0.0001$); and 73 ± 12% ($p = 0.004$) vs. 99 ± 15% ($p = 0.0002$).

Similarly, both strains of three-week old WT mice hyperventilated throughout hypoxia, as $\dot{V}_E/\dot{V}_{O_2}$ increased by over double in P20–22 FVB mice at 2 min (130 ± 11%, $p < 0.0001$), at 4 min (133 ± 12%, $p < 0.0001$) and at the end of hypoxia (141 ± 12%, $p < 0.0001$) whereas $\dot{V}_E/\dot{V}_{O_2}$ remained 40% above baseline in C57BL/6J animals (2 min: 90 ± 16%, $p < 0.0001$; 4 min: 60 ± 12%, $p = 0.0001$; 10 min: 40 ± 8%, $p = 0.01$).

Comparing the adult WT mice, P49–56 C57BL/6J mice, but not P49–57 FVB animals increased $\dot{V}_E/\dot{V}_{O_2}$ significantly at 2 minutes in hypoxia (104 ± 23%, $p = 0.03$). Afterwards, both FVB and C57BL/6J mice hyperventilated through the remainder of the hypoxic challenge. The relative change in $\dot{V}_E/\dot{V}_{O_2}$ for FVB and C57BL/6J mice, respectively was 154 ± 43% ($p = 0.01$) and 116 ± 54% ($p = 0.02$) at 4 min and 175 ± 28% ($p = 0.0005$) and 96 ± 31% ($p = 0.03$) at 10 min.

Data demonstrate that the $\dot{V}_E/\dot{V}_{O_2}$ response to hypoxia is immature in neonate C57BL/6J mice, whereas FVB mice produce a sustained increase in $\dot{V}_E/\dot{V}_{O_2}$ during hypoxia from P1 through adulthood.

Fig. 4.2D–F show the relative change of $\dot{V}_E$, $\dot{V}_{O_2}$ and $\dot{V}_E/\dot{V}_{O_2}$ from baseline during the steady-state period of hypoxia (average of minutes 7–10 in hypoxia) in both sets of WT mice. Asterisks in Figure 4.2D–F designate when each parameter at 10 minutes in hypoxia was different from baseline at a specific age within strains, similar to what is shown in Figure 4.2A–C. Further analysis between the strains revealed that there were no significant differences in the steady state $\dot{V}_E$ response at any age (Figure 4.2D). In contrast, steady state changes in $\dot{V}_{O_2}$ and $\dot{V}_E/\dot{V}_{O_2}$ were significantly different between strains at P1–2 and P20–23. Figure 4.2E shows that the changes in

$\dot{V}O_2$ were significantly different in neonate P1–2 (FVB: -49 ± 4%, vs. C57BL/6J: 67 ± 24%, $p < 0.0001$) and juvenile P20–23 mice (FVB: -43 ± 3%, vs. C57BL/6J: -12 ± 6%, $p = 0.04$). The steady-state hyperventilatory response to hypoxia was also different in neonate P1–2 (FVB: 104 ± 24%, vs. C57BL/6J: -19 ± 13%, $p = 0.0005$) and juvenile P20–23 wild-type animals (FVB: 141 ± 12%, vs. C57BL/6J: 40 ± 8%, $p = 0.0001$) (Figure 4.2F).

4.3.3 Postnatal emergence of a hypoxia-induced depression of metabolic rate in C57BL/6J mice.

That ventilatory and metabolic response to hypoxia change during postnatal development is well-established (Bissonnette, 2000; Mortola, 1999, 1996; Moss, 2000) and supported by my developmental analyses of FVB and C57BL/6J mice. Neonatal mammals typically do not produce a sustained increase in $\dot{V}E$ during hypoxia. $\dot{V}E$ returns to or below baseline while hypoxia persists, which underlies the hypothesis that the adaptive, responses of newborns to hypoxia are immature/inadequate and newborns are more vulnerable to hypoxic injury. The alternative view is that the greater secondary reduction in $\dot{V}E$ in neonates simply reflects that the metabolic rate of neonates is more sensitive to hypoxia (Dzal et al., 2020; Frappell et al., 1992; Mortola, 1999; Mortola et al., 1989). Thus, neonates, like adults, are fully capable of responding to hypoxia with an adaptive sustained increase in $\dot{V}E/\dot{V}O_2$. The strategies employed by neonates to achieve the sustained increase in $\dot{V}E/\dot{V}O_2$ (primarily a hypoxic depression of $\dot{V}O_2$) differ from adults (primarily a sustained increase in $\dot{V}E$), but the homeostatic responses of neonates are intact. That hypoxic responses of neonates are not compromised is supported by a substantial but incomplete body of literature in which most studies did not include measurements from the earliest postnatal period. Key assumptions are that all neonates respond to hypoxia with a reduction in $\dot{V}O_2$, that the magnitude of the hypoxic metabolic depression is greatest in the youngest animals and that it decreases with development; i.e. the mechanisms via which hypoxia inhibits metabolism are well developed at birth and decrease thereafter. The observation that hypoxia does not depress $\dot{V}O_2$ in P0–3 C57BL/6J mice is therefore potentially very significant. It suggests either that C57BL/6J mice are an exception, or that the mechanisms underlying the hypoxic depression of $\dot{V}O_2$ emerge postnatally, in which case neonates will be more vulnerable to hypoxia until they reach that critical age when hypoxia depresses $\dot{V}O_2$.

My first objective was to gain further insight into when in postnatal development C57BL/6J mice respond to hypoxia with a reduction in $\dot{V}O_2$ and produce a sustained increase in $\dot{V}E/\dot{V}O_2$. Data in Chapter 3 that first revealed that neonatal C57BL/6J did not reduce $\dot{V}O_2$ during hypoxia represented data averaged from animals ranging in age from P0–3. P0 animals from this group (data not shown) did not depress $\dot{V}O_2$ or increase $\dot{V}E/\dot{V}O_2$ to hypoxia so I examined P1, P2 and P6 animals to start.

As expected, P1, P2 and P6 mice all responded to hypoxia with an immediate, 20–40% increase in $\dot{V}E$ at the onset of hypoxia that fell to or below baseline by the end of hypoxia (P1: Baseline: 1244 ± 102 ml/min/kg, 10-min hypoxia: 1357 ± 79 ml/min/kg, $p = 0.79$; P2: Baseline: 1803 ± 154 ml/min/kg, 10-min hypoxia: 1654 ± 115 ml/min/kg, $p = 0.87$; P6: Baseline: 2926 ± 196 ml/min/kg, 10-min hypoxia: 2243 ± 159 ml/min/kg, $p < 0.0001$) (Fig. 4.3A–C). In contrast to the prevailing view but consistent with data in Chapter 3, $\dot{V}O_2$ in P1 and P2 C57BL/6J mice did not decrease in response to hypoxia; it actually increased. At the end of the 10 min hypoxic period, $\dot{V}O_2$ was significantly greater than pre-hypoxic levels in P1 (Baseline: 38 ± 4 ml/min/kg, hypoxia: 54 ± 5 ml/min/kg, $p = 0.01$) and P2 animals (Baseline: 49 ± 4 ml/min/kg, hypoxia: 79 ± 1 ml/min/kg, $p = 0.002$). In contrast, in P6 mice hypoxia reduced $\dot{V}O_2$. At the end of the 10 min hypoxic exposure metabolic was ~50% of pre-hypoxic levels (Baseline: 60 ± 3 ml/min/kg, hypoxia: 31 ± 2 ml/min/kg, $p = 0.005$) (Fig. 4.3D–F). The lack of a hypoxic metabolic depression in the P1 and 2 mice but its emergence by P6 meant that only the P6 C57BL/6J mice produced a sustained hyperventilatory response to hypoxia. The air convection requirement ($\dot{V}E/\dot{V}O_2$) did not increase during hypoxia and was not different from baseline at P1 (Baseline: 35 ± 4 a.u., hypoxia: 28 ± 4 a.u., $p = 0.48$) or P2 (Baseline: 37 ± 2 a.u., hypoxia: 21 ± 1 a.u., $p = 0.13$), but it was increased at P6 (Baseline: 49 ± 3 a.u., hypoxia: 72 ± 6 a.u., $p = 0.02$) (Fig. 4.3G-I).

I did not complete the day-by-day analysis of $\dot{V}O_2$ and $\dot{V}E/\dot{V}O_2$ responses to 10% O_2, but instead started the developmental time series again but this time I measured responses to 8% O_2. My rationale was based on the possibility that C57BL/6J mice might be less sensitive to hypoxia such that the "typical" responses of neonatal mammals to hypoxia, a transient increase in $\dot{V}E$ and a reduction in $\dot{V}O_2$, would require a stronger hypoxic stimulus. C57BL/6J mice at each age (P1–3, 7-8) showed the expected transient $\dot{V}E$ response to hypoxia; $\dot{V}E$ increased during the first 1-2

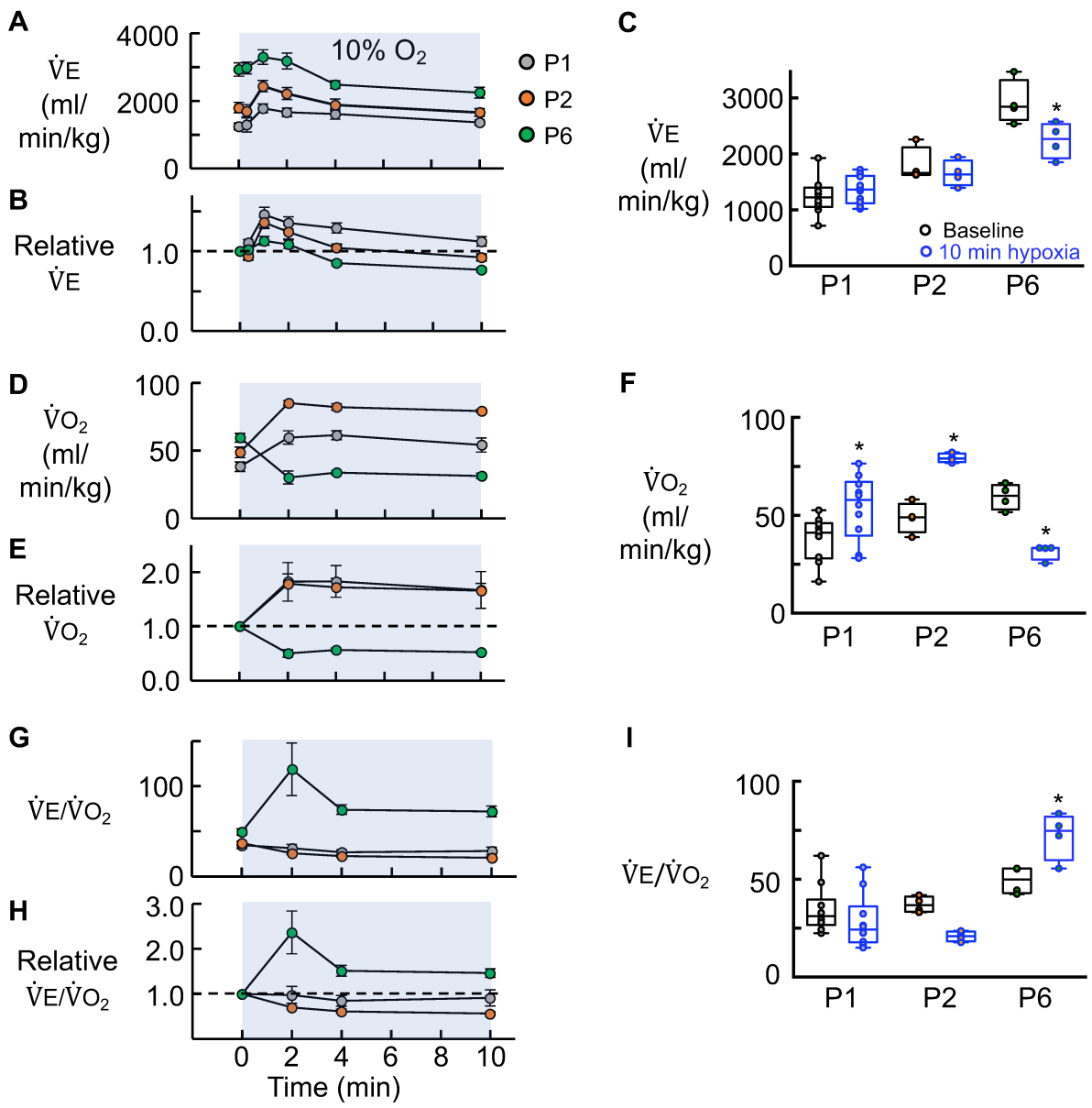

Figure 4.3. Comparison of $\dot{V}E$, $\dot{V}O_2$, $\dot{V}E/\dot{V}O_2$ responses to 10% O_2 in P1, P2, and P6 C57BL/6J mice.

Time-course graphs show absolute and relative changes in A,B) $\dot{V}E$, D,E) $\dot{V}O_2$ and G,H) $\dot{V}E/\dot{V}O_2$ evoked by a 10-minute exposure to 10% O_2 in P1, P2 and P6 C57BL/6J mice. Box and whisker plots show the values of C) $\dot{V}E$, F) $\dot{V}O_2$ and I) $\dot{V}E/\dot{V}O_2$ at baseline (pre-hypoxia) and at the end of hypoxia (average of minute 7–10). Measurements were made in P1 (n = 8), P2 (n= 6), and P6 mice (n = 4). *indicates for each age group a significant difference ($P < 0.05$) from its own baseline (in absolute terms) determined using a two-way ANOVA with Sidak's *post hoc* test.

minutes of hypoxia but fell back to baseline before the end 10-minute hypoxic exposure (Fig. 4.4A–C). $\dot{V}_E$ at the end of 10 minutes of 8% O_2 was not significantly different from baseline at any day of the youngest neonates studied (P1: Baseline: 1403 ± 197 ml/min/kg, 10-min hypoxia: 1673 ± 183 ml/min/kg, p = 0.91; P2: Baseline: 1578 ± 293 ml/min/kg, 10-min hypoxia: 1770 ± 129 ml/min/kg, p = 0.57; P3: Baseline: 1774 ± 92 ml/min/kg, 10-min hypoxia: 1851 ± 174 ml/min/kg, p = 0.99), nor the P7–8 age group (Baseline: 3153 ± 174 ml/min/kg, 10-min hypoxia: 2963 ± 193 ml/min/kg, p = 0.84) (Fig. 4.4C).

8% O_2, like 10%, did not cause a reduction $\dot{V}_{O_2}$ in P1, P2 or P3 mice (Fig 4.4D–E) (P1: Baseline: 42 ± 4 ml/min /kg, hypoxia: 37 ± 6 ml/min/kg, p = 0.99; P2: Baseline: 45 ± 12 ml/min/kg, hypoxia: 53 ± 11 ml/min/kg, p = 0.82; P3: Baseline: 56 ± 3 ml/min/kg, hypoxia: 41 ± 3 ml/min/kg, p = 0.34). However, the "typical" hypoxic depression of metabolic rate was present at P7–8 when hypoxia caused $\dot{V}_{O_2}$ to fall by more than 50% from baseline (Baseline: 61 ± 4 ml/min/kg, hypoxia: 24 ± 1 ml/min/kg, p < 0.0001) (Fig. 4.4F).

The expression of a sustained hyperventilatory response (sustained increase in $\dot{V}_E/\dot{V}_{O_2}$) followed the same developmental time course as the capacity for hypoxia to reduce metabolic rate. Only P7–8 mice produced a sustained hyperventilation during hypoxia (Baseline: 52 ± 4 a.u., 10-min hypoxia: 129 ± 11 a.u., p < 0.0001). $\dot{V}_E/\dot{V}_{O_2}$ was not different from baseline at the end of the hypoxic episode in P1, P2 or P3 mice (P1: Baseline: 34 ± 5 a.u., hypoxia: 46 ± 6 a.u., p = 0.94; P2: Baseline: 50 ± 19 a.u., hypoxia: 37 ± 7 a.u., p = 0.90; P3: Baseline: 32 ± 2 a.u., hypoxia: 47 ± 7 a.u., p = 0.84) (Fig. 4.4G–I). These data that show that hypoxia does not inhibit $\dot{V}_{O_2}$ in C57BL/6J until after P3 and the lack of a hypoxic metabolic depression, neonates cannot mount a sustained adaptive hyperventilatory response to hypoxia.

4.3.4 The hypoxia-induced depression of metabolic rate emerges postnatally in FVB mice.

While the data from C57BL/6J mice clearly show that the depression of metabolic rate by hypoxia emerges postnatally, they do not distinguish whether C57BL/6J mice are unique in the postnatal emergence of the hypoxic metabolic depression or whether postnatal emergence of metabolic

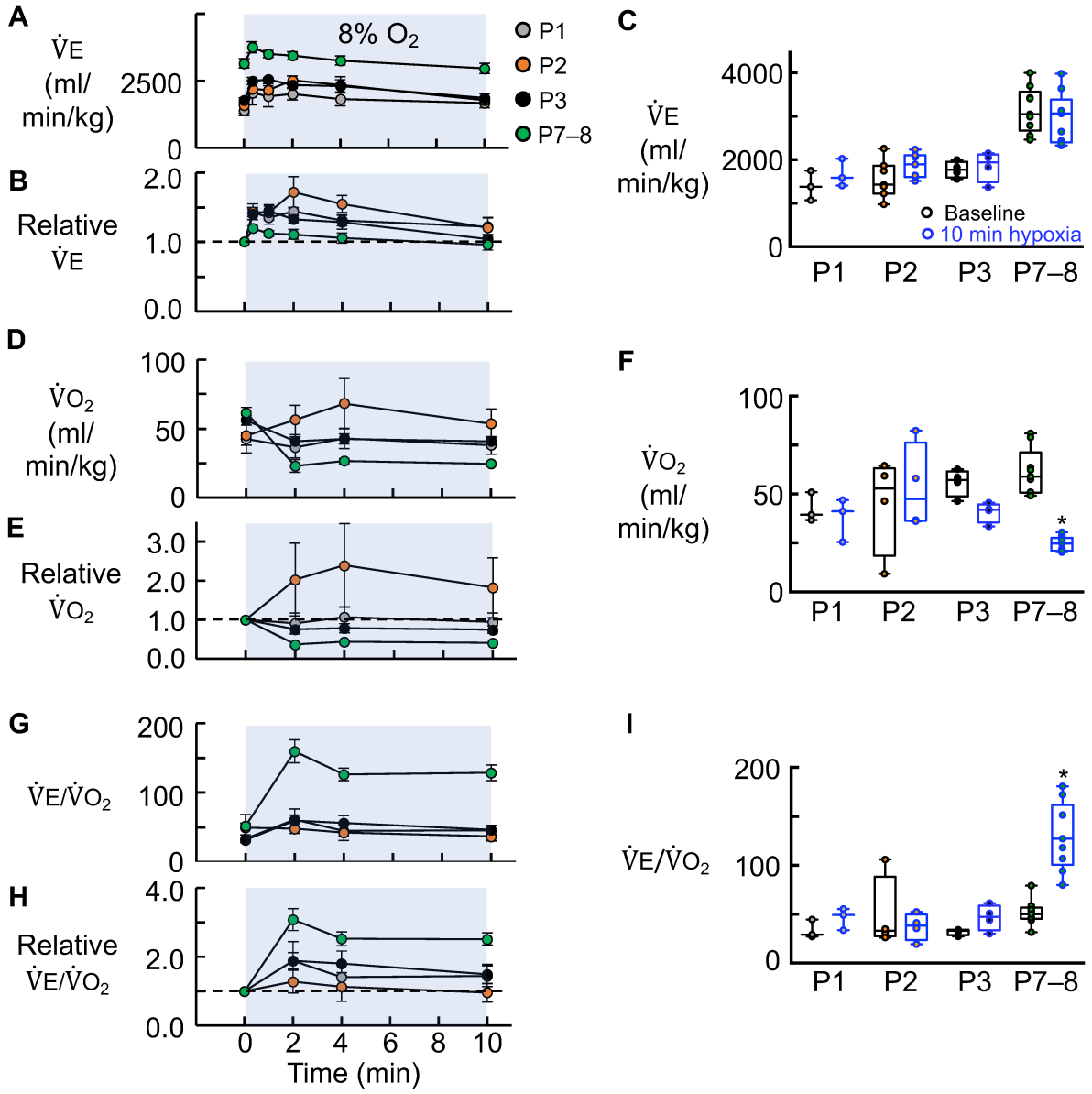

Figure 4.4. Comparison of $\dot{V}_E$, $\dot{V}O_2$, $\dot{V}_E/\dot{V}O_2$ responses to 8% O_2 in P1, P2, P3 and P7–8 C57BL/6J mice.

Time-course graphs show absolute and relative changes in A,B) $\dot{V}_E$, D,E) $\dot{V}O_2$, and G,H) $\dot{V}_E/\dot{V}O_2$ evoked by a 10-minute exposure to 8% O_2 in P1, P2, P3 and P6 C57BL/6J mice. Box and whisker plots show the values of C) $\dot{V}_E$, F) $\dot{V}O_2$ and I) $\dot{V}_E/\dot{V}O_2$ at baseline (pre-hypoxia) and at the end of hypoxia (average of minute 7–10). Measurements were made in P1 (n = 8), P2 (n= 6), and P6 mice (n = 4). *indicates for each age group a significant difference ($P < 0.05$) from its own baseline (in absolute terms) determined using a two-way ANOVA with Sidak's *post hoc* test.

depression is common. I therefore tested in FVB mice whether the hypoxic depression of $\dot{V}O_2$, and the ability to produce a sustained increase in $\dot{V}E/\dot{V}O_2$, are present at birth or emerge postnatally.

As seen in C57BL/6J mice, 10% O2 evoked a transient, ~45% increase in $\dot{V}E$ during the first minute in P0, P1, P2 and P3 mice but this increase was not sustained at any of these ages. $\dot{V}E$ returned back to baseline in P0 and P2 mice and fell below baseline in P1 and P3 animals (P0: Control: 1340 ± 182 ml/min/kg; hypoxia: 1359 ± 58 ml/min/kg, $p > 0.99$; P1: 2278 ± 106 ml/min/kg; hypoxia: 1946 ± 61 ml/min/kg, $p = 0.03$; P2: 2384 ± 124 ml/min/kg; hypoxia: 2063 ± 53 ml/min/kg, $p = 0.10$; P3: 2525 ± 116 ml/min/kg; hypoxia: 2131 ± 63 ml/min/kg, $p = 0.03$) (Fig. 4.5A–C).

Similar to observation in C57BL/6J mice, and in contrast to dominant view that the hypoxic depression of $\dot{V}O_2$ is present at birth and decreases thereafter, hypoxia did not depress $\dot{V}O_2$ in P0 FVB mice. Moreover, the magnitude of the metabolic depression did not diminish with development. The depression was first seen at P1 and it appeared to increase, rather than decrease, between P1 and P3. (Fig. 4.5D–E) (P0: Baseline: 36 ± 7 ml/min/kg, hypoxia: 33 ± 9 ml/min/kg, $p = 0.99$; P1: Baseline: 51 ± 5 ml/min/kg, hypoxia: 28 ± 2 ml/min/kg, $p = 0.0003$; P2: Baseline: 58 ± 5 ml/min/kg, hypoxia: 20 ± 3 ml/min/kg, $p < 0.0001$; P3: Baseline: 71 ± 4 ml/min/kg, hypoxia: 23 ± 4 ml/min/kg, $p < 0.0001$) (Fig. 4.5F).

The magnitude of the $\dot{V}E/\dot{V}O_2$ response to hypoxia and capacity for mice to produce a sustained hyperventilatory response to hypoxia correlated precisely with the capacity for hypoxia to reduce metabolic rate. $\dot{V}E/\dot{V}O_2$ did not change during hypoxia in P0 FVB mice (Baseline: 41 ± 6 a.u., hypoxia: 55 ± 11 a.u., $p = 0.86$). A sustained hyperventilation was apparent at P1 and this appeared to increase between P1 and P3 (Fig. 4.5G–H) (P1: Baseline: 52 ± 7 a.u., hypoxia: 80 ± 9 a.u., $p = 0.04$; P2: Baseline: 44 ± 5 a.u., hypoxia: 119 ± 14 a.u., $p < 0.0001$; P3: Baseline: 37 ± 3 a.u., hypoxia: 117 ± 14 a.u., $p < 0.0001$) (Fig. 4.5I). These data establish that the lack of a hypometabolic response to hypoxia at birth is not unique to C57BL/6J mice; the hypoxic hypometabolic response also emerges postnatally in FVB mice. Moreover, the magnitude of the hypoxic metabolic depression does not decrease during early postnatal life; if anything it increases.

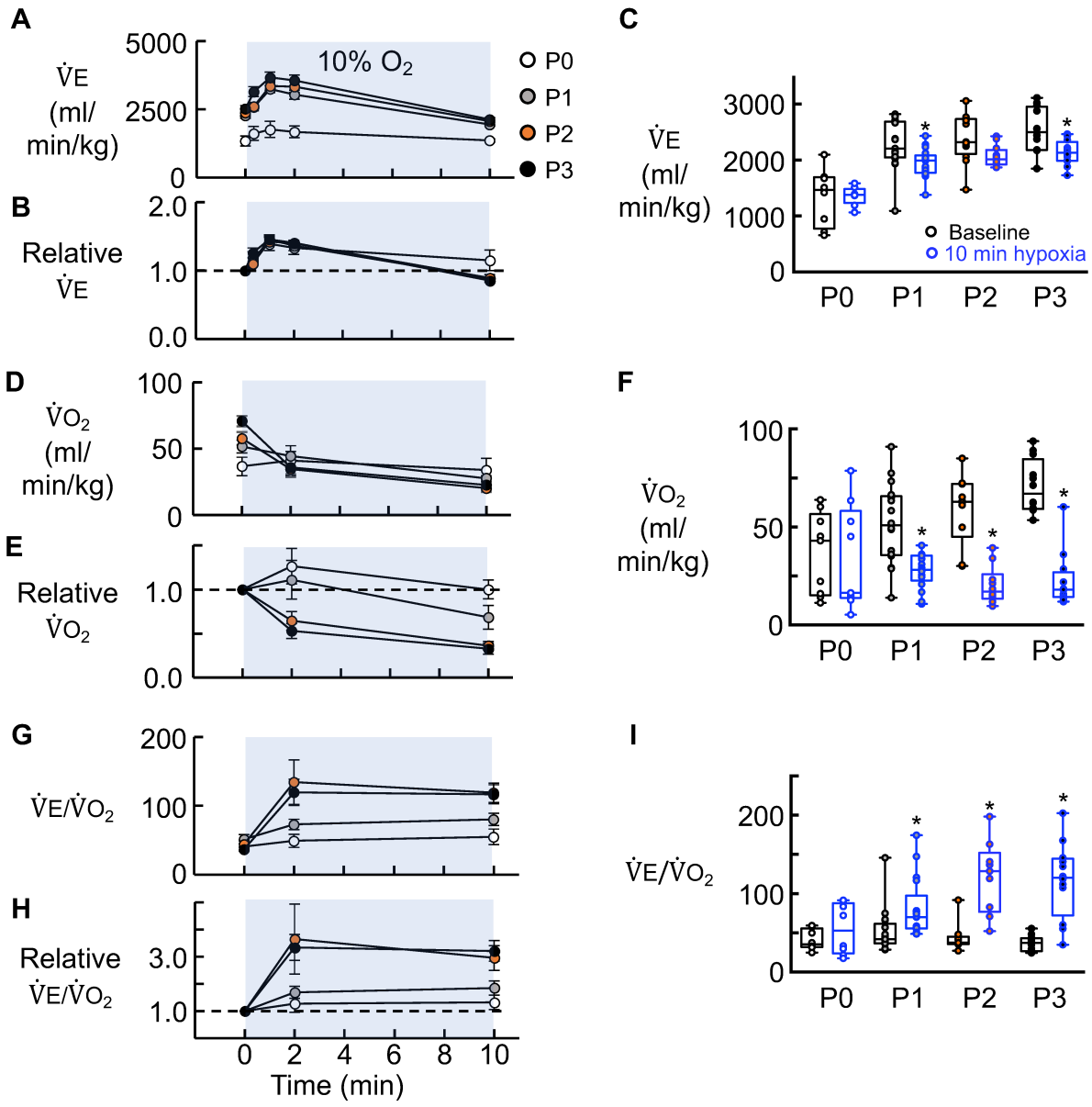

Figure 4.5. Comparison of $\dot{V}_E$, $\dot{V}O_2$, $\dot{V}_E/\dot{V}O_2$ responses to 10% O_2 in P0–3 FVB mice.
Time-course graphs show absolute and relative changes in A,B) $\dot{V}_E$, D,E) $\dot{V}O_2$ and G,H) $\dot{V}_E/\dot{V}O_2$ evoked by hypoxia (10 minute, 10% O_2) in P0, P1, P2 and P3 FVB mice. Box and whisker plots show the values of C) $\dot{V}_E$, F) $\dot{V}O_2$ and I) $\dot{V}_E/\dot{V}O_2$ at baseline (pre-hypoxia) and at the end of hypoxia (average of minute 7–10). Measurements were made in P0 (n = 8), P1 (n = 17), P2 (n = 12), and P3 mice (n = 12). *indicates a significant, within age group difference ($P < 0.05$) between the parameter at 10 min compared to its own baseline (in absolute terms), as determined using a two-way ANOVA with Sidak's *post hoc* test.

4.3.5 Lack of a hypoxia-induced metabolic depression in P0 FVB mice is not due restraint/stress.

The observation that hypoxia does not evoke a decrease in metabolic rate in P0 FVB mice, like the observations in C57BL/6J mice, contradicts a significant body of literature. While most of this literature did not examine the effects of hypoxia on $\dot{V}O_2$ in the immediate postnatal period, I wanted to exclude any possible confounders. I therefore addressed the possibility that the lack of a $\dot{V}O_2$ decrease at P0 FVB animals reflected that youngest mice were more stressed by the head-out plethysmograph chamber, and that stress-induced increases in $\dot{V}O_2$ obscured the normal hypoxic depression of $\dot{V}O_2$ in P0 FVB mice. Therefore, I measured changes in $\dot{V}O_2$ evoked by hypoxia in P0 and P3 FVB mice when mice were placed in a whole-body plethysmograph rather than the head-out plethysmograph. The type of chamber did not alter the metabolic response to hypoxia. P0 mice did not depress metabolic rate at any point in the 10-minute hypoxic challenge (Baseline $\dot{V}O_2$: 38 ± 2 ml/min/kg compared to 2 min: 32 ± 2 ml/min/kg, p = 0.84; and 10 min of hypoxia: 21 ± 1 ml/min/kg, p = 0.06). In contrast, in P3 FVB mice, $\dot{V}O_2$ fell within 2 minutes of exposure to hypoxia and remained depressed throughout hypoxia (Baseline: 64 ± 2 ml/min/kg vs. 2 min hypoxia: 41 ± 2 ml/min/kg, p = 0.01; and 10 min hypoxia: 32 ± 1 ml/min/kg, p = 0.0002) (Fig. 4.6A–C). These results support that P0 FVB mice do not depress metabolism in response to hypoxia.

4.3.6 The hypoxia-induced depression of metabolic rate also emerges postnatally in Sprague-Dawley rats

As demonstrated here for C57BL/6J and FVB mice, previous studies using SD rats suggest that capacity for hypoxia to depress metabolism emerges postnatally at P2 (Liu et al., 2009; Liu and Wong-Riley, 2013). My next objective was to revisit this question in SD rats and determine if the hypoxic hypometabolism is present at birth and, if not, when does it first emerge. As seen in FVB and C57BL/6J mice, 10% O_2 evoked a transient increase in $\dot{V}E$ in the first min of hypoxia that was between ~30 and 75% above baseline and increased with age (Fig. 4.7A–C). The initial increase in $\dot{V}E$, however, was not sustained, falling back to baseline before the end of the hypoxic episode (P0: Baseline: 826 ± 81 ml/min/kg; hypoxia: 1083 ± 95 ml/min/kg, p = 0.58; P1: Baseline: 2089 ± 105 ml/min/kg; hypoxia: 2011 ± 101 ml/min/kg, p = 0.99; P2: Baseline: 1989 ± 262 ml/min/kg;

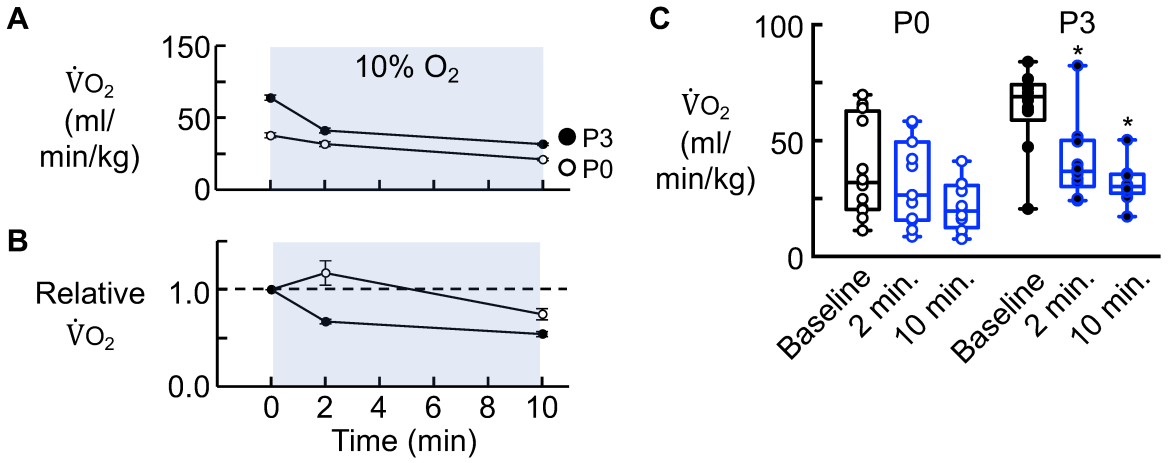

Figure 4.6. Comparison of $\dot{V}O_2$ responses to 10% O_2 in unrestrained P0 and P3 FVB mice. Time-course graphs show absolute A) and relative B) changes in $\dot{V}O_2$ evoked by hypoxia (10-minute, 10% O_2) stimulus in P0 (white) and P3 (black) FVB mice. C) Box and whisker plots show $\dot{V}O_2$ at baseline (pre-hypoxia) and at 2 and 10 min of hypoxia. Measurements were made in P0 (n = 12) and P3 mice (n = 10). *indicates for each age group a significant difference ($P < 0.05$) from its own baseline (in absolute terms) determined using a two-way ANOVA with Sidak's *post hoc* test.

hypoxia: 2226 ± 135 ml/min/kg, p = 0.71; P3: Baseline: 1837 ± 164 ml/min/kg; hypoxia: 2205 ± 167 ml/min/kg, p = 0.30) (Fig. 4.7C). In response to 10% O_2, time-course data showed that there was a smaller $\dot{V}O_2$ depression in P0 rats compared to the P1–3 neonates (Fig. 4.7D–E).

In addition, hypoxia did not depress $\dot{V}O_2$ in SD rats at P0; $\dot{V}O_2$ after 10 min of hypoxia (15 ± 2 ml/min/kg) was not different that baseline (19 ± 3 ml/min/kg, p = 0.35). The hypoxic depression of $\dot{V}O_2$ first emerged at P1 and remained relatively constant at ~50% between P1–P3 (P1: Baseline: 50 ± 2 ml/min/kg; hypoxia: 23 ± 1 ml/min/kg; P2: Baseline: 44 ± 3 ml/min/kg; hypoxia: 24 ± 1 ml/min/kg; P3: Baseline: 44 ± 3 ml/min/kg; hypoxia: 22 ± 2 ml/min/kg, For P1–3: $p < 0.0001$) (Fig. 4.7F). Modest, but insignificant increases in $\dot{V}E$ combined to modest insignificant decreases in $\dot{V}O_2$ resulted in a modest but significant, ~50% increase in the hypoxia-induced increase in $\dot{V}E/\dot{V}O_2$ at P0. The magnitude of the hypoxia-induced steady-state increase in $\dot{V}E/\dot{V}O_2$ appeared to increase thereafter (Fig. 4.7G–H) (P0: Baseline: 44 ± 3 a.u., hypoxia: 79 ± 11 a.u., p = 0.0002; P1: Baseline: 42 ± 2 a.u., hypoxia: 86 ± 5 a.u.; P2: Baseline: 44 ± 3 a.u., hypoxia: 95 ± 6 a.u.; P3: Baseline: 42 ± 2 a.u., 10-min hypoxia: 101 ± 7 a.u., For P1–3: $p < 0.0001$) (Fig. 4.7I).

4.4 Discussion

The first objective of this study was to compare side-by-side the hypoxic ventilatory and metabolic responses of FVB and C57BL/6J mice throughout postnatal life from birth to adulthood. These data were first presented in Chapter 3 where FVB were the WT mice used to assess the effects of ENT 1/2 KO on hypoxic responses and C57BL/6J mice were the WT strain used to assess the effects of ADK-S overexpression. Responses of the two strains were not compared directly in Chapter 3. As suggested in Chapter 3, the most dramatic difference in the hypoxic responses of FVB and C57BL/6J mice was that P1–2 C57BL/6J mice did not respond to hypoxia (10% O_2) with a decrease in metabolic rate. Hypoxia actually caused an increase in $\dot{V}O_2$ in the P1–2 C57BL/6J mice, which is opposite to the hypoxic depression of $\dot{V}O_2$ I saw in P1–2 FVB mice and that has been reported in the majority of developmental studies. The ventilatory response of the youngest age group to hypoxia, which comprised a transient increase in $\dot{V}E$ that fell back to baseline, was similar between strains. Thus, another important strain difference in the hypoxic responses was

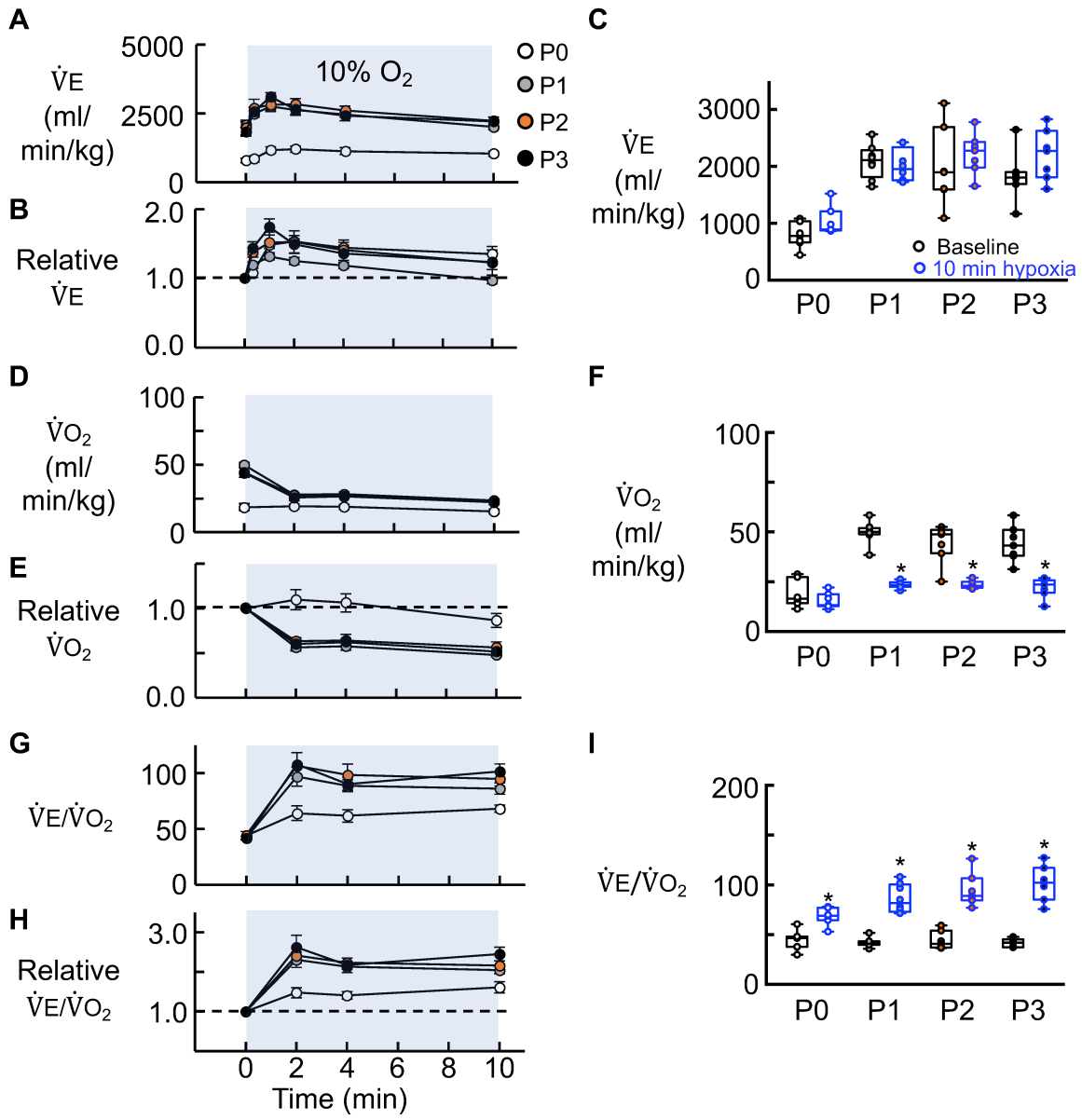

Figure 4.7. Comparison of $\dot{V}E$, $\dot{V}O_2$, $\dot{V}E/\dot{V}O_2$ responses to 10% O_2 hypoxia in P0–3 SD rats.
Time-course graphs show absolute and relative changes in A,B) $\dot{V}E$, D,E) $\dot{V}O_2$ and G,H) $\dot{V}E/\dot{V}O_2$ evoked by hypoxia (10 minute, 10% O_2) in P0, P1, P2, and P3 SD rats. Box and whisker plots show the values of C) $\dot{V}E$, F) $\dot{V}O_2$ and I) $\dot{V}E/\dot{V}O_2$ at baseline (pre-hypoxia) and at the end of hypoxia (average of minute 7–10). Sample size for each group; n = 7). *indicates for each age group a significant difference ($P < 0.05$) from its own baseline (in absolute terms) determined using a two-way ANOVA with Sidak's *post hoc* test.

that only neonatal FVB mice hyperventilated (i.e., increased $\dot{V}_E/\dot{V}_{O_2}$) throughout hypoxia. This apparently anomalous observation in P1–2 C57BL/6J mice directly contradicts a substantial literature that a key feature of homeostatic hypoxic response of neonatal mammals is that the well-documented, transient increase in $\dot{V}_E$ combined with a metabolic depression that is greatest in younger animals underlie the ability of neonatal mammals to produce a sustained, adaptive increase in $\dot{V}_E/\dot{V}_{O_2}$. In this context, neonates are not more vulnerable to hypoxia than older animals; they all hyperventilate during hypoxia. Thus, the observation that neonatal C57BL/6J mice do not depress $\dot{V}_{O_2}$ in response to hypoxia led me to challenge the prevailing view that the mechanisms via which hypoxia depresses $\dot{V}_{O_2}$ are functional, and in fact more potent, at birth. If my hypothesis is correct and the capacity for hypoxia to depress $\dot{V}_{O_2}$ emerges postnatally, a hypoxic depression of $\dot{V}_{O_2}$ should not be present at birth but its emergence will correlate with the ability of neonates to respond to hypoxia with a sustained increase in $\dot{V}_E/\dot{V}_{O_2}$. None of rodents examined, not C57BL/6J, FVB nor SD rats responded to hypoxia with a reduction in metabolic rate at birth; in all strains/species the hypoxic depression of $\dot{V}_{O_2}$ emerged after P0. The time point at which the depression emerged, however, differed between rodent species and between mouse strains; in FVB mice and SD rats the hypometabolic response was first apparent at P1 in FVB mice and SD rats, but not until after P3 in C57BL/6J mice. The capacity to for hypoxia to depress metabolic rate was adaptive as this capacity correlated in mice with the emergence of the capacity to mount a sustained hypoxia-induced hyperventilation.

4.4.1 Hypometabolic responses to hypoxia mature in the very young postnatal period

My results support the conclusion that reducing metabolic demand in response to hypoxia does not occur in all newborn rodents; i.e. this response matures in early postnatal development at least in the species studied here. Reducing metabolic demand has long been considered a critical adaptive mechanism to counteract hypoxia in neonate animals in which hypoxia causes a much stronger secondary inhibition of breathing compared to adults. Indeed, a substantial literature that has documented developmental changes in hypoxic ventilatory and metabolic responses supported the widely held view that newborn mammals respond to hypoxia with a powerful depression of $\dot{V}_{O_2}$ and that this decrease is critical in the ability of these animals to mount a homeostatic, hyperventilatory response to hypoxia that counteract reductions on O_2 (Frappell et al., 1992; Hill, 1959; Mortola and Dotta, 1992; Mortola et al., 1989). Closer examination of these studies revealed,

however, these data did not include studies from newborn mammals. Rodent data did not include animals younger than P2. Our data in FVB and C57BL/6J mice and SD rats, daily analysis of hypoxic responses in SD rats (Liu et al., 2009; Liu and Wong-Riley, 2013) and older studies showing hypoxic responses of premature infants (Cross et al., 1958) all suggest that the hypoxic depression of $\dot{V}O_2$ emerges postnatally.

The time-course and mechanisms via which hypoxia depresses $\dot{V}O_2$ newborns are not completely understood. The factors that contribute a sustained increase in $\dot{V}E/\dot{V}O_2$ are well described and change developmentally. Specifically, the relative contribution of metabolic depression vs. a hypoxic excitation of $\dot{V}E$ is greater earlier in development. With progressive age, the sustained increase in $\dot{V}E$ become more important as in many species the hypoxic depression of $\dot{V}O_2$ disappears in adulthood. This description, however, does not reveal underlying mechanism(s). More detailed daily analysis of developmental changes in ventilatory and metabolic activity suggest that at P0–P1, rats exhibit higher $\dot{V}E$ and lower $\dot{V}O_2$ at baseline compared to any other day in the first week of life (Liu et al., 2009; Liu and Wong-Riley, 2013). Between P1–P7, baseline $\dot{V}O_2$ increases before falling in the second week of life, whereas baseline $\dot{V}E$ steadily increases through P13. These authors attribute the high $\dot{V}E$ in P0 rats to poor alveolar gas exchange, whereas depressed baseline $\dot{V}O_2$ arises from immature thermogenic capacity; this combination blunts further hyperventilation during hypoxia since $\dot{V}E/\dot{V}O_2$ is already elevated compared to the older rats under baseline conditions. Other studies, including the results presented in this chapter, both support and challenge these conclusions. First, baseline $\dot{V}O_2$ appears to increase from minimal levels in newborn rodents. However, baseline $\dot{V}E$ also increases postnatally from birth (Sprenger et al., 2019). If metabolic rate is depressed in the youngest newborn rodents, $\dot{V}E$ is also expected to be reduced as a result of homeostatic mechanisms that match $\dot{V}E$ to metabolic demand. At rest, $\dot{V}E/\dot{V}O_2$ was similar during early postnatal development in each of the strains tested suggesting that mechanisms that match $\dot{V}E$ to $\dot{V}O_2$ are present from birth and contradicts previous data showing that resting $\dot{V}E/\dot{V}O_2$ is elevated in P0 rats (Liu et al., 2009; Liu and Wong-Riley, 2013). My data agree that baseline $\dot{V}O_2$ is lower in newborn rodents. In cross-species comparisons, the magnitude of the hypoxic hypometabolic response is correlated to higher resting $\dot{V}O_2$ measurements (Frappell et al., 1992; Mortola, 1999; Mortola et al., 1989). Taken together, the capacity to decrease metabolic rate

even further during hypoxia may be hampered in the youngest mammals until baseline $\dot{V}O_2$ increases in the first days of life, which appeared to occur in each of the rodent strains used here.

4.4.2 $\dot{V}E$ falls during hypoxia in newborn rodents independent of metabolic depression.

Another interesting aspect of my data in P0–3 C57BL/6J mice and P0 FVB mice and SD rats, that $\dot{V}E$ falls back to or below baseline during hypoxia in each neonate species studied, even in those that do not depress metabolic rate. This argues strongly against the view that the secondary depression of $\dot{V}E$ during hypoxia is merely the consequence of a progressive fall in $\dot{V}O_2$ and functional homeostatic control mechanism. These data also suggest the presence in neonates of stronger inhibitory mechanisms in these neonates and support the longstanding hypothesis that the strong, secondary depression of breathing in neonates during hypoxia arises from powerful, centrally-mediated inhibitory processes affecting $\dot{V}E$ (Bissonnette, 2000; Darnall, 1985; Koos et al., 2016, 2004; Moss, 2000). Of these inhibitory neuromodulators, ADO has long been implicated in the strong secondary depression in neonates. The observation that nearly all premature infants with apnea receive methylxanthine treatment to support breathing and prevent apnea of prematurity (Fiore et al., 2013; Mathew, 2011; Mitchell and MacFarlane, 2019), supports the involvement of ADO-mediated inhibition. However, these clinical data must be interpreted with caution because the mechanism(s) via which clinically-relevant caffeine are not entirely clear (Ballanyi, 2004; Comer et al., 2001). My data in Chapters 2 and 3 show that at birth in central inspiratory networks, the expression and activity of the adenosine kinase (ADK), which supports ENT-mediated ADOe clearance, is very low. Inhibition of ADK and ENT activity has greater depressive effects on rhythmic preBötC activity later in postnatal development, suggesting that the importance of these clearance mechanisms in modulating the activity of central respiratory networks increases developmentally. In humans, block of ENT activity blunts hypoxia-induced increases in $\dot{V}E$, presumably via actions of ADO since these actions could be reversed by ADOR antagonists (Yamamoto et al., 1994). In addition to its effects on preBötC rhythm and respiratory activity in vivo, my data also show that genetic introduction of ADK-S in neonate C57BL/6J mice produces an adaptive, hypometabolic response to hypoxia, that inhibition of ADK activity depresses $\dot{V}O_2$ in FVB mice and attenuates the hypometabolic responses of juvenile animals to hypoxia. In many parts of the brain, ADO depresses neuronal activity and decreases metabolic demand and reductions in ADO are associated with disturbances in sleep when metabolism is

normally reduced (Rytkönen et al., 2010). In rats, ADK activity in the cortex and basal forebrain are higher during periods of wakefulness suggesting that ADOe metabolism is associated with periods of increased metabolic demand (Alanko et al., 2003; Mackiewicz et al., 2003). Since ADO levels influence metabolic activity, these data could point to a role of ADO metabolism by ADK in contributing to changes in $\dot{V}O_2$. Experiments using naked mole rats however, suggest that ADO has no role in the hypoxic depression of $\dot{V}O_2$ (Pamenter et al., 2015). A caveat is that these rodents have evolved to live underground in chronic hypoxic conditions, and may have evolved unique strategies to cope with hypoxia; e.g., in severe hypoxia they simply stop breathing whereas most mammals hyperventilate. Thus, the effects of ADOe on metabolic rate (and $\dot{V}E$ for that matter) in fossorial mammals may not translate to non-fossorial mammals like mice, rats and humans. The underlying mechanisms via which ADK activity, which reduces ADOe by metabolizing ADOi, contributes to adaptive, hypoxic $\dot{V}O_2$ responses remain to be answered. Regardless, data clearly support the hypothesis that ADO signaling alters metabolic activity and that effective ADOe clearance supports both adaptive ventilatory and metabolic responses to hypoxia that mature after birth.

4.4.3 Differences between strains of species and considerations in respiratory research

My results also show that development of the hypoxic ventilatory and metabolic responses are different between C57BL/6J and FVB mouse strains. Hypometabolic responses to hypoxia are present in FVB mice (and SD rats) within days after birth, similar to previous reports (Liu et al., 2009; Liu and Wong-Riley, 2013). In marked contrast, C57BL/6J mice do not respond to hyoxia with a metabolic decrease or a sustained increase in $\dot{V}E/\dot{V}O_2$ until after P3. By adulthood, neither these strains depress metabolic rate in hypoxia, although animals still increased $\dot{V}E/\dot{V}O_2$ by the end of hypoxia. The onset of this change occurred more quickly in C57BL/6J mice by P20. Nonetheless, data from older mice suggests that strong $\dot{V}E$ increases during hypoxia that are sustained at higher levels than neonates, maintain $\dot{V}E/\dot{V}O_2$ above pre-hypoxic levels even though $\dot{V}O_2$ does not significantly change.

While differences in metabolism or metabolic responses of C57BL/6J mice to hypoxia, particularly in newborns, have not been reported previously to the best of my knowledge, differences in breathing pattern and hypoxic $\dot{V}E$ responses have been reported in C57BL/6J mice (Tankersley et

al., 1994). First, they have lower resting frequency and greater variability in breathing pattern (i.e. more disordered) during hypoxia and hypercapnia the post-hypoxic period compared to B6AF1 and Swiss-Webster mice (Gaston et al., 2014; Getsy et al., 2014). C57BL/6J mice also show larger roll-offs in breathing frequency during hypoxia after an initial increase (Getsy et al., 2014; Palmer et al., 2013), which may be consistent with my data showing that the duration of the $\dot{V}_E$ increase in C57BL/6J mice shorter than FVB mice (Fig. 4.2). Previously, I reported that frequency either did not increase above baseline in young C57BL/6J mice or fell back to baseline during a 10-minute 10% O_2 stimulus in more developed animals, both of which were not observed in FVB mice (Fig. 3.3, 3.7). Thus, C57BL/6J mice may have distinct developmental hypoxic ventilatory and metabolic trends, particularly in early development that must be accounted for if these mice are compared to other strains or species. While the development of hypoxic hypometabolic responses in C57BL/6J mice are delayed, my conclusion that the youngest newborn rodents do not adaptively depress $\dot{V}_{O_2}$ in hypoxia remains supported by the literature (Liu et al., 2009; Liu and Wong-Riley, 2013). Therefore, in addition to stronger reductions in the $HVR_{\dot{V}_E}$, an immature $\dot{V}_{O_2}$ response may also compromise an adaptive "back-up" mechanism employed by the young mammals to alternatively support the $HVR_{\dot{V}_E/\dot{V}_{O_2}}$.

4.4.4 Physiological Significance

Neonate mammals, with very few exceptions, depress metabolic rate in response to hypoxia, which is an adaptive strategy to overcome the challenges associated with limited O_2 supply. The consistent observation that hypoxia depresses $\dot{V}_{O_2}$ most strongly in neonates led to the suggestion the greater $\dot{V}_E$ depression of newborns simply reflects functioning homeostatic processes whereby greater reductions in $\dot{V}_{O_2}$ will result in greater reductions in $\dot{V}_E$; i.e., the greater fall in in $\dot{V}_E$ in neonates does not represent a problem with respiratory control nor does it indicate greater vulnerability to hypoxia (Dzal et al., 2020; Frappell et al., 1992, 1991; Mortola, 1999; Mortola and Dotta, 1992; Mortola et al., 1989; Waters and Gozal, 2003). The main limitation of these developmental data, however, is developmental analyses often excluded the youngest animals. Data from over 60 years ago in humans and more recent data from newborn rats challenged this dogma and suggest that the youngest mammals do not depress metabolic rate in hypoxia (Cross et al., 1958; Liu et al., 2009). These data and my work in the different rodents supports the possibility that adaptive metabolic responses to hypoxia are not present at birth in newborn rodents, as each

species tested here only began to depress $\dot{V}O_2$ in response to hypoxia over the first days of life. Since $\dot{V}E$ is more strongly depressed during hypoxia in the youngest rodents, increases in $\dot{V}E/\dot{V}O_2$ during hypoxia can be compromised. This effect would be compounded if adaptive $\dot{V}O_2$ responses normally thought to support the $HVR_{\dot{V}E/\dot{V}O_2}$ are also immature. Importantly, these data strongly support that neonatal rodents are more susceptible to a powerful hypoxic depression of $\dot{V}E$ and that the greater $\dot{V}E$ depression is not attributed to a greater metabolic depression; i.e. $\dot{V}E$ fell back to baseline in all rodents tested even in those in which there was no decrease in $\dot{V}O_2$. While data suggest that the development of hypometabolic responses to hypoxia occurs after birth in rodents, further studies are needed to confirm if this is also the case in other mammalian species. Overall, my data highlight that metabolic responses to hypoxia and how these change during development are key in understanding alternative adaptive mechanisms that can be utilized to counteract hypoxia if breathing is susceptible to depression. Enhanced characterization of the mechanisms underlying the depression of $\dot{V}O_2$ and $\dot{V}E$ during the latter stages of hypoxia and how these change developmentally, as well as how these mechanisms differ between species may inform development of treatments that facilitate adaptive hypoxic responses that minimize apneas and stabilize breathing in at risk populations including premature infants with apnea (Paolillo and Picone, 2013), patients with epilepsy at risk of SUDEP (Boison, 2012a; Ryvlin et al., 2013), as well those suffering from neurodegenerative disorders the feature degeneration of respiratory networks (Howell and Newman, 2017; Presti et al., 2014; Schwarzacher et al., 2011).

Chapter 5: General Discussion

"*Human knowledge is never contained in one person. It grows from the relationships we create between each other and the world, and still it is never complete*."

- Paul Kalanithi, *When Breath Becomes Air*

5.1 Summary of Contributions

This thesis centered on the general objective to characterize mechanisms underlying postnatal changes in the hypoxic ventilatory and metabolic responses, specifically focusing on developing elements that influence purinergic signaling in the preBötC inspiratory network. First, I completed a comprehensive analysis of the purinome in the preBötC network over the first two postnatal weeks, in vitro (Chapter 2). Data suggest mechanisms responsible for ADOe clearance are immature at birth in the preBötC, which may underlie stronger inhibitory P1 effects during the secondary phase of the HVR$\dot{V}_E$ in the very young. Therefore, I then characterized ENT1/2 and ADK activity affected developmental changes in the ventilatory and metabolic responses to hypoxia (Chapter 3). Experiments suggest that ADOe clearance by both ENT1/2 and ADK-S activity reduce the secondary respiratory depression of the HVR$\dot{V}_E$ in adult mice. These experiments also highlighted an unexpected, albeit important finding that hypometabolic responses to hypoxia in newborns are immature, and implicated limited ADK-S activity in this effect. Subsequent experiments revealed that newborns of three experimental rodent models do not evoke significant reductions in metabolic rate during hypoxia, which has previously been characterized as an important adaptive response to counteract stronger reductions in the HVR$\dot{V}_E$ at this age (Chapter 4).

Based on results described in this thesis, there are five major contributions that support our understanding of how development influences hypoxic ventilatory and metabolic responses, as well as how purinergic signaling in the preBötC changes postnatally and influences these responses. These are:

(i) Excitatory effects of ATP within the preBötC inspiratory network increase over the first two weeks of development in FVB mice, as a result of reduced A_1R-mediated inhibition evoked following ATP metabolism to ADO;

(ii) Postnatal increases in ADK-S activity, which supports the removal of ADOe through ENTs that are present from birth, affects basal ADOe tone (and therefore excitability) in the preBötC and limits the duration of ADO-evoked reductions in network activity;

(iii) ADK-S and ENT activity, which support ADOe clearance, contribute to developmental reductions in the secondary ventilatory depression of the HVR$\dot{V}_E$;

(iv) Central ADK-S activity, presumably by helping remove ADOe, influences basal metabolic rate in juvenile mice after P11 and imparts an adaptive hypometabolic responses to hypoxia in newborn rodents through a yet-to-be determined mechanism;

(v) The hypometabolic response to hypoxia is an important adaptive strategy to counteract drops in O_2 in young rodents, however this response is not present at birth and develops at different times over the first days of life in C57BL/6J and FVB mice, as well as SD rats.

In the following sections, I will detail both the physiological and clinical significance of my findings, and then discuss what questions remain and the strengths and limitations of various approaches that could elucidate answers to these queries. In each data chapter, I have summarized the physiological relevance of each study, specific to the results observed in those experiments. Thus, in the preceding section, I provide a comprehensive summary of the significance of all of my results and discuss the complete story that has emerged related to developmental changes in the hypoxic ventilatory and metabolic responses, and the impact that dynamic elements of the purinome contribute to these postnatal changes.

5.2 Physiological Significance

5.2.1 Net effect of purinergic signaling in the preBötC during development shifts toward excitation

The secondary respiratory depression during hypoxia is speculated to arise from central mechanisms, which includes the inhibitory actions of ADO (Bissonnette, 2000; Moss, 2000). Past research suggested that contributions of the CNS were solely inhibitory (Funk, 2013), however recent results suggest that excitatory actions of ATP released during hypoxia can stimulate breathing and reduce the magnitude of the secondary depression (Angelova et al., 2015; Gourine et al., 2005; Rajani et al., 2017). Given that ATP excites breathing by activating $P2Y_1Rs$ in the preBötC inspiratory network but is also broken down by ECTOs to produce ADO that inhibits this network at A_1Rs, ATP release can cause competing effects that are ultimately determined by a host of elements collectively termed the *purinome* (Reklow et al., 2019; Volonté and D'Ambrosi, 2009). These data supported my original hypothesis that changes in elements of the purinome contribute to developmental reductions in the magnitude of the hypoxic respiratory depression,

which is strongest and life-threatening in premature and newborn infants. Indeed, comprehensive analysis in vitro suggest that the preBötC network's sensitivity to excitatory-actions of ATP are reduced at birth, but increases over the first two weeks of life, due to diminished A_1-mediated inhibition evoked by ATP degradation, therefore unmasking the full excitatory effects of ATP via $P2Y_1$ receptor stimulation (Chapter 2). Data also suggest that sensitivity to excitatory $P2Y_1$ or inhibitory P1 receptor activation remains constant over the first two weeks after birth, while ECTO-mediated metabolism of ATP increases postnatally. However, postnatal increases in ADK activity appear to reduce basal ADOe tone and support clearance of high levels of ADOe through passively-active ENTs, contributing to an overall excitatory shift in the effects of the purinome within the preBötC network.

Inhibiting ENT and ADK activity significantly reduces preBötC rhythm in slices from P9–12 mice yet were without effect in slices from neonates. The duration of inhibition of preBötC activity evoked by a bolus of ADO, which replicates in the slice accumulating ADOe levels seen during hypoxia in vivo, decreases developmentally and this inhibition can be prolonged or shortened by removing ADO transporters (ENTs) or increasing ADOi metabolism through ADK-S activity, respectively. Results are significant since i) the purinome exerts greater overall inhibitory effects in the preBötC at birth that may underlie in the larger magnitude secondary hypoxic respiratory depression of the $HVR_{\dot{V}E}$ in newborns, and ii) changes or dysfunction in any element of the purinome active in the preBötC network, such as ENTs and ADK, may explain variability in network sensitivity to ATP and ADO across mammalian strains, species, and development. These in vitro results provided the framework to then complete in vivo assays that assess how ENT and ADK activity influenced the overall HVR during postnatal development.

5.2.2 Ventilatory and metabolic responses to hypoxia are differentially modulated during development by elements of the purinome that affect ADOe and ADOi.

A caveat of my data presented in Chapter 2 was that these results were obtained in vitro meaning i) inputs and feedback that will affect the preBötC during hypoxia are removed; ii) oxygenation throughout the slice was not homogenous; and iii) hypoxic conditions were simulated by injecting purinergic agents that do not perfectly match the spatiotemporal profile of endogenous modulatory transmitter release during hypoxia. To address this, I utilized pharmacological and genetic

interventions targeting ADOe clearance elements and compared the developmental changes in ventilatory and metabolic responses to hypoxia to wild-type mice, in vivo. ENT activity influenced breathing pattern responses to hypoxia in young mice, as ENT1/2 KO shortened the tachypnea response evoked by hypoxia, however ENT activity attenuated the secondary $\dot{V}_E$ depression to greater degrees as development progressed. This suggests that ENT activity influences ventilatory responses to hypoxia, and that its effects on the HVR$_{\dot{V}_E}$ increase developmentally, presumably through its function to remove inhibitory ADOe that accumulates during hypoxia. This could reflect direct actions of increasing ENT expression or activity, or indirect actions by changes in elements influencing the ADOi–ADOe gradient. ENTs operate passively, therefore any element that metabolizes intracellular ADO (ADOi) will support ENT activity. ADK activity has been shown to functionally increase developmentally, as its expression shifts from the ADK-L isoform, whose primary function an epigenetic regulator in the nucleus of neurons, to the ADK-S isoform, that metabolizes ADOi and is expressed primarily in the cytoplasm of astrocytes (Gebril et al., 2021, 2020; Studer et al., 2006). Data demonstrates that ADK-S expression in the medulla also increases postnatally maturing around three-weeks of age in mice, and its activity impacts both basal ventilation and metabolism in normoxia and under hypoxic conditions. Inhibition of endogenous ADK activity had minimal effects on newborn WT mice, however by the second and third weeks of development, this inhibition significantly reduced basal $\dot{V}_E$, which appeared to homeostatically follow reductions in basal $\dot{V}_{O_2}$. Overexpression of ADK-S in juvenile and adult mice potentiated excitatory increases in $\dot{V}_E$ during the secondary phase of hypoxia, suggesting that ADK-supported clearance of ADOe attenuates the hypoxic respiratory depression in developed animals.

These results collectively suggest elements that support central ADOe clearance increase their activity postnatally and contribute to adaptive developmental changes in the HVR$_{\dot{V}_E}$. With development, reducing ADOe clearance had greater depressive effects on basal inspiratory-related activity in vitro and ventilation in vivo, compared to newborns. At birth, when ADOe clearance is limited or when ENT1/2 were genetically removed, the ADO-meditated inhibition of preBötC activity in vitro is prolonged, whereas the duration of inhibition is shortened as endogenous ADOe clearance increases (via increases in ADK-S), or when ADK-S expression is introduced in newborns. In vivo, ENT KO and overexpression of ADK-S had smaller effects on the HVR$_{\dot{V}_E}$ in

early development compared to mice studied after P20. Enhanced ADOe clearance in developed mice prolonged increases in $\dot{V}_E$, largely mediated by increases in breathing frequency, which could reflect reduced effects of ADO in networks involved in respiratory rhythm including the preBötC.

5.2.3 Reduced capacity for hypoxia to depress metabolism in newborns, but greater capacity to depress ventilation may compromise homeostatic hyperventilatory responses in the very young

Much of the previous literature in our field that characterizes the impact of purinergic modulation on hypoxic responses focuses on its effects on the secondary $\dot{V}_E$ depression, developing the hypothesis that accumulating ADO potentiates this depression by inhibiting central respiratory networks, whereas ATP released from astrocytes in the preBötC inspiratory network attenuate the reduction in breathing (Angelova et al., 2015; Rajani et al., 2017). There has been considerable data supporting that the secondary depression of breathing during hypoxia is strongest and life-threatening in newborns since $\dot{V}_E$ falls back to or below baseline levels, however neonate mammals can also reduce $\dot{V}_{O_2}$ therefore reducing oxygen demand, increasing $\dot{V}_E/\dot{V}_{O_2}$, and protecting against further drops in PaO_2 (Mortola, 1999). Recent data however, suggest metabolic responses to hypoxia are also immature at birth (Liu et al., 2009; Liu and Wong-Riley, 2013). In Chapter 4, I observed that although P0 rats fail to significantly depress $\dot{V}_{O_2}$, these animals have marginal changes in $\dot{V}_E$ and $\dot{V}_{O_2}$ such that $\dot{V}_E/\dot{V}_{O_2}$ is elevated above baseline by the end of hypoxia. In contrast, neither P0 FVB nor P1–3 C57BL/6J mice depressed $\dot{V}_{O_2}$, and $\dot{V}_E/\dot{V}_{O_2}$ was not increased suggesting the $HVR_{\dot{V}_E/\dot{V}_{O_2}}$ is compromised in the very young mice. With varying degrees of development, each of the neonate rodent models studied developed the adaptive hypoxic hypometabolic response.

Interestingly, data suggests that ADK-S activity affects both basal metabolic rate and the $HVR_{\dot{V}_E/\dot{V}_{O_2}}$. When endogenous ADK activity was inhibited using ABT 702, there was a significant depression of $\dot{V}_{O_2}$ in mice older than P11, but not neonates suggesting that as ADK-S levels increase, it has modulatory effects on basal metabolic rate, presumably by affecting ADOe equilibrium in the brain. In the older ABT 702-treated mice, $\dot{V}_E$ fell proportionally to the reduction in $\dot{V}_{O_2}$ suggesting that homeostatic control of breathing is not affected by ADK inhibition, therefore $\dot{V}_E/\dot{V}_{O_2}$ was similar to vehicle-injected animals. On the other hand, transgenic introduction and

overexpression of ADK-S throughout the brain imparted a significant, adaptive reduction in metabolic rate in neonate mice during hypoxia which was not seen in C57BL/6J controls. This suggests mature ADK activity that affects ADOe equilibrium has influences on the adaptive reduction in $\dot{V}_{O_2}$ in the youngest mice. Coupled with the observation that ADK inhibition depressed basal $\dot{V}_{O_2}$ in older animals, this could reflect that ADK activity and regulation of ADOe levels in the brain appears important for not only setting metabolism at rest but also impacts the $HVR_{\dot{V}_E/\dot{V}_{O_2}}$. While data suggests the more inhibitory effects of the purinome shift towards excitation during second week of development in the preBötC network, it is possible the appearance of the hypometabolic hypoxic response in the first days results from diminished adenosinergic inhibition, possibly mediated in part by increases ADK-S activity, in other areas of the brain important for regulating metabolism.

5.3 Clinical Relevance

In humans, incidence of apnea of prematurity is correlated with gestational age as nearly all infants < 29 weeks are affected, but only ~15% of infants are affected at 32–33 weeks gestation (Paolillo and Picone, 2013). ~20% of infants with apnea of prematurity do not respond to caffeine (Schmidt et al., 2012, 2007), which is the preferred treatment to stimulate breathing and prevent apnea in these vulnerable infants (Shrestha and Jawa, 2017). Data from this thesis, which is supported by evidence showing substantial differences in sensitivity to ATP and ADO in Swiss CD mice and SD rats (Zwicker et al., 2011), demonstrates that there are a host of unique elements that collectively influence the overall balance between excitation and inhibition of the preBötC network following the release of ATP during hypoxia. Just as there are substantial strain and species differences in purinergic modulation of the postnatal rodent preBötC network, variations in any element of the purinome through development could underlie differences in the response to reduced oxygen or create susceptibility to life-threatening apnea during hypoxia. Sensitivity of the preBötC network to $P2Y_1$ receptor stimulation appears consistent during the first two weeks of life and through development (Lorier et al., 2007; Rajani et al., 2017; Zwicker et al., 2011). The overall effects of ATP mediated by P2 and P1 stimulation, however, are affected by developmental changes in activity of different ECTOs and accumulation of puringeric metabolites that activate P2 (i.e. ADP) and P1 receptors (i.e. ADO), (Zwicker et al., 2011), as well as clearance of ADO through ENTs, which is affected by intracellular enzymes that metabolize ADO such as ADK. In

medullary slices from newborn SD rats and FVB mice, ATP injection elicits short, but powerful increases in preBötC frequency (Huxtable et al., 2009; Lorier et al., 2007), yet in Swiss CD mice, ATP has no effect on rhythm unless inhibitory A_1Rs are first blocked using DPCPX (Zwicker et al., 2011). Data from my thesis shows ATP evokes stronger increases in preBötC activity in slices from P9–12 FVB mice than those from P0–6 animals, except when ATP is applied immediately after DPCPX. Additionally, in mice, ADO evokes reductions in preBötC frequency until at least P12, yet does not affect rhythm in P0–P4 SD rats (Zwicker et al., 2011). These differences highlight variability of purinergic modulation of the preBötC between species, and even between strains, during postnatal development. This is significant clinically, as it may help explain differences in the incidence of apnea of prematurity and provide clues as to why some infants are unresponsive to caffeine therapy. New data ultimately spawn new questions, including: i) do increases in central ADK-S activity, which enhances ENTs removal of ADOe, increase excitability of respiratory networks and contribute to reductions in the incidence of AOP; ii) do certain purinome phenotypes (i.e. ECTO isoform expression/activity, altered function of ENTs and ADK, etc.) correlate to efficacy of treatments like caffeine to prevent AOP; and iii) are the elements identified in this thesis and recent literature new therapeutic targets to prevent life-threatening apneas?

The emergence of personalized medicine may be instrumental to translating developmental observations made in mice and rats, to effective treatments in the neonatal intensive care unit (National Research Council, 2011). Characterization of individual genotypes could reveal specific therapies should be utilized to best address a specific patients deficits, however, a caveat is that interventions affecting central purinergic modulation need to be specific to a region or network in order to prevent off-target side effects. For instance, while data suggests ADOe clearance limits the inhibitory effects of ADO on preBötC activity and breathing during hypoxia, greater ADK functioning in higher regions of the brain reduces ADO tone and is associated with greater seizure risk, which is a hallmark of SUDEP (Boison, 2013b). While greater ADK activity is correlated with increased seizure incidence, it also prevents fatal apneas, mediated at least in part by enhanced clearance of ADOe in central respiratory networks (Shen et al., 2022). Furthermore, as demonstrated by this thesis, the purinome is comprised of many elements that contribute to the overall effects of ATP and ADO in the brain, therefore it is important to understand how targeting

one component may impact activity of another. Further studies in animal and human subjects are needed to determine the efficacy and feasibility of clinical treatments that specifically support excitability of breathing networks by modulating one or more elements of the purinome. My thesis focused characterizing the overall output of modulation of breathing networks by the purinome changes developmentally, specifically related to hypoxia, nonetheless data may also be instructive for translation to therapies to prevent apnea in multiple pathophysiological conditions throughout life.

Data also suggest that endogenous increases in ADOe clearance mechanisms in the CNS contribute to developmental reductions in the hypoxic respiratory depression, which supports the hypotheses that i) ADO is implicated in the stronger hypoxic respiratory depression in newborns and ii) maturation of endogenous mechanisms that limit ADO inhibitory actions attenuate the depression of breathing in adults. This also supports the hypothesis that caffeine, the primary treatment for apnea of prematurity, stimulates breathing by blocking ADO-mediated inhibitory effects in central respiratory networks, which are greatest at birth. ADK activity, possibly by influencing central ADOe tone, increases basal metabolic rate and affects the hypoxic hypometabolic response, which is a second adaptive mechanism that counteracts falling oxygen levels in the blood. The exact mechanism underlying the role ADK has in metabolism, particularly with respect to its changes during hypoxia, will require further investigation and is discussed in section 5.4.3. Nonetheless, data suggests mechanisms limiting ADO inhibitory effects (i.e. methylxanthine therapy) may also impact metabolic responses during hypoxia.

Finally, this thesis characterized the development of the $HVR_{\dot{V}E/\dot{V}O_2}$ in the first days after birth in rodents and found that reductions in $\dot{V}O_2$ in response to hypoxia are not present at birth in each of rodent models studied. Previous data suggested that, given the secondary depression of $\dot{V}E$ during hypoxia is strongest in neonate mammals, a rapid reduction in $\dot{V}O_2$ is utilized by newborns to maintain $\dot{V}E/\dot{V}O_2$ above baseline levels (Frappell et al., 1992; Hill, 1959; Mortola, 1999, 1996). Closer examination of these studies, however, revealed there were no data from animals younger than P2 (Fahey and Lister, 1989; Frappell et al., 1992; Mortola et al., 1989; Rohlicek et al., 1998). Recently, studies in SD rats showed metabolic responses to hypoxia were blunted over the first two days of life (Liu et al., 2009; Liu and Wong-Riley, 2013), but also characterized another

developmental period at P12–13 in these rats, deemed the "critical period", during which there are significant, discrete changes in neurotransmitter signaling and activity in respiratory networks of the brain that may underlie disruptions in the ventilatory and metabolic responses to hypoxia at this age (Liu et al., 2006; Liu and Wong-Riley, 2002; Wong-Riley et al., 2019). While human brain development occurs on a much longer time-scale than a mouse or rat, the sequence of development is largely consistent. A comprehensive comparison of human and rodent data suggests that rodents studied at P1–3 correlate roughly to 23–32 week gestation pre-term infant, while P7–10 is representative of a 36–40 week gestation full-term infant (Semple et al., 2013). Therefore, developmental changes in rodents younger than P3 are likely more relevant to understanding potential mechanisms underlying apnea of prematurity that occurs in nearly all infants < 29 weeks old (Paolillo and Picone, 2013). Here, data shows that P0 SD rats can still elicit a significant increase in $\dot{V}_E/\dot{V}_{O_2}$ by the end of hypoxia, but the lack of a reduction in $\dot{V}_{O_2}$ in both newborn FVB and C57BL/6J mice limits their ability to raise $\dot{V}_E/\dot{V}_{O_2}$ above baseline during a hypoxic challenge and counteract falls in PaO_2. Collectively, these data suggest that in the very young, not only is $\dot{V}_E$ depressed to a greater magnitude during the secondary phase of hypoxia, adaptive $\dot{V}_{O_2}$ responses are also blunted. Human data supports this observation, as the magnitude of the adaptive $\dot{V}_{O_2}$ reduction during hypoxia increases over the first two weeks of life in preterm infants and the hypoxic hypometabolic response is greater in full-term babies (Cross et al., 1958). Together, data suggest metabolic responses to hypoxia are not fully developed in the youngest rodents and humans, which may be a clinically relevant contributing factor to the susceptibility of premature and newborn infants to life-threatening apneas associated with very early development.

5.4 Future Work

This thesis provides evidence that development changes in the purinome in the brain, specifically an increased capacity for ADOe clearance, reduces inhibitory adenosingergic modulation of the preBötC inspiratory network and contributes to developmental adaptation in both the hypoxic ventilatory and metabolic responses. As discussed above, these results have several significant physiological and clinical implications, however there are a number of unanswered questions and outstanding caveats that can be resolved in future experimental studies, which I discuss below.

5.4.1 Unexplored elements of the purinome that may contribute to development changes in purinergic signaling in the preBötC network

In Chapter 2, I demonstrated how individual elements of the purinome influence basal preBötC activity and affect the responses to locally-applied ATP or ADO. My data suggests developmental increases in elements supporting ADOe clearance, mediated through increases in ADK-S expression that supports ENT activity, contribute to developmental increases in the overall excitatory effects of the purinome within the inspiratory network. This is supported by evidence *in vivo* that suggests ENT and ADK activity support reductions of the secondary ventilatory depression during hypoxia in developed mice. Nonetheless, there are a number of unexplored avenues that could provide important information supporting the observations presented in this thesis.

i) $P2Y_1$ or A_1 receptors

The preBötC of FVB mice remains consistently sensitive to $P2Y_1$ receptor activation through P12, which is supported by the observation that blocking A_1R-mediated inhibition unmasks the full excitatory effects of ATP from birth in the preBötC. Likewise, the magnitude of the ADO-mediated inhibition of preBötC activity was consistent, collectively suggesting that changes in excitatory or inhibitory receptor sensitivity within the network is not responsible for early developmental changes in the overall effects of the purinome of preBötC activity during early development in mice. Data supports the hypothesis that caffeine stimulates breathing to prevent apnea of prematurity by blocking ADO receptors and suggests A_1R inhibition in the preBötC specifically can produce a mature excitatory response to ATP. Functional data presented in Chapter 2 could reflect that expression of the $P2Y_1$ or A_1/P1 receptors mediating excitatory and inhibitory effects arising from ATP release are consistent through this period, or, albeit unlikely, that expression of these receptors increases while their sensitivity to their respective agonists decreases, or vice versa. Characterization of changes in $P2Y_1$ and ADO receptor expression within the preBötC would add to our understanding of the postnatal development of the purinome. Collecting viable rhythmic preBötC slices from mice older than P12 to obtain functional data is challenging, however characterizing changes in receptor expression before and after P12 could provide insight as to whether the effects of ATP or ADO in the preBötC may change into adulthood. This approach is not perfect since expression changes do not necessarily mean

sensitivity to agonists functionally changes, therefore developing methods to obtain adult preBötC slices will need to be optimized or the brainstem network will need to be accessed in vivo using surgical methods in order to infuse agonists while recording changes in ventilatory behaviour under anesthesia. While data are not yet available, I expect that sensitivity of the preBötC network to $P2Y_1$ receptor-mediated excitation will remain constant and the P1-mediated inhibition will stay the same or slightly decrease as seen in rats (Herlenius et al., 2002, 1997; Huxtable et al., 2009).

The identity of signaling cascades and ion channels through which the different receptors modulate breathing rhythm also requires clarification. Existing literature supports my observation that the inhibitory effects of ADO on preBötC activity are mediated through activation of A_1 receptors (Brockhaus and Ballanyi, 2000; Huxtable et al., 2009; Kawai et al., 1995; Kobayashi et al., 2001; Koos et al., 2001, 2004; Mironov et al., 1999; Schmidt et al., 1995; Wang et al., 2005; Zwicker et al., 2011). Evidence suggests that both pre- and postsynaptic A_1 receptors can reduce preBötC rhythm [as reviewed in Chapter 1 and (Reklow et al., 2019), however extrasynaptic sites on astrocytes or microglia may also be involved. Determining which cell types A_1 receptors are expressed on may provide clues for alternative therapies to attenuate ADO-mediated reductions in breathing. For example, if ADO preferentially inhibits excitatory glutamatergic neurons in the preBötC, then therapies that potentiate the activity of these neurons may alleviate the induced depression of breathing by ADO. Specifically altering the activity of one network of the brain without unintended consequences arising from affecting others is extremely challenging however, as demonstrated by exploratory therapies designed to reduce seizure by increasing ADO levels by inhibiting ADK activity globally, which can cause respiratory-related unexpected death as ADO increases in respiratory nuclei (Shen et al., 2022).

The mechanism by which $P2Y_1$ receptors increases preBötC activity also remains elusive. These receptors exclusively mediate the frequency increase evoked by ATP in the network of neonate rodents (Huxtable et al., 2009; Lorier et al., 2008, 2007) and supports ventilation during the secondary phase of $HVR_{\dot{V}E}$ in adult rats (Rajani et al., 2017). $P2Y_1$ receptor activation increases $[Ca^{2+}]_i$ to enhance frequency, although other non-Ca^{2+} mechanisms may also be involved since EGAT-AM (Ca^{2+} chelator) and thapsigargin (SERCA inhibitor) only partially blocked the $P2Y_1$-mediated increase in preBötC frequency evoked by MRS 2365 (Rajani et al., 2017). $P2Y_1$ receptors

have been shown to signal through $G_{\alpha q/11}$ pathway, which activates phospholipase C and activation of protein kinase C, the former of which stimulates release intracellular stores of Ca^{2+} (Kugelgen and Wetter, 2000; Sak and Illes, 2005; Simon et al., 1995). $P2Y_1$ receptors can also modulate ion channel activity via the Ca^{2+}-independent $G_{\alpha i}$ pathway (Aoki et al., 2004; Brown et al., 2000; Filippov et al., 2000). A number of candidate downstream ion channel(s) have been postulated to mediate the effects of $P2Y_1$ activation in the preBötC, however the exact mechanism remains unanswered (Rajani et al., 2016). Identifying the mechanism by which $P2Y_1$ receptors increase preBötC frequency is important to determining if alternative therapies could be utilized to replicate or enhance the excitatory effects of ATP directly in the inspiratory network.

ii) Ectonucleotidases

Results from this thesis underscore the importance that non-receptor elements of the purinome have in determining the overall balance between P2 and P1 effects in the preBötC network. Data supports the previous observation that ECTO activity increases postnatally (Huxtable et al., 2009), however the profile of ECTO expression, which was not tested here, is also essential to characterizing the balance between ATP and ADP-mediated excitation and ADO-mediated inhibition (Zwicker et al., 2011). Developmental increases in ATP metabolism would not be expected to underlie increases in the excitatory effects of ATP, however previous data shows different ATP metabolites can preferentially activate either excitatory P2 or inhibitory P1 receptors depending on which ECTO isoform is predominant in a given region (Zwicker et al., 2011). Thus, future work characterizing the expression of ECTO isoforms in the preBötC from birth could be instructive not only to understand if enhanced excitatory effects of ATP arise from increases in ECTO isoforms that produce excitatory metabolites like ADP (i.e. ENTPDase2), but also confirm whether specific ECTOs that produce ADO are present (i.e. TNAP), which could elucidated new pharmacological targets to reduce the accumulation of ADOe following ATP release in the preBötC network.

iii) Mechanisms Mediating ADOe Clearance

Data suggest ADK-S activity, which supports ENT-mediated removal of ADOe, increases postnatally to influence baseline preBötC activity and the temporal profile of ADO-mediated reductions in network activity, which contributes to the reduction in the magnitude of the hypoxic

respiratory depression in adult mice. In vitro experiments suggest that ADO is removed from the extracellular space within the preBötC by ENT1 and ENT2, although my experiments did not differentiate whether each transporter are expressed at equal levels, nor whether other NTs exist in the network. Previous data suggests that ENT1 and ENT2 are the most abundant extracellular NTs in the brain (Parkinson et al., 2011) and that concentrative nucleoside transporters (CNTs), which actively move ADO against its concentration gradient, do not contribute to setting central ADOe levels (Chu et al., 2013). NBMPR, which is normally used to block ENT1 but will inhibit ENT2 activity at higher μM concentrations (Crawford et al., 1998), did not potentiate or prolong the ADO evoked inhibition of preBötC activity throughout development, however the ADO-mediated reduction of frequency was significantly prolonged in P0–12 ENT1/2 KO mice. This cannot exclude that NBMPR did not completely block ENT2 activity, especially if ENT2 is expressed at higher levels than ENT1. Another pharmacological inhibitor for ENT1 and 2, dipyridamole, was tested in preliminary experiments but also did not appear to affect the preBötC response to ATP or ADO. Dipyridamole, however, is a phosphodiesterase inhibitor that increases cAMP and cGMP levels (Gresele et al., 2011; Harker and Kadatz, 1983) which have been shown to stimulate and reduce preBötC output, respectively (Mironov et al., 1999; Mironov and Langohr, 2007; Shao et al., 2003; Zhang et al., 2019). Thus, NBMPR was a better option to limit off-target effects. Characterizing the expression of ENT isoforms within the preBötC would be useful to explain if the lack of effect on ADO-mediated inhibition using NBMPR was due to an incomplete block of ENT2 activity, provide insight about other ENTs expressed in the network, and inform predictions as to how manipulating ENTs may influence respiratory behaviour as inhibitors are used clinically to prevent tumor growth, treat pain, and promote cardioprotective effects by increasing peripheral ADO levels (Young et al., 2013). In terms of increasing ADOe clearance to support breathing in newborns, ENT function would need to be potentiated, which is difficult to achieve pharmacologically particularly with a passive transporter. Interventions that increase intracellular ADO metabolism would increase ENT-mediated removal of ADOe, however increasing the activity of an enzyme or protein that is not expressed in the very young (i.e. ADK-S) is impossible without exogenous introduction of the functional protein or replication of its activity through another method. While my data shows that ENT and ADK activity supports ADOe clearance in the preBötC, and their activity reduces the hypoxic respiratory depression in adult

mice, future studies will be needed to elucidate therapies that reduce ADOe, either by enhancing the systems presented here or through other novel means.

Data also does not conclusively demonstrate whether ENT or ADK activity influences the response of the preBötC network to ATP, nor did pharmacological inhibitors influence the ADO-mediated reduction in network frequency. As discussed in Chapter 2, the spatiotemporal dynamics of endogenous ATP release within the preBötC during hypoxia are not perfectly replicated by exogenous injection of 100 μM ATP in vitro, therefore I cannot exclude that pharmacological inhibition of ENTs does not affect the network response to ATP if endogenous synaptic concentrations are lower, which also holds true for exogenous 500 μM ADO injections. Stimulated release of astrocytic ATP in the preBötC in vitro could be achieved by using an optogenetic or chemogenetic technique to better replicate the spatial profile of its endogenous ATP release in vivo. A caveat, however, is that intracellular levels of ATP may be reduced in the slice and the temporal profile of purinergic release may also differ, underscoring the difficulty to replicate in vivo hypoxia conditions in the preBötC slice. Therefore, as I will describe in the next section, experiments in the whole animal be needed to fully elucidate the role of ADOe clearance mechanisms in influencing puringeric signaling within the preBötC during acute hypoxia.

5.4.2 Confirming that ADOe clearance in the preBötC reduces the secondary hypoxic respiratory depression

Results suggest that ENT and ADK activity contribute to development of a sustained, mature $HVR_{\dot{V}E}$ in adult mice, however further experiments are needed to determine if activity of either ENTs or ADK in the preBötC mediate their effects on the $HVR_{\dot{V}E}$, or if other regions of the brain are also involved. In my experiments, ENT1/2 were removed throughout the mouse meaning there could be large compensatory changes throughout the body that contributed to my observations, whereas in ADKtg mice, the endogenous *Adk* gene was replaced with a transgene that specifically overexpressed ADK-S throughout the brain. While sensitivity of the preBötC network to ATP and ADO appeared unchanged in ENT1/2 KO mice, this transgenic manipulation may have altered purinergic sensitivity in other central respiratory networks, or affected centres outside the CNS that transduce peripheral information to modulate ventilation using purinergic signaling, such as the carotid bodies (Conde et al., 2017; Lahiri et al., 2007; Leonard et al., 2018; Nurse et al., 2018).

The overexpression of ADK-S was specific to the brain unlike ENT1/2 KO, however this still does not conclusively demonstrate that ADOe clearance in the preBötC reduces the magnitude of the hypoxic respiratory depression in adult mice. In the following sections, I will detail the strengths and caveats of using either pharmacological or viral genetic approaches that could elucidate the role of ENTs and ADK specifically within the preBötC network in the HVR$\dot{V}_E$.

i) Pharmacological Interventions

Future studies that manipulate ENT and ADK activity specifically in the preBötC network during a hypoxic stimulus will elucidate whether the effects of these elements on the HVR$\dot{V}_E$ are mediated locally in the brainstem inspiratory network or exert effects elsewhere in the CNS. The first experiments that could be used are by directly infusing drugs in the preBötC to reduce/block the activity of ENTs and ADK and expose these animals to hypoxia. In anesthetized, vagotomized rats, unilateral application of MRS 2279 ($P2Y_1$ antagonist) to the preBötC during a hypoxic stimulus potentiated the hypoxic ventilatory depression suggesting that breathing is supported by $P2Y_1$ activation in this network during the secondary phase of hypoxia (Rajani et al., 2017). Infusion of ADO had no effect in anesthetized rats, which may reflect that P1-mediated inhibition of the preBötC disappears around 2–3 days after birth in these animals (Huxtable et al., 2009; Rajani et al., 2017; Zwicker et al., 2011). Data suggests that adult humans remain sensitive to central, ADO-mediated reductions in breathing (Yamamoto et al., 1994), therefore studying how the purinome affect the HVR in mice or other animal models that remain sensitive to central ADO through development will inform better predictions of what may be observed in humans.

A major caveat to any preBötC-specific interventions in vivo is that this requires complex, invasive surgeries in order to expose the brainstem, which is difficult to achieve in small rodents like mice. Furthermore, locally inhibiting either ENTs or ADK in the preBötC using drug infusion will require an animal to be kept under anesthesia during a hypoxic exposure, since the metabolism and diffusion of these drugs requires application throughout a hypoxic stimulus. The HVR has been measured extensively in animals kept under anesthesia (Gourine et al., 2005; Mayer et al., 2006; Rajani et al., 2017; Schmidt et al., 1995; Wessberg et al., 1984), however animals must be thermoregulated using a heating pad or other heating device. Thus, while it is possible to observe how pharmacological manipulation of ENT or ADK affects the HVR$\dot{V}_E$, effects of anesthesia on

basal metabolism would preclude measurement of whether ADOe clearance in the preBötC also affects the HVR$\dot{V}_E/\dot{V}_{O_2}$.

ii) Genetic Interventions

In order to assess ENT or ADK activity locally within the preBötC network influence the HVR, genetic tools that reduce either elements activity could also be utilized to alleviate issues related to measuring metabolic rate under anesthesia. While surgery would still be needed to access the brainstem network, animals would recover as expression of the transporter or enzyme is altered over 4–6 weeks, thus allowing both metabolic and ventilatory parameters of the HVR to be measured before and after the surgical intervention. Previously, viral constructs expressing the cytosolic isoform of ADK in the sense (overexpression) or antisense orientation (knockdown) have been used to manipulate the enzyme activity specifically in the striatum (Shen et al., 2011) and hippocampus (Theofilas et al., 2011). RNA interference (RNAi) could also be utilized to locally reduce the expression of ENTs in the brainstem. In culture, short interfering (si)RNA has been used to knockdown ENT1 (Hu et al., 2010; Lee et al., 2014), ENT2 (Dickens et al., 2018; Zeng et al., 2019), and ADK-S (Fassett et al., 2011), however future studies are needed to optimize this assay to induce preBötC-specific knockdown of ADOe clearance elements in a whole animal. Previous work has shown short hairpin (sh)RNA, which are transfected into target cells to produce siRNA, reduce the expression of Trpc3 and Trpm4 ion channels in the preBötC of mice (Picardo et al., 2019) demonstrating that this technology can be used to manipulate the inspiratory network. ADK-S levels, and ADOe clearance, increase in the preBötC network first three weeks of development, which means in vivo protocols to locally knockdown ADK activity could not be used in mice until ADK activity matures. Therefore, viral techniques to utilize conditional knock-in/out targeting ENT or ADK activity within the preBötC network may be a more viable tool to demonstrate their local activity are necessary to attenuate the hypoxic respiratory depression in neonates or contribute to reducing the hypoxic respiratory depression in adult mice.

5.4.3 The role of ADO and ADOe clearance in the hypoxic depression of metabolism

A major contribution of this thesis was demonstrating that reductions in $\dot{V}_{O_2}$ in response to hypoxia are an important adaptive strategy for the newborn rodents to sustain HVR$\dot{V}_E/\dot{V}_{O_2}$ above baseline like adults. Furthermore, my experiments suggest that inhibition of ADK can reduce $\dot{V}_{O_2}$ in developed

mice and block the hypometabolic response to hypoxia in P20 animals, whereas introduction of an overexpressed ADK-S transgene imparted a significant reduction in $\dot{V}O_2$ during hypoxia in newborn mice under a C57BL/6J background. Overall, this suggests that central ADO equilibrium may have significant effects on both baseline metabolic rate, as well as the $HVR_{\dot{V}E/\dot{V}O_2}$ through development. ADOe reduces neuronal activity and metabolic demand in the CNS, which is supported by data showing reductions in ADO increase sleep disruption (Rytkönen et al., 2010) and ADK activity in the cortex and basal forebrain increases to enhance metabolic demand during wakefulness (Alanko et al., 2003; Mackiewicz et al., 2003). Data suggests that peripheral chemoception at carotid bodies, which mediate the primary increase of the $HVR_{\dot{V}E}$, is not necessary to reduce metabolic rate in response to hypoxia (Matsuoka et al., 1994). In the brain, the hypothalamus is a major centre regulating energy intake and metabolism (Gu and Jun, 2018; Roh and Kim, 2016). Interestingly, this region has extensive reciprocal connections to the brainstem, specifically the NTS (Kooy et al., 1984), that is a relay network that transmits signals from carotid bodies to stimulate breathing networks when PaO_2 levels fall (Guyenet et al., 2010). ADO has been speculated to modulate metabolic networks in the hypothalamus since intracisternal injections of 2-chloroadenosine (A_1 receptor agonist) induces reductions in body temperature (Yarbrough and McGuffin-Clineschmidt, 1981), whereas DPCPX (A_1 antagonist) attenuates drops in body temperature during hypoxia when it is locally infused into the anteroventral preoptic region of the hypothalamus (Barros et al., 2006). ADK activity generates AMP, which activates metabolic pathways regulated by AMPK. AMPK activity is implicated not only in depressing metabolic activity but has also been implicated in shaping the $HVR_{\dot{V}E}$ (Evans, 2019) . Conditional deletion from catecholaminergic or adrenergic neurons can attenuate or potentiate the $HVR_{\dot{V}E}$, respectively (MacMillan and Evans, 2023; Mahmoud et al., 2016) This may explain my observation that ADK inhibition using ABT 702, which presumably increases in ADOe in two- and three-week old mice, depresses basal $\dot{V}O_2$. While previous data suggests that increasing ADOe should enhance the hypoxic hypometabolic response, the attenuation of this response in P20 mice treated with ABT 702 may be due to the significant drop in baseline metabolism. As described in Frappell et al., 1991, the magnitude of the hypoxic hypometabolic response is proportional to resting $\dot{V}O_2$ in most mammals, i.e. greater basal metabolic rate is associated with greater reductions in $\dot{V}O_2$ during hypoxia. Therefore, when ADK is inhibited in P20 mice, further reductions in $\dot{V}O_2$ during hypoxia may be limited by a "floor" that $\dot{V}O_2$ must remain above to maintain normal physiological processes

and thermogenesis. In ADKtg newborns, basal ADOe levels in the brain would be expected to be lower than WTs. These mice did not have significantly different basal $\dot{V}O_2$ relative to their WT counterparts, which may reflect compensatory changes due to transgene expression from before birth. Similarly, while ADOe levels should be diminished in ADKtg mice, therefore attenuating the hypoxic hypometabolic response, the $\dot{V}O_2$ of WT mice may already be closer to the endogenous "floor" under normoxia conditions and cannot fall as much as transgenic mice that have altered ADOe equilibrium and $\dot{V}O_2$ homeostasis. This hypothesis attempts to merge my observations with previous literature, however further investigation is needed to unravel the complex mechanisms that have evolved to overcome drops in available O_2. If nothing else, my data highlight the importance in measuring both ventilatory and metabolic changes during hypoxia as each are crucial in determining the odds of survival for vulnerable populations.

5.5 Conclusion

Development has large effects on both ventilatory and metabolic responses to hypoxia, highlighting the lengths evolution has progressed to maintain energy homeostasis in a rapidly changing period of life. Longstanding data suggested that newborns are susceptible to greater reductions in breathing during hypoxia due to greater inhibition of respiratory networks in the brain, which was believed to be the only contribution of the CNS to this response. Recent results challenged this dogma, showing that ATP is not only released in the brainstem inspiratory network during hypoxia, but stimulates breathing and attenuates secondary reductions in ventilation (Angelova et al., 2015; Gourine et al., 2005; Rajani et al., 2017). In this thesis, I tested the hypotheses that elements influencing purinergic signaling in the preBötC inspiratory network, termed the purinome, underlie developmental increases in the excitatory effects of ATP in the network and contribute to postnatal reductions in the secondary respiratory depression of the HVR$\dot{V}_E$. This work suggests that clearance of inhibitory ADOe in the preBötC is immature at birth, as ADK-S is minimally expressed and as levels increase to adult-like levels during the first three weeks, the HVR$\dot{V}_E$ also matures. My experiments led me to also test whether the HVR$\dot{V}_E/\dot{V}O_2$ of newborn rodents was attenuated due to immature hypometabolic responses to hypoxia. Results supports previous data from rats (Liu et al., 2009; Liu and Wong-Riley, 2013) showing that newborn rodents do not reduce $\dot{V}O_2$ during hypoxia and the HVR$\dot{V}_E/\dot{V}O_2$ is compromised in the youngest mice.

Studies exploring the roles of ADO transporters (ENTs), and intracellular enzymes important in controlling ADOi and ADOe clearance (e.g., ADK), on the $HVR_{\dot{V}E}$ are only in their infancy. Furthermore, understanding how/if the purinome affects metabolic responses during hypoxia is crucial, since data suggests while neonates exhibit an inadequate $HVR_{\dot{V}E,}$ the $HVR_{\dot{V}E/\dot{V}O2}$ can be compensated by greater reductions in $\dot{V}O_2$. The developmental dynamics of purinergic signaling in the respiratory network also requires investigation, especially given the potential involvement of the immature purinome in the greater susceptibility of premature and newborn mammals to hypoxic respiratory depression. Additional key areas of future investigation not discussed above include how the effects of purinergic signaling on cerebral vasculature could affect network excitability, and how the mechanisms and dynamics of purinergic signaling differ between conditions like hypoxia, when ATP is released through physiologically-relevant processes, and traumatic injury where ATP is released in high concentration from damaged/ruptured cells including red blood cells. A key translational challenge is to selectively manipulate the balance between ATP/ADO signaling to stimulate ventilation without simultaneously interfering with the beneficial actions of ADOe in other brain regions. To do so will require detailed understanding, not only of the purinome within the preBötC and other respiratory nuclei, but the rest of the CNS.

In conclusion, this thesis expands our understanding of the physiological mechanisms that mediate the HVR through development and across species. This work may inform future studies that ultimately elucidate novel therapeutic targets to prevent respiratory depression in apnea of prematurity and SUDEP, amongst other pathologies. While therapies will require rigorous experimental testing and optimization that may take years, bedside therapies breakthrough from a swell of observations amassed by physiological studies much like those presented here.

References

Abbracchio, M., Brambilla, R., Ceruti, S., Kim, H., Lubitz, D. von, Jacobson, K., Cattabeni, F., 1995. G protein-dependent activation of phospholipase C by adenosine A3 receptors in rat brain. Mol Pharmacol 48, 1038–45.

Abbracchio, M.P., Burnstock, G., Boeynaems, J.-M., Barnard, E.A., Boyer, J.L., Kennedy, C., Knight, G.E., Fumagalli, M., Gachet, C., Jacobson, K.A., Weisman, G.A., 2006. International Union of Pharmacology LVIII: Update on the P2Y G Protein-Coupled Nucleotide Receptors: From Molecular Mechanisms and Pathophysiology to Therapy. Pharmacol Rev 58, 281–341. https://doi.org/10.1124/pr.58.3.3

Abbracchio, M.P., Burnstock, G., Verkhratsky, A., Zimmermann, H., 2009. Purinergic signallingsignaling in the nervous system: an overview. Trends Neurosci 32, 19–29. https://doi.org/10.1016/j.tins.2008.10.001

Abbracchio, M.P., Cattabeni, F., Clementi, F., Sher, E., 1989. Adenosine receptors linked to adenylate cyclase activity in human neuroblastoma cells: Modulation during cell differentiation. Neuroscience 30, 819–825. https://doi.org/10.1016/0306-4522(89)90173-5

Ackley, M., Governo, R., Cass, C., Young, J., Baldwin, S., King, A., 2003. Control of glutamatergic neurotransmission in the rat spinal dorsal horn by the nucleoside transporter ENT1. The Journal of Physiology 548, 507–517. https://doi.org/10.1113/jphysiol.2002.038091

Alanko, L., Heiskanen, S., Stenberg, D., Porkka-Heiskanen, T., 2003. Adenosine kinase and 5′-nucleotidase activity after prolonged wakefulness in the cortex and the basal forebrain of rat. Neurochem Int 42, 449–454. https://doi.org/10.1016/s0197-0186(02)00155-9

Alanko, L., Porkka-Heiskanen, T., Soinila, S., 2006. Localization of equilibrative nucleoside transporters in the rat brain. Journal of Chemical Neuroanatomy 31, 162–168. https://doi.org/10.1016/j.jchemneu.2005.12.001

al-Rashida, M., Iqbal, J., 2014. Therapeutic Potentials of Ecto-Nucleoside Triphosphate Diphosphohydrolase, Ecto-Nucleotide Pyrophosphatase/Phosphodiesterase, Ecto-5′-Nucleotidase, and Alkaline Phosphatase Inhibitors. Med. Res. Rev. 34, 703–743. https://doi.org/10.1002/med.21302

Altaweraqi, R.A., Yao, S.Y., Smith, K.M., Cass, C.E., Young, J.D., 2020. HPLC reveals novel features of nucleoside and nucleobase homeostasis, nucleoside metabolism and nucleoside transport. Biochimica et biophysica acta. Biomembranes 1862, 183247. https://doi.org/10.1016/j.bbamem.2020.183247

Alvares, T., Revill, A., Huxtable, A., Lorenz, C., Funk, G., 2014. P2Y1 receptor-mediated potentiation of inspiratory motor output in neonatal rat in vitro 592. https://doi.org/10.1113/jphysiol.2013.268136

Alvaro, R., Alvarez, J., Kwiatkowski, K., Cates, D., Rigatto, H., 1992. Small Preterm Infants (≤1500 g) Have Only a Sustained Decrease in Ventilation in Response to Hypoxia. Pediatr Res 32, 403–406. https://doi.org/10.1203/00006450-199210000-00007

Ambrósio, A.F., Malva, J.O., Carvalho, A.P., Carvalho, C.M., 1997. Inhibition of N-, P/Q- and other types of Ca2+ channels in rat hippocampal nerve terminals by the adenosine A1 receptor. Eur J Pharmacol 340, 301–310. https://doi.org/10.1016/s0014-2999(97)01451-9

Anderson, C., Xiong, W., Geiger, J., Young, J., Cass, C., Baldwin, S., Parkinson, F., 1999. Distribution of equilibrative, nitrobenzylthioinosine-sensitive nucleoside transporters (ENT1) in brain. Journal of neurochemistry 73, 867–73.

Anderson, T.M., Ramirez, J.-M., 2017. Respiratory rhythm generation: triple oscillator hypothesis. F1000research 6, 139. https://doi.org/10.12688/f1000research.10193.1

Angelova, P., Kasymov, V., Christie, I., Sheikhbahaei, S., Turovsky, E., Marina, N., Korsak, A., Zwicker, J., Teschemacher, A., Ackland, G., Funk, G., Kasparov, S., Abramov, A., Gourine, A., 2015. Functional Oxygen Sensitivity of Astrocytes. J Neurosci 35, 10460–73. https://doi.org/10.1523/JNEUROSCI.0045-15.2015

Aoki, Y., Yamada, E., Endoh, T., Suzuki, T., 2004. Multiple actions of extracellular ATP and adenosine on calcium currents mediated by various purinoceptors in neurons of nucleus tractus solitarius. Neurosci Res 50, 245–255. https://doi.org/10.1016/j.neures.2004.07.012

Aoyama, T., Koga, S., Nakatsuka, T., Fujita, T., Goto, M., Kumamoto, E., 2010. Excitation of rat spinal ventral horn neurons by purinergic P2X and P2Y receptor activation. Brain Res 1340, 10–17. https://doi.org/10.1016/j.brainres.2010.04.053

Araque, A., Parpura, V., Sanzgiri, R.P., Haydon, P.G., Araque, A., Parpura, V., Sanzgiri, R.P., Haydon, P.G., 1999. Tripartite synapses: glia, the unacknowledged partner. Trends Neurosci 22, 208–215. https://doi.org/10.1016/s0166-2236(98)01349-6

Aronica, E., Zurolo, E., Iyer, A., Groot, M. de, Anink, J., Carbonell, C., Vliet, E.A. van, Baayen, J.C., Boison, D., Gorter, J.A., 2011. Upregulation of adenosine kinase in astrocytes in experimental and human temporal lobe epilepsy. Epilepsia 52, 1645–55. https://doi.org/10.1111/j.1528-1167.2011.03115.x

Ashraf, O., Huynh, T., Purnell, B.S., Murugan, M., Fedele, D.E., Chitravanshi, V., Boison, D., 2021. Suppression of phrenic nerve activity as a potential predictor of imminent sudden unexpected death in epilepsy (SUDEP). Neuropharmacology 184, 108405. https://doi.org/10.1016/j.neuropharm.2020.108405

Atterbury, A., Wall, M.J., 2009. Adenosine signalling at immature parallel fibre–Purkinje cell synapses in rat cerebellum. J Physiology 587, 4497–4508. https://doi.org/10.1113/jphysiol.2009.176420

Augusto, E., Matos, M., Sévigny, J., El-Tayeb, A., Bynoe, M.S., Müller, C.E., Cunha, R.A., Chen, J.-F., 2013. Ecto-5′-Nucleotidase (CD73)-Mediated Formation of Adenosine Is Critical for the Striatal Adenosine A2A Receptor Functions. J Neurosci 33, 11390–11399. https://doi.org/10.1523/jneurosci.5817-12.2013

Baertsch, N.A., Baertsch, H.C., Ramirez, J.M., 2018. The interdependence of excitation and inhibition for the control of dynamic breathing rhythms. Nature communications 9, 843. https://doi.org/10.1038/s41467-018-03223-x

Baldwin, S.A., Beal, P.R., Yao, S.Y., King, A.E., Cass, C.E., Young, J.D., 2004. The equilibrative nucleoside transporter family, SLC29. Pflugers Archiv : European journal of physiology 447, 735–43. https://doi.org/10.1007/s00424-003-1103-2

Baldwin, S.A., Yao, S.Y.M., Hyde, R.J., Ng, A.M.L., Foppolo, S., Barnes, K., Ritzel, M.W.L., Cass, C.E., Young, J.D., 2005. Functional Characterization of Novel Human and Mouse Equilibrative Nucleoside Transporters (hENT3 and mENT3) Located in Intracellular Membranes*. J Biol Chem 280, 15880–15887. https://doi.org/10.1074/jbc.m414337200

Ballanyi, K., 2004. Neuromodulation of the Perinatal Respiratory Network. Current neuropharmacology 2, 221–243. https://doi.org/10.2174/1570159043476828

Ballarín, M., Fredholm, B.B., Ambrosio, S., Mahy, N., 1991. Extracellular levels of adenosine and its metabolites in the striatum of awake rats: inhibition of uptake and metabolism. Acta Physiol Scand 142, 97–103. https://doi.org/10.1111/j.1748-1716.1991.tb09133.x

Barnes, K., Dobrzynski, H., Foppolo, S., Beal, P.R., Ismat, F., Scullion, E.R., Sun, L., Tellez, J., Ritzel, M.W.L., Claycomb, W.C., Cass, C.E., Young, J.D., Billeter-Clark, R., Boyett, M.R., Baldwin, S.A., 2006. Distribution and Functional Characterization of Equilibrative Nucleoside Transporter-4, a Novel Cardiac Adenosine Transporter Activated at Acidic pH. Circ Res 99, 510–519. https://doi.org/10.1161/01.res.0000238359.18495.42

Barros, R.C., Zimmer, M.E., Branco, L.G., Milsom, W.K., 2001. Hypoxic metabolic response of the golden-mantled ground squirrel. Journal of applied physiology (Bethesda, Md. : 1985) 91, 603–12. https://doi.org/10.1152/jappl.2001.91.2.603

Barros, R.C.H., Branco, L.G.S., Cárnio, E.C., 2006. Respiratory and body temperature modulation by adenosine A1 receptors in the anteroventral preoptic region during normoxia and hypoxia. Resp Physiol Neurobi 153, 115–125. https://doi.org/10.1016/j.resp.2005.09.013

Bélanger, M., Allaman, I., Magistretti, P.J., 2011. Brain Energy Metabolism: Focus on Astrocyte-Neuron Metabolic Cooperation. Cell Metab 14, 724–738. https://doi.org/10.1016/j.cmet.2011.08.016

Bellingham, M.C., Berger, A.J., 1994. Adenosine suppresses excitatory glutamatergic inputs to rat hypoglossal motoneurons in vitro. Neurosci Lett 177, 143–146. https://doi.org/10.1016/0304-3940(94)90065-5

Bhatt-Mehta, V., Schumacher, R.E., 2003. Treatment of Apnea of Prematurity. Pediatr Drugs 5, 195–210. https://doi.org/10.2165/00128072-200305030-00006

Bissonnette, J.M., 2000. Mechanisms regulating hypoxic respiratory depression during fetal and postnatal life. American journal of physiology. Regulatory, integrative and comparative physiology 278, R1391-400. https://doi.org/10.1152/ajpregu.2000.278.6.R1391

Bissonnette, J.M., Hohimer, A.R., Chao, C.R., Knopp, S.J., Notoroberto, N.F., 1990. Theophylline stimulates fetal breathing movements during hypoxia. Pediatric research 28, 83–6. https://doi.org/10.1203/00006450-199008000-00002

Bissonnette, J.M., Hohimer, A.R., Knopp, S.J., 1991. The effect of centrally administered adenosine on fetal breathing movements. Resp Physiol 84, 273–285. https://doi.org/10.1016/0034-5687(91)90123-z

Boison, D., 2016. Adenosinergic signaling in epilepsy. Neuropharmacology 104, 131–139. https://doi.org/10.1016/j.neuropharm.2015.08.046

Boison, D., 2013a. Adenosine and Seizure Termination: Endogenous Mechanisms. Epilepsy Curr 13, 35–37. https://doi.org/10.5698/1535-7511-13.1.35

Boison, D., 2013b. Adenosine kinase: exploitation for therapeutic gain. Pharmacological reviews 65, 906–43. https://doi.org/10.1124/pr.112.006361

Boison, D., 2012a. A Breather for SUDEP. Epilepsy Curr 12, 111–112. https://doi.org/10.5698/1535-7511-12.3.111

Boison, D., 2012b. Adenosine Augmentation Therapy, in: Noebels, J.L., Avoli, M., Rogawski, M.A., Olsen, R.W., Delgado-Escueta, A.V. (Eds.), Jasper's Basic Mechanisms of the Epilepsies [Internet]. Oxford University Press, USA.

Boison, D., 2011. Methylxanthines, Seizures, and Excitotoxicity. Handb Exp Pharmacol 251–266. https://doi.org/10.1007/978-3-642-13443-2_9

Boison, D., 2008. The adenosine kinase hypothesis of epileptogenesis. Prog Neurobiol 84, 249–262. https://doi.org/10.1016/j.pneurobio.2007.12.002

Boison, D., Chen, J.-F.F., Fredholm, B.B., 2010. Adenosine signaling and function in glial cells. Cell death and differentiation 17, 1071–82. https://doi.org/10.1038/cdd.2009.131

Boison, D., Scheurer, L., Zumsteg, V., Rülicke, T., Litynski, P., Fowler, B., Brandner, S., Mohler, H., 2002. Neonatal hepatic steatosis by disruption of the adenosine kinase gene.

Proceedings of the National Academy of Sciences of the United States of America 99, 6985–90. https://doi.org/10.1073/pnas.092642899

Bonora, M., Marlot, D., Gautier, H., Duron, B., 1984. Effects of hypoxia on ventilation during postnatal development in conscious kittens. Journal of applied physiology: respiratory, environmental and exercise physiology 56.

Bouzier-Sore, A., Merle, M., Magistretti, P., Pellerin, L., 2002. Feeding active neurons: (re)emergence of a nursing role for astrocytes 96.

Brockhaus, J., Ballanyi, K., 2000. Anticonvulsant A(1) receptor-mediated adenosine action on neuronal networks in the brainstem-spinal cord of newborn rats. Neuroscience 96, 359–71.

Brown, D.A., Filippov, A.K., Barnard, E.A., 2000. Inhibition of potassium and calcium currents in neurones by molecularly-defined P2Y receptors. J Autonom Nerv Syst 81, 31–36. https://doi.org/10.1016/s0165-1838(00)00150-8

Brundege, J.M., Dunwiddie, T.V., 1996. Modulation of Excitatory Synaptic Transmission by Adenosine Released from Single Hippocampal Pyramidal Neurons. J Neurosci 16, 5603–5612. https://doi.org/10.1523/jneurosci.16-18-05603.1996

Burnstock, G., 2015. Purinergic signalling and the autonomic nervous system in health and disease. Autonomic Neurosci 191, 1. https://doi.org/10.1016/j.autneu.2015.05.006

Burnstock, G., 2006. Purinergic P2 receptors as targets for novel analgesics. Pharmacol Therapeut 110, 433–454. https://doi.org/10.1016/j.pharmthera.2005.08.013

Burnstock, G., Dale, N., 2015. Purinergic signalling during development and ageing. Purinerg Signal 11, 277–305. https://doi.org/10.1007/s11302-015-9452-9

Burnstock, G., Fredholm, B.B., Verkhratsky, A., 2011. Adenosine and ATP Receptors in the Brain. Curr Top Med Chem 11, 973–1011. https://doi.org/10.2174/156802611795347627

Calker, D. van, Biber, K., 2005. The Role of Glial Adenosine Receptors in Neural Resilience and the Neurobiology of Mood Disorders. Neurochem Res 30, 1205–1217. https://doi.org/10.1007/s11064-005-8792-1

Calker, D. van, Müller, M., Hamprecht, B., 1979. Adenosine Regulates Via Two Different Types of Receptors, The Accumulation of Cyclic AMP in Cultured Brain Cells. J Neurochem 33, 999–1005. https://doi.org/10.1111/j.1471-4159.1979.tb05236.x

Canada, S., 2022. Live births, by weeks of gestation [WWW Document]. URL https://www150.statcan.gc.ca/t1/tbl1/en/tv.action?pid=1310042501 (accessed 5.3.23).

Canas, P.M., Porciúncula, L.O., Simões, A., Augusto, E., Silva, H.B., Machado, N.J., Gonçalves, N., Alfaro, T.M., Gonçalves, F.Q., Araújo, I.M., Real, J.I., Coelho, J.E., Andrade, G.M.,

Almeida, R.D., Chen, J.-F., Köfalvi, A., Agostinho, P., Cunha, R.A., 2018. Neuronal Adenosine A2A Receptors Are Critical Mediators of Neurodegeneration Triggered by Convulsions. Eneuro 5, ENEURO.0385-18.2018. https://doi.org/10.1523/eneuro.0385-18.2018

Carroll, J., Bureau, M., 1987. Decline in peripheral chemoreceptor excitatory stimulation during acute hypoxia in the lamb. Journal of applied physiology (Bethesda, Md. : 1985) 63.

Cheffer, A., Castillo, A., Corrêa-Velloso, J., Gonçalves, M., Naaldijk, Y., Nascimento, I., Burnstock, G., Ulrich, H., 2018. Purinergic system in psychiatric diseases. Mol Psychiatr 23, 94–106. https://doi.org/10.1038/mp.2017.188

Chen, C.-Y., Chou, F.-Y., Chang, Y.-G., Ho, C.-J., Wu, K.-C., Hsu, C.-L., Chern, Y., Lin, C.-J., 2023. Deletion of equilibrative nucleoside transporter 2 disturbs energy metabolism and exacerbates disease progression in an experimental model of Huntington's disease. Neurobiol Dis 177, 106004. https://doi.org/10.1016/j.nbd.2023.106004

Cheung, K.K., Chan, W.Y., Burnstock, G., 2005. Expression of P2X purinoceptors during rat brain development and their inhibitory role on motor axon outgrowth in neural tube explant cultures. Neuroscience 133, 937–45. https://doi.org/10.1016/j.neuroscience.2005.03.032

Cheung, K.-K.K., Ryten, M., Burnstock, G., 2003. Abundant and dynamic expression of G protein-coupled P2Y receptors in mammalian development. Dev. Dyn. 228, 254–66. https://doi.org/10.1002/dvdy.10378

Choi, D.-S., Cascini, M.-G., Mailliard, W., Young, H., Paredes, P., McMahon, T., Diamond, I., Bonci, A., Messing, R.O., 2004. The type 1 equilibrative nucleoside transporter regulates ethanol intoxication and preference. Nat Neurosci 7, 855–861. https://doi.org/10.1038/nn1288

Chrościńska-Krawczyk, M., Jargiełło-Baszak, M., Wałek, M., Tylus, B., Czuczwar, S.J., 2011. Caffeine and the anticonvulsant potency of antiepileptic drugs: experimental and clinical data. Pharmacol Rep 63, 12–18. https://doi.org/10.1016/s1734-1140(11)70394-2

Chu, S., Xiong, W., Zhang, D., Soylu, H., Sun, C., Albensi, B.C., Parkinson, F.E., 2013. Regulation of adenosine levels during cerebral ischemia. Acta Pharmacol Sin 34, 60–66. https://doi.org/10.1038/aps.2012.127

Comer, A.M., Perry, C.M., Figgitt, D.P., 2001. Caffeine Citrate. Paediatr Drugs 3, 61–79. https://doi.org/10.2165/00128072-200103010-00005

Conde, S.V., Monteiro, E.C., Sacramento, J.F., 2017. Purines and Carotid Body: New Roles in Pathological Conditions. Frontiers in pharmacology 8, 913. https://doi.org/10.3389/fphar.2017.00913

Corti, F., Cellai, L., Melani, A., Donati, C., Bruni, P., Pedata, F., 2013. Adenosine is present in rat brain synaptic vesicles. Neuroreport 24, 982–987. https://doi.org/10.1097/wnr.0000000000000033

Covelo, A., Araque, A., 2018. Neuronal activity determines distinct gliotransmitter release from a single astrocyte. Elife 7, e32237. https://doi.org/10.7554/elife.32237

Crawford, C.R., Patel, D.H., Naeve, C., Belt, J.A., 1998. Cloning of the human equilibrative, nitrobenzylmercaptopurine riboside (NBMPR)-insensitive nucleoside transporter ei by functional expression in a transport-deficient cell line. The Journal of biological chemistry 273, 5288–93. https://doi.org/10.1074/jbc.273.9.5288

Cronberg, T., Greer, D.M., Lilja, G., Moulaert, V., Swindell, P., Rossetti, A.O., 2020. Brain injury after cardiac arrest: from prognostication of comatose patients to rehabilitation. Lancet Neurology 19, 611–622. https://doi.org/10.1016/s1474-4422(20)30117-4

Cross, K., Oppe, T., 1952. The effect of inhalation of high and low concentrations of oxygen on the respiration of the premature infant. The Journal of physiology 117.

Cross, K., Tizard, J., Trythall, D., 1958. The Gaseous Metabolism of the New-born Infant Breathing 15 % Oxygen. Acta Pædiatrica 47, 217–237. https://doi.org/10.1111/j.1651-2227.1958.tb07879.x

Cunha, R.A., 2016. How does adenosine control neuronal dysfunction and neurodegeneration? J Neurochem 139, 1019–1055. https://doi.org/10.1111/jnc.13724

Cunha, R.A., 2005. Neuroprotection by adenosine in the brain: From A1 receptor activation to A2A receptor blockade. Purinerg Signal 1, 111–134. https://doi.org/10.1007/s11302-005-0649-1

Cunha, R.A., Sebastião, A.M., Ribeiro, J., 1998. Inhibition by ATP of Hippocampal Synaptic Transmission Requires Localized Extracellular Catabolism by Ecto-Nucleotidases into Adenosine and Channeling to Adenosine A1 Receptors. J Neurosci 18, 1987–1995. https://doi.org/10.1523/jneurosci.18-06-01987.1998

Curran, A.K., Rodman, J.R., Eastwood, P.R., Henderson, K.S., Dempsey, J.A., Smith, C.A., 2000. Ventilatory responses to specific CNS hypoxia in sleeping dogs. J Appl Physiol 88, 1840–1852. https://doi.org/10.1152/jappl.2000.88.5.1840

Dale, N., Frenguelli, B.G., 2009. Release of Adenosine and ATP During Ischemia and Epilepsy. Curr Neuropharmacol 7, 160–179. https://doi.org/10.2174/157015909789152146

Daristotle, L., Engwall, M., Niu, W., Bisgard, G., 1991. Ventilatory effects and interactions with change in PaO2 in awake goats. J Appl Physiol 71, 1254–1260. https://doi.org/10.1152/jappl.1991.71.4.1254

Darnall, Jr.R., 1985. Aminophylline reduces hypoxic ventilatory depression: possible role of adenosine. Pediatric Research 19. https://doi.org/10.1203/00006450-198507000-00014

Dejours, P., 1981. Principles of comparative respiratory physiology.

Del Negro, C.A., Funk, G.D., Feldman, J.L., 2018. Breathing matters. Nature reviews. Neuroscience 19, 351–367. https://doi.org/10.1038/s41583-018-0003-6

Dempsey, J.A., Smith, C.A., 2019. Update on Chemoreception Influence on Cardiorespiratory Regulation and Pathophysiology. Clin Chest Med 40, 269–283. https://doi.org/10.1016/j.ccm.2019.02.001

Dempsey, J.A., Smith, C.A., Blain, G.M., Xie, A., Gong, Y., Teodorescu, M., 2012. Role of Central/Peripheral Chemoreceptors and Their Interdependence in the Pathophysiology of Sleep Apnea, in: Nurse, C.A., Gonzalez, C., Peers, C., Prabhakar, N. (Eds.), Arterial Chemoreception, Advances in Experimental Medicine and Biology. pp. 343–349. https://doi.org/10.1007/978-94-007-4584-1_46

Dempsey, J.A., Veasey, S.C., Morgan, B.J., O'Donnell, C.P., 2010. Pathophysiology of Sleep Apnea. Physiol Rev 90, 47–112. https://doi.org/10.1152/physrev.00043.2008

Devinsky, O., 2011. Sudden, Unexpected Death in Epilepsy. New Engl J Medicine 365, 1801–1811. https://doi.org/10.1056/nejmra1010481

Devinsky, O., Hesdorffer, D.C., Thurman, D.J., Lhatoo, S., Richerson, G., 2016. Sudden unexpected death in epilepsy: epidemiology, mechanisms, and prevention. Lancet Neurology 15, 1075–1088. https://doi.org/10.1016/s1474-4422(16)30158-2

Dickens, D., Rädisch, S., Chiduza, G.N., Giannoudis, A., Cross, M.J., Malik, H., Schaeffeler, E., Sison-Young, R.L., Wilkinson, E.L., Goldring, C.E., Schwab, M., Pirmohamed, M., Nies, A.T., 2018. Cellular Uptake of the Atypical Antipsychotic Clozapine Is a Carrier-Mediated Process. Mol Pharmaceut 15, 3557–3572. https://doi.org/10.1021/acs.molpharmaceut.8b00547

Díez-Zaera, M., Díaz-Hernández, J.I., Hernández-Álvarez, E., Zimmermann, H., Díaz-Hernández, M., Miras-Portugal, M.T., 2011. Tissue-nonspecific alkaline phosphatase promotes axonal growth of hippocampal neurons. Molecular biology of the cell 22, 1014–24. https://doi.org/10.1091/mbc.E10-09-0740

Disease, N.A. on and on on for a of, 2011. Toward Precision Medicine: Building a knowledge network for biomedical research and a new taxonomy of disease. National Academies Press.

Dixon, A.K., Gubitz, A.K., Sirinathsinghji, D.J.S., Richardson, P.J., Freeman, T.C., 1996. Tissue distribution of adenosine receptor mRNAs in the rat. Brit J Pharmacol 118, 1461–1468. https://doi.org/10.1111/j.1476-5381.1996.tb15561.x

Dong, X., Feldman, J., 1995. Modulation of inspiratory drive to phrenic motoneurons by presynaptic adenosine A1 receptors. J Neurosci 15, 3458–3467. https://doi.org/10.1523/jneurosci.15-05-03458.1995

Drorbaugh, J., Fenn, W., 1955. A barometric method for measuring ventilation in newborn infants. Pediatrics 16, 81–7.

Dunwiddie, T.V., Diao, L., Kim, H.O., Jiang, J.-L., Jacobson, K.A., 1997a. Activation of Hippocampal Adenosine A3 Receptors Produces a Desensitization of A1 Receptor-Mediated Responses in Rat Hippocampus. J Neurosci 17, 607–614. https://doi.org/10.1523/jneurosci.17-02-00607.1997

Dunwiddie, T.V., Diao, L., Proctor, W.R., 1997b. Adenine Nucleotides Undergo Rapid, Quantitative Conversion to Adenosine in the Extracellular Space in Rat Hippocampus. J Neurosci 17, 7673–7682. https://doi.org/10.1523/jneurosci.17-20-07673.1997

Dunwiddie, T.V., Masino, S.A., 2001. THE ROLE AND REGULATION OF ADENOSINE IN THE CENTRAL NERVOUS SYSTEM. Annu Rev Neurosci 24, 31–55. https://doi.org/10.1146/annurev.neuro.24.1.31

Dzal, Y.A., Milsom, W.K., 2021. Effects of hypoxia on the respiratory and metabolic responses to progressive cooling in newborn rodents that range in heterothermic expression. Exp Physiol 106, 1005–1023. https://doi.org/10.1113/ep089085

Dzal, Y.A., Sprenger, R.J., Milsom, W.K., 2020. Postnatal changes in O2 and CO2 sensitivity in rodents. Resp Physiol Neurobi 272, 103313. https://doi.org/10.1016/j.resp.2019.103313

Easton, P., Anthonisen, N., 1988. Ventilatory response to sustained hypoxia after pretreatment with aminophylline. Journal of applied physiology (Bethesda, Md. : 1985) 64.

Eichenwald, E.C., 2016. Apnea of Prematurity. Pediatrics 137, e20153757. https://doi.org/10.1542/peds.2015-3757

Eldridge, F.L., Millhorn, D.E., Kiley, J.P., 1984. Respiratory effects of a long-acting analog of adenosine. Brain research 301, 273–80. https://doi.org/10.1016/0006-8993(84)91096-5

Evans, A.M., 2019. AMPK breathing and oxygen supply. Respiratory Physiology & Neurobiology 265, 112–120. https://doi.org/10.1016/j.resp.2018.08.011

Fábera, P., Uttl, L., Kubová, H., Tsenov, G., Mareš, P., 2022. Adenosine Kinase Isoforms in the Developing Rat Hippocampus after LiCl/Pilocarpine Status Epilepticus. Int J Mol Sci 23, 2510. https://doi.org/10.3390/ijms23052510

Fahey, J.T., Lister, G., 1989. Response to Low Cardiac Output: Developmental Differences in Metabolism during Oxygen Deficit and Recovery in Lambs. Pediatr Res 26, 180–187. https://doi.org/10.1203/00006450-198909000-00003

Fassett, J.T., Hu, X., Xu, X., Lu, Z., Zhang, P., Chen, Y., Bache, R.J., 2011. Adenosine kinase regulation of cardiomyocyte hypertrophy. Am J Physiol-heart C 300, H1722–H1732. https://doi.org/10.1152/ajpheart.00684.2010

Fedele, D., Gouder, N., Güttinger, M., Gabernet, L., Scheurer, L., Rülicke, T., Crestani, F., Boison, D., 2005. Astrogliosis in epilepsy leads to overexpression of adenosine kinase, resulting in seizure aggravation. Brain : a journal of neurology 128, 2383–95. https://doi.org/10.1093/brain/awh555

Fedele, D.E., Koch, P., Scheurer, L., Simpson, E.M., Möhler, H., Brüstle, O., Boison, D., 2004. Engineering embryonic stem cell derived glia for adenosine delivery. Neurosci Lett 370, 160–165. https://doi.org/10.1016/j.neulet.2004.08.031

Fedele, D.E., Li, T., Lan, J.Q., Fredholm, B.B., Boison, D., 2006. Adenosine A1 receptors are crucial in keeping an epileptic focus localized. Exp Neurol 200, 184–190. https://doi.org/10.1016/j.expneurol.2006.02.133

Feldman, J., Del Negro, C., 2006. Looking for inspiration: new perspectives on respiratory rhythm 7. https://doi.org/10.1038/nrn1871

Filippov, A.K., Brown, D.A., Barnard, E.A., 2000. The P2Y1 receptor closes the N-type Ca2+ channel in neurones, with both adenosine triphosphates and diphosphates as potent agonists. Brit J Pharmacol 129, 1063–1066. https://doi.org/10.1038/sj.bjp.0703185

Fiore, J.M., Martin, R.J., Gauda, E.B., 2013. Apnea of prematurity – Perfect storm. Respiratory Physiology & Neurobiology 189, 213–222. https://doi.org/10.1016/j.resp.2013.05.026

Fong, A.Y., Krstew, E.V., Barden, J., Lawrence, A.J., 2002. Immunoreactive localisation of P2Y1 receptors within the rat and human nodose ganglia and rat brainstem: comparison with [α33P]deoxyadenosine 5′-triphosphate autoradiography. Neuroscience 113, 809–823. https://doi.org/10.1016/s0306-4522(02)00237-3

Franke, H., Illes, P., 2006. Involvement of P2 receptors in the growth and survival of neurons in the CNS. Pharmacol Therapeut 109, 297–324. https://doi.org/10.1016/j.pharmthera.2005.06.002

Frappell, P., Lanthier, C., Baudinette, R.V., Mortola, J.P., 1992. Metabolism and ventilation in acute hypoxia: a comparative analysis in small mammalian species. Am J Physiology-regulatory Integr Comp Physiology 262, R1040–R1046. https://doi.org/10.1152/ajpregu.1992.262.6.r1040

Frappell, P., Saiki, C., Mortola, J.P., 1991. Metabolism during normoxia, hypoxia and recovery in the newborn kitten. Resp Physiol 86, 115–24. https://doi.org/10.1016/0034-5687(91)90043-i

Fredholm, B., Abbracchio, M., Burnstock, G., Daly, J., Harden, T., Jacobson, K., Leff, P., Williams, M., 1994. Nomenclature and classification of purinoceptors. Pharmacol Rev 46, 143–56.

Fredholm, B., IJzerman, A., Jacobson, K., Klotz, K., Linden, J., 2001. International Union of Pharmacology. XXV. Nomenclature and classification of adenosine receptors. Pharmacological reviews 53, 527–52.

Fredholm, B.B., Arslan, G., Halldner, L., Kull, B., Schulte, G., Wasserman, W., 2000. Structure and function of adenosine receptors and their genes. Naunyn-schmiedeberg's Archives Pharmacol 362, 364–374. https://doi.org/10.1007/s002100000313

Fuller, D.D., Mitchell, G.S., 2017a. Special Issue: Respiratory Neuroplasticity. Exp Neurol 287, 91–92. https://doi.org/10.1016/j.expneurol.2016.11.004

Fuller, D.D., Mitchell, G.S., 2017b. Respiratory neuroplasticity – Overview, significance and future directions. Exp Neurol 287, 144–152. https://doi.org/10.1016/j.expneurol.2016.05.022

Funk, G., 2013. Neuromodulation: purinergic signaling in respiratory control. Comprehensive Physiology 3, 331–63. https://doi.org/10.1002/cphy.c120004

Funk, G., Greer, J., 2013. The rhythmic, transverse medullary slice preparation in respiratory neurobiology: contributions and caveats. Respiratory Physiology & Neurobiology 186. https://doi.org/10.1016/j.resp.2013.01.011

Funk, G., Smith, J., Feldman, J., 1994. Development of thyrotropin-releasing hormone and norepinephrine potentiation of inspiratory-related hypoglossal motoneuron discharge in neonatal and juvenile mice in vitro 72. https://doi.org/10.1152/jn.1994.72.5.2538

Funk, G.D., Gourine, A.V., 2018a. CrossTalk proposal: a central hypoxia sensor contributes to the excitatory hypoxic ventilatory response. J Physiology 596, 2935–2938. https://doi.org/10.1113/jp275707

Funk, G.D., Gourine, A.V., 2018b. Rebuttal from Gregory D. Funk and Alexander V. Gourine. J Physiology 596, 2943–2944. https://doi.org/10.1113/jp276282

Funk, G.D., Huxtable, A.G., Lorier, A.R., 2008. ATP in central respiratory control: a three-part signaling system. Respiratory physiology & neurobiology 164, 131–42. https://doi.org/10.1016/j.resp.2008.06.004

Gaston, B., May, W.J., Sullivan, S., Yemen, S., Marozkina, N.V., Palmer, L.A., Bates, J.N., Lewis, S.J., 2014. Essential role of hemoglobin beta-93-cysteine in posthypoxia facilitation of breathing in conscious mice. J Appl Physiol 116, 1290–1299. https://doi.org/10.1152/japplphysiol.01050.2013

Gebril, H., Wahba, A., Zhou, X., Lai, T., Alharfoush, E., DiCicco-Bloom, E., Boison, D., 2021. Developmental Role of Adenosine Kinase in the Cerebellum. eNeuro 8. https://doi.org/10.1523/ENEURO.0011-21.2021

Gebril, H.M., Rose, R.M., Gesese, R., Emond, M.P., Huo, Y., Aronica, E., Boison, D., 2020. Adenosine kinase inhibition promotes proliferation of neural stem cells after traumatic brain injury. Brain communications 2, fcaa017. https://doi.org/10.1093/braincomms/fcaa017

Gendron, F., Benrezzak, O., Krugh, B., Kong, Q., Weisman, G., Beaudoin, A., 2002. Purine Signaling and Potential New Therapeutic Approach: Possible Outcomes of NTPDase Inhibition. Curr Drug Targets 3, 229–45. https://doi.org/10.2174/1389450023347713

Getsy, P.M., Davis, J., Coffee, G.A., May, W.J., Palmer, L.A., Strohl, K.P., Lewis, S.J., 2014. Enhanced non-eupneic breathing following hypoxic, hypercapnic or hypoxic–hypercapnic gas challenges in conscious mice. Respiratory Physiology & Neurobiology 204, 147–159. https://doi.org/10.1016/j.resp.2014.09.006

Gill, M., Pugh, L., 1964. Basal metabolism and respiration in men living at 5,800 m (19,000 ft). J Appl Physiol 19, 949–954. https://doi.org/10.1152/jappl.1964.19.5.949

Golder, F.J., Ranganathan, L., Satriotomo, I., Hoffman, M., Lovett-Barr, M.R., Watters, J.J., Baker-Herman, T.L., Mitchell, G.S., 2008. Spinal Adenosine A2a Receptor Activation Elicits Long-Lasting Phrenic Motor Facilitation. J Neurosci 28, 2033–2042. https://doi.org/10.1523/jneurosci.3570-07.2008

Gomes, C.V., Kaster, M.P., Tomé, A.R., Agostinho, P.M., Cunha, R.A., 2011. Adenosine receptors and brain diseases: Neuroprotection and neurodegeneration. Biochimica Et Biophysica Acta Bba - Biomembr 1808, 1380–1399. https://doi.org/10.1016/j.bbamem.2010.12.001

Gonçalves, F.Q., Pires, J., Pliassova, A., Beleza, R., Lemos, C., Marques, J.M., Rodrigues, R.J., Canas, P.M., Köfalvi, A., Cunha, R.A., Rial, D., 2015. Adenosine A2b receptors control A1 receptor-mediated inhibition of synaptic transmission in the mouse hippocampus. Eur J Neurosci 41, 878–888. https://doi.org/10.1111/ejn.12851

Gouder, N., Scheurer, L., Fritschy, J.-M.M., Boison, D., 2004. Overexpression of adenosine kinase in epileptic hippocampus contributes to epileptogenesis. The Journal of neuroscience : the official journal of the Society for Neuroscience 24, 692–701. https://doi.org/10.1523/JNEUROSCI.4781-03.2004

Gourine, A.V., Funk, G.D., 2017. On the existence of a central respiratory oxygen sensor. J Appl Physiol 123, 1344–1349. https://doi.org/10.1152/japplphysiol.00194.2017

Gourine, A.V., Kasymov, V., Marina, N., Tang, F., Figueiredo, M.F., Lane, S., Teschemacher, A.G., Spyer, K.M., Deisseroth, K., Kasparov, S., 2010. Astrocytes Control Breathing Through

pH-Dependent Release of ATP. Science 329, 571–575. https://doi.org/10.1126/science.1190721

Gourine, A.V., Llaudet, E., Dale, N., Spyer, K.M., 2005. Release of ATP in the Ventral Medulla during Hypoxia in Rats: Role in Hypoxic Ventilatory Response. J Neurosci 25, 1211–1218. https://doi.org/10.1523/jneurosci.3763-04.2005

Gourine, A.V., Llaudet, E., Thomas, T., Dale, N., Spyer, M.K., 2002. Adenosine release in nucleus tractus solitarii does not appear to mediate hypoxia-induced respiratory depression in rats. J Physiology 544, 161–170. https://doi.org/10.1113/jphysiol.2002.024174

Gozal, D., Reeves, S.R., Row, B.W., Neville, J.J., Guo, S.Z., Lipton, A.J., 2003. Respiratory Effects of Gestational Intermittent Hypoxia in the Developing Rat. Am J Resp Crit Care 167, 1540–1547. https://doi.org/10.1164/rccm.200208-963oc

Gray, P., Janczewski, W., Mellen, N., McCrimmon, D., Feldman, J., 2001. Normal breathing requires preBotzinger complex neurokinin-1 receptor-expressing neurons. Nature Neuroscience 4. https://doi.org/10.1038/nn0901-927

Gray, P., Rekling, J., Bocchiaro, C., Feldman, J., 1999. Modulation of respiratory frequency by peptidergic input to rhythmogenic neurons in the preBotzinger complex 286. https://doi.org/10.1126/science.286.5444.1566

Greene, R.W., Haas, H.L., 1991. The electrophysiology of adenosine in the mammalian central nervous system. Prog Neurobiol 36, 329–341. https://doi.org/10.1016/0301-0082(91)90005-l

Gresele, P., Momi, S., Falcinelli, E., 2011. Anti-platelet therapy: phosphodiesterase inhibitors. Brit J Clin Pharmaco 72, 634–646. https://doi.org/10.1111/j.1365-2125.2011.04034.x

Grković, I., Bjelobaba, I., Mitrović, N., Lavrnja, I., Drakulić, D., Martinović, J., Stanojlović, M., Horvat, A., Nedeljković, N., 2016. Expression of ecto-nucleoside triphosphate diphosphohydrolase3 (NTPDase3) in the female rat brain during postnatal development. J Chem Neuroanat 77, 10–18. https://doi.org/10.1016/j.jchemneu.2016.04.001

Grkovic, I., Bjelobaba, I., Nedeljkovic, N., Mitrovic, N., Drakulic, D., Stanojlovic, M., Horvat, A., 2014. Developmental Increase in Ecto-5′-Nucleotidase Activity Overlaps with Appearance of Two Immunologically Distinct Enzyme Isoforms in Rat Hippocampal Synaptic Plasma Membranes. J Mol Neurosci 54, 109–118. https://doi.org/10.1007/s12031-014-0256-0

Gu, C., Jun, J.C., 2018. Does Hypoxia Decrease the Metabolic Rate? Front Endocrinol 9, 668. https://doi.org/10.3389/fendo.2018.00668

Guyenet, P., Stornetta, R., Bayliss, D., 2010. Central respiratory chemoreception 518. https://doi.org/10.1002/cne.22435

Guyenet, P.G., 2014. Regulation of Breathing and Autonomic Outflows by Chemoreceptors. Compr Physiol 4, 1511–1562. https://doi.org/10.1002/cphy.c140004

Guyenet, P.G., 2006. The sympathetic control of blood pressure. Nat Rev Neurosci 7, 335–346. https://doi.org/10.1038/nrn1902

Haas, H.L., Selbach, O., 2000. Functions of neuronal adenosine receptors. Naunyn-schmiedeberg's Archives Pharmacol 362, 375–381. https://doi.org/10.1007/s002100000314

Haddad, G.G., Gandhi, M.R., Mellins, R.B., 1982. Maturation of ventilatory response to hypoxia in puppies during sleep. J Appl Physiol 52, 309–314. https://doi.org/10.1152/jappl.1982.52.2.309

Harker, L., Kadatz, R., 1983. Mechanism of action of dipyridamole. Thrombosis research. Supplement 4, 39–46.

Haselkorn, L.M., Shellington, D.K., Jackson, E.K., Vagni, V.A., Janesko-Feldman, K., Dubey, R.K., Gillespie, D.G., Cheng, D., Bell, M.J., Jenkins, L.W., Homanics, G.E., Schnermann, J., Kochanek, P.M., 2010. Adenosine A1 Receptor Activation as a Brake on the Microglial Response after Experimental Traumatic Brain Injury in Mice. J Neurotraum 27, 901–910. https://doi.org/10.1089/neu.2009.1075

Hedner, T., Hedner, J., Bergman, B., Mueller, R.A., Jonason, J., 1985. Characterization of Adenosine-Induced Respiratory Depression in the Preterm Rabbit. Neonatology 47, 323–332. https://doi.org/10.1159/000242135

Hedner, T., Hedner, J., Jonason, J., Wessberg, P., 1984. Effects of theophylline on adenosine-induced respiratory depression in the preterm rabbit. Eur J Respir Dis 65, 153–6.

Heitzmann, D., Buehler, P., Schweda, F., Georgieff, M., Warth, R., Thomas, J., 2016. The in vivo respiratory phenotype of the adenosine A1 receptor knockout mouse. Respiratory Physiology & Neurobiology 222, 16–28. https://doi.org/10.1016/j.resp.2015.11.005

Herlenius, E., Aden, U., Tang, L., Lagercrantz, H., 2002. Perinatal respiratory control and its modulation by adenosine and caffeine in the rat. Pediatric Research 51. https://doi.org/10.1203/00006450-200201000-00004

Herlenius, E., Lagercrantz, H., 1999. Adenosinergic modulation of respiratory neurones in the neonatal rat brainstem in vitro. The Journal of Physiology 518, 159–172. https://doi.org/10.1111/j.1469-7793.1999.0159r.x

Herlenius, E., Lagercrantz, H., Yamamoto, Y., 1997. Adenosine modulates inspiratory neurons and the respiratory pattern in the brainstem of neonatal rats. Pediatric research 42, 46–53. https://doi.org/10.1203/00006450-199707000-00008

Hill, A., 3rd, G.A., of …, Z.-S., 2011. Graded reductions in oxygenation evoke graded reconfiguration of the isolated respiratory network. https://doi.org/10.1152/jn.00237.2010

Hill, J.R., 1959. The oxygen consumption of new-born and adult mammals. Its dependence on the oxygen tension in the inspired air and on the environmental temperature. J Physiology 149, 346–373. https://doi.org/10.1113/jphysiol.1959.sp006344

Howell, B.N., Newman, D.S., 2017. Dysfunction of central control of breathing in amyotrophic lateral sclerosis. Muscle Nerve 56, 197–201. https://doi.org/10.1002/mus.25564

Hu, X., Chen, W., Xu, J., 2010. Downregulation of human equilibrative nucleoside transporter 1 by RNAi enhances 5-fluorouracil response in pancreatic cancer. Hepato-gastroenterol 57, 1567–72.

Huxtable, A., Zwicker, J., Alvares, T., Ruangkittisakul, A., Fang, X., Hahn, L., Chaves, P.E. de, Baker, G., Ballanyi, K., Funk, G., 2010. Glia contribute to the purinergic modulation of inspiratory rhythm-generating networks. The Journal of neuroscience : the official journal of the Society for Neuroscience 30. https://doi.org/10.1523/JNEUROSCI.6027-09.2010

Huxtable, A., Zwicker, J., Poon, B., Pagliardini, S., Vrouwe, S., Greer, J., Funk, G., 2009. Tripartite purinergic modulation of central respiratory networks during perinatal development: the influence of ATP, ectonucleotidases, and ATP metabolites. The Journal of neuroscience : the official journal of the Society for Neuroscience 29. https://doi.org/10.1523/JNEUROSCI.2660-09.2009

Jackson, E.K., Kotermanski, S.E., Menshikova, E.V., Dubey, R.K., Jackson, T.C., Kochanek, P.M., 2017. Adenosine production by brain cells. J Neurochem 141, 676–693. https://doi.org/10.1111/jnc.14018

Jacobson, K.A., Balasubramanian, R., Deflorian, F., Gao, Z.-G., 2012. G protein-coupled adenosine (P1) and P2Y receptors: ligand design and receptor interactions. Purinerg Signal 8, 419–436. https://doi.org/10.1007/s11302-012-9294-7

Jansen, N.A., Schenke, M., Voskuyl, R.A., Thijs, R.D., Maagdenberg, A.M.J.M.M. van den, Tolner, E.A., 2019. Apnea Associated with Brainstem Seizures in Cacna1aS218L Mice Is Caused by Medullary Spreading Depolarization. The Journal of neuroscience : the official journal of the Society for Neuroscience 39, 9633–9644. https://doi.org/10.1523/JNEUROSCI.1713-19.2019

Jarvis, M.F., Yu, H., Kohlhaas, K., Alexander, K., Lee, C.H., Jiang, M., Bhagwat, S.S., Williams, M., Kowaluk, E.A., 2000. ABT-702 (4-amino-5-(3-bromophenyl)-7-(6-morpholinopyridin-3-yl)pyrido[2, 3-d]pyrimidine), a novel orally effective adenosine kinase inhibitor with analgesic and anti-inflammatory properties: I. In vitro characterization and acute antinociceptive effects in the mouse. The Journal of pharmacology and experimental therapeutics 295, 1156–64.

Jennings, L.L., Hao, C., Cabrita, M.A., Vickers, M.F., Baldwin, S.A., Young, J.D., Cass, C.E., 2001. Distinct regional distribution of human equilibrative nucleoside transporter proteins 1 and 2 (hENT1 and hENT2) in the central nervous system. Neuropharmacology 40, 722–731. https://doi.org/10.1016/s0028-3908(00)00207-0

Johnson, R.A., Mitchell, G.S., 2013. Common mechanisms of compensatory respiratory plasticity in spinal neurological disorders. Resp Physiol Neurobi 189, 419–428. https://doi.org/10.1016/j.resp.2013.05.025

Johnson, S., Koshiya, N., Smith, J., 2001. Isolation of the kernel for respiratory rhythm generation in a novel preparation: the pre-Bötzinger complex "island". Journal of neurophysiology 85, 1772–6.

Johnson, S.M., Randhawa, K.S., Baker, T.L., Watters, J.J., 2019. Respiratory frequency plasticity during development. Resp Physiol Neurobi 266, 54–65. https://doi.org/10.1016/j.resp.2019.04.014

Kao, Y.-H., Lin, M.-S., Chen, C.-M., Wu, Y.-R., Chen, H.-M., Lai, H.-L., Chern, Y., Lin, C.-J., 2017. Targeting ENT1 and adenosine tone for the treatment of Huntington's disease. Hum Mol Genet 26, ddw402. https://doi.org/10.1093/hmg/ddw402

Kawai, A., Okada, Y., Muckenhoff, K., Scheid, P., 1995. Theophylline and hypoxic ventilatory response in the rat isolated brainstem-spinal cord. Respiration physiology 100. https://doi.org/10.1016/0034-5687(94)00124-i

Kawamura, M., Gachet, C., Inoue, K., Kato, F., 2004. Direct Excitation of Inhibitory Interneurons by Extracellular ATP Mediated by P2Y 1 Receptors in the Hippocampal Slice. J Neurosci 24, 10835–10845. https://doi.org/10.1523/jneurosci.3028-04.2004

Kiese, K., Jablonski, J., Boison, D., Kobow, K., 2016. Dynamic Regulation of the Adenosine Kinase Gene during Early Postnatal Brain Development and Maturation. Front Mol Neurosci 9, 99. https://doi.org/10.3389/fnmol.2016.00099

Kimura, M., Saitoh, N., Takahashi, T., 2003. Adenosine A1 receptor-mediated presynaptic inhibition at the calyx of Held of immature rats. J Physiology 553, 415–426. https://doi.org/10.1113/jphysiol.2003.048371

King, A.E., Ackley, M.A., Cass, C.E., Young, J.D., Baldwin, S.A., 2006. Nucleoside transporters: from scavengers to novel therapeutic targets. Trends Pharmacol Sci 27, 416–425. https://doi.org/10.1016/j.tips.2006.06.004

Klein, P., Dingledine, R., Aronica, E., Bernard, C., Blümcke, I., Boison, D., Brodie, M.J., Brooks-Kayal, A.R., Engel, J., Forcelli, P.A., Hirsch, L.J., Kaminski, R.M., Klitgaard, H., Kobow, K., Lowenstein, D.H., Pearl, P.L., Pitkänen, A., Puhakka, N., Rogawski, M.A., Schmidt, D., Sillanpää, M., Sloviter, R.S., Steinhäuser, C., Vezzani, A., Walker, M.C.,

Löscher, W., 2018. Commonalities in epileptogenic processes from different acute brain insults: Do they translate? Epilepsia 59, 37–66. https://doi.org/10.1111/epi.13965

Kleinfeld, D., Deschênes, M., Wang, F., Moore, J.D., 2014a. More than a rhythm of life: breathing as a binder of orofacial sensation. Nat Neurosci 17, 647–651. https://doi.org/10.1038/nn.3693

Kleinfeld, D., Moore, J.D., Wang, F., Deschênes, M., 2014b. The Brainstem Oscillator for Whisking and the Case for Breathing as the Master Clock for Orofacial Motor Actions. Cold Spring Harb Sym 79, 29–39. https://doi.org/10.1101/sqb.2014.79.024794

Klyuch, B.P., Dale, N., Wall, M.J., 2012. Receptor-mediated modulation of activity-dependent adenosine release in rat cerebellum. Neuropharmacology 62, 815–824. https://doi.org/10.1016/j.neuropharm.2011.09.007

Klyuch, B.P., Richardson, M.J., Dale, N., Wall, M.J., 2011. The dynamics of single spike-evoked adenosine release in the cerebellum. J Physiology 589, 283–295. https://doi.org/10.1113/jphysiol.2010.198986

Kobayashi, K., Lemke, R.P., Greer, J.J., 2001. Ultrasound measurements of fetal breathing movements in the rat. J Appl Physiol 91, 316–20. https://doi.org/10.1152/jappl.2001.91.1.316

Koles, L., Furst, S., Illes, P., 2005. P2X and P2Y receptors as possible targets of therapeutic manipulations in CNS illnesses. Drug News Perspect 18, 85. https://doi.org/10.1358/dnp.2005.18.2.886479

Koos, B., Chau, A., 1998. Fetal cardiovascular and breathing responses to an adenosine A2a receptor agonist in sheep. The American journal of physiology 274, R152-9.

Koos, B., Maeda, T., Jan, C., 2001. Adenosine A(1) and A(2A) receptors modulate sleep state and breathing in fetal sheep. Journal of applied physiology (Bethesda, Md. : 1985) 91, 343–50.

Koos, B., Matsuda, K., 1990. Fetal breathing, sleep state, and cardiovascular responses to adenosine in sheep. J Appl Physiol 68, 489–495. https://doi.org/10.1152/jappl.1990.68.2.489

Koos, B.J., Chau, A., Matsuura, M., Punla, O., Kruger, L., 2000. Thalamic lesions dissociate breathing inhibition by hypoxia and adenosine in fetal sheep. Am J Physiology-regulatory Integr Comp Physiology 278, R831–R837. https://doi.org/10.1152/ajpregu.2000.278.4.r831

Koos, B.J., Chau, A., Matsuura, M., Punla, O., Kruger, L., 1998. Thalamic Locus Mediates Hypoxic Inhibition of Breathing in Fetal Sheep. J Neurophysiol 79, 2383–2393. https://doi.org/10.1152/jn.1998.79.5.2383

Koos, B.J., Kawasaki, Y., Kim, Y.-H., Bohorquez, F., 2004. Adenosine A2A-receptor blockade abolishes the roll-off respiratory response to hypoxia in awake lambs. American journal of

physiology. Regulatory, integrative and comparative physiology 288, R1185-94. https://doi.org/10.1152/ajpregu.00723.2004

Koos, B.J., Kruger, L., Murray, T.F., 1997. Source of extracellular brain adenosine during hypoxia in fetal sheep. Brain Res 778, 439–442. https://doi.org/10.1016/s0006-8993(97)01207-9

Koos, B.J., Maeda, T., 2001. Adenosine A2A receptors mediate cardiovascular responses to hypoxia in fetal sheep. Am J Physiol-heart C 280, H83–H89. https://doi.org/10.1152/ajpheart.2001.280.1.h83

Koos, B.J., Maeda, T., Jan, C., Lopez, G., 2002. Adenosine A2A receptors mediate hypoxic inhibition of fetal breathing in sheep. American Journal of Obstetrics and Gynecology 186, 663–668. https://doi.org/10.1067/mob.2002.122129

Koos, B.J., Mason, B.A., Punla, O., Adinolfi, A.M., 1994. Hypoxic inhibition of breathing in fetal sheep: relationship to brain adenosine concentrations. J Appl Physiol 77, 2734–9. https://doi.org/10.1152/jappl.1994.77.6.2734

Koos, B.J., Rajaee, A., Ibe, B., Guerra, C., Kruger, L., 2016. Thalamic mediation of hypoxic respiratory depression in lambs. American Journal of Physiology-Regulatory, Integrative and Comparative Physiology 310, R586–R595. https://doi.org/10.1152/ajpregu.00412.2015

Kooy, D. van der, Koda, L.Y., McGinty, J.F., Gerfen, C.R., Bloom, F.E., 1984. The organization of projections from the cortes, amygdala, and hypothalamus to the nucleus of the solitary tract in rat. J Comp Neurol 224, 1–24. https://doi.org/10.1002/cne.902240102

Kowaluk, E.A., Jarvis, M.F., 2000. Therapeutic potential of adenosine kinase inhibitors. Expert Opin Inv Drug 9, 551–564. https://doi.org/10.1517/13543784.9.3.551

Kugelgen, I. von, Wetter, A., 2000. Molecular pharmacology of P2Y-receptors. Naunyn-Schmiedeberg's Archives of Pharmacology 362. https://doi.org/10.1007/s002100000310

Kull, B., Svenningsson, P., Fredholm, B.B., 2000. Adenosine A2A Receptors are Colocalized with and Activate Golf in Rat Striatum. Mol Pharmacol 58, 771–777. https://doi.org/10.1124/mol.58.4.771

Lagercrantz, H., 1987. Neuromodulators and Respiratory Control in the Infant. Clin Perinatol 14, 683–695. https://doi.org/10.1016/s0095-5108(18)30757-7

Lagercrantz, H., Yamamoto, Y., Fredholm, B., Prabhakar, N., Euler, C. von, 1984. Adenosine Analogues Depress Ventilation in Rabbit Neonates. Theophylline Stimulation of Respiration via Adenosine Receptors? Pediatr Res 18, 387–390. https://doi.org/10.1203/00006450-198404000-00018

Lahiri, S., Mitchell, C.H., Reigada, D., Roy, A., Cherniack, N.S., 2007. Purines, the carotid body and respiration. Resp Physiol Neurobi 157, 123–129. https://doi.org/10.1016/j.resp.2007.02.015

Langer, D., Hammer, K., Koszalka, P., Schrader, J., Robson, S., Zimmermann, H., 2008. Distribution of ectonucleotidases in the rodent brain revisited. Cell and tissue research 334, 199–217. https://doi.org/10.1007/s00441-008-0681-x

Latini, S., Pedata, F., 2001. Adenosine in the central nervous system: release mechanisms and extracellular concentrations. J Neurochem 79, 463–484. https://doi.org/10.1046/j.1471-4159.2001.00607.x

Leabman, M.K., Huang, C.C., DeYoung, J., Carlson, E.J., Taylor, T.R., Cruz, M. de la, Johns, S.J., Stryke, D., Kawamoto, M., Urban, T.J., Kroetz, D.L., Ferrin, T.E., Clark, A.G., Risch, N., Herskowitz, I., Giacomini, K.M., Investigators¶¶, P. of M.T., 2003. Natural variation in human membrane transporter genes reveals evolutionary and functional constraints. Proc National Acad Sci 100, 5896–5901. https://doi.org/10.1073/pnas.0730857100

Lee, Y., Koay, E.J., Zhang, W., Qin, L., Kirui, D.K., Hussain, F., Shen, H., Ferrari, M., 2014. Human Equilibrative Nucleoside Transporter-1 Knockdown Tunes Cellular Mechanics through Epithelial-Mesenchymal Transition in Pancreatic Cancer Cells. Plos One 9, e107973. https://doi.org/10.1371/journal.pone.0107973

Leonard, E.M., Salman, S., Nurse, C.A., 2018. Sensory Processing and Integration at the Carotid Body Tripartite Synapse: Neurotransmitter Functions and Effects of Chronic Hypoxia. Front Physiol 9, 225. https://doi.org/10.3389/fphys.2018.00225

Leung, R.S., Bradley, D.T., 2001. Sleep Apnea and Cardiovascular Disease. Am J Resp Crit Care 164, 2147–2165. https://doi.org/10.1164/ajrccm.164.12.2107045

Li, B., Gu, L., Hertz, L., Peng, L., 2013. Expression of nucleoside transporter in freshly isolated neurons and astrocytes from mouse brain. Neurochemical research 38, 2351–8. https://doi.org/10.1007/s11064-013-1146-5

Li, P., Janczewski, W.A., Yackle, K., Kam, K., Pagliardini, S., Krasnow, M.A., Feldman, J.L., 2016. The peptidergic control circuit for sighing. Nature 530, 293–297. https://doi.org/10.1038/nature16964

Li, T., Lan, J.Q., Fredholm, B.B., Simon, R.P., Boison, D., 2007. Adenosine dysfunction in astrogliosis: cause for seizure generation? Neuron Glia Biol 3, 353–366. https://doi.org/10.1017/s1740925x0800015x

Li, T., Ren, G., Lusardi, T., Wilz, A., Lan, J.Q., Iwasato, T., Itohara, S., Simon, R.P., Boison, D., 2008. Adenosine kinase is a target for the prediction and prevention of epileptogenesis in mice. J Clin Invest 118, 571–582. https://doi.org/10.1172/jci33737

Lietsche, J., Imran, I., Klein, J., 2016. Extracellular levels of ATP and acetylcholine during lithium-pilocarpine induced status epilepticus in rats. Neurosci Lett 611, 69–73. https://doi.org/10.1016/j.neulet.2015.11.028

Linden, J., 1991. Structure and function of A1 adenosine receptors1. Faseb J 5, 2668–2676. https://doi.org/10.1096/fasebj.5.12.1916091

Linden, J., Tucker, A.L., Lynch, K.R., 1991. Molecular cloning of adenosine A1 and A2 receptors. Trends Pharmacol Sci 12, 326–328. https://doi.org/10.1016/0165-6147(91)90589-k

Liu, G., Feldman, J., neurophysiology, S.-J. of, 1990. Excitatory amino acid-mediated transmission of inspiratory drive to phrenic motoneurons. https://doi.org/10.1152/jn.1990.64.2.423

Liu, Q., Fehring, C., Lowry, T.F., Wong-Riley, M.T.T., 2009. Postnatal development of metabolic rate during normoxia and acute hypoxia in rats: implication for a sensitive period. J Appl Physiol 106, 1212–1222. https://doi.org/10.1152/japplphysiol.90949.2008

Liu, Q., Lowry, T.F., Wong-Riley, M.T.T., 2006. Postnatal changes in ventilation during normoxia and acute hypoxia in the rat: implication for a sensitive period. J Physiology 577, 957–970. https://doi.org/10.1113/jphysiol.2006.121970

Liu, Q., Wong-Riley, M., 2013. Gender considerations in ventilatory and metabolic development in rats: Special emphasis on the critical period. Respiratory Physiology & Neurobiology 188, 200–207. https://doi.org/10.1016/j.resp.2013.06.013

Liu, Q., Wong-Riley, M.T.T., 2002. Postnatal expression of neurotransmitters, receptors, and cytochrome oxidase in the rat pre-Bötzinger complex. J Appl Physiol 92, 923–934. https://doi.org/10.1152/japplphysiol.00977.2001

Liu, Y., Chen, J., Li, X., Zhou, X., Hu, Y., Chu, S., Peng, Y., Chen, N., 2019. Research progress on adenosine in central nervous system diseases. Cns Neurosci Ther 25, 899–910. https://doi.org/10.1111/cns.13190

Lloyd, H.G.E., Fredholm, B.B., 1995. Involvement of adenosine deaminase and adenosine kinase in regulating extracellular adenosine concentration in rat hippocampal slices. Neurochem Int 26, 387–395. https://doi.org/10.1016/0197-0186(94)00144-j

Lloyd, H.G.E., Lindström, K., Fredholm, B.B., 1993. Intracellular formation and release of adenosine from rat hippocampal slices evoked by electrical stimulation or energy depletion. Neurochem Int 23, 173–185. https://doi.org/10.1016/0197-0186(93)90095-m

Lopes, J.P., Pliássova, A., Cunha, R.A., 2019. The physiological effects of caffeine on synaptic transmission and plasticity in the mouse hippocampus selectively depend on adenosine A1 and A2A receptors. Biochem Pharmacol 166, 313–321. https://doi.org/10.1016/j.bcp.2019.06.008

Lopes, L.V., Cunha, R.A., Kull, B., Fredholm, B.B., Ribeiro, J.A., 2002. Adenosine A2A receptor facilitation of hippocampal synaptic transmission is dependent on tonic A1 receptor inhibition. Neuroscience 112, 319–329. https://doi.org/10.1016/s0306-4522(02)00080-5

Lopes, L.V., Cunha, R.A., Ribeiro, J., 1999. Cross Talk Between A1 and A2A Adenosine Receptors in the Hippocampus and Cortex of Young Adult and Old Rats. J Neurophysiol 82, 3196–3203. https://doi.org/10.1152/jn.1999.82.6.3196

Lopes, L.V., Rebola, N., Pinheiro, P.C., Richardson, P.J., Oliveira, C.R., Cunha, R.A., 2003. Adenosine A3 receptors are located in neurons of the rat hippocampus. Neuroreport 14, 1645–1648. https://doi.org/10.1097/00001756-200308260-00021

Lorier, A., Huxtable, A., Robinson, D., Lipski, J., Housley, G., Funk, G., 2007. P2Y1 receptor modulation of the pre-Botzinger complex inspiratory rhythm generating network in vitro. Journal of Neuroscience 27. https://doi.org/10.1523/JNEUROSCI.3948-06.2007

Lorier, A., Lipski, J., Housley, G., Greer, J., Funk, G., 2008. ATP sensitivity of preBotzinger complex neurones in neonatal rat in vitro: mechanism underlying a P2 receptor-mediated increase in inspiratory frequency. The Journal of Physiology 586. https://doi.org/10.1113/jphysiol.2007.143024

Lu, H., Chen, C., Klaassen, C., 2004. Tissue Distribution of Concentrative and Equilibrative Nucleoside Transporters in Male and Female Rats and Mice. Drug Metab Dispos 32, 1455–1461. https://doi.org/10.1124/dmd.104.001123

Mackiewicz, M., Nikonova, E.V., Zimmerman, J.E., Galante, R.J., Zhang, L., Cater, J.R., Geiger, J.D., Pack, A.I., 2003. Enzymes of adenosine metabolism in the brain: diurnal rhythm and the effect of sleep deprivation. J Neurochem 85, 348–357. https://doi.org/10.1046/j.1471-4159.2003.01687.x

MacMillan, S., Evans, M.A., 2023. AMPK facilitates the hypoxic ventilatory response through non-adrenergic mechanisms at the brainstem. Pflügers Archiv - European Journal of Physiology 475, 89–99. https://doi.org/10.1007/s00424-022-02713-8

Mahan, L.C., McVittie, L.D., Smyk-Randall, E.M., Nakata, H., Monsma, F.J., Gerfen, C.R., Sibley, D.R., 1991. Cloning and expression of an A1 adenosine receptor from rat brain. Mol Pharmacol 40, 1–7.

Mahmoud, A.D., Lewis, S., Juričić, L., Udoh, U.-A., Hartmann, S., Jansen, M.A., Ogunbayo, O.A., Puggioni, P., Holmes, A.P., Kumar, P., Navarro-Dorado, J., Foretz, M., Viollet, B., Dutia, M.B., Marshall, I., Evans, A.M., 2016. AMP-activated Protein Kinase Deficiency Blocks the Hypoxic Ventilatory Response and Thus Precipitates Hypoventilation and Apnea. American Journal of Respiratory and Critical Care Medicine 193, 1032–1043. https://doi.org/10.1164/rccm.201508-1667OC

Marina, N., Turovsky, E., Christie, I.N., Hosford, P.S., Hadjihambi, A., Korsak, A., Ang, R., Mastitskaya, S., Sheikhbahaei, S., Theparambil, S.M., Gourine, A.V., 2018. Brain metabolic sensing and metabolic signaling at the level of an astrocyte. Glia 66, 1185–1199. https://doi.org/10.1002/glia.23283

Martín, E.D., Fernández, M., Perea, G., Pascual, O., Haydon, P.G., Araque, A., Ceña, V., 2007. Adenosine released by astrocytes contributes to hypoxia-induced modulation of synaptic transmission. Glia 55, 36–45. https://doi.org/10.1002/glia.20431

Martin, R.J., Abu-Shaweesh, J.M., 2005. Control of breathing and neonatal apnea. Biology of the neonate 87, 288–95. https://doi.org/10.1159/000084876

Martin-Body, R.L., Robson, G.J., Sinclair, J.D., 1985. Respiratory effects of sectioning the carotid sinus glossopharyngeal and abdominal vagal nerves in the awake rat. The Journal of physiology 361, 35–45. https://doi.org/10.1113/jphysiol.1985.sp015631

Mathew, O.P., 2011. Apnea of prematurity: pathogenesis and management strategies. Journal of perinatology : official journal of the California Perinatal Association 31, 302–10. https://doi.org/10.1038/jp.2010.126

Matsuoka, T., Saiki, C., Mortola, J.P., 1994. Metabolic and ventilatory responses to anemic hypoxia in conscious rats. J Appl Physiol 77, 1067–1072. https://doi.org/10.1152/jappl.1994.77.3.1067

Matti, S., Shlomo, S., 2010. Long-Term Mortality in Childhood-Onset Epilepsy. New Engl J Med 363, 2522–2529. https://doi.org/10.1056/nejmoa0911610

Matyash, M., Zabiegalov, O., Wendt, S., Matyash, V., Kettenmann, H., 2017. The adenosine generating enzymes CD39/CD73 control microglial processes ramification in the mouse brain. Plos One 12, e0175012. https://doi.org/10.1371/journal.pone.0175012

Mayer, C.A., Haxhiu, M.A., Martin, R.J., Wilson, C.G., 2006. Adenosine A2A receptors mediate GABAergic inhibition of respiration in immature rats. Journal of applied physiology (Bethesda, Md. : 1985) 100, 91–7. https://doi.org/10.1152/japplphysiol.00459.2005

McPherson, C., Neil, J.J., Tjoeng, T., Pineda, R., Inder, T.E., 2015. A pilot randomized trial of high-dose caffeine therapy in preterm infants. Pediatr Res 78, 198–204. https://doi.org/10.1038/pr.2015.72

Meghji, P., Tuttle, J.B., Rubio, R., 1989. Adenosine Formation and Release by Embryonic Chick Neurons and Glia in Cell Culture. J Neurochem 53, 1852–1860. https://doi.org/10.1111/j.1471-4159.1989.tb09252.x

Mendonça, A. de, Sebastião, A.M., Ribeiro, A.J., 1995. Inhibition of NMDA receptor-mediated currents in isolated rat hippocampal neurones by adenosine A1 receptor activation. Neuroreport 6, 1097–1100. https://doi.org/10.1097/00001756-199505300-00006

Miller, S.R., Hau, R.K., Jilek, J.L., Morales, M.N., Wright, S.H., Cherrington, N.J., 2020. Nucleoside Reverse Transcriptase Inhibitor (NRTI) Interaction with Human Equilibrative Nucleoside Transporters 1 and 2. Drug Metab Dispos 48, dmd.120.090720. https://doi.org/10.1124/dmd.120.090720

Mironov, S.L., Langohr, K., 2007. Modulation of synaptic and channel activities in the respiratory network of the mice by NO/cGMP signalling pathways. Brain Res 1130, 73–82. https://doi.org/10.1016/j.brainres.2006.09.114

Mironov, S.L., Langohr, K., Richter, D.W., 1999. A1 adenosine receptors modulate respiratory activity of the neonatal mouse via the cAMP-mediated signaling pathway. Journal of neurophysiology 81, 247–55. https://doi.org/10.1152/jn.1999.81.1.247

Mitchell, L., MacFarlane, P.M., 2019. Mechanistic actions of oxygen and methylxanthines on respiratory neural control and for the treatment of neonatal apnea. Respiratory physiology & neurobiology 273, 103318. https://doi.org/10.1016/j.resp.2019.103318

Montandon, G., Horner, R.L., Kinkead, R., Bairam, A., 2009. Caffeine in the neonatal period induces long-lasting changes in sleep and breathing in adult rats. J Physiology 587, 5493–5507. https://doi.org/10.1113/jphysiol.2009.171918

Moore, R.E., Underwood, M.C., 1963. The thermogenic effects of noradrenaline in new-born and infant kittens and other small mammals. A possible hormonal mechanism in the control of heat production. J Physiology 168, 290–317. https://doi.org/10.1113/jphysiol.1963.sp007193

Mortola, J., 1999. How newborn mammals cope with hypoxia. Respiration physiology 116. https://doi.org/10.1016/s0034-5687(99)00038-9

Mortola, J., Dotta, A., 1992. Effects of hypoxia and ambient temperature on gaseous metabolism of newborn rats. The American journal of physiology 263, R267-72.

Mortola, J., Morgan, C., Virgona, V., 1986. Respiratory adaptation to chronic hypoxia in newborn rats. J Appl Physiol 61, 1329–1336. https://doi.org/10.1152/jappl.1986.61.4.1329

Mortola, J.P., 2004. Implications of hypoxic hypometabolism during mammalian ontogenesis. Resp Physiol Neurobi 141, 345–356. https://doi.org/10.1016/j.resp.2004.01.011

Mortola, J.P., 1996. Ventilatory Responses to Hypoxia in Mammals, in: Haddad, G.G., Lister, G. (Eds.), Tissue Oxygen Deprivation. CRC Press, New York, pp. 433–477.

Mortola, J.P., Frappell, P.B., 2013. Measurements of air ventilation in small vertebrates. Resp Physiol Neurobi 186, 197–205. https://doi.org/10.1016/j.resp.2013.02.001

Mortola, J.P., Rezzonico, R., Lanthier, C., 1989. Ventilation and oxygen consumption during acute hypoxia in newborn mammals: a comparative analysis. Resp Physiol 78, 31–43. https://doi.org/10.1016/0034-5687(89)90140-0

Moss, I., 2000. Respiratory responses to single and episodic hypoxia during development: mechanisms of adaptation. Respiration physiology 121.

Moss, I., Inman, J., 1989. Neurochemicals and respiratory control during development. J Appl Physiol 67, 1–13. https://doi.org/10.1152/jappl.1989.67.1.1

Mouro, F.M., Rombo, D.M., Dias, R.B., Ribeiro, J.A., Sebastião, A.M., 2018. Adenosine A2A receptors facilitate synaptic NMDA currents in CA1 pyramidal neurons. Brit J Pharmacol 175, 4386–4397. https://doi.org/10.1111/bph.14497

Mulkey, D.K., Henderson, R.A., Olson, J.E., Putnam, R.W., Dean, J.B., 2001. Oxygen measurements in brain stem slices exposed to normobaric hyperoxia and hyperbaric oxygen. J Appl Physiol 90, 1887–1899. https://doi.org/10.1152/jappl.2001.90.5.1887

Nagai, K., Nagasawa, K., Fujimoto, S., 2005. Transport mechanisms for adenosine and uridine in primary-cultured rat cortical neurons and astrocytes. Biochem Bioph Res Co 334, 1343–1350. https://doi.org/10.1016/j.bbrc.2005.07.032

Neubauer, J., Melton, J., Edelman, N., 1990. Modulation of respiration during brain hypoxia. J Appl Physiol 68, 441–451. https://doi.org/10.1152/jappl.1990.68.2.441

Nguyen, M.D., Ross, A.E., Ryals, M., Lee, S.T., Venton, B.J., 2015. Clearance of rapid adenosine release is regulated by nucleoside transporters and metabolism. Pharmacology research & perspectives 3, e00189. https://doi.org/10.1002/prp2.189

Nicholson, C., 1985. Diffusion from an injected volume of a substance in brain tissue with arbitrary volume fraction and tortuosity. Brain research 333, 325–9. https://doi.org/10.1016/0006-8993(85)91586-0

Novak, C.M., Ozen, M., Burd, I., 2018. Perinatal Brain Injury Mechanisms, Prevention, and Outcomes. Clin Perinatol 45, 357–375. https://doi.org/10.1016/j.clp.2018.01.015

Nurse, C.A., Leonard, E.M., Salman, S., 2018. Role of glial-like type II cells as paracrine modulators of carotid body chemoreception. Physiol Genomics 50, 255–262. https://doi.org/10.1152/physiolgenomics.00142.2017

Nurse, C.A., Piskuric, N.A., 2013. Signal processing at mammalian carotid body chemoreceptors. Seminars in cell & developmental biology 24, 22–30. https://doi.org/10.1016/j.semcdb.2012.09.006

Osato, D.H., Huang, C.C., Kawamoto, M., Johns, S.J., Stryke, D., Wang, J., Ferrin, T.E., Herskowitz, I., Giacomini, K.M., 2003. Functional characterization in yeast of genetic

variants in the human equilibrative nucleoside transporter, ENT1. Pharmacogenetics 13, 297–301. https://doi.org/10.1097/00008571-200305000-00010

Otsuguro, K., Tomonari, Y., Otsuka, S., Yamaguchi, S., Kon, Y., Ito, S., 2015. An adenosine kinase inhibitor, ABT-702, inhibits spinal nociceptive transmission by adenosine release via equilibrative nucleoside transporters in rat. Neuropharmacology 97, 160–170. https://doi.org/10.1016/j.neuropharm.2015.05.035

Otsuguro, K., Wada, M., Ito, S., 2011. Differential contributions of adenosine to hypoxia-evoked depressions of three neuronal pathways in isolated spinal cord of neonatal rats. Brit J Pharmacol 164, 132–144. https://doi.org/10.1111/j.1476-5381.2011.01333.x

Owen, R.P., Lagpacan, L.L., Taylor, T.R., Cruz, M., Huang, C.C., Kawamoto, M., Johns, S.J., Stryke, D., Ferrin, T.E., Giacomini, K.M., 2006. Functional Characterization And Haplotype Analysis of Polymorphisms in the Human Equilibrative Nucleoside Transporter, ENT2. Drug Metab Dispos 34, 12–15. https://doi.org/10.1124/dmd.105.006270

Pak, M.A., Haas, H.L., Decking, U.K.M., Schrader, J., 1994. Inhibition of adenosine kinase increases endogenous adenosine and depresses neuronal activity in hippocampal slices. Neuropharmacology 33, 1049–1053. https://doi.org/10.1016/0028-3908(94)90142-2

Palmer, L.A., May, W.J., deRonde, K., Brown-Steinke, K., Gaston, B., Lewis, S.J., 2013. Hypoxia-induced ventilatory responses in conscious mice: Gender differences in ventilatory roll-off and facilitation. Resp Physiol Neurobi 185, 497–505. https://doi.org/10.1016/j.resp.2012.11.010

Pamenter, M.E., Dzal, Y.A., Milsom, W.K., 2015. Adenosine receptors mediate the hypoxic ventilatory response but not the hypoxic metabolic response in the naked mole rat during acute hypoxia. Proceedings. Biological sciences 282, 20141722. https://doi.org/10.1098/rspb.2014.1722

Paolillo, P., Picone, S., 2013. Apnea of Prematurity. J Pediatric Neonatal Individ Medicine Jpnim 2. https://doi.org/10.7363/020213

Parkinson, F.E., Damaraju, V.L., Graham, K., Yao, S.Y., Baldwin, S.A., Cass, C.E., Young, J.D., 2011. Molecular Biology of Nucleoside Transporters and their Distributions and Functions in the Brain. Curr Top Med Chem 11, 948–972. https://doi.org/10.2174/156802611795347582

Parkinson, F.E., Xiong, W., Zamzow, C.R., 2005. Astrocytes and neurons: different roles in regulating adenosine levels. Neurological research 27, 153–60. https://doi.org/10.1179/016164105X21878

Pascual, O., Casper, K.B., Kubera, C., Zhang, J., Revilla-Sanchez, R., Sul, J.-Y., Takano, H., Moss, S.J., McCarthy, K., Haydon, P.G., 2005. Astrocytic Purinergic Signaling Coordinates Synaptic Networks. Science 310, 113–116. https://doi.org/10.1126/science.1116916

Patodia, S., Somani, A., O'Hare, M., Venkateswaran, R., Liu, J., Michalak, Z., Ellis, M., Scheffer, I.E., Diehl, B., Sisodiya, S.M., Thom, M., 2018. The ventrolateral medulla and medullary raphe in sudden unexpected death in epilepsy. Brain : a journal of neurology 141, 1719–1733. https://doi.org/10.1093/brain/awy078

Pearson, T., Currie, A.J., Etherington, L.V., Gadalla, A.E., Damian, K., Llaudet, E., Dale, N., Frenguelli, B., 2003. Plasticity of purine release during cerebral ischemia: clinical implications? J Cell Mol Med 7, 362–375. https://doi.org/10.1111/j.1582-4934.2003.tb00239.x

Pedata, F., Corsi, C., Melani, A., Bordoni, F., Latini, S., 2001. Adenosine Extracellular Brain Concentrations and Role of A2A Receptors in Ischemia. Ann Ny Acad Sci 939, 74–84. https://doi.org/10.1111/j.1749-6632.2001.tb03614.x

Peyronnet, J., Roux, J.C., Géloën, A., Tang, L.Q., Pequignot, J.M., Lagercrantz, H., Dalmaz, Y., 2000. Prenatal hypoxia impairs the postnatal development of neural and functional chemoafferent pathway in rat. J Physiology 524, 525–537. https://doi.org/10.1111/j.1469-7793.2000.00525.x

Picardo, M.D., Sugimura, Y.K., Dorst, K.E., Kallurkar, P.S., Akins, V.T., Ma, X., Teruyama, R., Guinamard, R., Kam, K., Saha, M.S., Del Negro, C.A., 2019. Trpm4 ion channels in pre-Bötzinger complex interneurons are essential for breathing motor pattern but not rhythm. PLOS Biology 17, e2006094. https://doi.org/10.1371/journal.pbio.2006094

Presti, M.F., Schmeichel, A.M., Low, P.A., Parisi, J.E., Benarroch, E.E., 2014. Degeneration of Brainstem Respiratory Neurons in Dementia with Lewy Bodies. Sleep 37, 373–378. https://doi.org/10.5665/sleep.3418

Psarropoulou, C., Kostopoulos, G., Haas, H.L., 1990. An electrophysiological study of the ontogenesis of adenosine receptors in the CA1 area of rat hippocampus. Dev Brain Res 55, 147–150. https://doi.org/10.1016/0165-3806(90)90116-g

Punjabi, N.M., 2008. The Epidemiology of Adult Obstructive Sleep Apnea. Proc Am Thorac Soc 5, 136–143. https://doi.org/10.1513/pats.200709-155mg

Rajani, V., Zhang, Y., Jalubula, V., Rancic, V., SheikhBahaei, S., Zwicker, J.D., Pagliardini, S., Dickson, C.T., Ballanyi, K., Kasparov, S., Gourine, A.V., Funk, G.D., 2017. Release of ATP by pre-Bötzinger complex astrocytes contributes to the hypoxic ventilatory response via a Ca2+ -dependent P2Y1 receptor mechanism. The Journal of physiology 596, 3245–3269. https://doi.org/10.1113/JP274727

Rajani, V., Zhang, Y., Revill, A.L., Funk, G.D., 2016. The role of P2Y1 receptor signaling in central respiratory control. Respiratory physiology & neurobiology 226, 3–10. https://doi.org/10.1016/j.resp.2015.10.003

Rau, A.R., Ariwodola, O.J., Weiner, J.L., 2015. Postsynaptic Adenosine A2A Receptors Modulate Intrinsic Excitability of Pyramidal Cells in the Rat Basolateral Amygdala. Int J Neuropsychoph 18, pyv017. https://doi.org/10.1093/ijnp/pyv017

Rebola, N., Canas, P.M., Oliveira, C.R., Cunha, R.A., 2005. Different synaptic and subsynaptic localization of adenosine A2A receptors in the hippocampus and striatum of the rat. Neuroscience 132, 893–903. https://doi.org/10.1016/j.neuroscience.2005.01.014

Rebola, N., Lujan, R., Cunha, R.A., Mulle, C., 2008. Adenosine A2A Receptors Are Essential for Long-Term Potentiation of NMDA-EPSCs at Hippocampal Mossy Fiber Synapses. Neuron 57, 121–134. https://doi.org/10.1016/j.neuron.2007.11.023

Rebola, N., Pinheiro, P.C., Oliveira, C.R., Malva, J.O., Cunha, R.A., 2003. Subcellular localization of adenosine A1 receptors in nerve terminals and synapses of the rat hippocampus. Brain Res 987, 49–58. https://doi.org/10.1016/s0006-8993(03)03247-5

Reklow, R.J., Alvares, T.S., Zhang, Y., Tapia, A.P.M., Biancardi, V., Katzell, A.K., Frangos, S.M., Hansen, M.A., Toohey, A.W., Cass, C.E., Young, J.D., Pagliardini, S., Boison, D., Funk, G.D., 2019. The Purinome and the preBötzinger Complex - A Ménage of Unexplored Mechanisms That May Modulate/Shape the Hypoxic Ventilatory Response. Frontiers in cellular neuroscience 13, 365. https://doi.org/10.3389/fncel.2019.00365

Reppert, S.M., Weaver, D.R., Stehle, J.H., Rivkees, S.A., 1991. Molecular Cloning and Characterization of a Rat A1-Adenosine Receptor that is Widely Expressed in Brain and Spinal Cord. Mol Endocrinol 5, 1037–1048. https://doi.org/10.1210/mend-5-8-1037

Richerson, G.B., Boison, D., Faingold, C.L., Ryvlin, P., 2016. From unwitnessed fatality to witnessed rescue: Pharmacologic intervention in sudden unexpected death in epilepsy. Epilepsia 57, 35–45. https://doi.org/10.1111/epi.13236

Richter, D.W., Schmidt-Garcon, P., Pierrefiche, O., Bischoff, A.M., Lalley, P.M., 1999. Neurotransmitters and neuromodulators controlling the hypoxic respiratory response in anaesthetized cats. J Physiology 514, 567–578. https://doi.org/10.1111/j.1469-7793.1999.567ae.x

Roberts, B.M., Lambert, E., Livesey, J.A., Wu, Z., Li, Y., Cragg, S.J., 2022. Dopamine Release in Nucleus Accumbens Is under Tonic Inhibition by Adenosine A 1 Receptors Regulated by Astrocytic ENT1 and Dysregulated by Ethanol. J Neurosci 42, 1738–1751. https://doi.org/10.1523/jneurosci.1548-21.2021

Robinson, D.M., Kwok, H., Adams, B.M., Peebles, K.C., Funk, G.D., 2000. Development of the ventilatory response to hypoxia in Swiss CD-1 mice. Journal of applied physiology (Bethesda, Md. : 1985) 88, 1907–14. https://doi.org/10.1152/jappl.2000.88.5.1907

Robinson, D.M., Peebles, K.C., Kwok, H., Adams, B.M., Clarke, L., Woollard, G.A., Funk, G.D., 2002. Prenatal nicotine exposure increases apnoea and reduces nicotinic potentiation of

hypoglossal inspiratory output in mice. J Physiology 538, 957–973. https://doi.org/10.1113/jphysiol.2001.012705

Robson, S.C., Sévigny, J., Zimmermann, H., 2006. The E-NTPDase family of ectonucleotidases: Structure function relationships and pathophysiological significance. Purinergic signalling 2, 409–30. https://doi.org/10.1007/s11302-006-9003-5

Rodrigues, R.J., Almeida, T., Richardson, P.J., Oliveira, C.R., Cunha, R.A., 2005. Dual Presynaptic Control by ATP of Glutamate Release via Facilitatory P2X1, P2X2/3, and P2X3 and Inhibitory P2Y1, P2Y2, and/or P2Y4 Receptors in the Rat Hippocampus. J Neurosci 25, 6286–6295. https://doi.org/10.1523/jneurosci.0628-05.2005

Roh, E., Kim, M.-S., 2016. Brain Regulation of Energy Metabolism. Endocrinol Metab 31, 519–524. https://doi.org/10.3803/enm.2016.31.4.519

Rohlicek, C., Saiki, C., Matsuoka, T., Mortola, J., 1996. Cardiovascular and Respiratory Consequences of Body Warming during Hypoxia in Conscious Newborn Cats. Pediatr Res 40, 1–5. https://doi.org/10.1203/00006450-199607000-00001

Rohlicek, C.V., Saiki, C., Matsuoka, T., Mortola, J.P., 1998. Oxygen transport in conscious newborn dogs during hypoxic hypometabolism. J Appl Physiol 84, 763–8. https://doi.org/10.1152/jappl.1998.84.3.763

Rosin, D.L., Robeva, A., Woodard, R.L., Guyenet, P.G., Linden, J., 1998. Immunohistochemical localization of adenosine A2A receptors in the rat central nervous system. The Journal of comparative neurology 401, 163–86.

Ruangkittisakul, A., Panaitescu, B., Ballanyi, K., 2011. K+ and Ca2+ dependence of inspiratory-related rhythm in novel "calibrated" mouse brainstem slices. Resp Physiol Neurobi 175, 37–48. https://doi.org/10.1016/j.resp.2010.09.004

Runold, M., Lagercrantz, H., Fredholm, B.B., 1986. Ventilatory effect of an adenosine analogue in unanesthetized rabbits during development. J Appl Physiol 61, 255–259. https://doi.org/10.1152/jappl.1986.61.1.255

Runold, M., Lagercrantz, H., Prabhakar, N.R., Fredholm, B.B., 1989. Role of adenosine in hypoxic ventilatory depression. Journal of applied physiology (Bethesda, Md. : 1985) 67, 541–6. https://doi.org/10.1152/jappl.1989.67.2.541

Rytkönen, K.-M., Wigren, H.-K., Kostin, A., Porkka-Heiskanen, T., Kalinchuk, A.V., 2010. Nitric oxide mediated recovery sleep is attenuated with aging. Neurobiol Aging 31, 2011–2019. https://doi.org/10.1016/j.neurobiolaging.2008.10.006

Ryvlin, P., Nashef, L., Lhatoo, S.D., Bateman, L.M., Bird, J., Bleasel, A., Boon, P., Crespel, A., Dworetzky, B.A., Høgenhaven, H., Lerche, H., Maillard, L., Malter, M.P., Marchal, C., Murthy, J.M., Nitsche, M., Pataraia, E., Rabben, T., Rheims, S., Sadzot, B., Schulze-

Bonhage, A., Seyal, M., So, E.L., Spitz, M., Szucs, A., Tan, M., Tao, J.X., Tomson, T., 2013. Incidence and mechanisms of cardiorespiratory arrests in epilepsy monitoring units (MORTEMUS): a retrospective study. The Lancet Neurology 12, 966–977. https://doi.org/10.1016/S1474-4422(13)70214-X

Sacramento, J.F., Olea, E., Ribeiro, M.J., Prieto-Lloret, J., Melo, B.F., Gonzalez, C., Martins, F.O., Monteiro, E.C., Conde, S.V., 2019. Contribution of adenosine and ATP to the carotid body chemosensory activity in ageing. J Physiology 597, 4991–5008. https://doi.org/10.1113/jp274179

Saiki, C., Matsuoka, T., Mortola, J.P., 1994. Metabolic-ventilatory interaction in conscious rats: effect of hypoxia and ambient temperature. J Appl Physiol 76, 1594–9. https://doi.org/10.1152/jappl.1994.76.4.1594

Sak, K., Illes, P., 2005. Neuronal and glial cell lines as model systems for studying P2Y receptor pharmacology. Neurochem Int 47, 401–412. https://doi.org/10.1016/j.neuint.2005.05.012

Sandau, U.S., Colino-Oliveira, M., Jones, A., Saleumvong, B., Coffman, S.Q., Liu, L., Miranda-Lourenço, C., Palminha, C., Batalha, V.L.L., Xu, Y., Huo, Y., Diógenes, M.J., Sebastião, A.M., Boison, D., 2016. Adenosine Kinase Deficiency in the Brain Results in Maladaptive Synaptic Plasticity. The Journal of neuroscience : the official journal of the Society for Neuroscience 36, 12117–12128. https://doi.org/10.1523/JNEUROSCI.2146-16.2016

Scanziani, M., Capogna, M., Gähwiler, B.H., Thompson, S.M., 1992. Presynaptic inhibition of miniature excitatory synaptic currents by baclofen and adenosine in the hippocampus. Neuron 9, 919–927. https://doi.org/10.1016/0896-6273(92)90244-8

Schmidt, B., Anderson, P.J., Doyle, L.W., Dewey, D., Grunau, R.E., Asztalos, E.V., Davis, P.G., Tin, W., Moddemann, D., Solimano, A., Ohlsson, A., Barrington, K.J., Roberts, R.S., Investigators, C. for A. of P. (CAP) T., 2012. Survival without disability to age 5 years after neonatal caffeine therapy for apnea of prematurity. JAMA 307, 275–82. https://doi.org/10.1001/jama.2011.2024

Schmidt, B., Roberts, R.S., Davis, P., Doyle, L.W., Barrington, K.J., Ohlsson, A., Solimano, A., Tin, W., Group, C. for A. of P.T., 2007. Long-Term Effects of Caffeine Therapy for Apnea of Prematurity. New Engl J Medicine 357, 1893–1902. https://doi.org/10.1056/nejmoa073679

Schmidt, C., Bellingham, M.C., Richter, D.W., 1995. Adenosinergic modulation of respiratory neurones and hypoxic responses in the anaesthetized cat. J Physiology 483, 769–781. https://doi.org/10.1113/jphysiol.1995.sp020621

Scholz, K.P., Miller, R.J., 1992. Inhibition of quantal transmitter release in the absence of calcium influx by a G protein-linked adenosine receptor at hippocampal synapses. Neuron 8, 1139–1150. https://doi.org/10.1016/0896-6273(92)90134-y

Schulte, G., Fredholm, B.B., 2003. Signalling from adenosine receptors to mitogen-activated protein kinases. Cell Signal 15, 813–827. https://doi.org/10.1016/s0898-6568(03)00058-5

Schurr, A., Miller, J.J., Payne, R.S., Rigor, B.M., 1999. An increase in lactate output by brain tissue serves to meet the energy needs of glutamate-activated neurons. J Neurosci Official J Soc Neurosci 19, 34–9.

Schwarzacher, S., Rüb, U., Brain, D.-T., 2011. Neuroanatomical characteristics of the human pre-Bötzinger complex and its involvement in neurodegenerative brainstem diseases. https://doi.org/10.1093/brain/awq327

Sebastião, A.M., Ribeiro, J.A., 2009. Adenosine Receptors in Health and Disease. Handb Exp Pharmacol 471–534. https://doi.org/10.1007/978-3-540-89615-9_16

Semple, B.D., Blomgren, K., Gimlin, K., Ferriero, D.M., Noble-Haeusslein, L.J., 2013. Brain development in rodents and humans: Identifying benchmarks of maturation and vulnerability to injury across species. Progress in neurobiology 106–107, 1–16. https://doi.org/10.1016/j.pneurobio.2013.04.001

Serra, A., Brozoski, D., Hedin, N., Franciosi, R., Forster, H.V., 2001. Mortality after carotid body denervation in rats. Journal of applied physiology (Bethesda, Md. : 1985) 91, 1298–306. https://doi.org/10.1152/jappl.2001.91.3.1298

Shao, X.M., Ge, Q., Feldman, J.L., 2003. Modulation of AMPA receptors by cAMP-dependent protein kinase in PreBötzinger complex inspiratory neurons regulates respiratory rhythm in the rat. J Physiology 547, 543–553. https://doi.org/10.1113/jphysiol.2002.031005

Sheikhbahaei, S., Turovsky, E.A., Hosford, P.S., Hadjihambi, A., Theparambil, S.M., Liu, B., Marina, N., Teschemacher, A.G., Kasparov, S., Smith, J.C., Gourine, A.V., 2018. Astrocytes modulate brainstem respiratory rhythm-generating circuits and determine exercise capacity. Nature communications 9, 370. https://doi.org/10.1038/s41467-017-02723-6

Shen, H., Li, T., Boison, D., 2010. A novel mouse model for sudden unexpected death in epilepsy (SUDEP): Role of impaired adenosine clearance. Epilepsia 51, 465–468. https://doi.org/10.1111/j.1528-1167.2009.02248.x

Shen, H.-Y., Baer, S.B., Gesese, R., Cook, J.M., Weltha, L., Coffman, S.Q., Wu, J., Chen, J.-F., Gao, M., Ji, T., 2022. Adenosine-A2A Receptor Signaling Plays a Crucial Role in Sudden Unexpected Death in Epilepsy. Front Pharmacol 13, 910535. https://doi.org/10.3389/fphar.2022.910535

Shen, H.-Y.Y., Lusardi, T.A., Williams-Karnesky, R.L., Lan, J.-Q.Q., Poulsen, D.J., Boison, D., 2011. Adenosine kinase determines the degree of brain injury after ischemic stroke in mice. Journal of cerebral blood flow and metabolism: official journal of the International Society of Cerebral Blood Flow and Metabolism 31, 1648–59. https://doi.org/10.1038/jcbfm.2011.30

Shen, H.-Y.Y., Singer, P., Lytle, N., Wei, C.J., Lan, J.-Q.Q., Williams-Karnesky, R.L., Chen, J.-F.F., Yee, B.K., Boison, D., 2012. Adenosine augmentation ameliorates psychotic and cognitive endophenotypes of schizophrenia. The Journal of clinical investigation 122, 2567–77. https://doi.org/10.1172/JCI62378

Shrestha, B., Jawa, G., 2017. Caffeine citrate – Is it a silver bullet in neonatology? Pediatrics & Neonatology 58, 391–397. https://doi.org/10.1016/j.pedneo.2016.10.003

Silinsky, E.M., 1984. On the mechanism by which adenosine receptor activation inhibits the release of acetylcholine from motor nerve endings. J Physiology 346, 243–256. https://doi.org/10.1113/jphysiol.1984.sp015019

Simon, J., Webb, T.E., King, B.F., Burnstock, G., Barnard, E.A., 1995. Characterisation of a recombinant P2Y purinoceptor. European J Pharmacol Mol Pharmacol 291, 281–289. https://doi.org/10.1016/0922-4106(95)90068-3

Smith, J., Ellenberger, H., Ballanyi, K., Richter, D., Feldman, J., 1991. Pre-Botzinger complex: a brainstem region that may generate respiratory rhythm in mammals 254, 726–9. https://doi.org/10.1126/science.1683005

Sprenger, R.J., Kim, A.B., Dzal, Y.A., Milsom, W.K., 2019. Comparison of the CO2 ventilatory response through development in three rodent species: Effect of fossoriality. Resp Physiol Neurobi 264, 19–27. https://doi.org/10.1016/j.resp.2019.03.006

Stella, L., Berrino, L., Maione, S., Novellis, V. de, Rossi, F., 1993. Cardiovascular effects of adenosine and its analogs in anaesthetized rats. Life Sci 53, 755–763. https://doi.org/10.1016/0024-3205(93)90497-q

Studer, F.E., Fedele, D.E., Marowsky, A., Schwerdel, C., Wernli, K., Vogt, K., Fritschy, J.M., Boison, D., 2006. Shift of adenosine kinase expression from neurons to astrocytes during postnatal development suggests dual functionality of the enzyme. Neuroscience 142, 125–37. https://doi.org/10.1016/j.neuroscience.2006.06.016

Svenningsson, P., Hall, H., Sedvall, G., Fredholm, B.B., 1997a. Distribution of adenosine receptors in the postmortem human brain: An extended autoradiographic study. Synapse 27, 322–335. https://doi.org/10.1002/(sici)1098-2396(199712)27:4<;322::aid-syn6>3.0.co;2-e

Svenningsson, P., Moine, L.C., Kull, B., Sunahara, R., Bloch, B., Fredholm, B.B., 1997b. Cellular expression of adenosine A2A receptor messenger RNA in the rat central nervous system with special reference to dopamine innervated areas. Neuroscience 80, 1171–1185. https://doi.org/10.1016/s0306-4522(97)00180-2

Takahashi, M., Fujita, M., Asai, N., Saki, M., Mori, A., 2018. Safety and effectiveness of istradefylline in patients with Parkinson's disease: interim analysis of a post-marketing surveillance study in Japan. Expert Opin Pharmaco 19, 1635–1642. https://doi.org/10.1080/14656566.2018.1518433

Tanaka, A., Nishida, K., Okuda, H., Nishiura, T., Higashi, Y., Fujimoto, S., Nagasawa, K., 2011. Peroxynitrite treatment reduces adenosine uptake via the equilibrative nucleoside transporter in rat astrocytes. Neurosci Lett 498, 52–56. https://doi.org/10.1016/j.neulet.2011.04.060

Tankersley, C.G., Fitzgerald, R.S., Kleeberger, S.R., 1994. Differential control of ventilation among inbred strains of mice. Am J Physiology-regulatory Integr Comp Physiology 267, R1371–R1377. https://doi.org/10.1152/ajpregu.1994.267.5.r1371

Teppema, L.J., 2018a. CrossTalk opposing view: the hypoxic ventilatory response does not include a central, excitatory hypoxia sensing component. J Physiology 596, 2939–2941. https://doi.org/10.1113/jp275708

Teppema, L.J., 2018b. Rebuttal from Luc J. Teppema. J Physiology 596, 2945–2945. https://doi.org/10.1113/jp276281

Teppema, L.J., Dahan, A., 2010. The Ventilatory Response to Hypoxia in Mammals: Mechanisms, Measurement, and Analysis. Physiol Rev 90, 675–754. https://doi.org/10.1152/physrev.00012.2009

Tetzlaff, W., Schubert, P., Kreutzberg, G.W., 1987. Synaptic and extrasynaptic localization of adenosine binding sites in the rat hippocampus. Neuroscience 21, 869–875. https://doi.org/10.1016/0306-4522(87)90043-1

Thauerer, B., Nedden, S. zur, Baier-Bitterlich, G., 2012. Purine nucleosides: endogenous neuroprotectants in hypoxic brain. J Neurochem 121, 329–342. https://doi.org/10.1111/j.1471-4159.2012.07692.x

Theofilas, P., Brar, S., Stewart, K., Shen, H., Sandau, U.S., Poulsen, D., Boison, D., 2011. Adenosine kinase as a target for therapeutic antisense strategies in epilepsy. Epilepsia 52, 589–601. https://doi.org/10.1111/j.1528-1167.2010.02947.x

Thomas, T., Spyer, K., 2000. ATP as a mediator of mammalian central CO2 chemoreception. J Physiology 523, 441–447. https://doi.org/10.1111/j.1469-7793.2000.00441.x

Tomaselli, B., Nedden, S. zur, Podhraski, V., Baier-Bitterlich, G., 2008. p42/44 MAPK is an essential effector for purine nucleoside-mediated neuroprotection of hypoxic PC12 cells and primary cerebellar granule neurons. Mol Cell Neurosci 38, 559–568. https://doi.org/10.1016/j.mcn.2008.05.004

Tronche, F., Kellendonk, C., Kretz, O., Gass, P., Anlag, K., Orban, P.C., Bock, R., Klein, R., Schütz, G., 1999. Disruption of the glucocorticoid receptor gene in the nervous system results in reduced anxiety. Nat Genet 23, 99–103. https://doi.org/10.1038/12703

Vandam, R., Shields, E., Kelty, J., 2008. Rhythm generation by the pre-Botzinger complex in medullary slice and island preparations: effects of adenosine A(1) receptor activation. BMC neuroscience 9. https://doi.org/10.1186/1471-2202-9-95

Vilella, L., Lacuey, N., Hampson, J.P., Rani, S.M., Sainju, R.K., Friedman, D., Nei, M., Strohl, K., Scott, C., Gehlbach, B.K., Zonjy, B., Hupp, N.J., Zaremba, A., Shafiabadi, N., Zhao, X., Reick-Mitrisin, V., Schuele, S., Ogren, J., Harper, R.M., Diehl, B., Bateman, L., Devinsky, O., Richerson, G.B., Ryvlin, P., Lhatoo, S.D., 2018. Postconvulsive central apnea as a biomarker for sudden unexpected death in epilepsy (SUDEP). Neurology 92, e171–e182. https://doi.org/10.1212/wnl.0000000000006785

Volonté, C., D'Ambrosi, N., 2009. Membrane compartments and purinergic signalling: the purinome, a complex interplay among ligands, degrading enzymes, receptors and transporters. Febs J 276, 318–329. https://doi.org/10.1111/j.1742-4658.2008.06793.x

Wall, M., Dale, N., 2008. Activity-Dependent Release of Adenosine: A Critical Re-Evaluation of Mechanism. Curr Neuropharmacol 6, 329–337. https://doi.org/10.2174/157015908787386087

Wall, M.J., Dale, N., 2013. Neuronal transporter and astrocytic ATP exocytosis underlie activity-dependent adenosine release in the hippocampus. The Journal of physiology 591, 3853–71. https://doi.org/10.1113/jphysiol.2013.253450

Wall, M.J., Dale, N., 2007. Auto-inhibition of rat parallel fibre–Purkinje cell synapses by activity-dependent adenosine release. J Physiology 581, 553–565. https://doi.org/10.1113/jphysiol.2006.126417

Wang, J.-L., Wu, Z.-H., Pan, B.-X., Li, J., 2005. Adenosine A1 receptors modulate the discharge activities of inspiratory and biphasic expiratory neurons in the medial region of Nucleus Retrofacialis of neonatal rat in vitro. Neurosci Lett 379, 27–31. https://doi.org/10.1016/j.neulet.2004.12.042

Wang, X., Hayes, J.A., Revill, A.L., Song, H., Kottick, A., Vann, N.C., LaMar, M.D., Picardo, M.C.D., Akins, V.T., Funk, G.D., Del Negro, C.A., 2014. Laser ablation of Dbx1 neurons in the pre-Bötzinger complex stops inspiratory rhythm and impairs output in neonatal mice. Elife 3, e03427. https://doi.org/10.7554/elife.03427

Waters, K., Gozal, D., 2003. Responses to hypoxia during early development 136.

Wei, C.J., Li, W., Chen, J.-F., 2011. Normal and abnormal functions of adenosine receptors in the central nervous system revealed by genetic knockout studies. Biochimica Et Biophysica Acta Bba - Biomembr 1808, 1358–1379. https://doi.org/10.1016/j.bbamem.2010.12.018

Weltha, L., Reemmer, J., Boison, D., 2019. The role of adenosine in epilepsy. Brain Res Bull 151, 46–54. https://doi.org/10.1016/j.brainresbull.2018.11.008

Wessberg, P., Hedner, J., Hedner, T., Persson, B., Jonason, J., 1984. Adenosine mechanisms in the regulation of breathing in the rat. European journal of pharmacology 106, 59–67.

Wilson, C., Martin, R., Jaber, M., Abu-Shaweesh, J., Jafri, A., Haxhiu, M., Zaidi, S., 2004. Adenosine A2A receptors interact with GABAergic pathways to modulate respiration in

neonatal piglets. Respiratory physiology & neurobiology 141. https://doi.org/10.1016/j.resp.2004.04.012

Winn, H., Rubio, R., Berne, R., 1981. Brain adenosine concentration during hypoxia in rats. Am J Physiol-heart C 241, H235–H242. https://doi.org/10.1152/ajpheart.1981.241.2.h235

Wölkart, G., Stessel, H., Fassett, E., Teschl, E., Friedl, K., Trummer, M., Schrammel, A., Kollau, A., Mayer, B., Fassett, J., 2022. Adenosine kinase (ADK) inhibition with ABT-702 induces ADK protein degradation and a distinct form of sustained cardioprotection. Eur J Pharmacol 927, 175050. https://doi.org/10.1016/j.ejphar.2022.175050

Wong-Riley, M.T.T., Liu, Q., Gao, X., 2019. Mechanisms underlying a critical period of respiratory development in the rat. Respiratory physiology & neurobiology 264, 40–50. https://doi.org/10.1016/j.resp.2019.04.006

Wu, K.-C., Lee, C.-Y., Chou, F.-Y., Chern, Y., Lin, C.-J., 2020. Deletion of equilibrative nucleoside transporter-2 protects against lipopolysaccharide-induced neuroinflammation and blood-brain barrier dysfunction in mice. Brain Behav Immun 84, 59–71. https://doi.org/10.1016/j.bbi.2019.11.008

Wu, L.-G., Saggau, P., 1994. Adenosine inhibits evoked synaptic transmission primarily by reducing presynaptic calcium influx in area CA1 of hippocampus. Neuron 12, 1139–1148. https://doi.org/10.1016/0896-6273(94)90321-2

Xiao, Q., Suguihara, C., Hehre, D., Devia, C., Huang, J., Bancalari, E., 2000. Effects of GABA Receptor Blockade on the Ventilatory Response to Hypoxia in Hypothermic Newborn Piglets. Pediatr Res 47, 663–668. https://doi.org/10.1203/00006450-200005000-00018

Yacoubi, E.M., Ledent, C., Parmentier, M., Daoust, M., Costentin, J., Vaugeois, J.-M., 2001. Absence of the adenosine A2A receptor or its chronic blockade decrease ethanol withdrawal-induced seizures in mice. Neuropharmacology 40, 424–432. https://doi.org/10.1016/s0028-3908(00)00173-8

Yacoubi, M., Ledent, C., Parmentier, M., Costentin, J., Vaugeois, J.-M., 2009. Adenosine A2A receptor deficient mice are partially resistant to limbic seizures. Naunyn-schmiedeberg's Archives Pharmacol 380, 223–232. https://doi.org/10.1007/s00210-009-0426-8

Yamamoto, M., Nishimura, M., Kobayashi, S., Akiyama, Y., Miyamoto, K., Kawakami, Y., 1994. Role of endogenous adenosine in hypoxic ventilatory response in humans: a study with dipyridamole. J Appl Physiol 76, 196–203. https://doi.org/10.1152/jappl.1994.76.1.196

Yan, S., Laferrière, A., Zhang, C., Moss, I.R., 1995. Microdialyzed adenosine in nucleus tractus solitarii and ventilatory response to hypoxia in piglets. J Appl Physiol 79, 405–10. https://doi.org/10.1152/jappl.1995.79.2.405

Yarbrough, G.G., McGuffin-Clineschmidt, J.C., 1981. In vivo bahavioral assessment of central nervous system purinergic receptors. Eur J Pharmacol 76, 137–144. https://doi.org/10.1016/0014-2999(81)90495-7

Yawo, H., Chuhma, N., 1993. Preferential inhibition of oω-conotoxin-sensitive presynaptic Ca2+ channels by adenosine autoreceptors. Nature 365, 256–258. https://doi.org/10.1038/365256a0

Yoshioka, T., Tanaka, O., 1989. Histochemical localization of Ca2+, Mg2+-ATPase of the rat cerebellar cortex during postnatal development. Int J Dev Neurosci 7, 181–193. https://doi.org/10.1016/0736-5748(89)90068-3

Young, J.D., Yao, S., Baldwin, J.M., Cass, C.E., Baldwin, S.A., 2013. The human concentrative and equilibrative nucleoside transporter families, SLC28 and SLC29. Mol Aspects Med 34, 529–547. https://doi.org/10.1016/j.mam.2012.05.007

Young, J.D., Yao, S.Y., Sun, L., Cass, C.E., Baldwin, S.A., 2008. Human equilibrative nucleoside transporter (ENT) family of nucleoside and nucleobase transporter proteins. Xenobiotica; the fate of foreign compounds in biological systems 38, 995–1021. https://doi.org/10.1080/00498250801927427

Young, T., Palta, M., Dempsey, J., Skatrud, J., Weber, S., Badr, S., 1993. The Occurrence of Sleep-Disordered Breathing among Middle-Aged Adults. New Engl J Medicine 328, 1230–1235. https://doi.org/10.1056/nejm199304293281704

Young, T., Peppard, P., 2000. Sleep-disordered breathing and cardiovascular disease: epidemiologic evidence for a relationship. Sleep 23 Suppl 4, S122-6.

Zaidi, S.I., Jafri, A., Martin, R.J., Haxhiu, M.A., 2006. Adenosine A2A receptors are expressed by GABAergic neurons of medulla oblongata in developing rat. Brain research 1071, 42–53. https://doi.org/10.1016/j.brainres.2005.11.077

Zannin, E., Stoecklin, B., Choi, J.Y., Simpson, S.J., Veneroni, C., Dellaca, R.L., Pillow, J.J., 2023. Ventilatory response and stability of oxygen saturation during a hypoxic challenge in very preterm infants. Pediatr. Pulmonol. https://doi.org/10.1002/ppul.26343

Zeng, Q., Bai, M., Li, C., Lu, S., Ma, Z., Zhao, Y., Zhou, H., Jiang, H., Sun, D., Zheng, C., 2019. Multiple Drug Transporters Contribute to the Placental Transfer of Emtricitabine. Antimicrob Agents Ch 63. https://doi.org/10.1128/aac.00199-19

Zhang, D., Xiong, W., Albensi, B.C., Parkinson, F.E., 2011. Expression of human equilibrative nucleoside transporter 1 in mouse neurons regulates adenosine levels in physiological and hypoxic-ischemic conditions. Journal of Neurochemistry 118, 4–11. https://doi.org/10.1111/j.1471-4159.2011.07242.x

Zhang, D., Xiong, W., Chu, S., Sun, C., Albensi, B.C., Parkinson, F.E., 2012. Inhibition of Hippocampal Synaptic Activity by ATP, Hypoxia or Oxygen-Glucose Deprivation Does Not Require CD73. Plos One 7, e39772. https://doi.org/10.1371/journal.pone.0039772

Zhang, Y., Biancardi, V., Tapia, A.M., Jaib, T.A., Gourine, A., Kasparov, S., Funk, G.D., 2019. cAMP-dependent modulation of Ih underlies the P2Y1 receptor-mediated excitation of the preBötzinger Complex inspiratory network in vitro. Faseb J 33, 551.8-551.8. https://doi.org/10.1096/fasebj.2019.33.1_supplement.551.8

Zwicker, J., Rajani, V., Hahn, L., Funk, G., 2011. Purinergic modulation of preBotzinger complex inspiratory rhythm in rodents: the interaction between ATP and adenosine. The Journal of physiology 589. https://doi.org/10.1113/jphysiol.2011.210930